The First Reconstruction of the Head Anatomy of a Cretaceous Insect, †Gerontoformica gracilis (Hymenoptera: Formicidae), and the Early Evolution of Ants

Authors: Richter, Adrian, Boudinot, Brendon, Yamamoto, Shûhei, Katzke, Julian, and Beutel, Rolf Georg

Morphology and Ontology

The First Reconstruction of the Head Anatomy of a Cretaceous Insect, †*Gerontoformica gracilis* (Hymenoptera: Formicidae), and the Early Evolution of Ants

Adrian Richter,[1,2,5,] **Brendon Boudinot,**[1,] **Shûhei Yamamoto,**[3,] **Julian Katzke,**[4,] **and Rolf Georg Beutel**[1]

[1]Institut für Zoologie und Evolutionsforschung, Friedrich-Schiller-Universität Jena, Erbertstraße 1, 07743 Jena, Germany,[2]Max-Planck-Institut für evolutionäre Anthropologie, Deutscher Pl. 6, 04103 Leipzig,[3]Hokkaido University Museum, Hokkaido University, Kita 10, Nishi 8, Kita-ku, Sapporo 060-0810, Japan,[4]Biodiversity and Biocomplexity Unit, Okinawa Institute of Science and Technology Graduate University, Onna, Japan, and [5]Corresponding author, e-mail: adrichter@gmx.de

Subject Editor: István Mikó

Abstract

The fossil record allows a unique glimpse into the evolutionary history of organisms living on Earth today. We discovered a specimen of the stem group ant †*Gerontoformica gracilis* (Barden and Grimaldi, 2014) in Kachin amber with near-complete preservation of internal head structures, which we document employing μ-computed-tomography-based 3D reconstructions. We compare †*Gerontoformica* to four outgroup taxa and four extant ant species, employing parsimony and Bayesian ancestral state reconstruction to identify morphological differences and similarities between stem and crown ants and thus improve our understanding of ant evolution through the lens of head anatomy. Of 149 morphological characters, 87 are new in this study, and almost all applicable to the fossil. †*Gerontoformica gracilis* shares shortened dorsal tentorial arms, basally angled pedicels, and the pharyngeal gland as apomorphies with other total clade Formicidae. Retained plesiomorphies include mandible shape and features of the prepharynx. Implications of the reconstructed transitions especially for the ant groundplan are critically discussed based on our restricted taxon sampling, emphasizing the crucial information derived from internal anatomy which is applied to deep time for the first time. Based on the falcate mandible in †*Gerontoformica* and other Aculeata, we present hypotheses for how the shovel-shaped mandibles in crown Formicidae could have evolved. Our results support the notion of †*Gerontoformica* as 'generalized' above-ground predator missing crucial novelties of crown ants which may have helped the latter survive the end-Cretaceous extinction. Our study is an important step for anatomical research on Cretaceous insects and a glimpse into the early evolution of ant heads.

1

Graphical Abstract
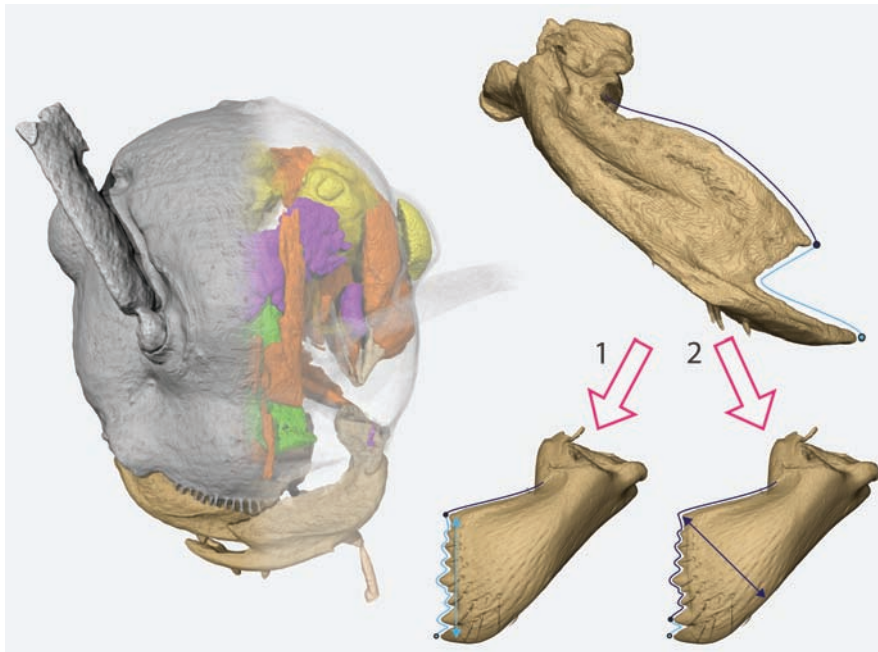
Keywords: Cenomanian, Kachin amber, preservation, μ-computed tomography, anatomy

Since the first discovery of a Mesozoic stem group ant fossil by Wilson et al. (1967a, b), much has been learned about the early evolution of the Formicidae through the study of amber fossils from Cretaceous deposits. The study of late Mesozoic ants has distinctly accelerated in recent years, with bizarre and impressive taxa described in a considerable number of studies, including the 'hell ants' (†Haidomyrmecinae) with scythe-like mandibles (e.g., Dlussky 1996; Perrichot et al. 2008, 2016, 2020; Lattke et al. 2020; Barden and Grimaldi 2012; Barden et al. 2017, 2020) and the recently discovered 'iron maiden ants' (†Zigrasimeciinae) with mandibles, labrum, and clypeus set with stout, spine-like setae (e.g., Barden and Grimaldi 2013, Perrichot 2014, Cao et al. 2020). Furthermore, the †*Camelomecia*-clade is characterized by deeply cup-shaped mandibles (Barden and Grimaldi 2016; Boudinot et al. 2020, 2022c), whereas the comparatively more generalized †Sphecomyrminae have short bidentate mandibles (e.g., Nel and Perrault 2004, Engel and Grimaldi 2005, Perrichot et al. 2008, Barden and Grimaldi 2014, Boudinot et al. 2022b), and the similarly shaped and sized mandibles of the monotypic †*Brownimecia clavata* Grimaldi, Agosti, Carpenter 1997 (Grimaldi et al. 1997) are edentate. Including several described species of currently unknown systematic affinity which are known from compression fossils (Boudinot et al. 2020), the stem group of ants currently consists of 46 valid species preserved in amber and about 10 as compression fossils.

The first recognized Cretaceous ant species, †*Sphecomyrma freyi* Wilson and Brown, 1967, was considered upon its discovery as an almost perfect mosaic of wasp-like and ant-like morphological features (Wilson et al. 1967a, b), with narrow bidentate mandibles, long filiform antennal flagellae, and the distinctly developed mesothoracic scutum and scutellum all identified as plesiomorphic features. Nevertheless, the authors interpreted the fossil as belonging within the crown group Formicidae, with closer affinities to the 'myrmecioid' rather than the 'poneroid' complex of subfamilies based on features such as presence of the metapleural gland opening and the deeply constricted petiole. Taylor (1978) then transferred it to the stem group, arguing that it was not morphologically close to any of the recent subfamilies; this intuitive action was weakly supported by subsequent cladistic analysis (Grimaldi et al. 1997, Grimaldi and Agosti 2000). Later cladistic study (Barden and Grimaldi 2016) strongly supported the stem group placement of the †Sphecomyrminae plus the †Haidomyrmecinae and †Zigrasimeciinae, recovering the highly divergent †Haidomyrmecinae as sister group to all other Formicidae. In the most recent phylogenetic analysis of fossil ant phylogeny based on a larger taxon sampling and character set, Boudinot et al. (2022c) were not able to resolve the relationships among these three subfamilies; thus, the exact phylogenetic placement of the relatively speciose taxa of the ant stem group remains unclear. Only the placement of †*Brownimecia clavata* as sister to the crown group of the ants seems unambiguous at present (Barden and Grimaldi 2016; Boudinot et al. 2020, 2022c). This persistent difficulty of resolving stem-group relationships highlights the need for new and hopefully incisive morphological characters and data.

Most of these critical discoveries regarding early ant evolution and diversity of total clade Formicidae were only possible due to the excellent preservational properties of amber fossils. Amber fossils originate when an organism is trapped in plant resin, becomes entombed, and subsequently deposited in sediment and fossilized over time (Martínez-Delclòs et al. 2004). Although most amber fossils are empty shells in which the original organism has completely decayed (e.g., Grimaldi et al. 1997, Grimaldi and Engel 2005), there is some chance for the organism itself to be preserved, possibly through desiccation or other means. Although such preservation of internal tissue seems to be possible for most amber sources in principle, there is considerable variation in the degree of preservation for amber from different deposits (McCoy et al. 2016). Partly, this can be explained by processes after the fossilization of the amber.

Different chemical and physical factors can affect the amber matrix and its inclusions, such as the pressure and temperature of the fossil deposit (Martínez-Delclòs et al. 2004). Additionally, it is likely that the chemical composition of the resin and even the gut microbiome of entombed insects can influence soft tissue preservation (McCoy et al. 2018).

Earlier studies on soft tissue of amber preserved insects were most commonly being conducted employing electron microscopy of broken or sectioned amber pieces (e.g., Poinar and Hess 1982, Henwood 1992a,b, Grimaldi et al. 1994). While these early approaches required near complete destruction of the fossil specimen, more recent non-destructive methods such as µ-CT scanning have become available. µ-CT scans can reveal fine morphological details of fossils that would have otherwise been inaccessible, including internal features (e.g., Dunlop et al. 2011, van de Kamp et al. 2014). Grimaldi et al. (2019) and Li et al (2021) were the first to show internal soft tissue of insect fossils (an apoid wasp and archostematan beetle, respectively) from the mid-Cretaceous-dated (Albian-Cenomanian boundary) Kachin amber (~99 Mya) using µ-CT-scans, but the preservation of their specimens and scan resolution were not sufficient for 3D reconstruction. The only example of an almost complete reconstruction of the internal anatomy of an insect fossil is †*Mengea tertiaria* (Menge, 1866) (Mengeidae) from Baltic amber, a species belonging to the stem group of the endoparasitic Strepsiptera (Pohl et al. 2010).

We present here the first discovery and 3D reconstruction of the almost completely preserved soft tissue in the head of a Cretaceous insect, belonging to the stem group ant genus †*Gerontoformica* (†Sphecomyrminae) from Burmese amber. The amber piece was first presented by Boudinot et al. (2022b) who identified the specimen as †*Gerontoformica gracilis* (Barden and Grimaldi, 2014). The amber piece was initially µ-CT scanned due to the discovery of a synincluded ant pupa, but preliminary examination of those scans revealed surprising and excellent preservation of internal structures, prompting further, higher resolution scans of different body parts. Based on these scans, we were able to reconstruct almost the complete anatomy of the head. The head was studied specifically in the context of an ongoing project on the evolution of ant head morphology and its analysis was strongly facilitated by recent advances in knowledge on the head anatomy of living ant species (Richter et al. 2019, 2020, 2021), which also heavily relied on results from µ-CT scans.

To put our anatomical results in an evolutionary context, we compared our reconstructions of †*Gerontoformica* Nel & Perrault, 2004 not only with extant ants carefully chosen to represent all major formicid clades, but also four outgroup taxa from several clades of aculeate wasps. This especially included *Methocha* sp. Latreille, 1804 (Hymenoptera, Tiphiidae), that was previously hypothesized to be morphologically close to the ant ancestor (Wilson et al. 1967a, b) and two species of Apoidea, with this superfamily now confirmed to be the sister group of ants based on phylogenomic analyses (Branstetter et al. 2017, Peters et al. 2017). Although this taxon sampling is still too fragmented for a detailed phylogenetic reconstruction of character evolution, we assembled a large list of anatomical characters and performed character mapping/ancestral state reconstruction using parsimony and Bayesian approaches to present new, revised, and incipient working hypotheses about important morphological transitions in the early evolution of ants. Because we took the 'node-spanning' approach to taxon choice among extant Formicidae, i.e., choosing taxa from reciprocally monophyletic groups to represent nodes which are well-supported in molecular phylogenetic analysis (e.g., Brady et al. 2006, Moreau

et al. 2006, Branstetter et al. 2017), we are confident that our results will be insightful especially at the level of the ant groundplan and transitions in the early evolution of the group. The express goal of our analysis here is to provide a step on the way to reconstruct the morphological evolution of the ant head; future study directly addressing the relationships of stem-group taxa will benefit from inclusion of character systems across body tagma. We hope this work will be a starting point and inspiration for future attempts to study the internal anatomy of insects fossilized in amber, and for the reconstruction and understanding of their evolution in unprecedented detail.

Materials and Methods

Material

The studied fossil was preserved in a single clear yellow piece of Kachin amber (Fig. 1A) from the northern Hukawng Valley, Kachin State. There is evidence that amber pieces from this site date to the Albian–Cenomanian boundary ('mid-Cretaceous'), based on included marine fauna (e.g., Mao et al. 2018, Yu et al. 2019) and U-PB dating (Shi et al. 2012), although an older age was also suggested (Balashov 2021). It is likely that fossils from this region cover a range of ages, which is difficult to assign exactly due to the mining circumstances (Xing and Qiu 2020). The focal specimen is synincluded with a conspecific pupa and two less well-preserved workers of a different species, plus a small unidentified hemipteran and a scydmaenine rove beetle (Coleoptera, Staphylinidae). The fossil piece and the external morphology of all ant specimens were first described in Boudinot et al. (2022b). Those authors identified the specimen treated here as †*Gerontoformica gracilis* (Barden and Grimaldi, 2014), and assigned the amber piece the identification number AMNH Bu-SY23 and the adult specimen of †*G. gracilis* the identifier CASENT0741232. The amber piece has been deposited in the American Museum of Natural History (AMNH). We used two high-resolution µ-CT scans of the head of CASENT0741232 for our analysis.

For our comparisons, we used the already published data on extant ant head anatomy by Richter et al. (2019, *Wasmannia affinis* Santschi, 1929), Richter et al. (2020, *Formica rufa* Linnaeus, 1761, Hymenoptera, Formicidae and *Brachyponera luteipes* [Mayr, 1862]) and Richter et al. (2021, *Protanilla lini* Terayama, 2009), covering the three major extant ant clades (Formicidae). For outgroups, we generated µ-CT scan data from *Parischnogaster* sp. (de Saussure, 1852) (Hymenoptera, Vespidae, keyed to genus using Carpenter and Starr 2000), *Methocha* sp., *Ampulex* sp. (Fabricius, 1781) (Hymenoptera, Ampulicidae), and *Sceliphron caementarium* (Drury, 1773) (Sphecidae, keyed to species using Jacobs 2007). *Parischnogaster* and *Ampulex* were chosen as they represent the sister-groups to the remainder of the Vespidae and Apoidea, respectively (Piekarski et al. 2018; Sann et al. 2018, 2021).

As we compared worker ant heads to individuals of the non-eusocial outgroup taxa, we also used a µ-CT scan of a queen of *B. luteipes* to evaluate the degree of comparability of worker and reproductive female heads. Although there are some differences in head anatomy between the queen and worker *B. luteipes*, almost none of the phylogenetic characters used here would have been coded differently between the queen and the worker, leading us to the tentative conclusion that the heads of adult female (worker and queen) ants are generally suitable for comparative analysis with other (solitary) Aculeata. Collection data of newly analyzed specimens are summarized in Table 1.
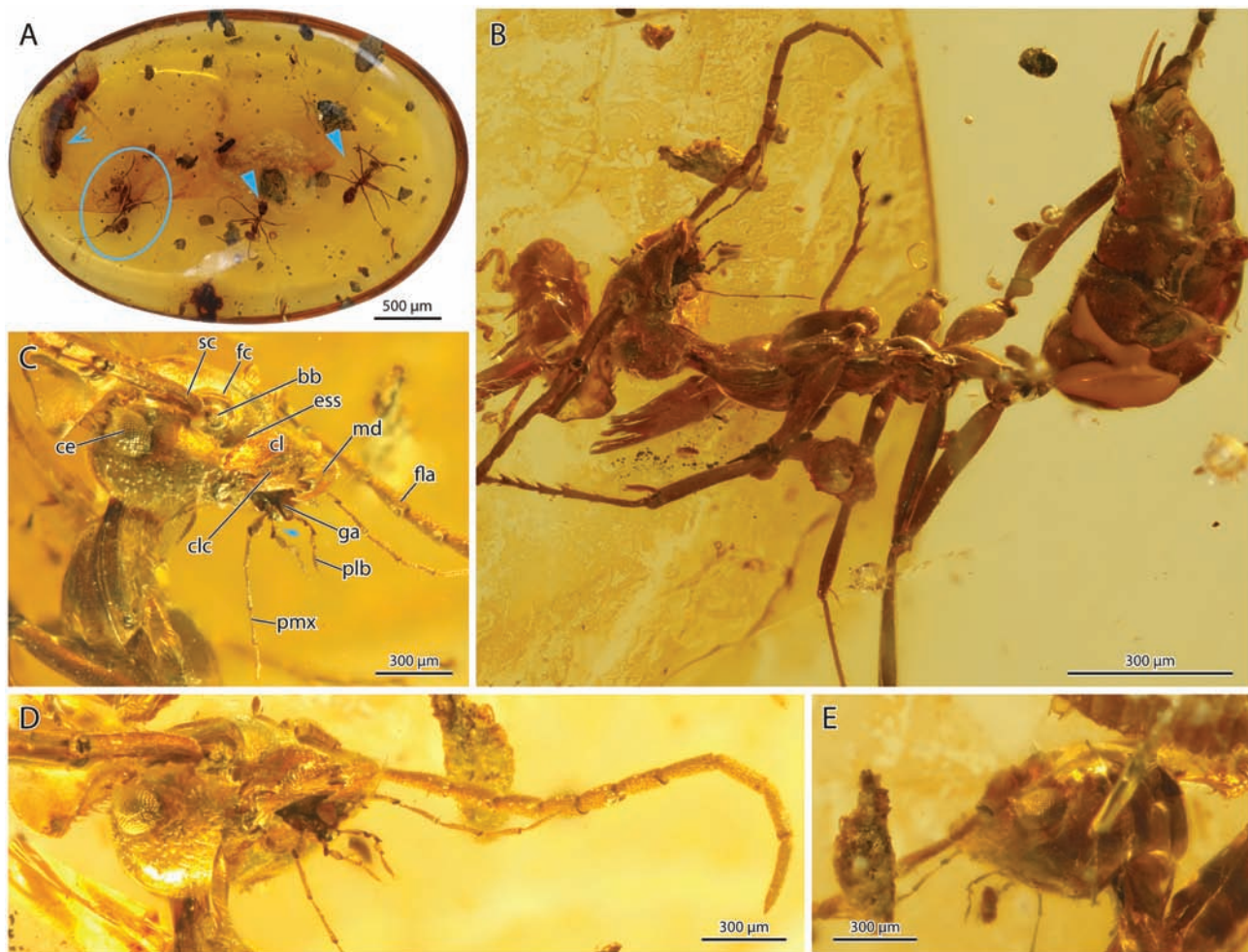
Fig. 1. Photographic images of the amber fossil. (A) Overview of the amber piece: the solid arrowheads indicate synincluded adult †*Gerontoformica sternorhabda*, the open arrowhead indicates synincluded †*G. gracilis* pupa, and the circle outlines focal †*G. gracilis* specimen CASENT0741232. (B) Overview of specimen CASENT0741232 in ventrolateral view. (C) Head of †*G. gracilis* in frontolateral view (oblique dorsal); the short blue arrow indicates the process on the first labial palpomere. (D) Head of †*G. gracilis* in frontolateral view (oblique ventral). (E) Head of †*G. gracilis* in posterolateral view. Abbreviations: **bb,** bulbus; **cl,** clypeus; **clc,** clypeal chaetae; **ce,** compound eye; **ess,** epistomal sulcus; **fc,** frontal carina; **fla,** antennal flagellum; **ga,** galea; **md,** mandible; **plb,** labial palp; **pmx,** maxillary palp; **sc,** scapus. The photographs in A, B and D were also used in Boudinot et al. 2022b.

Table 1. Collection data of newly analyzed specimens

Species	Collection Label	Located at
Methocha sp.	Thailand, Surat Thani, Khlong Sok, Our Jungle House resort, 75 m, 25.V.2018, 8.908°N, 98.534°E, hand collected, R. Malee. FFP18TH115	BEBC
Ampulex sp.	Ghana, Western Region, Nini Suhien NP, Ankasa Game Reserve, 80 m, 2014.IV.24, 5.248°N, -2.648°E, M. Hauser, S. D. Gaimari. FFP14GHA53	BEBC
Sceliphron caementarium	Italy, Umbria, south of Monte del Lago, Castelle di Zocco, ruins, 260 m, 25.VIII.2019, 43.1358°N, 12.167686°E, A. Richter IT/2019/02	ARC
Parischnogaster sp.	Thailand, Krabi, 14 km NNE Krabi; Phnom Bencha Mountain Resort, 90 m, 02.IV.2017, 8.210°N, 98.935°E, Borkent, C. J. FFP17TH060	BEBC
Brachyponera luteipes (q)	Okinawa, Uruma-shi, Ishikawa, Precious One Appartment, 24.VI.2019, 26.4376°N, 127.8321°E, by hand at night, A. Richter	ARC

BEBC, Brendon Boudinot research collection; ARC, Adrian Richter research collection (Phyletisches Museum Jena).

X-Ray Microtomography (μ-CT)

The fossil was μ-CT scanned using a Zeiss Xradia 510 Versa 3D X-ray Microscope (Zeiss, Jena, Germany) operated with the Zeiss Scout-and-Scan Control System software (v.11.16411.17883) at the Okinawa Institute of Science and Technology Graduate University, Okinawa, Japan. Two scans of the head were performed. The first includes the complete head and was used for 3D-reconstruction. The second scan with higher resolution has parts of the mandibles and mouthparts cut off and was used to resolve fine details of tissues as a reference to improve the

3D-reconstruction, and for analysis of histological details, such as the muscle sarcomeres and gland cells. The scanning parameters were as follows, with high resolution scan values presented in parentheses where they differ: 25 s (80 s) exposure time; 40 keV source voltage; 3 W source power; 4× (20×) magnification; source to sample distance: 26.027 mm (51.004 mm); detector to sample distance: 100.02 mm (17.002 mm); 3001 projections; and 1.394 (0.956) resulting pixel image size. Both scans were reconstructed using the Zeiss Scout-and-Scan Control System Reconstructor (version 11.1.6411.17883) and exported as TIFF image series. The lower resolution scan was used for the 3D-reconstruction, the higher resolution one to show histological details (Fig. 2). The scans can be accessed in the Zenodo archive (DOI: 10.5281/zenodo.5608454).

All outgroup taxa were stained in a 2% iodine solution in ethanol for a week prior to scanning. They were transferred to a sealed off pipette tip of appropriate size filled with ethanol and mounted on a metal sample holder. They were scanned at a SkyScan 2211 (Bruker, Billerica, USA) at the Max Planck Institute for the Science of Human History in Jena, equipped with a high resolution (4000 × 2600 pixel) X-ray sensitive CCD camera in the nanofocus mode. Scanning parameters for the extant taxa are summarized in Table 2. The tomographic reconstructions were done in NRecon (Version: 1.7.3.1) and exported as a 16-bit TIFF image series. Scanning procedures of the included extant ants can be found in their respective publications (Richter et al. 2019, 2020, 2021).

3D Reconstruction

The lower resolution TIFF image stack was imported into ORS Dragonfly 2020.1 (Object Research Systems, Montreal, Canada) to segment individual structures into discrete regions of interest (ROI). The ORS file with labeled ROIs is uploaded to the Zenodo archive (DOI:10.5281/zenodo.5825697). The ROIs were then used to export TIFF image stacks containing only the marked structures. VG-Studio Max 3.4 (Volume Graphics GmbH, Heidelberg, Germany) was used to create volume renders (Phong) of the TIFF image series. A video showing all reconstructed structures, simplified (e.g., all muscles in the same color), was also exported from VG Studio Max and can be found in Supp Video S1 (online only).

Additionally, a surface mesh of all external structures (head capsule, antennae, and mouthparts) was created in Dragonfly and imported to Blender 2.8 (Blender Foundation, Amsterdam, Netherlands). It was simplified and smoothed with the modifier functions of blender and a video showing the head from different angles was rendered (Supp Video S2 [online only]).

Scans of all outgroup taxa were imported to Amira 6.0 (Visage Imaging GmbH, Berlin, Germany). Selected structures of phylogenetic interest were pre-segmented every 20th slice and semiautomatically segmented using Biomedisa (Lösel et al. 2020). To complete the segmentation, the semiautomatic results were corrected manually and via the 'remove island' and 'smooth labels' functions of Amira. The plugin script 'multiExport' (Engelkes et al. 2018) was used to automatically export the image information of all segmented materials as TIFF image series. Rendering was also performed in VG-Studio Max 3.4.

All images were edited with Adobe Photoshop CS6 (Adobe System Incorporated, San Jose, USA) and arranged into figure plates. Adobe Illustrator CS6 (Adobe Systems Incorporated, San Jose, USA) was used to label the figure plates.

Measurements

To measure the volume of different brain regions of †*Gerontoformica gracilis*, volumes of the segmented materials were calculated in ORS Dragonfly 2020.1 (Object Research Systems, Montreal, Canada) (see Supp File S1 [online only]). To determine sarcomere length, we imported the higher resolution scan of †*G. gracilis* in Amira 6.0 (Visage Imaging GmbH, Berlin, Germany) and used the Orthoslice function to to find planes that cut parallel to the direction of the muscle fibers. We exported three slices to 4000 × 4000 pixel images with known pixel size using the extract image module of Amira. We measured the pixel length of individual sarcomeres as the length from the proximal end of one light band to the proximal end of the next one in Adobe Photoshop CS6 (Adobe System Incorporated, San Jose, USA) and calculated the individual and average sarcomere lengths in µm multiplying length by image pixel size. The measurements can be found in Supp File S2 (online only), and the used images are part of the Zenodo archive (DOI:10.5281/zenodo.5825697).

In our phylogenetic character definitions, we use a few measurements that were taken on images of our volume renderings with the measurement tool of Adobe Illustrator CS6 (Adobe Systems Incorporated, San Jose, USA). The respective measurements are described in the character list and illustrated in the accompanying images (see *Character List* section).

Character Coding

We coded 149 characters for the specific purpose of reconstructing character evolution across our taxon sampling (see *Character List* section). Our main inspirations for the inclusion of previously used characters were Prentice (1998), Keller (2011), Zimmermann and Vilhelmsen (2016), and Boudinot et al. (2022c), but all character statements are newly written for this work and 87 of them are used for systematic analysis for the first time (marked by asterisk *). Most of these newly defined characters relate to internal features that were not investigated in this way before (40 characters), or to the shape of external features that is easier to access and analyze with three-dimensional (µ-CT) data (40 characters). Additionally, seven characters are very specific to one of the included taxa. Another factor is our purpose of reconstructing character evolution only rather than topology, for which we relaxed some of the usual 'good coding practices' (e.g., Sereno 2007) for morphological characters (see last paragraph of this section).

Our underlying concept of what constitutes a character follows the 'developmental character concept' of Wagner (2007, 2014), recently specified in McKenna et al. (2021). Accordingly, we conceive of 'characters' as phenotypic objects, object systems (combination of phenotypic objects), or regions that are developmentally specified by different levels of genetic regulatory networks and systems, and which have different genetically specified variants that are considered as character 'states'. In other words, discrete phenotypic objects are characters, whereas continuous variation of a given character constitutes state space, which we discretized into two or more states.

In our practical process of character coding, we recognize 'expression' and 'variation characters', with the former being columns representing 'presence' or 'absence' of a specified developmental character, and the latter being columns representing two or more discretized variants of a given developmental character, following the suggestions of Brazeau (2011). Where both 'expression' and 'variation characters' are scored in the matrix, i.e., where state variation is scored separately from character presence/absence, we employ reductive coding (also called 'contingent coding', e.g., Brazeau 2011, or 'hierarchical coding', e.g., Hopkins and St. John 2021). We also

use this in cases where we hypothesize that a variation character depends on a certain state of another variation character. We mark reductive characters as '(Reductive)' at the beginning of the character statement and specify the character and state they are dependent on at the end of the character's discussion section. Taxa in which the dependent state is not present were therefore coded as inapplicable (–) in the matrix.

Most characters here defined are more-or-less independent from each other; in cases where this principle is potentially violated, we discuss it in the character statement. Due to the high number of newly defined characters (marked by an asterisk, *) and characters for which the exact definitions are revised (marked by a tilde, ~), we provide at least a short discussion of each character as part of the character list and additionally visualize the different character states in 45 image plates (Char. 1–149). Our character set is biased towards characters that allow for a good delimitation of clades within ants and of total clade Formicidae as a clade within Aculeata. We therefore mostly excluded characters that would be suited for analyses among different groups of wasps and also omitted many possible 'among ant' characters that would not have been informative with our limited sampling. In some cases, we include such 'among ant' characters even though they are not phylogenetically informative with our sampling due to either too much or too little variation, which violates the good practices of character coding for phylogenetic analysis (e.g., Sereno 2007). However, we retain these characters as they 1) provide interesting insight for discussion purposes and 2) will provide useful systematic information with expanded taxon sampling at lower taxonomic level. We risked biases in the chosen characters and took these liberties in character coding as our singular purpose here is to analyze and discuss character evolution, and not topology estimation. Individual reasoning is also given in the discussion of relevant characters (see *Character List* section).

Parsimony Analysis

Our taxon sampling is highly limited; we address this potential problem by very carefully discussing the validity of any character transitions recovered by our analyses in the discussion section and description of each character (see *Character List* section). We believe that even with its limitations, the formal parsimony and Bayesian analyses add a stronger foundation to our discussion of the early evolution of ants than would be possible without these estimations. We also hope that our open approach to the character coding and analysis will make it easy for future workers to build on our results and refine them. The character matrix (149 characters, 9 OTUs) was first assembled as an Excel file (Supp File S3 [online only]). Based on this, a Mesquite (Maddison and Maddison 2021) file with the matrix and a tree was constructed. The phylogenetic tree for the taxa analyzed here is based on the results of Branstetter et al. (2017) and Boudinot et al. (2022c). The following branching pattern was used: (*Methocha* + *Parischnogaster*) + ((*Ampulex* + *Sceliphron*) + (†*Gerontoformica* + (*Protanilla* + (*Brachyponera* + (*Formica* + *Wasmannia*)))))). Peters et al. (2017) recovered a slightly different branching pattern, i.e. *Parischnogaster* + (*Methocha* + ((*Ampulex* + *Sceliphron*) + (†*Gerontoformica* + (*Protanilla* + (*Brachyponera* + (*Formica* + *Wasmannia*))))))); use of this alternative hypothesis did not change the results of the parsimony-based character mapping and is thus not shown in our results. We imported the tree and matrix into WinClada (Nixon 1999–2001), where we first executed the 'mop uninformative characters' function and deactivated characters without any phylogenetic information. Next, we displayed unambiguous character transformations based on the criterium of maximum

parsimony along the tree. Conservatively, only unambiguous transformations are discussed here, but character transformations using ACCTRAN and DELTRAN optimizations can be found in the Zenodo repository to this article (DOI:10.5281/zenodo.5825697).

Bayesian Analysis

Because parsimony analysis results in absolute character mapping, we employed statistical ancestral state estimation via MrBayes 3.2.6 (Ronquist et al. 2003) in order to gain a more-nuanced perspective on potential character transitions among our sampled taxa. Characters were partitioned by state count, resulting in four total partitions. For each partition, we applied an Mkv model (Lewis 2001) with among-character rate variation modeled by gamma (+Γ). We set coding to 'variable', unlinked the Q-matrices, the shape parameter for gamma (α), and set the branch length prior as an unconstrained gamma Dirichlet (1,1,1,1). We constrained all nodes because we were not concerned with topology estimation.

As †*G. gracilis* is a fossil tip, we set its age as a uniform distribution spanning 94.3–99.7 Mya and evaluated the fit of a uniform (UNI), birth-death (BD), and fossilized birth-death (FBD) clock model using stepping-stone sampling (SSS, Xie et al. 2011). Each clock model implemented an independent gamma rates clock variation prior (IGR; Ronquist et al. 2012), an exponential (mean = 37) IGR variation prior, a lognormal (mean = –5, variance = 1.2) clock rate prior, and an offset exponential tree age prior (100, 175). For the BD and FBD models, the speciation and extinction priors were set as exponential (10) and beta (1, 1), respectively, with the fossilization prior for the FBD also set as a beta (1, 1) distribution. Only the results of the UNI analysis will be presented and discussed as this model had the highest likelihood as determined by SSS (UNI: LnL = –777.37; BD: LnL = –779.88; FBD: LnL = 782.25).

MCMC analyses were run for at least 10 million generations, sampling every 1 thousand generations across two runs with four chains each, with a temperature set a 0.01 and burnin fraction for diagnosis of 0.25. To increase the potential of sampling at stationarity, we only let analyses finish when the average standard deviation of split frequencies (ASDSF) was below 0.001, and when potential scale reduction factors (PSRF) for each parameter were approximately 1.000. We then checked the shape of estimated distributions, their traces, and estimated sample sizes (ESSs) via Tracer (Rambaut et al. 2018); ESSs for all parameters across all analyses were well over the suggested threshold of 300.

To gauge the support for character/state estimates and transformations resulting from our analysis, we constructed a reporting workbook in Excel, with separate worksheets for each partition (Supp File S4 [online only]). As our approach to comparative analysis and evaluation is apparently novel (see, e.g., Boudinot et al. 2022c), we propose our evaluation criteria as a first idea to gauge support for character state transformations. Parameter estimates were first sorted by character number, node index, then by probability (highest to lowest). These estimates were then piped into a side-by-side comparison frame, where the scale of support for each state was determined by dividing the highest probability by the lowest for the two-state partition, and the second lowest divided by the third lowest and so on for the other partitions. For each state at each node, we employed the following interpretation scheme for the coefficients of support (CS): CS < 5 = state not supported; 5 < CS < 10 = state moderately supported; 10 < CS < 100 = state well-supported; 100 < CS < 1000 = state very well-supported; 1000 < CS = state maximally supported.

Table 2. Scanning parameters of the newly generated µCT scans at the MPI-SHH in Jena

Species	Image pixel size (µm)	Exposure time (s)	Voltage (kV)	Current (µA)	Rotation step
Methocha sp.	0.7	4.1	50	300	0.2°
Ampulex sp.	0.9	1.9	40	300	0.18°
Sceliphron caementarium	1.5	1.7	40	300	0.18°
Parischnogaster sp.	1	5.9	40	300	0.17°
Brachyponera luteipes (q)	0.5	5.9	40	300	0.18°

With CS calculated for each state by each node across all characters and partitions, we then interpreted the support for state transitions. To do so, we evaluated if the best-supported states differed between sequential nodes (state identity), and if the CS values for each best-supported state of the paired nodes were well-supported (state polarity). When state identities differed between sequential nodes, we interpreted this as potential support for a transition, with the degree of support determined by the CS values and state polarities. We then employed the following interpretation scheme: 'synapomorphies' have different state identities and well-supported CS values for each node; a state may be 'fixed' when the CS for the shallower node is well-supported and that of the deeper node is less supported; 'unstable' or 'possibly diverging' states have different identities but negligible support (CS < 10); 'certain' and 'uncertain plesiomorphies' have the same state identity between the deeper and shallower node, and differ in CS; 'uncertain' states have negligible support for both nodes.

Terminology

The terminology of head structures generally follows Richter et al. (2020, 2021). The head orientation of Aculeata, including ants such as †*Gerontoformica*, is always somewhat ambiguous due to the highly mobile head that can assume both forward (prognathous), downward (orthognathous), or backward directed (hypognathous) positions. This is apparent, for example, via the rather anteriorly directed head in our fossil (Fig. 1B and C), although some morphological features indicate a more orthognathous head compared to extant ants (see Results and Discussion). Therefore, we decided to treat the head as prognathous in our description mainly to facilitate easy comparison with previously published descriptions of extant ant heads (Richter et al. 2019, 2020, 2021). Where we are comparing prognathous and more orthognathous species, we give the positional term for the orthognathous orientation in parentheses. Where necessary, we indicate term equivalencies to the Hymenoptera Anatomy Ontology (HAO, Yoder et al. 2010) in parentheses. A table of all important terms used and their equivalency to HAO terms is provided in Supp File S5 (online only).

The hypostomal region has rarely been investigated in detail in Hymenoptera before, so for the purpose of our comparisons we introduce several new terms here, marked by an asterisk (*) and bolded. A visual overview of the described features can be found in Fig. 3 and the character image plate for Char. 25, 28, 37–40, 45–47. With the head in oral view, the ***oral margin of the hypostoma** is the lower margin of the oral foramen between the pleurostomal fossae (vma, Fig. 3), i.e., it is the portion of the head which rims the oral foramen ventrally if the head is prognathous or posteriorly if the head is orthognathous. The central portion of the oral hypostomal margin laterally extended into the ***cardinal condyle of hypostoma** is referred to as the ***oral hypostomal carina** (hysc$_{or}$, Fig. 3; see also the magenta dotted line, Char. 39). The cardo rests in a deep notch laterad the condyle, the ***cardinal notch**. A broad, triangular process

reaches into the oral foramen (hysp, Fig. 3; also Char. 45) laterad this notch. It is often termed 'paramandibular process' in the literature (e.g., Prentice et al. 1998, Porto et al. 2016, HAO) but we choose to retain the term (**triangular**) **hypostomal process** (e.g., Richter et al. 2019) here to make its association to the hypostoma clear. The hypostomal surface is separated from the remaining ventral head capsule (postgenal bridge) by the ***outer hypostomal carina**, which terminates laterally at the pleurostomal fossae, thus demarcating the hypostomal surface between it and the oral hypostomal margin (hysc$_{ou}$, Fig. 3; also, the yellow dotted line, Char. 40). This carina is traditionally referred to simply as the 'hypostomal carina' (HAO), but we specify it here as there is a second hypostomal carina that we want to distinguish it from, the ***inner hypostomal carina** (this corresponds to the "paramandibular carina" of Prentice 1998). It runs from the tip of the triangular hypostomal process downward towards the sagittal line where it sometimes meets in the middle right above the outer carina (hysc$_i$, Fig. 3; also, the blue dotted line in Char. 38). The inner carina thus separates the concave hypostomal surface into a ***medial hypostomal groove** (hyg$_m$, Fig. 3) and one or two ***lateral hypostomal grooves** (hyg$_l$, Fig. 3). The outer hypostomal carina is usually concave to some degree in ventral (posterior) view and its distalmost lateral points are termed the ***hypostomal corners**. Often the hypostomal corners are flat or rounded, but sometimes they are produced into pointed ***hypostomal teeth** (the term was used for these processes before, e.g., HAO, but not in the specific distinction to the hypostomal corners as defined here). More exact terminology for the hypostoma may arise as this variable character system is studied in more detail in the future.

We also want to clarify a few terms of the mandible since they are not consistently used in the ant literature. The medial margin of the mandible is termed the gnathal edge or gnathal margin as is the convention for all Mandibulata (e.g., Edgecombe et al. 2003). Terminology of teeth on the mandible is complicated by their wide variation in shape, size, and position across the ants, aculeates, and insects more broadly. The limited developmental work on insect mandibles has indicated (e.g., Gotoh et al. 2017, see *Discussion*) that different teeth on the mandible may be shaped by different underlying developmental processes and networks, and may thus represent different developmental characters. As working hypoŁthesis, we roughly follow Bolton's (1994) distinction of ***incisors** and ***denticles** (new sense), with the former comprising larger and the latter smaller teeth, when two series of teeth are detectable. Across most Aculeata, two primary teeth occur on the mandibles, which we refer to as the ***apical** and ***subapical incisors** (at, sat, Fig. 4G and H). These two incisors correspond to the tooth of the 'rutellum' (apical) and 'pollex' (subapical) in the bee mandible terminology of Michener and Fraser (1978). Practically, incisors and denticles can be differentiated by a '2/3 rule', with denticles being < 2/3 the length of the incisors or the incisor series of teeth. We base the terms of mandibular grooves and carinae on Michener and Fraser (1978), where we find them broadly applicable to ant and other aculeate

mandibles: the ***fimbrial line** (fl, Fig. 4G and H) (fimbriate line in Michener and Fraser 1978) is a line of setae, often in a slight groove and sometimes accompanied by a carina that is located on the inner surface of the mandible and runs along part of the gnathal edge. The 'condylar carina' (cdc, Fig. 4E) runs from the mandibular condyle to the tip of the apical incisor. The ***adductor carina** (adc, Fig. 4E and H) (adductor ridge in Michener and Fraser 1978) runs on the inner surface of the mandible from the insertion point of the adductor apodeme also to the tip of the apical incisor. Between these two carinae on the distal ventral (posterior) margin of the mandible is the 'condylar groove' (cdg, Fig. 4E) in which a line of setae is usually set. Together, the condylar carina and the gnathal edge constitute the single, continuous ***carina mandibularis,** which separates the inner and outer surfaces of the mandible (ims, oms, Fig. 4G and H).

The 'oral arm' ('pharyngeal rod' of, e.g., Porto and Almeida 2019) of ants was previously established as an intricate sclerite stabilizing the prepharynx (Richter et al. 2019, 2020, 2021). We recognize here the proximal processes of the arms that receive the frontooral and tentoriooral muscles as ***oral arm processes** and the broad, dorsally directed plates that receive part of the longitudinal pharyngoepipharyngeal musculature as well as the transverse oral muscle as ***oral arm lamellae**. We additionally introduce a muscle symbol for the *Musculus pharyngoepipharyngalis* (previously Mpe, e.g., Zimmermann and Vilhelmsen 2016; Richter et al. 2020, 2021) that is an autapomorphy of Hymenoptera (Beutel and Vilhelmsen 2007): *0pe1, to fit with the muscle terminology of Wipfler et al. (2011) that we consistently use here.

To identify and name the different subregions of the brain, we used the insect brain database (https://insectbraindb.org/app/).

Classification System

The systematic concept in our study follows, as mentioned above, the phylogenetic hypotheses of Branstetter et al. (2017) and Boudinot et al. (2022c). These were translated into a classification of the higher clades of Aculeata by Boudinot et al. (2022c) and we use the terms introduced by those authors. For the higher clades applicable in our present work, we refer to the 'vespiform Aculeata' (Aculeata, excluding Chrysidoidea, Dryinoidea), the 'Vespoida' (Vespoidea + pompiloid families), and Formicapoidina (Formicoidea + Apoidea). Within the Formicoidea, we recognize a monophylum including the stem group subfamilies †Sphecomyrminae (including †*Gerontoformica*), †Haidomyrmecinae, †Zigrasimeciinae, and †Brownimeciinae, but not the more wasp-like stem group fossils of the †*Camelomecia* clade (Boudinot et al. 2020, 2022c). We refer to this grouping consistently as 'total clade Formicidae' in the text. Crown Formicidae exclusively refers to the extant subfamilies of ants and their stem groups, not including any of the aforementioned taxa. Within the crown group, 'Leptanillomorpha' refers to Leptanillinae + Martialinae, 'Poneroformicines' to crown ants excluding Leptanillomorpha, and 'Formicomyrmines' to Formicinae + (Ectatomminae *sensu lato* + Myrmicinae). Crown Formicidae are either referred to as 'Formicidae', or specifically as 'crown Formicidae'.

Cephalic Morphology of †*Gerontoformica gracilis*

Overall Preservation/Taphonomy

The fossil (about 5 mm body length) shows an astonishing level of preservation of soft tissue. Muscles, gland tissue, the central nervous system, and the cephalic digestive tract are very clearly recognizable

(Fig. 2). The structures show a minimal degree of shrinkage indicated for instance by the very densely arranged muscle fibers (insect muscle fibers usually separate upon shrinkage) (Fig. 2D). Fine histological details of several tissues are documented in the μ-CT scan, such as individual cells of the mandibular gland (Fig. 2A), individual brain regions (Fig. 2A, B, and E), and sarcomeres of the musculature (Fig. 2D and E). That some structures are not fully preserved or cannot be recognized in their fine details is mostly due to large bubbles within the cephalic lumen, possibly consisting of amber, as the contrast of these bubbles is very similar to that of the surrounding medium in X-ray tomographic images (Fig. 2D–F). As the bubbles are located in the ventral head region and, on one side, also dorsally and laterally, they displace most of the external muscles of the maxillolabial complex, part of the mandibular muscles and the posterior cephalic digestive tract. Additionally, they cause a shift and rupture of the central nervous system. Some structures not located in these regions are not entirely preserved, possibly due to decay prior to complete dehydration and fixation in resin. Therefore, it cannot be excluded that some soft parts completely disappeared even in regions not affected by the large bubbles. Nevertheless, the overall preservation is exceptional and allows the reconstruction of most internal structures, including an almost complete set of muscles with limited loss of information compared to extant ant workers.

Head Capsule

The head of the reconstructed specimen is held in an orthognathous position, with the mouthparts directed ventrad relative to the longitudinal body axis (Fig. 1B and C). As described in the Character section (Char. 1), we devised a measurement angle intended to capture 'anatomical head orientation', to evaluate the degree of prognathism in this ant. Our evaluation resulted in an angle of 82° but is complicated by the incomplete preservation of the postocciput. The head capsule is 0.83 mm long from the anterior clypeal margin to the hind margin of the head in dorsal (full face) view and reaches its maximum width of 0.85 mm between the compound eyes; it appears broadly oval in dorsal view, slightly widening posteriorly (Fig. 3A); in lateral view, the anterior cephalic region at the level of the clypeus is moderately flattened, and the remaining head is bulbous (Fig. 3C). The **occipital region** on the ventral side of the head is deeply concave (occ, Fig. 3B). In the center of the concavity, the collar-shaped **postocciput** (poc, Fig. 3B) surrounds the **occipital foramen** (ocf, Fig. 3B); its anterior arch is cup-shaped, and the dorsal arch is very short and straight (this part of the structure is only partly preserved); the occipital region directly surrounding the foramen is deeply countersunk into a triangular depression; especially the region directly anterad the postocciput is deeply sunk into a **subforaminal groove** (sfg, Fig. 3B); the occipital region is delimited by an **occipital carina** (oca, Fig. 3B) that forms a semi-circular arch posteriorly and extends straight, slightly converging anteriorly onto the ventral side of the head without closing anteriorly. The ventral head sclerotization is formed by a **postgenal bridge** (pgb, Fig. 3B) slightly more than half as long as the entire head capsule. The roughly trapezoidal **clypeus** (cl, Figs. 1C and 3A, C, and G) appears evenly convex in lateral view and so does its anterior margin in dorsal view; the latter is set with a row of short, stout **chaetae** ('traction setae') (preserved only on one side) (clc, Fig. 3A, C, and G); the lateral edges of the clypeus project as triangular **clypeal lobes** (clp, Fig. 3A and G) beyond its anterior margin, covering the mandibular bases; the clypeus is deeply inflected; the oral margin carrying the labrum is concealed by the extended anterior margin; the anterior surface of the **clypeal inflection** (cli, Fig. 3F) is deeply concave; the posterior clypeal
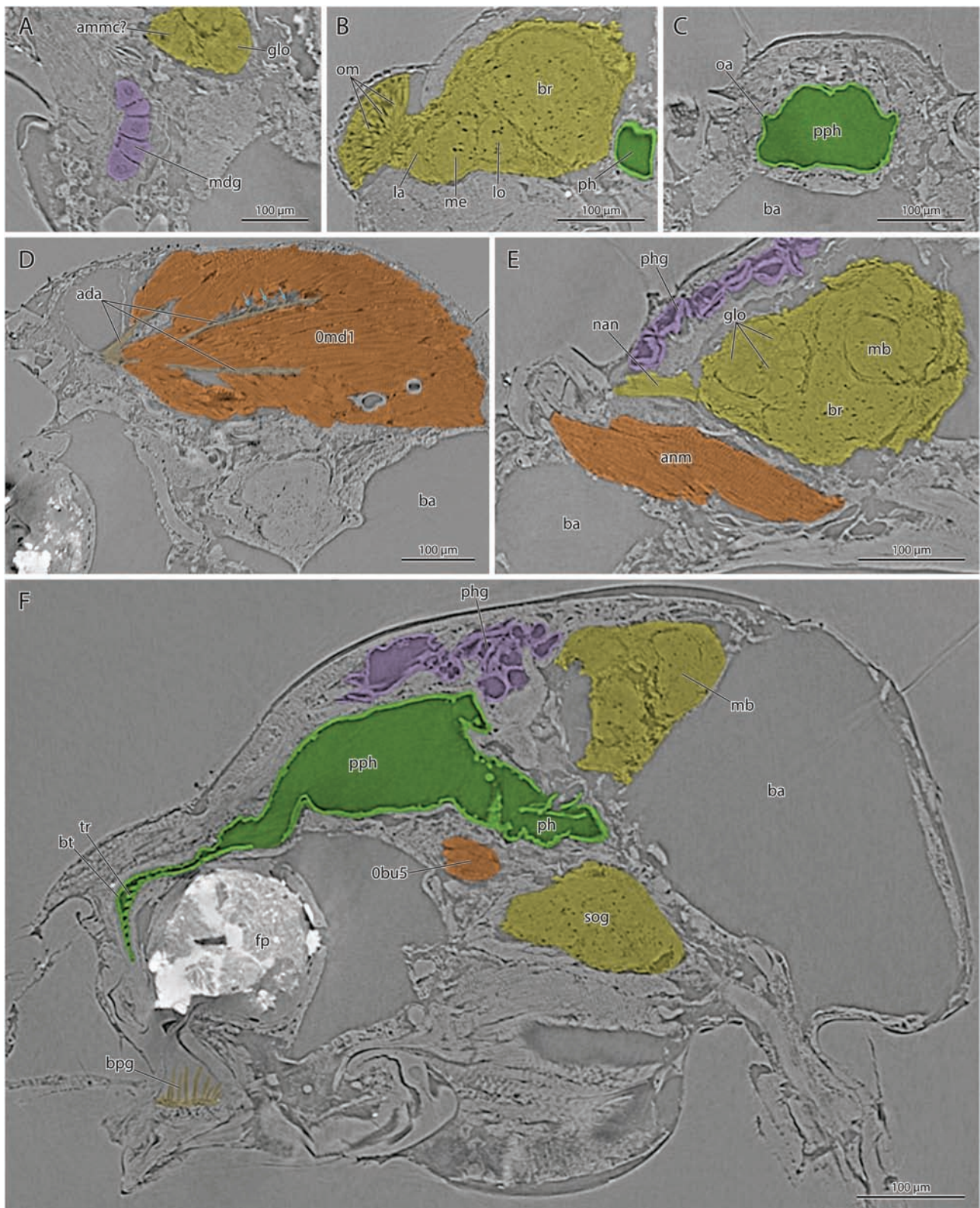
Fig. 2. Slices of the μ-CT dataset showing histological preservation in the head of †*Gerontoformica gracilis* specimen CASENT0741232. (A) Frontal section showing the cells of the mandibular gland. (B) Transverse section showing the optic neuropils of the brain. (C) Transverse section showing the prepharynx slightly posterad the antennal insertions. (D) Frontal section showing the mandibular adductor, arrows indicating the only possible cuticular filaments. (E) Longitudinal section showing antennal muscles, olfactory lobes, and part of the pharyngeal gland. (F) Overview of sagittal section. Abbreviations: **0bu5,** *M. tentoriobuccalis,* only fragments preserved; **0md1,** *M. craniomandibularis internus*; **ada**, adductor apodeme; **ammc?**, likely the antennal mechanosensory and motor center; **anm**, antennal musculature; **ba**, amber 'bubble' displacing tissue; **bpg**, basiparaglossal brush; **br**, brain; **bt**, buccal tube; **la**, lamina; **lo**, lobula; **mb**, mushroom body; **me**, medulla; **nan**, antennal nerve; **glo**, glomeruli of the olfactory lobe; **mdg**, mandibular gland; **om**, fold representing the oral arm; **om**, ommatidia of the compound eye; **ph**, pharynx; **pph**, prepharynx; **sog**, suboesophageal ganglion; **tr**, transverse prepharyngeal ridges. Colors: **beige/brown,** cuticular structures (ada & bpg); **green,** alimentary canal; **orange,** muscles; **purple,** glands; **yellow,** nervous system.

Fig. 3. 3D reconstructions of the head of †*Gerontoformica gracilis* specimen CASENT0741232, showing external and internal skeletal elements. (A and D) Dorsal view. (B and E) Ventral view. (C) Lateral view. (C′) Dorsolateral view of the torulus. (F) Sagittal view. (G) Frontal view of the oral foramen of the head capsule. (A–C) Complete head. (D–F) Internal skeleton. (H) Labrum outer surface. (I) Labrum inner surface. Abbreviations: **alf**, atalar fossa; **ant**, antennifer; **ata**, anterior tentorial arm; **atp**, anterior tentorial pit; **bb**, bulbus; **bbn**, bulbus neck; **ce**, compound eye; **cl**, clypeus; **cli**, clypeal inflection; **clp**, clypeal process; **clc**, clypeal chaetae; **cor**, circumocular ridge; **dma**, dorsal mandibular articulation; **dta**, dorsal tentorial arm; **ess**, epistomal sulcus; **esr**, epistomal ridge; **fc**, frontal carina; **fr**, frontal area; **hc**, cardinal condyle of hypostoma; **hygl**, lateral hypostomal groove; **hygm**, medial hypostomal groove; **hyp**, hypostomal triangular process; **hysci**, inner hypostomal carina; **hyscor**, oral hypostomal carina; **hyscou**, outer hypostomal carina; **hyt**, hypostomal corner; **ll**, lateral tentorial lamella; **lbre**, outer labral surface; **lbri**, inner labral surface; **ltra**, transverse row of labral setae; **md**, mandible; **ml**, medial tentorial lamella; **oc**, ocellus; **oca**, occipital carina; **occ**, occipital area; **ocf**, occipital foramen; **pgb**, postgenal bridge; **pgr**, postgenal ridge; **plb**, labial palp; **pmx**, maxillary palp; **poc**, postocciput; **pta**, posterior tentorial arm; **sc**, scapus; **sfg**, subforaminal groove; **st**, stipes; **tb**, tentorial bridge; **tba**, tentorial bridge anteriomedian process; **to**, torulus; **toi**, inner torular rim; **vma**, pleurostomal fossa. Symbols: **blue line**, epistomal sulcus.

margin does not reach the area between the antennal insertions (Fig. 3A); the **epistomal sulcus** is present (indistinct externally on 3D-reconstructions but clearly visible on photographs) (**ess**, Figs. 1C

and 3A). A **supraclypeal area** ('frontal triangle') is not differentiated. The semicircular **frontal carinae** surround the antennal insertions medially and dorsally (fc, Fig. 3A, C, and G), forming a complete

half circle; they do not form **frontal lobes**; the area enclosed by them is slightly countersunk and contains the antennal sockets; a deep groove containing the antennal scapus is visible dorsad the antennal insertion and above the compound eye on one side of the head (very likely a taphonomic artefact) (Fig. 3A). The simple ring-shaped **toruli** (**to**, Fig. 3A, C, and G) are directed dorsolaterad due to the bulging **frontal area** between them (Fig. 3G); their lateral arches are relatively high, nearly barrel-shaped; they are located close to the epistomal sulcus but clearly separated from it by about one **torulus** length (Fig. 1C); they are separated from each other by about a third of the head width (Fig. 3A) and lack the interior torular apodemes based on our reconstruction (Fig. 4F). The oval **compound eyes** are strongly convex, distinctly protruding beyond the surrounding areas (**ce**, Figs. 1C, and 3A–C and G); they contain ca. 200 ommatidia with slightly convex corneal lenses. Three very small **ocelli** are present on the dorsoposterior surface of the head (**oc**, Fig. 3A and F). The hypostomal area is complex: the **outer hypostomal carina** (**hysc**$_{ou}$, Fig. 3B, F, G) is the externally visible ridge that surrounds the hypostomal area ventrally and separates it from the postgenal bridge; it is distinctly raised above the surrounding cuticle; its anterior tips are extended into rounded **hypostomal corners** (**hyt**, Fig. 3B); in frontal view, the hypostomal surface is delimited by the outer hypostomal carina ventrally, the **hypostomal oral margin** (**hysc**$_{or}$, Fig. 3G) dorsally, and the pleurostomal fossae of the ventral mandibular articulation (**vma**, Fig. 3G) laterally; the lateral parts of the hypostomal surface are extended into very broad **triangular hypostomal processes** (**hysp**, Fig. 3F and G); the medial margins of the processes form **inner hypostomal carinae** (**hysc**$_i$, Fig. 3G) that are joined in the midline of the head close to the outer carina; these inner carinae separate the hypostomal surface into paired **lateral hypostomal grooves** (**hyg**$_i$, Fig. 3G), delimited by the hypostomal processes and outer and inner hypostomal carinae and the unpaired **medial hypostomal groove** (**hyg**$_m$, Fig. 3G) that is delimited by the hypostomal oral margin and the inner hypostomal carinae; the medial groove contains the base of the maxillolabial complex and the lateral grooves contain the lateral margins of the maxillary stipites when the mouthparts are retracted; the maxillary cardines are inserted in the deep **cardinal notches** between the hypostomal processes and the **cardinal condyles of the hypostoma**, which articulate with the bases of the cardines; the **hypostomal corners** are located between the tips of the hypostomal processes and the pleurostomal fossae. A secondary hump close to the pleurostomal fossa is not developed.

The cuticle appears mostly smooth (Fig. 1C–E); it bears a regular vestiture of short setae (ca. 20–30 µm on clypeus); the coloration is brownish, ranging from light orange to a very dark, almost black tone.

Endoskeleton

The long **anterior tentorial arms** (**ata**, Fig. 3D–F) extend diagonally through the cephalic lumen (note that portions are not well preserved, especially in the center of the left arm where there is a sinuous, very thin region that is likely an artefact); the **anterior tentorial pits** (**atp**, Fig. 3A) are located slightly anterolaterad the antennal sockets, distinctly separated from them. **Lateral** and **medial tentorial lamellae** (**ll**, **ml**, Fig. 3D–F) apparently form expanded lobes surrounding the anterior arm, serving as areas of origin for antennal and maxillary musculature (note: these lamellae are visible in the middle head region but only fragments are preserved, so their exact shape cannot be reconstructed; presence of the lamellae can partly be inferred from presence of muscle fibers, but this part is excluded from the reconstructed images). The **posterior arms** (**pta**, Fig. 3D–F) are very short.

The **tentorial bridge** (**tb**, Fig. 3D–F) (asymmetric shape likely due to deformation) is slightly arched upwards by about the height of the anterior arms and bears a triangular anteromedian process. The **dorsal tentorial arms** (**dta**, Fig. 3D and F) are very thin and short (possibly incompletely preserved). **Posterior tentorial processes** are not visible (possibly not preserved), and a **secondary tentorial bridge** is absent. A well-developed, wall-shaped **postgenal ridge** (**pgr**, Fig. 3F) is present mesally on the ventral side of the head along the whole length of the **postgenal bridge**. The **torulus** forms an internal barrel-shaped ring similar to the external one (**toi**, Fig. 3F); a **torular apodeme** is missing. The flat but distinct **epistomal (clypeofrontal) ridge** (**esr**, Fig. 3F) delimits the straight posterior margin of the clypeus.

Labrum

The broad, trapezoidal, and plate-like **labrum** (Fig. 3H and I) articulates with the inflected ventral clypeal edge (**cli**, Fig. 3F) and is directed directly downward at closure (preserved in closed position); its distal margin is almost straight; **proximolateral labral processes** (labral arms) could not be identified (proximolateral parts not entirely preserved; see Fig. 3I). Short, stout setae (potentially **chaetae**) are inserted in a distinct **transverse line** across the **external labral surface** (**ltra**, Fig. 3H); base of the labrum forms a transverse 'hump' with its apex along this transverse line (see, e.g., Fig. 5C and G for labrum in transverse view); several setae of varying length (likely not all entirely preserved/reconstructed) are present on the labral surface distad the transverse line.

Musculature: *M. frontoepipharyngalis* (M. 9/0bl2): A large muscle (Fig. 6A); **O** (= origin): in an elongated longitudinal frontal area directly mesad the frontal carina (Fig. 6C); **I** (= insertion): not visible (tendon not entirely preserved).

Antenna

The geniculate **antennae** consist of 12 antennomeres (Fig. 1D). They are almost half as long as the entire body (Fig. 1B). The **bulbus** is semi-spherical and almost completely visible externally (**bb**, Figs. 1C and 3A); it articulates with a long, thin **antennifer** (**ant**, Fig. 3C′) and rests in a flat acetabulum formed by the barrel-like torulus; the narrow and straight **bulbus neck** (**bbn**, Fig. 3A) is placed on the posterior surface of the bulbus. The **scapus** almost reaches the posterior margin of the head but makes up only about one fifth of the very long antenna (**sc**, Fig. 1B and D); its anterior margin is roundly notched to accommodate the base of the pedicel, resulting in formation of distolateral shoulders of the scapus framing the lateral pedicel base (**sc**, Fig. 4C′). The base of the **pedicel** is dorsoventrally flattened ('pinched' appearing in medial or lateral view) and curved anterad (**pd**, Fig. 4C′) into the distal notch of the scapus; it is overall slightly shorter and thicker than the first flagellomere, which is the longest; the other cylindrical flagellomeres are of similar length and width (Fig. 1D). The surface of the flagellomeres is regularly, but not very densely covered by a vestiture of erect setae; details on the sensilla could not be observed based on our data (Fig. 1D).

Musculature (Figs. 2E and 4A–C): four intrinsic scapus muscles (0an1–4) are present but very close to each other (only three of them could be clearly identified on one side). The homologization is based on the relative position to each other and the site of origin (most tendons are not preserved; the site of origin is partly an inference as the tentorium is only partly preserved in the relevant region). *M. tentorioscapalis anterior* (M. 1/0an1): **O**: on anterior half of anterior tentorial arm; **I**: not visible (tendon not preserved or not recognizable). *M. tentorioscapalis posterior* (M. 2/0an2): **O**: posterior part of medial tentorial lamella (only partly preserved); **I**: not visible (tendon not preserved or not recognizable). *M. tentorioscapalis lateralis*
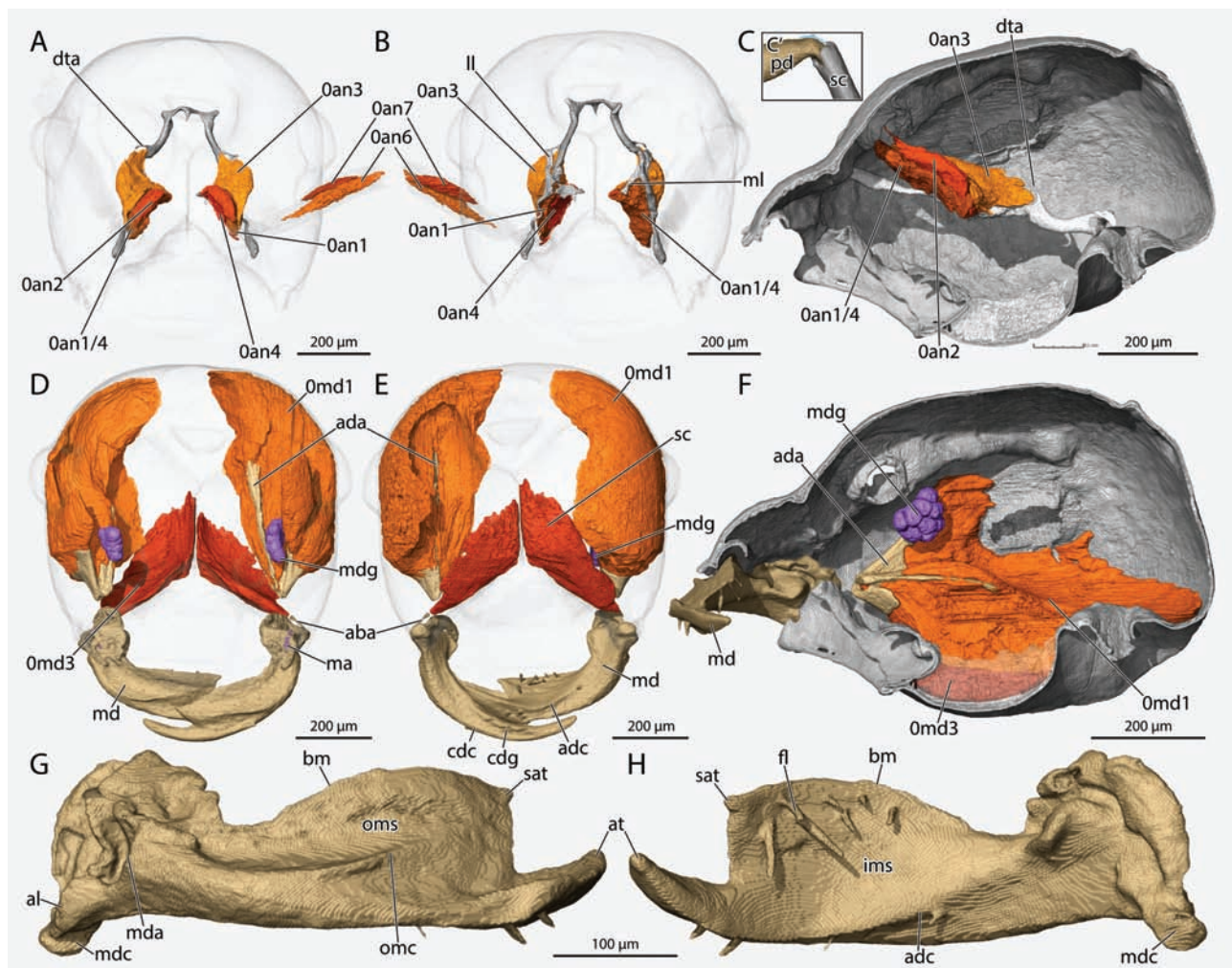
Fig. 4. 3D reconstructions of the head of †*Gerontoformica gracilis* specimen CASENT0741232, showing skeleton and musculature of mandible and antenna. (A and D) Dorsal view. (B and E) Ventral view. (C and F) Sagittal view. (G) Outer view. (H) Inner view. (A–C) Antennal musculature. (D–F) Mandibular musculature and mandibular gland. (G and H) Mandible. Abbreviations: **0an1**, *M. tentorioscapalis anterior*; **0an2**, *M. tentorioscapalis posterior*; **0an3**, *M. tentorioscapalis lateralis*; **0an4**, *M. tentorioscapalis medialis*; **0an6**, *M. scapopedicellaris lateralis*; **0an7**, *M. scapopedicellaris medialis*; **0md1**, *M. craniomandibularis internus*; **0md3**, *M. craniomandibularis externus*; **aba**, abductor apodeme; **ada**, adductor apodeme; **adc**, adductor carina; **al**, atala; **at**, apical tooth; **bm**, basal margin; **cdc**, condylar carina; **cdg**, condylar groove; **dta**, dorsal tentorial arm; **fl**, fimbriate line; **ims**, inner mandibular surface; **ll**, lateral tentorial lamella; **ma**, mandalus; **md**, mandible; **mda**, mandibular acetabulum; **mdc**, mandibular condyle; **mdg**, mandibular gland; **ml**, medial tentorial lamella; **omc**, outer mandibular carina; **oms**, outer mandibular surface; **pd**, pedicel; **sat**, subapical tooth; **sc**, scapus. Symbols: **blue line**, basal curvature of pedicel.

(M. 3/0an3): **O:** anterior tentorial arm posterad 0an1, lateral tentorial lamella and likely part of medial lamella laterad 0an2 (muscle boundaries not clearly defined) and also at least base of the dorsal tentorial arm; **I:** not visible (tendon not preserved or not recognizable). *M. tentorioscapalis medialis* (M. 4/0an4): **O:** medial tentorial lamella anterad 0an2; **I:** not visible (tendon not preserved or not recognizable). The two intrinsic muscles of the scapus are well preserved in one antenna (other antenna distinctly flattened) *M. scapopedicellaris lateralis* (M. 5/0an6): **O:** dorsal side of scapus; **I:** not visible (tendon not preserved or not recognizable) but inferring from the fiber direction dorsally on the pedicel. *M. scapopedicellaris medialis* (M. 6/0an7): **O:** ventrolaterally on the scapus; **I:** not visible (tendon apparently not preserved) but following the fiber direction ventrally on the pedicel.

Mandibles

The **mandibles** are sickle-shaped and curved inward, with a stronger curve close to the mandibular base (md, Fig. 4D); their

tips are overlapping in the resting position; from lateral view the mandible is straight, with only a minimal downward curve of the apical part relative to the base (Fig. 1D, see also Fig. 4F). The medial edge/margin of the mandible between its base and the tip of the apical incisor is the **gnathal edge/margin**. (Note: we term here the gnathal portion between mandible base and subapical tooth as 'basal margin' and the portion between apical and subapical tooth as 'masticatory margin'). The **basal margin** terminates at the medial mandible base, right above the insertion area of the adductor apodeme; the proximal part of the mandible is thin, with the basal margin concave in dorsofrontal view (Fig. 4G); its middle portion is much broader, with the broadly convex basal margin terminating in the wide subapical tooth. The **masticatory margin** encompasses only two teeth; the very long **apical tooth** is thin and pointed; on its ventral side it bears the **condylar carina** which marks the ventral margin of the mandible starting at the **mandibular condyle** and ending on the tooth (**cdc**, Fig. 4E); the carina is accompanied by a **condylar groove** with a line of hairs along it (**cdg**, Fig. 4E);

the broadly triangular **subapical tooth** (**sat,** Fig. 4G and H) is distinctly dorsoventrally flattened, together with the entire mesal part of the blade, thus appearing as a thin plate in sagittal view (Fig. 4F); the center of the subapical tooth is stabilized by a carina on the outer side of the mandible, which reaches from the mandibular acetabulum to almost the tip of the tooth and is here termed the **outer mandibular carina** (**omc,** Fig. 4G); between the apical and subapical tooth a flat groove is developed, reaching to the acetabulum; alternatively, this can be described as 'interspace' rather than groove as it encompasses the broad and flat space between outer and condylar carina. The mandibular base is only slightly broader than the proximal part of the blade in dorsal view (Fig. 4D). The secondary (dorsal) articulation is enlarged, with a dorsoventrally elongated **clypeal condyle**, reaching up to about mid-height of the mandible (**dma,** Fig. 3C, G), and a correspondingly expanded **mandibular acetabulum** (**mda,** Fig. 4G). The **mandibular condyle** of the primary (posterior) articulation is a short process with a bulbous tip (**mdc,** Fig. 4G and H), inserted deeply into a small acetabulum of the head capsule (**pleurostomal fossa**) (**vma,** Fig. 3G). A distinct **atala** is not developed; the lateral margin of the mandibular base is only slightly convex (**al,** Fig. 4G), resting in a slightly concave area of the head capsule between the primary and secondary mandibular articulation (**alf,** Fig. 3G). The **mandalus** (**ma,** Fig. 4D) (not very clearly recognizable on the µ-CT scans and thus only roughly reconstructed) with the duct of the **mandibular gland** (**mdg,** Figs. 2A, and 4D and F) is located laterally on the dorsal side of the mandibular base (a U-shaped groove visible directly distad the mandalus on one mandible is likely an artifact). On its inner surface, the mandible bears a longitudinally oriented field of thick setae close to the basal margin on the flattened part of the blade, representing the **fimbrial line** (**fl,** Fig. 4H). A carina obliquely runs across the inner surface, connecting the insertion region of the adductor apodeme and the tip of the apical tooth, thus termed **adductor carina** (**adc,** Fig. 4H); it forms the inner border of the condylar groove on the ventral margin of the mandible.

Musculature (Fig. 2D; 4 D–F): *M. craniomandibularis internus* (M. 11/0md1): largest cephalic muscle. Based on the µ-CT scan data, two different types of fibers appear to be present in the muscle. In some fibers, sarcomeres are clearly visible. The average sarcomere length of these fibers is 3.6 µm (min = 3 µm, max = 4.4 µm, *n* = 106 sarcomeres), although a few fibers have short regions of much longer sarcomeres (up to 7.2 µm, possibly a preservation artifact as these are restricted to short fragments of the fibers) (see Supp File S2 [online only]). In the central region of the muscle, fibers without any visible sarcomeres occur, indicating that these are a different type with much shorter sarcomeres (although regions without visible sarcomeres also occur in some of those fibers with visible sarcomeres, indicating that this may also be a preservation effect) (Fig. 2D). O: very large part of the ventral, lateral and posterior internal surface of the head capsule (muscle partly dislocated by bubbles); I: large apodeme (distal part normally connected to the mandibular base not preserved); the distal part of the preserved apodeme is halfcone-shaped laterally; from it expand short dorsolateral and ventral sheets; additionally, a longer sheet-like branch emerges from it centrally; an additional accessory branch emerges from the central branch (visible on one side of the head); it connects to a bundle of fibers originating dorsad the occipital foramen (attachment region of the muscle is partly affected by dislocation). The fibers of the muscle are directly inserted onto the large apodeme and its branches, even though some fibers may be indirectly attached via very short cuticular fibrillae (blue arrows Fig. 2D, possibly artefactual). *M. craniomandibularis externus* (M. 12/0md3): distinctly flattened on both sides (at least partly due to displacement by

bubbles); O: ventral head capsule and most of the postgenal ridge; I: tendon connected to slightly convex lateral mandibular margin (**aba,** Fig. 4D and E) (identified on one side). *M. tentoriomandibularis* (M. 13/0md8): not visible (probably not preserved).

Maxillae

The **maxillolabial complex** (largely extended in the reconstructed specimen, Figs. 1B–D, and 3B and C) consists of the maxillae, labium, and distal hypopharynx; the distal hypopharynx is completely fused to the prementum; stipes and prementum are connected by a ligament ("stipito-premental conjunctiva"), and cardines and postmentum by conjunctiva. The whole complex is connected to the head capsule by conjunctiva and through the maxillary cardines. The **cardo** is a rod with a T-shaped proximal end and a roughly club shaped and widening distal part (**cd,** Fig. 5D); even in the partly extended position, it is completely contained within the wide hypostomal groove (Fig. 5C and G); the medial base of the cardo articulates with the hypostomal cardinal condyle (**hc,** Fig. 3G). The **external stipital sclerite** (**st,** Fig. 5D–E) is ovoid, with a broader lateral side; no distinct process or shoulder is developed distally; its medial margin is formed by a carina extending beyond the stipital body and slightly bent outwards, the **median stipital flange** (/principal carina of the stipes) (**msf,** Fig. 5D and E); the stipes does not bear a groove, and its external surface is very slightly convex overall. The **maxillary palp** (**pmx,** Figs. 1C and 5D–F), inserted on the distalmost tip of the stipes, is six-merous and almost as long as the head capsule; **palpomere 1** is angled basally, club-shaped with a broadened distal end, and flattened; **palpomere 2** is similar in its general shape, but without the basal angle and longer and narrower (Fig. 5D–F); the following palpomeres are thin, long, and cylindrical, but also slightly broader distally (Fig. 1C); all palpomeres bear long setae that appear to be sparsely set based on our photographs (Fig. 1C and D). The **galea** is shaped as a rounded, long rectangle; the reconstructed part is about as long as palpomeres 1 and 2 combined and is only slightly bent downward distally; it bears the **maxillary comb** on its ventral side (**mxc,** Fig. 5D and E) with a row of closely set setae (only partly reconstructed on left maxilla and not preserved on right maxilla). The **lacinia** is present but only partly recognizable (**lc,** Fig. 5E and F) (not well preserved, apparently ripped from the galea and only a small fraction visible on µ-CT scan).

Musculature (Fig. 5A–C and G): *M. craniocardinalis externus* (M. 15/0mx1): O: head capsule close to the occipital foramen, but exact attachment site unclear (muscle displaced by bubble); I: with a long tendon on the lateral proximal end of the cardo. *M. tentoriocardinalis* (M. 17/0mx3) or *M. tentoriostipitalis posterior* (0mx5): only partly preserved on one side of the head (Fig. 5G); O: not preserved; I: area of the cardinostipital hinge but exact site of insertion not visible. *M. tentoriostipitalis* (M.18)/*M. tentoriostipitalis anterior* (0mx4): only preserved on one side, only one bundle visible; O: ventrally on the medial tentorial lamella; I: medial stipital wall, internal sclerite of the stipes. *M. stipitolacinialis* (M. 20/0mx6): well-preserved; O: laterally on the external stipital sclerite, along most of its length; I: lacinia (precise site unclear due to partial preservation of lacinia). *M. stipitogalealis* (M. 21/0mx7): fills out most of the stipes; O: proximally on the external stipital sclerite; I: with a short tendon proximolaterally on the galea. *M. stipitopalpalis externus* (M. 22/0mx8): very small (not well preserved); O: proximally on the external stipital sclerite; I: on the base of palpomere 1. *M. palpopalpalis maxillae primus, secundus, etc.* (M. 24, 25, 26, 27/0mx12, 13, 14, 15): the internal musculature of the maxillary palp is not preserved.
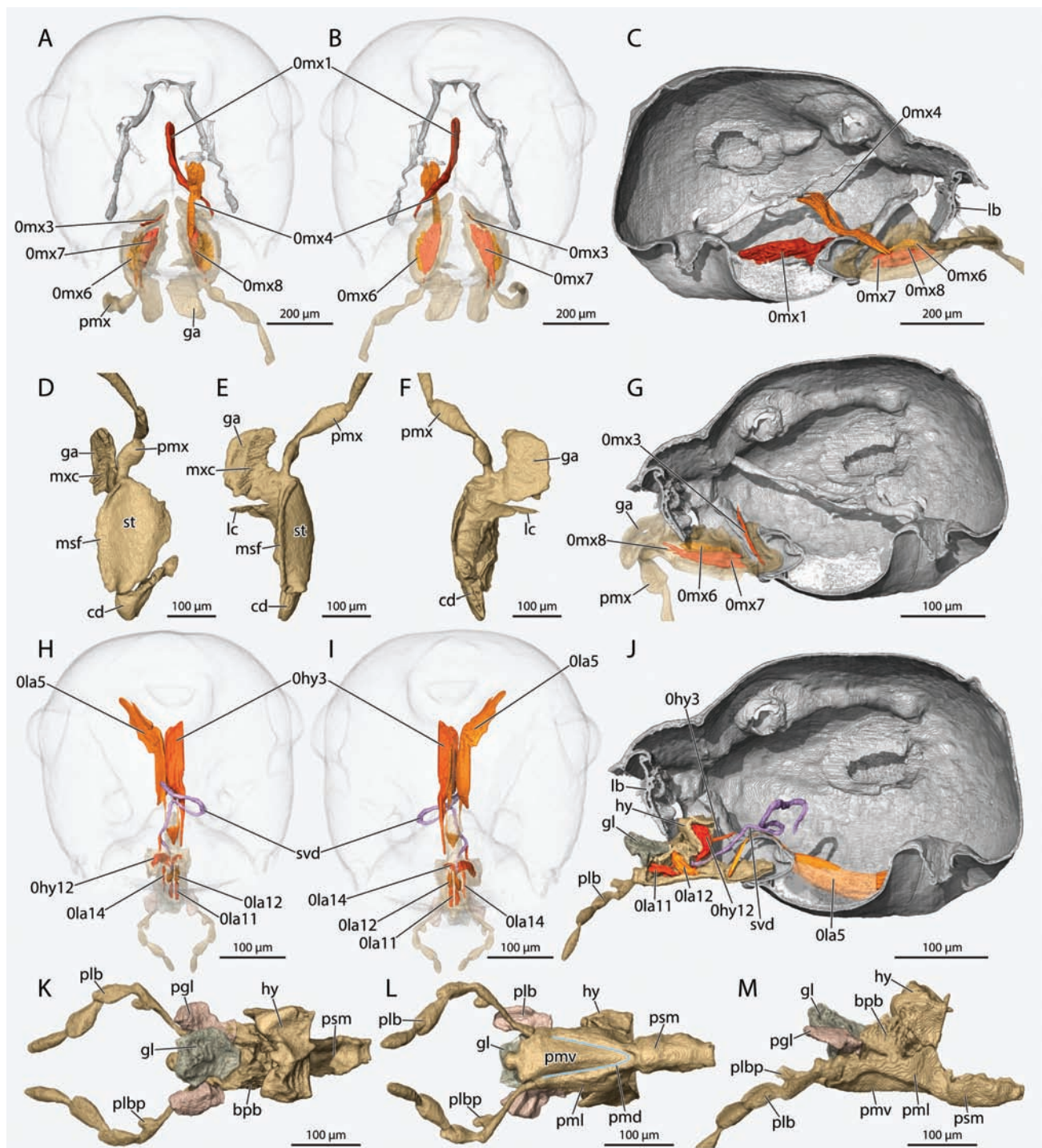
Fig. 5. 3D reconstructions of the head of †*Gerontoformica gracilis* specimen CASENT0741232, showing skeleton and musculature of maxilla and labium. (A, F, H, and K) Dorsal view. (B, E, I, and L) Ventral view. (C, G, and J) Sagittal view, in (C) the left instead of right side of the head is shown. (D) Frontal view. (M) Lateral view. (A–C and G) Maxillary musculature. (D–F) Maxilla. (H–J) Labial musculature and salivary duct. (K–M) Labium. Abbreviations: **0hy3**, *M. tentoriohypopharyngalis*; **0hy12**, *M. hypopharyngosalivaris*; **0la5**, *M. tentoriopraementalis*; **0la11**, *M. praementoparaglossalis*; **0la12**, *M. praementoglossalis*; **0la14**, *M. praementopalpalis externus*; **0mx1**, *M. craniocardinalis externus*; **0mx3**, *M. tentoriocardinalis*; **0mx4**, *M. tentoriostipitalis anterior*; **0mx6**, *M. stipitolacinialis*; **0mx7**, *M. stipitogalealis*; **0mx8**, *M. stipitopalpalis externus*; **bpb**, basiparaglossal brush; **cd**, cardo; **ga**, galea; **gl**, glossa; **hy**, distal hypopharynx; **lb**, labrum; **lc**, lacinia; **msf**, medial stipital flange; **mxc**, maxillary comb; **pgl**, paraglossa; **plb**, labial palp; **plbp**, process of the labial palp; **pmd**, premental ditch; **pml**, prementum lateral face; **pmv**, prementum ventral face; **pmx**, maxillary palp; **psm**, postmentum; **st**, stipes; **svd**, salivary duct. Symbols: **blue line**, premental ditch.

Labium and Distal Hypopharynx

The **labium** appears narrow and elongated; this applies to the **postmentum** (**psm**, Fig. 5K–M) with the conjunctiva connecting it to the prementum and head capsule and also the elongated oval, almost triangular **prementum** (**pm**, Figs. 3B and 5L); the **ventral premental face** (**pmv**, Fig. 5L and M) with a pointed base and truncated distal margin is distinctly convex and raised relative to the **lateral premental surface** (**pml**, Fig. 5L and M); the truncated distal

margin apparently bears a round, bell-shaped structure (likely an artifact caused by a bubble as suggested by its appearance in the μ-CT dataset); the **premental arms** are present (indistinct due to insufficient preservation) and stabilize the **distal hypopharynx** (**hy**, Fig. 5M), which forms the dorsal surface of the proximal labium. The distal hypopharynx is short and raised high above the labial level. The **basiparaglossal brushes** (**bpb**, Figs. 2F, and 5K and M) are visible distad the hypopharynx; their bases are continuous with well-developed, lobe-like, and irregularly shaped **paragossae** (**pgl**, Fig. 5K–M) (most likely with deformed soft parts). The **glossa** located between the paraglossae is also well-developed and of similar length (**gl**, Fig. 5K–M). The **labial palps** are four-segmented and about as long as the rest of the labium (**plb**, Figs. 1C and 5J–M); **palpomere 1** is long, thin, and cylindrical; it bears a distinct rounded mesal process close to its distal end (blue arrow Fig. 1C; **plbp**, Fig. 5K–M); **palpomeres 2** and **3** are flat, broad, and spatulate; **palpomere 4** is slightly shorter than 3 and fusiform.

Musculature (Fig. 5H–J): *M. tentoriopraementalis* (M. 29/0la5): mostly preserved on one side, about half of it preserved on the other; **O**: posterior head capsule laterad the occipital foramen (exact point of origin unclear due to displacement by bubble); **I**: the tendons of both sides fuse and the broad unpaired apical part inserts on the proximal margin of the prementum. *M. praementoparaglossalis* (M. 31/0la11): **O**: median premental region, distad 0la12; **I**: area of the ventral/distal margin of the glossa (likely on ventral glossal sclerite which is not preserved). *M. praementoglossalis* (M. 32/0la12): **O**: on the prementum proximad 0la11; **I**: dorsal margin of the glossa, dorsal glossal sclerites. *M. praementopalpalis externus* (M. 34/0la14): **O**: on the proximolateral surface of the prementum laterad 0la12; **I**: base of labial palpomere 1. *M. palpopalpalis labii primus/secundus* (M. 35/36 0la16/17): not clearly recognizable (not sufficiently preserved). *M. tentoriohypopharyngalis* (M37/0hy3): only partly preserved on one side; **O**: unclear but likely posterior head capsule (attachment area not preserved); **I**: with long tendon on hypopharynx (only tip of tendon preserved on one side, exact point of insertion not visible, Fig. 5J). *M. praementosalivaris anterior* (M38/0hy7): absent. *M. hypopharyngosalivaris* (M42/0hy12): **O**: hypopharynx, likely on hypopharyngeal sclerite (but this is not preserved); **I**: dorsally on the salivary duct close to the salivarium.

Digestive Tract

The cephalic digestive tract is subdivided into the buccal cavity, prepharynx, and pharynx. The **buccal cavity** is enclosed by the **distal epipharynx** (**ep**, Fig. 6D) on the dorsal side and the **distal hypopharynx** (**hy**, Fig. 6D) ventrally, both not fused along their lateral margins, thus leaving this space open laterally. Part of the buccal cavity is the **infrabuccal pouch**, a pocket formed by the hypopharynx between its distal portion above the labium and the prepharynx (**ibp**, Fig.6D); the pouch appears large and is filled with a refuse pellet (**fp**, Figs. 2F and 6D, no individual food items could be identified, but the material is heterogeneous). The free distal epipharyngeal part (only partly preserved) forms a distinct lobe. The laterally closed **prepharynx** (**pph**, Figs. 2C and F, and 6A and D–F), a tube formed by the fusion of the proximal epipharyngeal and hypopharyngeal portions is almost entirely preserved, but not the **functional mouth**, the distal end of the fusion. The distal part of the prepharynx is very flat and approximately crescent-shaped in cross section, forming the **buccal tube** (**bt**, Figs. 2F, and 6D and F); its posterior (hypopharyngeal) wall is set with thick transverse ridges (**tr**, Fig. 2F), which are ca. 5 μm high, angled toward the functional mouth opening and extending over the entire width of the buccal tube; it is bent relative to the remaining

prepharynx, both forming an angle of about 70°. Compared to the buccal tube, the middle region of the prepharynx has an expanded, more oval lumen, and the proximal portion close to the **anatomical mouth opening** is almost circular and expansive (Figs. 2F and 6D). The width of the prepharynx varies only slightly, with the distal buccal tube slightly wider than the proximal part close to the anatomical mouth. The insertion of *M. frontooralis* (**0hy2**, Fig. 6A) at the widest section of the cephalic digestive tract is likely closely adjacent to the **anatomical mouth**, but the main landmark, the **frontal ganglion**, is not preserved (or not recognizable in our scan data), and *M. frontobuccalis* anterior (**0bu2**, Fig. 6A and D) is only partly and very indistinctly preserved. The **oral arms**, the stabilizing sclerite rods of the prepharynx, are not preserved as distinct sclerites, but are likely represented by small folds in the prepharyngeal wall that correspond in position and orientation to the oral arms of other aculeates (see discussion) (**oa**, Figs. 2C, and 6E and F); the oral arm folds are on the lateral side of the prepharynx distally but curve onto the dorsal side proximally where they form large lobes at their proximal terminus, likely representing the oral arm processes (Fig. 6E and F, supported by insertion of *M. frontooralis* 0hy2 on these lobes, see Musculature section). The short visible portion of the **pharynx** (**ph**, Figs. 2F and 6D–F) (ruptured at the level of the brain, posterior pharynx not preserved) forms an angle of ca. 50° with the prepharynx, descending towards the occipital foramen.

Musculature (Fig. 6A–D, see Fig. 6C for most origins): The prepharyngeal musculature appears weakly developed and is only partly preserved. Statements on the probability of the presence of muscles that are not or not clearly visible (likely not preserved, possibly not preserved etc.) are based on conditions observed in extant ants. *M. clypeopalatalis* **a** (M. 43a/0ci1a): **F**: unpaired; **O**: middle region of clypeus; **I**: buccal tube, close to functional mouth. *M. clypeopalatalis* **b** (M. 43b/0ci1b): **F**: paired; **O**: distal clypeus laterad 0ci1; **I**: middle region of prepharynx, closer to functional mouth than to anatomical mouth opening. *M. clypeobuccalis* (M. 44/0bu1): **F**: paired; **O**: proximal clypeus close to epistomal ridge; **I**: central prepharyngeal region, closer to anatomical mouth, posterad 0ci1b. *M. frontobuccalis anterior* (M. 45/0bu2): **F**: unpaired, very indistinct, poorly preserved; **O**: frontal region, level of the anterior ocular margin; **I**: dorsal pharyngeal wall, between large folds likely representing the proximal oral arms. *M. frontobuccalis posterior* (M. 46/0bu3): absent (possibly not preserved). *M. tentoriobuccalis anterior* (M. 48/0bu5): only fragments visible, exact origin and insertion unrecognizable (Fig. 2F). *M. verticopharyngalis* (M. 51/0ph1): absent (preservation status unknown, posterodorsal region of cephalic lumen obscured by bubbles). *M. tentoriopharyngalis* (M. 52/0ph2): not visible (likely not preserved). *M. pharyngoepipharyngalis dorsalis* & *lateralis* (0pe1 d/l): **F**: well-developed, intrinsic longitudinal muscle of cranial digestive tract; unpaired median bundle partly preserved in central prepharyngeal region, insertion points not clearly recognizable, distal insertion likely located at level of 0ci1b insertion; paired lateral bundles broad, preserved at same level as median bundle; insertions also not clearly visible, but distal attachment site likely at similar level as median bundle. *M. frontooralis* (M. 41/0hy1): **F**: paired, well-developed; **O**: frontal area, laterad 0bu2 and further posterior, close to eye level; **I**: anteriorly on large prepharyngeal folds, conform with interpretation as oral arms. *M. tentoriooralis* (M. 47/0hy2): probably represented by short fragments preserved laterad to folds of oral arm, fragments suggesting origin on the epistomal ridge (but preservation insufficient for confident assignment, not reconstructed). *M. oralis transversalis* (0hy9) not visible (likely not preserved).
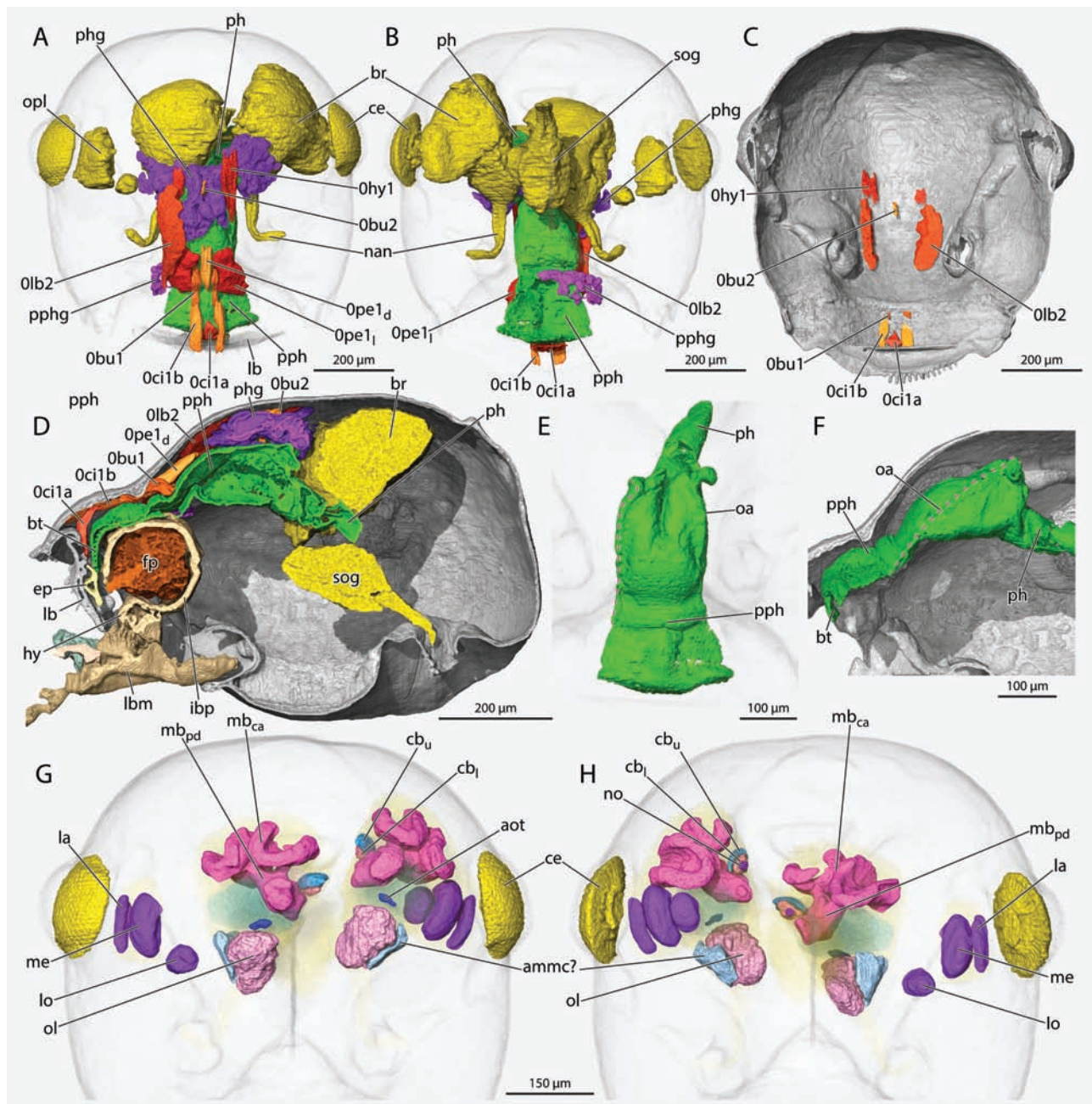
Fig. 6. 3D reconstructions of the head of †*Gerontoformica gracilis* specimen CASENT0741232, showing the digestive tract with its muscles and glands and the central nervous system. (A, E, and G) Dorsal view. (B, C, and H) Ventral view. (D and F) Sagittal view. (A, B, and D) Overview of digestive tract with muscles and glands and central nervous system. (C) Head capsule cut open to reveal origin sites of dorsal head muscles. (E and F) Prepharynx with oral arm folds. (G and H) Recognizable subregions of the brain. Abbreviations: **0ci1a**, *M. clypeopalatalis* a; **0ci1b**, *M. clypeopalatalis* b; **0bu1**, *M. clypeobuccalis*; **0bu2**, *M. frontobuccalis anterior*; **0hy1**, *M. frontooralis*; **0pe1d**, *M. pharyngoepipharyngalis* dorsal bundle; **0pe1l**, *M. pharyngoepipharyngalis* lateral bundle; **ammc?**, likely the antennal mechanosensory and motor center; **aot**, anterior optic tubercle; **br**, brain; **bt**, buccal tube; **cbl**, central body lower unit; **cbu**, central body upper unit; **ce**, compound eye; **ep**, epipharynx; **fp**, food pellet; **hy**, distal hypopharynx; **ibp**, infrabuccal pouch; **la**, lamina; **lb**, labrum; **lbm**, labium; **lo**, lobula; **me**, medulla; **mbpd**, mushroom body peduncle; **mbca**, mushroom body calyx; **nan**, antennal nerve; **no**, noduli; **oa**, oral arm fold; **ol**, olfactory lobe; **opl**, optic lobe; **ph**, pharynx; **phg**, pharyngeal gland; **pph**, prepharynx; **pphg**, prepharyngeal gland; **sog**, suboesophageal ganglion. Symbols: **dotted magenta line**, folds presumably representing the oral arms.

Brain and Suboesophageal Ganglion

The **brain** (ruptured along midline), placed in the posterior two thirds of the cephalic lumen, is moderately sized in relation to the entire head (br, Figs. 2B, E, and F and 6A, B, D, G, and H); it is distinctly separated from the wall of the head capsule (possibly due to shrinkage or displacement), with the minimum distance in the frontal region. The two halves of the brain are roughly drop-shaped, with

the large protocerebral hemispheres forming the wider posterodorsal parts, and the antennal lobes of the deutocerebrum the pointed anterior portions. The largest neuropils in the protocerebrum are the well-developed **mushroom bodies** (mb, Fig. 2E and F); they consist of the elongated, deeply cup-shaped **calyces** (mbca, Fig. 6G and H) and the thick **peduncles** (with very short and thick **mesal lobes** and slightly longer and thinner **vertical lobes**). The **optic neuropils**

are well developed; the thin, approximately cup-shaped **lamina ganglionaris** (**la,** Fig. 6G and H) appear separated from the retina, especially on the right side (as an artefact); the ellipsoid **medulla** (**me,** Fig. 6G and H) is the largest component, with a mesal concavity containing the almost spherical **lobula** (**lo,** Fig. 6G and H, strongly displaced on the right side). The central part of the protocerebrum is the **central body** (artefactually split in the middle region); it comprises two subdivisions, each crescent-shaped and closely adjacent, with the ventral part (**cb**$_l$, Fig. 6G and H) only slightly smaller than the dorsal one (**cb**$_u$, Fig. 6G and H); two-small spherical **noduli** (**no,** Fig. 6G and H) are present on the posterior side of the ventral subdivision. The **anterior optic tubercles** (**aot,** Fig. 6G) on the ventral side of the **protocerebrum** are small but clearly recognizable. The **antennal lobes** (**al,** Fig. 6G and H) of the **deutocerebrum** are also well developed; they release the long antennal nerves (**nan,** Fig. 6A and B) that strongly curve through the antennal foramina before entering the scapus; the nerves are clearly paired on each side but with closely adjacent halves. The brain forms a compact structural unit with the **suboesophageal ganglion** (**sog,** Figs. 2F, and 6B and D), leaving sufficient space for the passage of the cephalic digestive tract; the **suboesophageal ganglion** is almost as long as the brain but distinctly narrower, ca. 1/3 as wide as the **protocerebrum**; the connectives linking it with the prothoracic ganglion are closely adjacent medially but not fused. The frontal ganglion is not preserved.

Glands

The identity of the different gland cell clusters is clearly indicated by their position in the head, even though the tissue of most parts is in varying stages of decay. An exception are the cells of the **mandibular gland** (**mdg,** Figs. 2A, and 4D and E), which are exceedingly well-preserved, in contrast to the gland reservoir and duct connecting it to the mandibular lumen; nine cells are present on one side of the head and eleven on the other; the shape varies between spherical and rectangular, with a maximum diameter of about 38 μm. The **prepharyngeal gland** (**pphg,** Fig. 6A and B) is indistinctly preserved as a group of cells laterad the central portion of the tube. The **pharyngeal gland** (phg, Figs. 2E and F and 6A–C) is visible as a mass of bubble-like interconnected enclosures (likely in a state of decay, only indistinctly preserved), concentrated between the large anterior oral arm folds and continuous with two large lateral lobes above of this area. The precise shape and extent of the gland cluster could not be reconstructed due to the state of decay, but the reconstructed parts give a general impression of the overall shape.

Character Mapping

The 'mop uninformative characters' function applied in WinClada revealed 61 phylogenetically uninformative characters, which are listed in Supp File S6 (online only). To discuss these features in an evolutionary context, we retained them in the character list (see *Character List* section). The uninformative characters fall into three categories: 1) they are constant within the taxon sampling, 2) only one taxon differs from all others, or 3) most or all taxa display different states. In our mapping analysis (Fig. 7), we identified 30 unequivocal character transformations for the following clades: Apoidea (2), total clade Formicidae (7), Formicidae excl. †*Gerontoformica* (crown Formicidae) (11), Formicidae excl. *Protanilla* (Poneroformicines) (5), and (*Formica* + *Wasmannia*) (5). We did not find any apomorphies for the clade 'Vespoida', (*Parischnogaster* + *Methocha*) and (Formicidae + Apoidea). The reconstructed transformations are as follows (Fig. 7; newly defined

characters are marked by an asterisk, * and written in italics, modified ones by a tilde, ~):

Apoidea (2 characters): 2 and 24. *2: 1 › 0, loss of subforaminal groove (vs. groove present). 24: 1 › 0, toruli very close to each other (vs. at least one torulus diameter apart; homoplastic, toruli also narrowly separated in *Brachyponera*).

Total clade Formicidae (7 chars.): 25, 34, *57, *73, 79, 83, and *145. ~25: 0 › 1, frontal bulge present, resulting in more lateral orientation of antennae (vs. bulge absent). 34: 1 › 0, compound eyes reduced in size (vs. eyes large). *57: 1 › 0, dorsal tentorial arm shortened (vs. dorsal tentorial arm long). *73: 0 › 1, transverse line of setae on labrum present (vs. absent). ~79: 0 › 1, base of pedicel angled (vs straight). 83: 0 › 1, mandibular condyle elongated (vs. not or only slightly elongated). *145: 0 › 1, pharyngeal gland present in ants (vs. absent in outgroups).

Crown Formicidae (11 chars.): 7, 36, *42, *46, 78, *86, 94, *97, *108, *128, and *143. 7: 1 › 2, postgenal bridge very long (vs. of medium length). 36: 1 › 0, loss of ocelli in workers (vs. ocelli present). *42: 0 › 1, hypostomal teeth present (vs. hypostomal corners rounded, not projecting as teeth). *46: 1 › 0, triangular hypostomal (paramandibular) process aligned with hypostomal tooth/corner (vs. process shifted mesad relative to tooth/corner, with straight connection). 78: 0 › 1, scape elongated relative to flagellum (vs. scapus short relative to flagellum). *86: 0 › 1, atala (abductor swelling) developed as distinct, rounded process (vs. broad swelling of different shape). ~94: 0 › 1, mandibular denticles inserted proximad subapical incisor (vs. denticles absent). *97: 0 › 1, mandible broadened, with distinct basal margin forming angle with masticatory margin (vs. mandible not broadened and without such angle). *108: 0 › 1, 0md1 fibers attached with cuticular filaments (vs. no fibers attached with filaments). *128: 1 › 0, 0la11 with origin proximally on prementum (vs. distally; homoplastic, also occurring in *Sceliphron*, and reversal to distal origin in *Formica*). *143: 0 › 1, *M. pharyngoepipharyngalis* with two pairs of bundles (vs. one pair).

Poneroformicines, i.e., Formicidae excl. Leptanillinae (5 chars.): 17, *39, *64, *82, and *134. 17: 0 › 1, supraclypeal area distinct (vs. indistinct; homoplastic, also in *Methocha* and *Ampulex*). *39: 0 › 1, oral margin of hypostoma 'shouldered' (vs. straight or with even curvature). *64: 0 › 1, torular apodeme present (vs. absent). *82: 0 › 1, no 0an3 fibers originating on dorsal tentorial arm (vs. at least some fibers; homoplastic with respect to *Parischnogaster*). *134: 0 › 2, prepharynx (buccal tube) abruptly widened distally (vs. not or only slightly widened).

Formyrmines, i.e., *Formica* + *Wasmannia* (5 chars.): *46, *47, *50, *113, and *147. *46: 0 › 2, triangular hypostomal (paramandibular) process shifted mesad relative to hypostomal tooth, with concave connection (vs. process and tooth aligned in straight line). *47: 0 › 1, secondary hypostomal knob present (vs. absent). *50: 2 › 1, medial tentorial lamella forming lobe of medium size (vs. extending over most of anterior arm). *113: 2 › 0, stipital flange not raised (vs. distinctly raised above external stipital sclerite). *147: 0 › 1, gland of cardinal base (maxillary gland) present (vs. absent).

Constrained Bayesian Analysis

Bayesian analysis revealed that no character transitions are well supported with the present sampling. Table 3 lists a comparison of the parsimony results with the results of the Bayesian inference. The few supported fixations (as defined in *Methods*) are listed in the following:
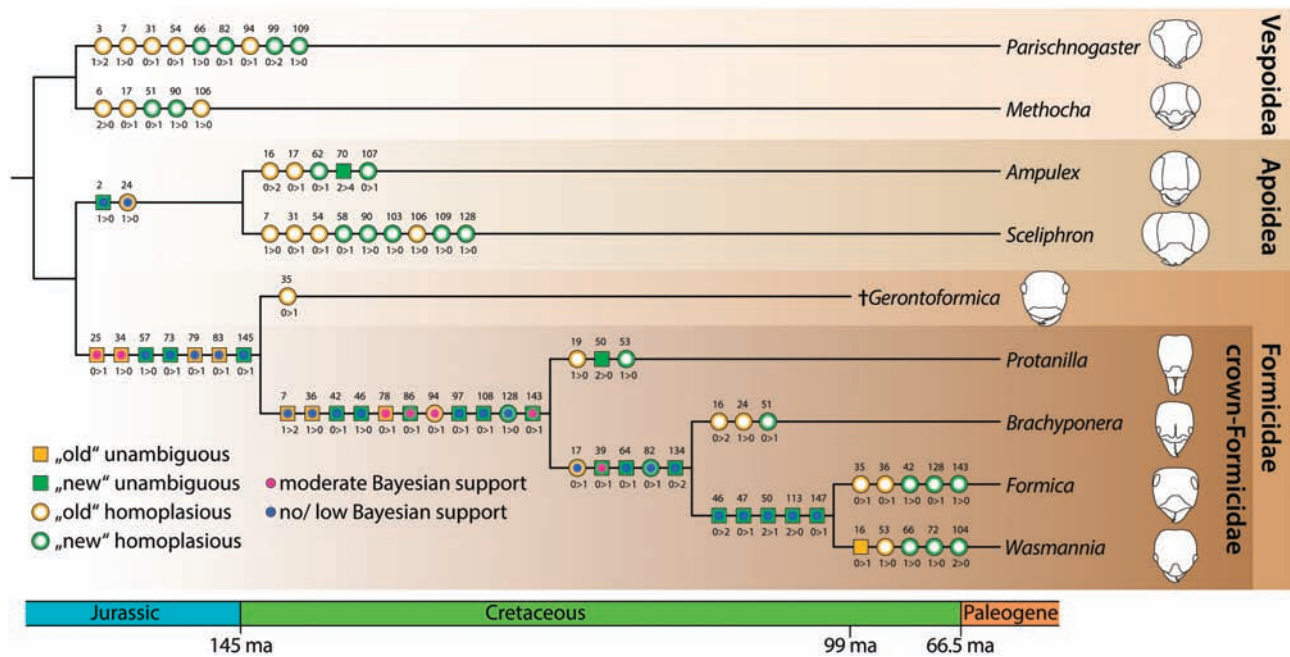
Fig. 7. Character state transformations recovered via parsimony and Bayesian analyses. Only unequivocally recovered transformations are shown. Topology fixed after Branstetter et al. (2017) and Boudinot et al. (2022c). Transformations are marked as open circles (homoplastic features) or solid boxes (unambiguous features), with the character number above and the transformation states below. Characters that are used here for the first time are marked in green, and those used in other analyses previously are marked in light orange. The timeline at the bottom is not to scale and not based on our analyses, but the marked time points (145, 99, and 66.5 ma) are positioned roughly to reflect current hypotheses on splitting events, mainly based on the divergence time estimations of Boudinot et al. (2022c). We set the branch tip of †*Gerontoformica* at 99 ma as this is the likely age of the fossil we investigated here.

Total clade Formicidae: *76: State 0, labrum directed downward in retracted state (vs. forward). *126: State 1, basiparaglossal brush position proximad of glossa (vs. on level of glossa).

Crown Formicidae: ~1: State 1, head more or less prognathous with an 'anatomical head orientation angle' of less than 70° (vs. more). 31: State 0, toruli situated directly at epistomal sulcus (vs. distinctly separated from it). *57: State 0, short dorsal arms (vs. long). 68: State 1, proximolateral labral processes present (vs. absent). *115: State 0, distance between setae of maxillary comb less than one diameter of seta base (vs. more than one diameter of seta base).

Poneroformicines: *39: State 1 in poneroformicines, oral hypostomal margin shouldered (vs. straight or evenly curved). *143: State 1 in poneroformicines, two pairs of bundles of *M. epipharyngopharyngalis* (vs. one pair).

Discussion

Overall, we found that most structures expected to be found in an ant head could be reconstructed based on our μ-CT scan. The features we observed in the head include plesiomorphies retained relative to crown-group Formicidae such as the shape of the mandibles and mandibular closer muscle, well-developed paraglossae, and the shape of the oral arms of the prepharynx. Furthermore, they share as apomorphies with all other ants a frontal bulge, compound eyes reduced in size, shortened dorsal tentorial arms, a transverse line of setae on the labrum, a basally angled pedicel, an elongated mandibular condyle, and a voluminous pharyngeal gland. Although the parsimony analysis suggests some very clear character transitions, our Bayesian inference shows that much denser taxon sampling would be necessary to confidently assess all of the analyzed characters. Nevertheless, as we think that the results of our analyses provide an interesting perspective of the early evolution of ants, we

discuss them in some detail, while stressing the preliminary nature of the results wherever appropriate. In other words, these are hypotheses to be deductively tested through extended taxon sampling and explicit statistical testing via phylogenetic methods. To outline the implications of our results, we provide a discussion of general considerations (*General Considerations*), and specific scenarios for the evolution of the ant head (*Evolution of the Ant Head*) and mandibles (*Evolution of the Ant Mandible*).

General Considerations

The level of preservation in the head of our fossil ant is exceptional. In addition to the mouthparts and internal sclerites, we were able to reconstruct the central nervous system including specific neuroanatomical structures, most parts of the cephalic digestive tract, several glands, and an almost complete set of muscles. The only two muscles that are found in all living species of Formicidae but were not preserved in our †*Gerontoformica* specimen are *M. tentoriooralis* 0hy2 and *M. tentoriopharyngalis* 0ph2. Although no trace of 0ph2 was visible, we found some fragments that possibly belong to 0hy2. Furthermore, the quality of preservation was such that we were able to observe fine histological details, such as sarcomere length, all individual cells of the mandibular gland, and to count individual olfactory glomeruli.

Our †*Gerontoformica* specimen represents the best-preserved insect amber fossil from the Cretaceous Period reported in the literature, and our work provides the most complete reconstruction of head anatomy of any fossil insect (Table 4). However, preservation of at least some soft tissue elements in amber is not as rare as one might expect based on the paucity of fossil anatomical reconstructions. For example, 67% of amber samples investigated by McCoy et al. (2016) had some degree of internal tissue preservation. Although the sample size in that study was relatively limited, their results indicate that soft tissue preservation can and does occur in

Table 3. Comparison of the parsimony and Bayesian results

Character	Character transformation Parsimony	Supported state at higher clade Bayesian	Supported state at clade Bayesian	Bayesian evaluation
Apoidea				
Char. 2	1 › 0	1, no s	0, moderate s	Unst. diverging
Char. 24	1 › 0	1, no s	0, moderate s	Unst. diverging
Total Formicidae				
Char. 25	0 › 1	0, good s	1, moderate s	Mod. diverging
Char. 34	1 › 0	1, good s	0, moderate s	Mod. diverging
Char. 57	1 › 0	0, no s	1, no s	Unst. diverging
Char. 73	0 › 1	1, no s	1, good s	Unst. plesiomorphy
Char. 76	No	1, no s	0, good s	Fixation
Char. 79	0 › 1	1, no s	1, good s	Unst. plesiomorphy
Char. 83	0 › 1	1, no s	1, good s	Unst. plesiomorphy
Char. 126	No	0, no s	1, good s	Fixation
Char. 145	0 › 1	1, no s	1, good s	Unst. plesiomorphy
Crown Formicidae				
Char. 1	No	0, no s	1, good s	Fixation
Char. 7	1 › 2	1, no s	2, no s	Unst. diverging
Char. 31	No	0, no s	0, good s	Fixation
Char. 36	1 › 0	1, good s	0, no s	Unst. diverging
Char. 42	0 › 1	0, good s	1, no s	Unst. diverging
Char. 46	1 › 0	1, no s	2, no s	No support
Char. 57	No	1, no s	0, good s	Fixation
Char. 68	No	0, no s	1, good s	Fixation
Char. 78	0 › 1	0, good s	1, moderate s	Mod. diverging
Char. 86	0 › 1	0, moderate s	1, moderate s	Mod. diverging
Char. 94	0 › 1	0, moderate s	1, moderate s	Mod. diverging
Char. 97	0 › 1	0, high s	0, high s	Sup. plesiomorphy
Char. 108	0 › 1	0, high s	0, high s	Sup. plesiomorphy
Char. 115	No	1, no s	0, good s	Fixation
Char. 128	1 › 0	1, moderate s	0, no s	Unst. diverging
Char. 143	0 › 1	0, good s	0, no s	Unst. plesiomorphy
Poneroformicines				
Char. 17	0 › 1	0, no s	1, no s	Unst. diverging
Char. 39	0 › 1	0, no s	1, good s	Fixation
Char. 64	0 › 1	1, high s	1, high s	Sup. plesiomorphy
Char. 82	0 › 1	1, no s	1, high s	Unst. plesiomorphy
Char. 134	0 › 2	2, no s	2, good s	Unst. plesiomorphy
Char. 143	No	0, no s	1, good s	Fixation
Formyrmines				
Char. 46	0 › 2	2, no s	2, no s	No support
Char. 47	0 › 1	0, no s	1, no s	Unst. diverging
Char. 50	2 › 1	1, no s	1, no s	No support
Char. 113	2 › 0	0, no s	0, no s	No support
Char. 147	0 › 1	0, high s	0, high s	Sup. plesiomorphy

The categories for Bayesian support for character states are based on the calculations detailed in *Material and Methods*. Generally, the higher the support for one of the character states over the others is at a particular node, the higher we interpret the support to be. No support means there is a close to equal likelihood recovered for either character state. Bayesian evaluation is 'unstable' if there is no support for at least one of the two relevant nodes, 'moderate' if both nodes have at least moderate support, and 'unsupported' if a plesiomorphy instead of transformation is recovered with low/no support. Dark green: at least good support and congruent with parsimony. Yellow: at least moderate support congruent with parsimony. Red: Low/no support in congruence with parsimony. Blue: Bayesian result not congruent with parsimony. Light green: fixation of a state at a node not recovered as transformation in parsimony.

Table 4. Overview of arthropod literature in which μ-CT methodology was used to document the internal anatomy of amber fossils to some degree

Structure(s)	Taxon	Deposit	Period	Reference
Skeletomusculature, nervous system, glands	Total Formicidae	Kachin	mid-Cretaceous	This study
Skeletomusculature, nervous system	Strepsiptera	Baltic	Eocene/Oligocene	Pohl et al. (2010)
Some muscle	Hymenoptera	Oise	Eocene	van de Kamp et al. (2014)
	Coleoptera	Kachin	mid-Cretaceous	Grimaldi et al (2019)
	Coleoptera	Kachin	mid-Cretaceous	Li et al. (2021)
General internal	Araneae	Paris	Eocene	Penney et al. (2007)
		Dominican Rep.	Miocene	Penney et al. (2012)
	Acari	Dominican Rep.	Miocene	Heethoff et al. (2009)
	Diplopoda	Chiapas	Oligocene/Miocene	Riquelme et al. (2014)
	Coleoptera	Spain	Early Cretaceous	Soriano et al. (2010)
		Baltic	Eocene/Oligocene	Schmidt et al. (2016)
Gills	Decapoda	Kachin	mid-Cretaceous	Luque et al. (2021)
Horn reinforcement	Formicidae s.l.	Kachin	mid-Cretaceous	Barden et al. (2017)
Endoparasitoidy	Braconidae	Baltic	Eocene/Oligocene	Belokobylskij et al. (2021)
Concealed juveniles	Araneae	Kachin	mid-Cretaceous	Guo et al. (2021)
Hindwing folding	Coleoptera	Kachin	mid-Cretaceous	Jałoszyński et al. (2020)
Mouthparts	Diplopoda	Kachin	mid-Cretaceous	Liu et al. (2017)
	Isopoda			Schädel et al. (2021)
	Coleoptera			Żyła et al. (2017)
	Mecoptera			Lin et al. (2019)
Genitalia	Coleoptera	Baltic/Rovno	Eocene	Perreau and Tafforeau (2011)
				Schmidt et al. (2016)
				Schmidt and Michalik (2017)
				Brunke et al. (2019)
				Bukejs and Legalov (2020)
				Bukejs et al. (2020a)
				Bukejs et al. (2020b)
				Kundrata et al. (2020)
				Nabozhenko et al. (2020)
				Alekseev et al. (2021)
				Kolibáč et al. (2021)
				Schmidt et al. (2021)
				Shavrin and Kairišs (2021)
				Yamamoto et al. (2021)
	Ostracoda			Keyser and Friedrich (2017)

most described sources of amber. Despite this, no prior study using μ-CT-based methods has provided complete tissue-by-tissue 3D reconstruction of any fossil insect in Mesozoic amber.

Previously, details of internal soft tissue of younger amber fossils have been revealed destructively using transmission electron microscopy (TEM) and scanning electron microscopy (SEM), achieving much higher resolution than is possible with μ-CT. Although we were able to visualize histological details such as muscle striation and larger individual cells such as those of the mandibular gland (Fig. 2), μ-CT scanning is currently not suitable to resolve tissue ultrastructure to the degree of electron microscopy. Poinar and Hess (1982) first documented ultrastructural details of a small strip of

preserved soft tissue in the abdomen of a fly in Baltic amber, imaging ultrathin sections with TEM. Henwood (1992a) documented the ultrastructure of the flight musculature of a fly from Dominican amber using TEM. In a follow-up study, Henwood (1992b) used SEM after crushing specimens into small pieces and employed TEM to investigate several types of tissue of fossil beetles, including the nervous system, digestive tract, respiratory organs, locomotor apparatus, and sensory organs. Using both TEM and SEM, Grimaldi et al. (1994) studied the mummified tissues of fossils from Baltic and Dominican amber, observing tracheae, flight musculature, and parts of the digestive tract and the central nervous system. By breaking the sample along the midline for SEM, Grimaldi et al. (1994) were

able to observe muscles in a natural position, and some of their samples showed a rather complete set of well-preserved muscles. Their ultrastructural TEM analysis yielded insights into the taphonomic process, such as the likely deposition of inorganic salts within muscle fibers and effects of tissue decomposition in the nervous system. More recently, Taniguchi et al. (2021) used petrological thin sectioning and confocal laser scanning microscopy to study the antennal sensilla of a cockroach preserved in Myanmar amber.

Although all these studies contributed important insights, the most critical advantage of µ-CT is non-destructive sampling, allowing preservation of the completely intact specimen in museum collections for perpetuity. This allows reexamination of the specimen, ensuring reproducibility and potentially including not yet developed techniques to reveal novel information about the fossil. Moreover, as Tafforeau et al. (2006) have previously indicated, destructive sampling methods provide little information on the three-dimensional structure of the tissue. In contrast, both shape and volume can be easily quantified using µ-CT data. Furthermore, as shown here, µ-CT can reveal the internal organization and tissues of soft organs such as the brain, which remain largely or completely obscured in SEM studies.

After reviewing the literature on the application of µ-CT to amber fossils, it is apparent that a minority of works have taken advantage of this methodology for the study of internal anatomy (Table 4). Most of these works have focused on the sclerotized elements of the male genital apparatus in Coleoptera, a character system well-known for alpha taxonomic and phylogenetic informativeness. A subset of works has shown cross sections or cross-sectional renders of general internal structures, without segmentation or detailed labeling, whereas an even smaller subset has specifically indicated or segmented musculature (Pohl et al. 2010, van de Kamp et al. 2014, Li et al. 2021, this study). Van de Kamp et al. (2014) studied wasp fossils from several ambers, uncovering vastly different levels of internal tissue preservation. They reconstructed the flight musculature of the best-preserved specimen in 3D. Li et al. (2021) used µ-CT scanning to reveal internal soft tissue preservation of an archostematan beetle (*Paraodontomma*) embedded in Burmese amber. Although they were not able to provide a detailed reconstruction due to limited resolution, poor preservation, and taphonomic artefacts, they tentatively identified a few muscles of possible systematic relevance, showing a thoracic bundle that is likely a plesiomorphy retained by Archostemata but missing in the other beetle suborders (Beutel and Haas 2000).

To date, the only other work to provide anatomical reconstructions of skeletomusculature and neuroanatomy of an amber fossil is that of Pohl et al. (2010). These authors documented the external and internal morphology of †*Mengea tertiaria*, a stem group strepsipteran of about 2 mm body length. Most elements of the skeletomuscular system could be reconstructed, as well as the shape and position of the brain and antennal nerves, most parts of the cephalic digestive tract, and the mouthparts. However, individual substructures of brain were not recognizable, and the preservation overall was too poor to differentiate individual cells, in contrast to the olfactory glomeruli and mandibular glands of †*Gerontoformica*. In contrast to our Cretaceous age fossil, †*Mengea tertiaria* was embedded in much younger Eocene Baltic amber (ca. 34–38 Ma).

Preservation and condition of amber specimens are difficult to predict, contributing to the rarity of detailed 3D morphological studies. Factors leading to a high level of preservation in amber are not well understood, but the original plant resin may need to access the body cavity through natural or artificial body openings. Statistical analysis of preservation level in different types of amber

(McCoy et al. 2016) and decay experiments with natural recent resin (McCoy et al. 2018) have shown that the type of resin and its chemical composition have an influence on how well organic tissue can be preserved. Additionally, the gut microbiome of the animal trapped in resin may have an influence on the process of tissue decay prior to complete entombment (McCoy et al. 2018). This is an interesting observation to consider in the present case, as the gut microbiome is known to vary within colonies (e.g., Ivens et al. 2018), among different castes of ants (Sinotte et al. 2020), and to have functional consequences across the ant tree of life (e.g., Anderson et al. 2012, Duplais et al. 2021). While speculative, this suggests that microbiomes of certain ant individuals may be better suited for preservation than those of others, thus possibly providing hints about colony lifestyle or division of labor in fossilized species.

Broad scale µ-CT scanning of fossils will increase the available information on the anatomy of extinct taxa dramatically, including or excluding internal soft parts. Even the documentation of exo- and endoskeletal features would greatly facilitate comparative investigations of insect communities of past periods. This has the potential to yield phylogenetically important characters and to reveal crucial character transformations. In the present study, we defined more than 80 new phylogenetic characters that were not used in phylogenetic studies before, many of them internal features. We were able to apply most of these features combined with previously used characters to evaluate the character evolution of the stem group ant †*Gerontoformica gracilis*. Of the newly defined characters, 32 were uninformative in parsimony analyses of the current dataset, but some of them will likely turn out as phylogenetically relevant at a lower taxonomic level. We recovered transformations of 19 newly defined characters as apomorphies for the clades of the total and crown Formicidae, and Formicidae excl. *Protanilla* and *Formica* + *Wasmannia*. Although the support for these transformations is limited based on our Bayesian analysis, this nevertheless underlines the potential of our approach to reconstruct character transformations in the early evolution of Formicidae by incorporating extensively analyzed fossils. Our aim in the current contribution was to reconstruct head anatomy, but the investigated fossil also shows significant preservation in the mesosoma, which may also be reconstructed in fine detail. As already suggested by Pohl et al. (2010) for the endoparasitic Strepsiptera, the detailed morphological analysis of insect fossils will yield crucial insights into the early evolution of a group that dominates and has dominated terrestrial ecosystems of our planet.

Evolution of the Ant Head

Application of µ-CT methodology has allowed us to characterize the heads of ants and other Aculeata in the greatest resolution to date, resulting in the estimation of 75 potential apomorphies, of which more than half (43) are newly defined (Fig. 7). With the presently available scan data alone, we recognize the possibility of scoring even more new characters, particularly for the outgroups. In total, we selected nine taxa for anatomical reconstruction and evolutionary analysis. Although this taxon sampling is quite limited, it reflects the very restricted knowledge of internal ant anatomy currently available. The taxa are furthermore selected specifically to represent a maximally diverse phylogenetic sample, spanning the major subgroups of ants and also the most relevant outgroups. Although we are cautious in interpreting the results based on this limited taxon set, we believe that it should allow a reasonable estimation, especially of the groundplan of ant head anatomy (crown Formicidae and to some extent total clade Formicidae). The included ant taxa represent all
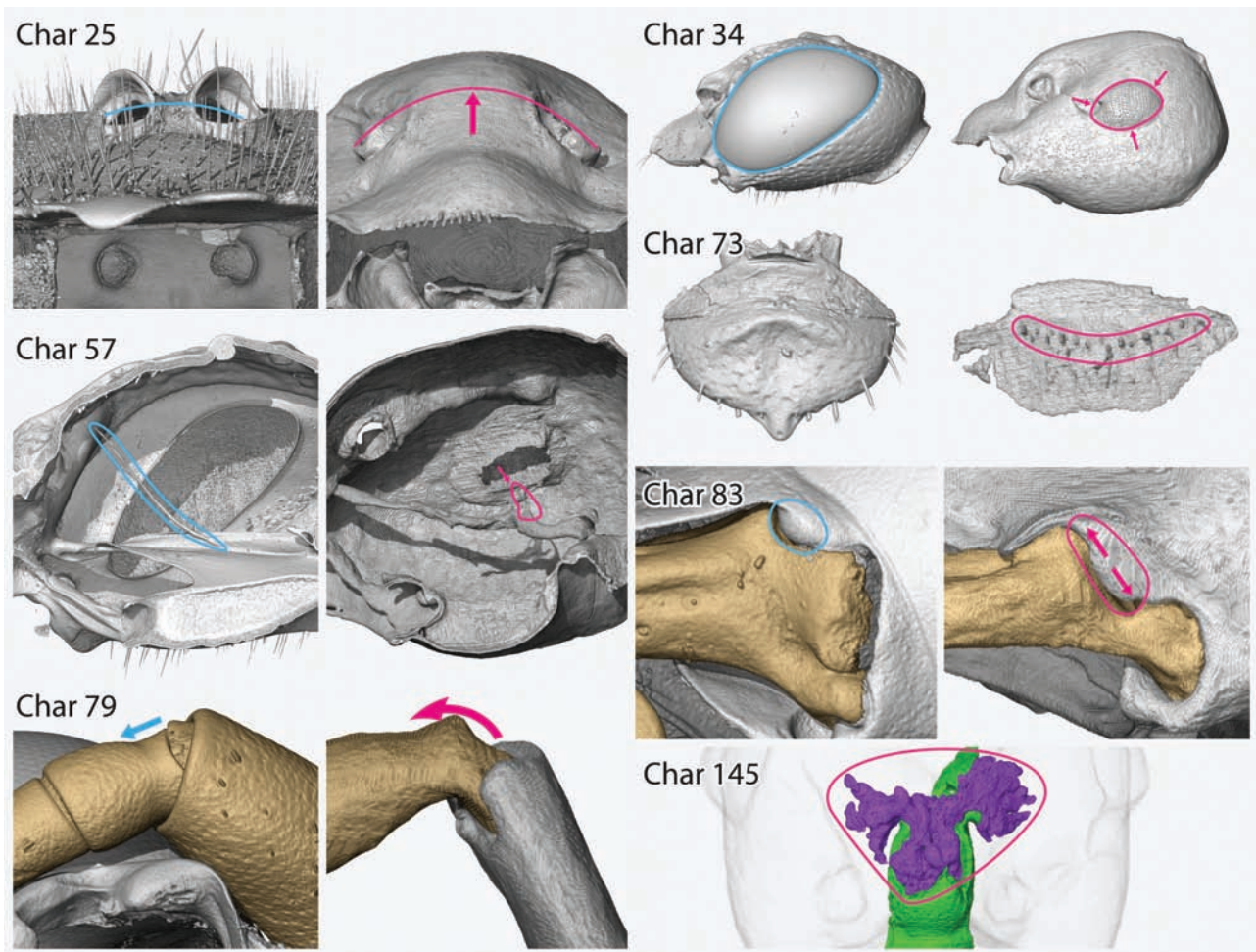
Fig. 8. 3D reconstructions of the heads of †*Gerontoformica gracilis* (on the right) and outgroup taxa (on the left) illustrating character transitions at the root of the total clade Formicidae. The relevant characters and states are marked with cyan outlines for plesiomorphies and magenta outlines for apomorphies; where applicable, physical directions of state changes are marked by arrows of the same colors. Complete illustrations of character states in all investigated taxa can be found in the character list at the end of this contribution. **Char. 24**: Frontal view on the head of *Sceliphron caementarium* and †*G. gracilis*, showing a flat versus bulging frontal region between the toruli. **Char. 34**: Lateral view of the head of *Ampulex* sp. and †*G. gracilis* showing large versus small compound eyes. **Char. 57**: Sagittal view of the tentorium of *Ampulex* sp. and †*G. gracilis* showing a long versus a short dorsal tentorial arm. **Char. 73**: Outer surface of the labrum of *Ampulex* sp. and †*G. gracilis* showing absence versus presence of a transverse line of setae. **Char. 79**: Frontal view of the scapopedicellar articulation of *Ampulex* sp. and †*G. gracilis* showing a basally straight and cylindrical versus a basally curved and flattened pedicel, in addition to an anteriorly deeply notched scapus tip. **Char. 83**: Lateral view of the mandibular articulation of *S. caementarium* and †*G. gracilis* showing a short versus elongated dorsal (secondary) mandibular articulation. **Char. 145**: Dorsal view of the cephalic digestive tract of †*G. gracilis* showing presence of the pharyngeal gland (absence in outgroups not shown).

species for which the complete external and internal head anatomy have been documented for workers (Richter et al. 2019, 2020, 2021; this study), whereas the four outgroups are newly evaluated. The parsimony analysis recovered numerous character transformations, but the Bayesian estimates are overwhelmed by uncertainty, thus more accurately reflecting the limits of our inferences and highlighting the need for extended taxon sampling. However, based on our results and a comparison with literature data, we can present a series of working hypotheses for the phenotypic transformations of head structures during the early evolution of the Formicidae.

Apoidea:

The two apomorphies reconstructed for Apoidea are unlikely to hold with broader taxon sampling. The first transformation is the reduction of the subforaminal groove (Char. 2), i.e., loss of a distinct angle on the surface of the ventral head capsule, beneath the postocciput. As head shape is generally highly variable across

Apoidea (Prentice 1998), it is quite possible that this transition was supported by the chance sampling of the two representatives included here. The second transformation is the strong spatial approximation of the antennal toruli (Char. 24), which otherwise only occurs in *Brachyponera*, among sampled taxa. This state is highly variable both within Apoidea and Formicidae, with gradual modification. Prentice (1998) evaluated a distance of about one torulus diameter as most common for Apoidea, with variation occurring both above and below this threshold and more or less wideset toruli are also likely the groundplan condition of ants.

Total Clade Formicidae

Among the reconstructed apomorphies of the total clade Formicidae (see *Classification System*), some appear more straightforward in interpretation than others. The presence of a frontal bulge (Fig. 8; Char. 25) conforms with an observation made by Boudinot et al. (2022c), who stated that the antennal insertion areas of ants

are laterally oriented in contrast to the dorsally directed antennal sockets in most other groups of Aculeata. Seemingly in contrast, Keller (2011) emphasized that the antennal socket of ants is almost always even relative to the surrounding frontal area. We reconcile these two perspectives with the observation that the frontal region bulges upwards between the antennal sockets in all ants we investigated. In fact, this condition is observed among most species of ants and results in a more lateral orientation of the antennal socket, compared to outgroup taxa. Obviously, this modification affects the orientation and movements of the antenna, the most important sensory and communication tool of ants. It is conceivable, however, that this is only a side-effect of rearrangements of internal structures. The median bulge likely provides additional space for the anterior digestive tract and its musculature. In this context, it should be noted that the frontal region is also variable across Aculeata and that a bulging frontal region also occurs in different groups of Apoidea, usually associated with elongated, nectar feeding mouthparts (Prentice 1998).

Size reduction of the compound eyes of workers (Fig. 8; Char. 34) is a well-known character of the ant groundplan, likely associated with the increasingly ground-based lifestyle of flightless worker females (Boudinot et al. 2022b), with evolutionary parallels in other surface-oriented aculeatan lineages (e.g., Boudinot et al. 2022c).

The length of the dorsal tentorial arm (Fig. 8; Char. 57) is a character included in a phylogenetic analysis for the first time. Zimmermann and Vilhelmsen (2016) stated that it is generally 'reduced' in Aculeata and never fused to the head capsule. We can confirm this general observation, but more specifically, the dorsal arms of outgroup taxa are distinctly longer than in any of the formicid terminals, being > 1/3 the length of the anterior arm. Among ants, the greatest length of the dorsal arm was observed in *Formica*, not quite reaching this threshold. Combined with the complete absence of the secondary tentorial bridge (Char. 52), this indicates a general trend toward reduction of the endoskeletal system in ants. Although the occurrence of the secondary bridge is highly variable across Aculeata (e.g., Prentice 1998), Zimmermann and Vilhelmsen (2016) reconstructed its presence as a synapomorphy of Aculeata and Evanioidea. A reliable assessment of the character state at the root node of the total clade Formicidae will require further taxon sampling, but it is very likely that the secondary bridge is generally absent in crown Formicidae (e.g., Richter et al. 2019, 2020, 2021, A. Richter, unpublished data). We propose two hypotheses for the reduction of the tentorium in Formicidae: optimization of intracranial space for musculature and other structures, or reduction of energy and material expenditure during development. The former hypothesis, as yet, has not been evaluated specifically; the latter aligns with the 'cheap worker' hypothesis of Peeters and Ito (2015), who proposed that small, simplified, and inexpensive workers are one of the keys to the evolutionary successes of ants. Although reduced investment into the cephalic endoskeleton would on principle fit with this idea, this appears unlikely considering the condition of the tentorium in ant queens: presently available data suggest that the cephalic endoskeleton is very similar to that of workers. Comparison of species with extreme worker-queen diphenism is necessary and comparison of worker/soldier polymorphism may also prove informative.

Interestingly, our analysis suggests that the presence of a 'transverse line of hairs' on the proximal region of the external labral surface (Fig. 8; Char. 73) is an autapomorphy of total clade Formicidae. The presence of stout labral setae has been previously remarked upon as a potential retained plesiomorphy of Leptanillinae and Amblyoponinae (e.g., Keller 2011, Boudinot 2015), but here we recognize the more generalized pattern of the transverse setal

arrangement. This character remains ambiguous to some degree, as we also defined the pair of longer setae occurring in *Protanilla*, *Brachyponera*, and *Wasmannia* as a 'line' of hairs as they correspond in position to the more clearly defined setal rows occurring in †*Gerontoformica* and *Formica*. No outgroup taxa that we examined showed such a labral hairline; we did not find any descriptions or depictions of the labrum in other aculeates that confirm the presence or absence of this feature. If the presence of the line of setae is confirmed as an autapomorphy of total clade Formicidae, it may indicate a new functional role of the labrum, such as sensory or manipulatory functions during object handling, screening the ground and detecting suitable prey or other items, or even involvement in prey capture, as was recently hypothesized for the specialized stout setae on the labrum of †*Zigrasimecia* (Cao et al. 2020).

A character that was always conceived as an apomorphy of total clade Formicidae is the geniculate antenna (e.g., Linnaeus 1758, p. 579). Here, we demonstrate that the defining feature of this antennal shape is the basally bent and flattened pedicel, thus resembling a beer can that is first transversely pinched at its base then tilted to one side, rather than evenly constricted around its proximal diameter, or not constricted at all (Fig. 8; Char. 79). This was previously suggested as a feature of the total clade Formicidae by Borysenko (2017) and Dlussky and Fedoseeva (1988); our analysis agrees with this assessment. Stem ants already displayed this key feature of the geniculate antenna, even though most of these extinct species retained relatively short scapes, apart from some species of †Haidomyrmecinae (e.g., Barden and Grimaldi 2016; Boudinot et al. 2022c). It is possible, therefore, that stem ants may have had increased capacity for antennating the ground and more efficient use of the antennae for communication, with further improvement attained in the crown ants via change in the proportions of the antennal segments. The condition of the basally flattened pedicel is not unique to ants and was, for example, also described in certain chalcidoid wasps that have geniculate antennae (Gibson 1986), although the basal curve observed in total clade Formicidae is not specifically mentioned. Biomechanical studies may further clarify how modifications of the antennal shape have influenced their use as sensorial structures and as organs of communication.

A feature that was only recently recognized as a characteristic of ants is the elongated dorsal (secondary) mandibular articulation (Fig. 8; Char. 83). This was supported as a autapomorphy of total clade Formicidae in the analyses of Boudinot et al. (2022c), confirming the result based on our more limited analysis. However, we also found unexpected variation of the shape of the articulatory area outside of Formicidae. The dorsal mandibular articulation of *Ampulex* is not as elongated as it is typical for ants, but clearly longer than the 'knob'-shaped condyle of other members of Aculeata and dicondylic insects in general (e.g., Beutel et al. 2014). The biomechanical consequences of the modified type of articulation are still unclear, but it is possible that this modifies or increases the degrees of freedom compared to typical dicondylic insects, indicated by the observation of biaxial rotation in the ant *Harpegnathos venator* (Smith, F., 1858) (Zhang et al. 2020b).

Another feature we inferred as an apomorphy of total clade Formicidae is the presence of the pharyngeal gland (Fig. 8; Char. 145). This is an interesting case, as a gland closely corresponding in position, shape, and biochemical contents was also found in several species of Philanthinae ("Crabronidae") (Herzner et al. 2007, Strohm et al. 2007). Due to the morphological similarities, Strohm et al. (2010) hypothesized a shared origin of the organ in ants and the crabronid subfamily. Additionally, a gland-like structure associated with the pharynx was identified in Ampulicidae, seemingly
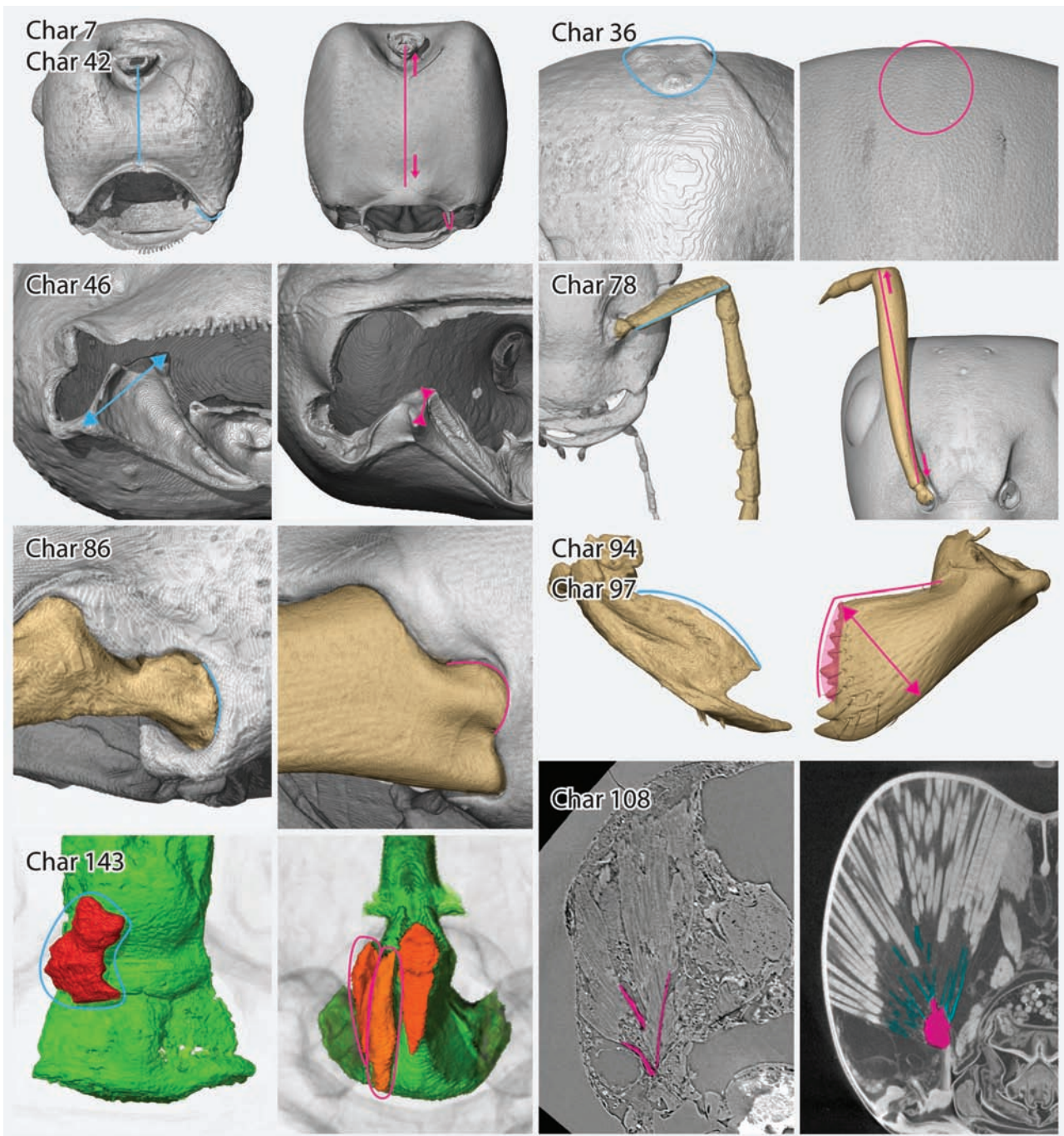
Fig. 9. 3D reconstructions of the heads of †*Gerontoformica gracilis* (on the left) and crown Formicidae (on the right) illustrating character transitions at the root of crown Formicidae, i.e., excluding †*Gerontoformica*. The relevant characters and states are marked with cyan outlines for plesiomorphies and magenta outlines for apomorphies; where applicable, physical directions of state changes are marked by arrows of the same colors. Complete illustrations of character states in all investigated taxa can be found in the character list at the end of this contribution. **Char. 7**: Ventral view on the head of †*G. gracilis* and *Brachyponera luteipes*, showing a medium versus a long postgenal bridge. **Char. 36**: Dorsal view on the posterior portion of the head of †*G. gracilis* and *Brachyponera luteipes*, showing presence versus absence of ocelli. **Char. 42**: Ventral view on the head of †*G. gracilis* and *Brachyponera luteipes*, showing a rounded versus projecting hypostomal tooth. **Char. 46**: Frontal view of the oral foramen of †*G. gracilis* and *Brachyponera luteipes*, showing a hypostomal corner situated far lateral of the tip of the hypostomal process versus a hypostomal corner aligned with the tip of the hypostomal triangular process. **Char. 78**: Frontal view of the scapus of †*G. gracilis* and *Formica rufa* showing a short scapus relative to the flagellum versus a long one. Only part of the antennal flagellum is shown, as this is not entirely imaged in the used µCT-scan data. **Char. 86**: Lateral view of the mandibular articulation of †*G. gracilis* and *F. rufa* showing the atala either broadly and flatly bulging or narrowly and highly bulging. **Char. 94** and **97**: Dorsal view of the mandible of †*G. gracilis* and *F. rufa* showing a narrow mandibular blade and gnathal edge without denticles proximad the subapical tooth versus a basally broadened mandibular blade with basal angle and denticles developed on the gnathal edge. **Char. 108**: Frontal section through the *M. craniomandibularis internus* (0md1) of †*G. gracilis* and *F. rufa* showing all fibers directly attaching to the main apodeme (magenta) versus some fibers attaching on thin cuticular fibrillae (cyan). **Char. 143**: Dorsal view of the prepharynx digestive tract of †*G. gracilis* and *Wasmannia* showing one bundle of the lateral portion of *M. pharyngoepipharyngalis* (0pe1l) versus two bundles.

lending additional support to this interpretation (Herzner et al. 2011). However, as we confirm here, this organ differs very distinctly from previously described pharyngeal glands. It consists of two long, sack-shaped, and unbranched structures which originate on the postcerebral pharynx. That these are in fact pharyngeal protrusions is clearly indicated by the insertion of the *M. verticopharyngalis* (0ph1) on the tip of these sacks. Considering the position and distinct structural differences, the homology of this structure with pharyngeal glands of Philanthinae and ants appears to be unlikely. In this context, it is also noteworthy that the glands are relatively large in the majority of Philanthinae, but smaller and less complex in species of a clade that forms the sister group of the remaining subfamily (Weiss et al. 2017). So far, the gland has not been reported in any other group of Aculeata and we also did not find it in our examined sphecid species. More broadly, the occurrence and morphology of glands deserves focused attention in social and solitary hymenopterans. It is conceivable that the genetic potential to form organs like the pharyngeal gland is at least shared by total clade Formicidae and Apoidea. However, the isolated occurrence rather suggests parallel evolution related to specific conditions. Extended taxon sampling is necessary.

Crown Formicidae

Our parsimony analysis suggests that the crown clade of the Formicidae is supported by more apomorphic conditions than the total clade Formicidae. This result should be treated with caution as our sampling of taxa, thus character space, was limited. Nevertheless, it appears likely that a series of evolutionary derivations may have contributed to the survival of the crown ants through the End Cretaceous crisis. Notably, apart from ocelli reduction (Char. 36), none of the apomorphies reconstructed for this clade are absences, all consisting of either 'present' or 'state change' features.

The first apomorphy we recovered is a very long postgenal bridge on the lower side of the head (Fig. 9; Char. 7), in contrast to medium length in outgroup taxa such as *Ampulex* and *Methocha* and †*Gerontoformica* (with *Parischnogaster* and *Sceliphron* having a very short bridge, which is presumably the groundplan state in most Aculeata, Prentice 1998). This is closely associated with the orientation of the head, as the elongation of the bridge moves the mouthparts anterad and upwards, basically leading to a prognathous condition. Although in the outgroups and †*Gerontoformica*, the postgenal bridge reaches at most 50% of the overall head length, it distinctly exceeds this threshold in all crown ants we examined, suggesting that the shift towards prognathism obtained a distinctive level in this taxon. It was suggested that the elevated posture of the head may have facilitated invasions of the subterranean sphere, allowing optimized movement and use of the mouthparts in narrow spaces (Wong and Guénard 2017, Richter et al. 2021), and enhanced their ability to carry loads (Nguyen et al. 2014) in combination with modifications of the mesosoma and its appendages (Keller et al. 2014, Boudinot 2015, Peeters et al. 2020, Boudinot et al. 2022c).

Another feature associated with a ground-dwelling lifestyle is the loss of ocelli in workers, which is here parsimoniously reconstructed as an apomorphy of crown Formicidae (Fig. 9; Char. 36). That the ancestor of the extant Formicidae had a lifestyle below or at least on the ground has been previously supported as a groundplan feature of the extant ants (Lucky et al. 2013, Nelsen et al. 2018). Given that the hypogaeic Martialinae and Leptanillinae are possible stable-niche relicts and supported as sister to the remainder of the Formicidae (Borowiec et al. 2019), it is conceivable that the most recent common ancestor of crown ants was more adapted to a subterranean lifestyle

than stem group representatives such as †*Gerontoformica*. In any case, characters potentially related to subterranean life are highly variable across modern ants, such as the shape of the head capsule, the ocelli, and the propectus. More detailed analyses are required for a reliable interpretation.

We also recovered the presence of 'hypostomal teeth' (Fig. 9; Char. 42) as an apomorphy of crown Formicidae. We use this term specifically for the more-or-less triangular projections of the lateral hypostomal corners. Similar structures also occur in other groups such as Scelionidae (Miko et al. 2007) and some Mutillidae (Brothers and Lelej 2017). Moreover, the projections are highly variable across Formicidae and missing in some cases (e.g., *Formica* from our sampling). Obviously, a reliable phylogenetic interpretation of this character requires a thorough evaluation with a broad taxon sampling. Another variable character of the hypostoma is the alignment of the hypostomal tooth/corner with the triangular hypostomal process (Fig. 9; Char. 46). As this feature was evaluated for the first time here and is rather variable, more taxa will have to be investigated. Nevertheless, the presently available results and some of the transitions reconstructed for other clades (see Poneroformicines section) show that the hypostoma is an interesting, potentially informative, and underexplored character system.

As discussed above, an important feature of Formicidae is their geniculate antenna. While the bent pedicel is clearly a feature of all Formicidae, an elongated scape relative to a shorter flagellum is recovered with our taxon sampling as an apomorphy of crown ants (Fig. 9; Char. 78). Boudinot et al. (2022c) retrieved this as an apomorphy of Antennoclypeata, a clade comprising the Cretaceous stem group subfamily †Brownimeciinae and all extant ants.

A very characteristic but phylogenetically problematic feature of ants is the atala, or 'abductor swelling', a lateral process of the mandible that receives the tendon of the *M. craniomandibularis externus* 0md3, the mandibular abductor. We found only a minute swelling in the outgroups *Parischnogaster* and *Methocha*, and a broad bulge on the lateral mandibular region in *Ampulex* and *Sceliphron*. A process is also present in Masarinae (Zimmermann et al. 2021) and Vespinae (Duncan 1939) but is apparently generally small in these taxa; it is developed as a broad, transverse column in Scoliidae (Osten 1982, Boudinot et al. 2022c). Additionally, protuberances or convexities on this mandibular region are highly variable across Apoidea (Bohart and Menke 1976, Michener and Fraser 1978). Although the process also shows a certain degree of variation across Formicidae (see, e.g., Khalife et al. 2018, Richter et al. 2021, Boudinot et al. 2022c), its shape appears relatively conserved, indicating a potential fixation of an optimal shape for the functional requirements of the ant mandible. Presently the structure is still underexplored across different aculeate clades and the biomechanical consequences of shape variations remain obscure.

Note that other characters of the mandible are only briefly treated here, as a more detailed discussion follows in *Evolution of the Ant Mandible* on the evolutionary transformations of these critical mouthparts. The transitions of Chars. 94 and 97 (Fig. 9) lead to the formation of the typical, 'triangular' or 'shovel-shaped' ant mandible with an elongated masticatory margin bearing additional teeth and a proximally broadened blade. Another highly characteristic, if not unique, feature of ants is a dual attachment mechanism of the large adductor muscle on its tendon: some of the fibers insert directly on the apodeme, whereas others are attached via thin cuticular fibrillae (Fig. 9; Char. 108). We could show that the latter are absent in †*Gerontoformica* and they are also missing in other groups of Aculeata. Consequently, the insertion mechanism involving fibrillae is a potential autapomorphic feature of crown Formicidae.

Two additional muscular features were recovered as apomorphies of crown Formicidae. The origin of *M. praementoparaglossalis* (0la11) proximally on the prementum, rather than distally (Fig. 9; Char. 128), is a highly variable character with reversal to the distal condition in *Formica*, and the proximal origin also occurring in Apoidea. Obviously, a more extensive taxon sampling would be required for a reliable interpretation. The second character is the presence of two pairs of bundles in the lateral portion of *M. pharyngoepipharyngalis* (0pe1), the longitudinal muscle of the prepharynx (Fig. 9; Char. 143). This possibly indicates an enhanced capacity of the prepharyngeal sucking pump in crown Formicidae. However, considering the very limited anatomical information for ants and other groups of Aculeata, a reliable interpretation is not possible at present. The development of oral arm lamellae (dorsal plates of the oral arms) may be related to this feature as one of these pairs originates on this structure (Char. 137). However, this was not supported as transformation in the parsimony analysis due to the uncertain state in †*Gerontoformica*. Our interpretation of the prepharyngeal folds as representing the oral arms would suggest that these arms are comparatively simple and no dorsal lamellae are developed in †*Gerontoformica*, but we conservatively retain the uncertain coding here. One possible driver of prepharyngeal variation may be the ability to perform trophallaxis, which is present in many lineages of ants but varies considerably across the family (Meurville and LeBoeuf 2021).

The size of the paraglossae (Char. 124) is another relevant feature with potential functional consequences. Even though transformations were neither recovered by parsimony nor by Bayesian inference, the character could be informative with a different coding scheme. In this study, we coded the paraglossa as small and partially reduced (state 1) for most Formicidae but as completely reduced (state 2) in *Protanilla*, while they are comparatively large and distinctly visible in †*Gerontoformica* and in the outgroup taxa. As we treated the character states as unordered, the phylogenetic position of *Protanilla* means that there is no clear signal for any of the states at any of the investigated clades. However, the character state of *Protanilla* could be pooled together with those of other extant ants for an analysis at this scale, in which case a size reduction of the paraglossae would be recovered as a autapomorphy of crown Formicidae.

Partial reduction of the paraglossae may be related to a switch in diet. Unusually large paraglossae often occur in species that are specialized nectar feeders such as many bees (e.g., Porto and Almeida 2021), but also members of other groups of Apoidea (Prentice et al. 1998, Krenn et al. 2005), Scoliidae (Osten 1982), Masarinae (Vespidae, Krenn et al. 2002), and to some extent even *Parischnogaster* from our taxon sampling. In this context, it should be noted that nectar producing plants, exclusively species of angiosperms, were likely undergoing major diversification (Barba-Montoya et al. 2018, Coiro et al. 2019, esp. Benton et al. 2021) when these hymenopteran lineages started to diversify in the late Mesozoic (Branstetter et al. 2017, Peters et al. 2017, Boudinot et al. 2022c). However, there is evidence that gymnosperm plants, still dominant in the Lower Cretaceous, produced pollination drops with a chemical composition similar to true nectar (Labandeira et al. 2007), and that some insects had independently evolved long mouthparts to feed on them, very similar to modern nectar feeders (Khramov et al. 2020). More generalist feeders that do not exclusively rely on plant exudates usually retain paraglossae about as large as the glossa (Khramov et al. 2020). This is also the case for example in Ampulicidae, which feed mainly on nectar and pollen as adults, but can ingest some of the hemolymph of the prey they

provide for their larvae (e.g. Jasso-Martínez et al. 2021) and have a similar paraglossa size as †*Gerontoformica*. This could indicate that †*Gerontoformica* was capable of feeding on plant secretions (such as pollination drops), at least facultatively, but considering the overall flexibility of these mouthparts and general restriction to liquid food in Hymenoptera, speculations about precise diet are tenuous.

Strongly reduced paraglossae in the crown ants could be related to a switch to almost exclusive carnivorous diets, as it is typical for members of Leptanillomorpha, Dorylinae, and many Poneria (e.g. Blüthgen and Feldhaar 2010). A potential argument against a diet relation of paraglossa reduction could be that the mouthparts of crown ants are still well-suited for uptake of liquid food even without well-developed paraglossae (Paul et al. 2002). It would thus have to be a very specific food source, not liquid feeding in general, that required retention of well-developed paraglossae in †Sphecomyrminae, for which there is currently no evidence. From another perspective, structural simplification while maintaining functional efficiency may have been an advantage of crown ants. Presently, precise data are only available for †*Gerontoformica* among stem group Formicidae. The documentation of the paraglossae and other mouthparts of fossil ants should have high priority, as this may reveal important transformations of the feeding apparatus and feeding behavior in the early evolution of the family.

Poneroformicines

Characters reconstructed as potential apomorphies of Formicidae excl. Leptanillinae (/*Protanilla*) are rather variable and will certainly require further scrutiny to confirm the evolutionary scenario suggested here. Nevertheless, we will discuss the individual features briefly.

The presence of a distinct supraclypeal area (Char. 17), also known as the 'frontal triangle' in the ant literature (see Keller 2011 for disambiguation), is supported as an autapomorphy of the poneroformicines. This feature also occurs in other groups of Aculeata (e.g., *Methocha* and *Ampulex*) and is currently not well understood from a functional perspective. Another presumptive apomorphy is the 'shouldered' oral carina between the cardinal condyles of the hypostoma, in contrast to a margin that is straight or evenly curved (Char. 39). This is one of several newly defined hypostomal characters that show an interesting pattern of variation. However, as virtually no reliable information can be found in the literature currently, we can only offer a preliminary interpretation of this character complex here.

A character that can be considered as an apomorphy of the poneroformicines with reasonable certainty (also supported by A. Richter, unpublished data) is the presence of a torular apodeme (Char. 64). This structure was observed for the first time by Lubbock (1877) but only recently rediscovered and described in detail (Richter et al. 2019, 2020, Boudinot et al. 2021). Even though this feature is not sufficiently documented across Formicidae at present, the current study tentatively suggests a new context for its evolution. In poneroformicines, the torular apodeme bears the origin of *M. tentoriooralis* (0hy2), for which the plesiomorphic origin is on the frontoclypeal strengthening ridge. In some aculeates, such as *Methocha* and *Sceliphron*, the formation of conspicuous lobes on this ridge results in an enlarged area of origin for the muscle and probably also an advantageous attachment angle to pull on the oral arm process/the proximal prepharynx. In crown ants, the origin is generally shifted to the inner rim of the torulus (Richter et al. 2021), although we could not confirm this in †*Gerontoformica* due to insufficient muscle preservation. Based on the visible fragments of

0hy2, an origin on the frontoclypeal ridge appears more likely than one on the torulus. This suggests that the torular apodeme may indeed have originated in the poneroformicine ancestor and is possibly analogous to the lobes of the frontoclypeal strengthening ridge, optimizing the attachment area and angle of the muscle.

Another variable character is the origin of a part of *M. tentorioscapalis lateralis* 0an3 on the dorsal tentorial arm. The parsimony analysis suggests that the complete absence of any components of this muscle on the dorsal arm is an apomorphy of poneroformicines, which may be related to the distinct reduction of this endoskeletal element in ants (see 'Total clade Formicidae'). Finally, we also retrieved an abruptly widened distal prepharynx (buccal tube) as an apomorphy of Formicidae excl. Leptanillinae. Although this is a conspicuous feature and likely related with dietary adaptations, the presently available data are not sufficient for a reliable interpretation.

Due to the highly limited taxon sampling, the retrieved shared derived features of *Formica* + *Wasmannia* are very uncertain as potential synapomorphies of monophyletic formicomyrmines. Therefore, we only treat them very briefly here. Two characters, the mesial shift of the hypostomal corners relative to the triangular hypostomal processes (Char. 46) and the occurrence of a hypostomal knob mesiad the pleurostomal fossa (Char. 47), underline that the hypostoma is a very variable and insufficiently explored character system. The presence of the medial tentorial lamella as a mid-sized lobe (Char. 50) will likely not be confirmed as an apomorphy of this clade with an expanded taxon sampling. A similar shape has been found in Leptanillinae (Lopez et al. 1994, Yamada et al. 2020) and likely also occurs in other groups. The cardo base gland (formerly 'maxillary gland') is likely an autapomorphy of a more inclusive clade within Formicidae. As this structure has previously been reported in Dorylinae (Gotwald and Schaefer 1982), it is a potential autapomorphy of the Doryloformicia, a group which is so far not supported by any morphological autapomorphy. However, in this context, it is important that Boonen and Billen (2016) noted some terminological confusion in the literature on ant glands, including a frequent confusion of the maxillary gland and prepharyngeal ('propharyngeal' or 'hypopharyngeal') gland. Clearly, a thorough screening and re-evaluation across a broad sample of ant taxa is necessary.

Bayesian Analysis Provides Additional Information

Accounting for the limited taxon sampling and uncertainty, the Bayesian analysis resulted in limited support for most of the transformations suggested by the parsimony analysis. We consider this to be important, as parsimony analysis results in 'absolute' reconstructions, regardless of uncertainty in character coding, state distribution, or branch lengths, and thus has higher potential to be misleading. Regardless, the Bayesian analysis did support fixation of some character states at certain nodes of the phylogeny that we will discuss briefly here (Table 3).

For the total clade Formicidae, fixation was supported for the hypostomally ('downward') directed condition of the labrum at closure (Char. 76). The state in other aculeatan groups is ambiguous due to the unusual forward orientation in *Ampulex* and the uncertain state in *Methocha*. The available information on the orientation in other groups of Aculeata (e.g., Scoliidae and different species of Pompiloidea and Apoidea; Osten 1982, Cowley 1959) suggests that the vertical orientation is a plesiomorphy retained in total clade Formicidae, and that several of our sampled outgroup taxa diverge from this groundplan condition. A downward directed labrum protects the maxillolabial complex and other, less sclerotized structures

during activities such as digging or prey capture (Osten 1982, Keller 2011). The functional implications of an anteriorly directed labrum as it occurs in Ampulicidae are presently unclear and deserve further attention. A second fixed state is the position of the basiparaglossal brush proximad the glossa (Char. 126). We observed this state also in †*Gerontoformica*, but the Bayesian analysis did not resolve the state in Formicapoidina (*Classification System*) due to the inapplicable state coded for *Parischnogaster* and *Methocha*. For the same reason, this was not unequivocally recovered in the parsimony analysis. Nevertheless, it is conceivable that the specific state of the basiparaglossal brush is unique to ants. Although this could suggest a specific mode of food uptake, the exact function of the brush is not known.

As in the parsimony analysis, the crown Formicidae are the group with the highest number of supported characters. Although a re-evaluation with a broader taxon sampling may reject some of the presumptive apomorphies for this clade, our analysis strongly suggests that important morphological transformations occurred at this stage of ant evolution.

The first fixation retrieved with Bayesian inference is the postgenal-postoccipital angle, or the 'head orientation angle', which is less than 70° in crown group ants (Char. 1), a condition that we consider as equivalent with the common concept of a prognathous head orientation. There is no support for any of the states for any other clade due to the highly variable condition of this character. The chosen threshold for 'prognathism' is clearly arbitrary, and prognathism is a complicated anatomical syndrome in Hymenoptera (see 'A Short Perspective on Hymenopteran Prognathy'). The low support values accurately reflect our current state of understanding of this feature. However, in correlation with the parsimony-supported elongation of the postgenal bridge in crown Formicidae, our results suggest that an increased ability to hold the head in a horizontal position is indeed a crucial derivation of crown ants, in clear contrast to the orthognathous condition in 'basal' hymenopteran groups (Beutel and Vilhelmsen 2007), in other groups of Aculeata, and in members of the formicid stem group. The supported stabilization of the toruli at the epistomal sulcus (Char. 31) is possibly an effect of insufficient taxon sampling as this character is rather variable both within Formicidae (Keller 2011) and other groups of Aculeata (e.g., Bohart and Menke 1976). The fixation of short dorsal tentorial arms (Char. 57) in crown Formicidae corroborates the interpretation as apomorphy for all total clade Formicidae in the parsimony analysis, although there is insufficient support in the Bayesian evaluation to determine the exact branch along which the transition occurred.

The Bayesian analysis also provided some support for transitions that were not recovered via parsimony due to the unknown state in †*Gerontoformica*. One prominent feature is the presence of proximolateral labral processes (Char. 68) in all crown group ants, which was recognized as a characteristic for the ant labrum by Keller (2011). The processes were also observed in stem group Formicidae (V. Perrichot, unpubl. data) but were not recognizable in †*Gerontoformica* (coded as '?'). Another feature is the dense arrangement of the setae of the maxillary comb on the inner side of the galea (Char. 115). Although we could not unambiguously assess the state in †*Gerontoformica* (also coded as '?'), our 3D-reconstruction suggests that this condition was in fact present. The setae are loosely arranged in Apoidea (*Ampulex, Sceliphron, Pison*: Cowley 1959), Tiphiidae (Gotwald 1969), and probably also in Scoliidae (Osten 1982: fig. 2). Both states occur in Masarinae according to Zimmermann et al. (2021: figs. 6, 7, and 8). Even though this is a likely an autapomorphy of total clade Formicidae or possibly only crown Formicidae, more taxa have to

be evaluated for a reliable interpretation. This feature is likely related to food uptake, but probably also to grooming and cleaning behavior in which the maxillae are involved in ants (e.g., Farish 1972).

Bayesian inference yielded two state fixations in poneroformicines. The 'shouldered' oral hypostomal margin (Char. 39) was also retrieved as an apomorphy of this clade in the parsimony analysis. The presence of two paired bundles of *M. epipharyngopharyngalis* (Char. 143) was only weakly supported in the Bayesian analysis and recovered as autapomorphy of crown Formicidae in the parsimony analysis.

Unique Features of †*Gerontoformica*

Several anatomical features were exclusively observed in our specimen of †*Gerontoformica gracilis*, of which two deserve special focus. First, we observed a medial, lobate process distally on the first maxillary palpomere. Due to its symmetry and appearance both in photos and in the µ-CT data, we do not consider these lobes to be artefactual. A similar process has never been described in any ant species to date, and this is a previously overlooked feature within the genus †*Gerontoformica* (Nel et al. 2004, Perrichot et al. 2008, Barden and Grimaldi 2014; see also Boudinot et al. 2022b). Based on preliminary scan data of another †*G. gracilis* wherein the lobes are present (B. Boudinot and T. van de Kamp, unpublished data), it is possible that this is a feature unique to this species, but it may also be found in other stem ants. Its function is entirely unknown; it could, for example, allow the labial palps to be used in manipulation of small objects or perhaps it may represent a special sensory structure. Further investigation is necessary.

As a unique feature of the cephalic digestive tract, we observed the occurrence of strong, transverse ridges on the lower wall of the anteriormost prepharynx, the buccal tube. It is well known that rows of microtrichia, often located on fine cuticular scales/ridges occur in this region of the prepharynx in ants (e.g., Janet 1905, Glancey et al. 1981, Richter et al. 2021) and Hymenoptera more generally (Beutel and Vilhelmsen 2007). However, similarly strong ridges in this position have not been reported before. It is conceivable that the ridges we observe may in fact represent rows of long microtrichia that are glued together by some material that has the same contrast in the µ-CT-scan as the surrounding prepharynx, but due to the regularity of the structures we consider this to be unlikely. The development of such strong ridges may have implications for the diet of †*Gerontoformica*. As these ants possessed a large infrabuccal pouch, their prepharynx likely functioned as an effective filter device, retaining food and debris particles of undesired sizes. This may, for example, be cuticular remains of pray insects or hard parts of plants or dirt particles from grooming (see, e.g., the pellet contents in *Colobopsis* sp., Davidson et al. 2016). Unfortunately, we were not able to identify food particles from the pellet of the infrabuccal pouch, but destructive sampling of such a pellet and subsequent chemical analysis could potentially reveal more about the diet of this Cretaceous animal.

A Short Perspective on Hymenopteran Prognathy

The phenomenon of prognathy was briefly touched on in the discussion of postgenal bridge elongation (Char. 7). However, we find it worthwhile to specifically note here that hymenopteran head orientation depends on several morphological conditions, and the 'prognathous' orientation is a gradual morphological syndrome affecting multiple character systems that can have evolved in different ways. Factors that can play a role in the overall appearance of the cephalic orientation are the relative length of the postgenal bridge (or other

sclerotized elements of the ventral/posterior cephalic wall), the orientation and shape of the postocciput surrounding the occipital foramen, the articulation and orientation of the mouthparts, the general head geometry, and the shape of the anterior prothorax. Another important factor is the flexibility of the head in the cervical region, based on the size of the occipital foramen and its connection to the prothorax. These different factors were previously discussed by Fedoseeva 2001, but so far, an evolutionary synthesis of the phenomenon based on modern phylogeny and anatomical data is missing.

In ant research, the assessment of head orientation is often obscured by the fact that dead ants usually have their mouthparts directed downwards (relative to the mesosoma), giving them an orthognathous appearance in samples in collections. Living individuals, however, can direct their mouthparts from strictly anterad ('prognathous orientation') to downwards ('orthognathous') or even further downward/backward ('hypognathous') depending on their current activities. This results in a broad functional spectrum and differs strongly from a largely fixed prognathous orientation in other groups with a retracted posterior head region, such as, for instance, Coleoptera or Raphidioptera (e.g., Beutel et al. 2011). Thus, we infer that 'prognathy' versus 'hypognathy' or 'orthognathy' are problematic character states for analyzing relationships in Hymenoptera. Instead, the individual features leading to different head orientations should be evaluated and their transformations in the groups under consideration. In the context of the Formicoidea, it will be especially valuable to make intersex comparisons (Boudinot et al. 2021), as the sexes differ in their apparent head orientation and in the construction of their cranial apparati.

Evolution of the Ant Mandible

What Is the Groundplan Shape of the Ant Mandible?

Mandibles are the primary tools available to ants for the manipulation of their environment. Ants handle and process food, brood, nestmates, nest substrates, detritus, enemies, and other objects with their mandibles (e.g., Gotwald 1969, Hölldobler and Wilson 1990, Gronenberg et al. 1997). The shape and size of the mandibles are arguably as diverse as the lifestyles of ants themselves. Over the course of ant evolutionary history, some extremely specialized variations have developed and received considerable research attention. Examples include the mandibles of various trap-jaw (e.g., Gronenberg 1995, Gronenberg 1996, Gronenberg et al. 1998, Larabee et al. 2017, Booher et al. 2021) and snap-jaw ants (Larabee et al. 2018), the pitchfork mandibles of *Thaumatomyrmex* (Brandão et al. 1991), the elongated, strongly toothed mandibles of many members of Amblyoponinae (Yoshimura and Fisher 2012), and the elongated curved upper jaws of *Protalaridris* (Lattke et al. 2018). Unusual mandibular shapes have also been a special point of interest in Cretaceous ants, especially in the †Haidomyrmecinae (Barden et al. 2020, Perrichot et al. 2020) and †Zigrasimeciinae (Cao et al. 2020). The biomechanics of the long, saber-shaped mandibles of *Harpegnathos* have been studied in several publications (Zhang et al. 2020a, b, 2021), whereas no ant species with 'normal' mandibles has received similar attention, with the arguable exception of leaf cutting ants (Püffel et al. 2021) and a single analysis of *Pheidole* mandibles (Klunk et al. 2021).

To understand the evolution of ant mandibles, it is crucial to determine what constitutes the groundplan conditions of the total and crown clades of the Formicidae from which all other mandibular forms derived. A formal, detailed analysis of this issue is still pending, but the most prevalent shape across different extant ant clades is certainly the so-called 'triangular' mandible (see, e.g.,
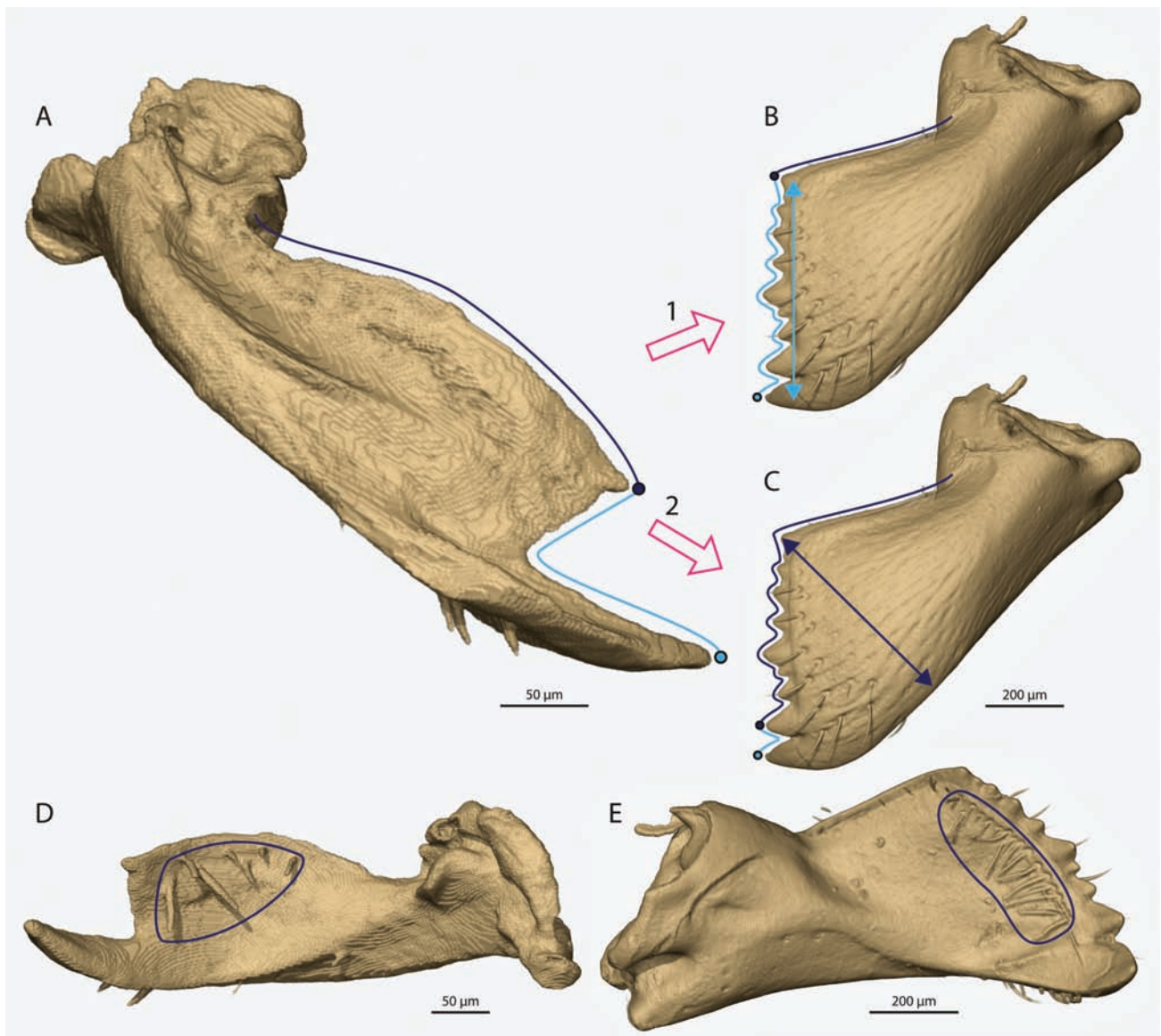
Fig. 10. 3D reconstructions of the mandible of †*Gerontoformica gracilis* (A and D) and *Formica rufa* (B, C, and E) illustrating our two hypotheses for the evolution of the shovel-shaped mandible of crown ants. According to hypothesis 1 (A → B), the position of the subapical tooth (purple dot in **A**) is shifted posteriorly so that the margin between it and the apical tooth (cyan dot) is elongated and additional teeth are inserted. Elongation of the masticatory margin (cyan line) leads to the modified orientation of the basal margin (purple line). The original subapical tooth becomes the basal margin (purple dot in B). According to hypothesis 2 (A → C), basal broadening of the mandibular blade leads to the formation of the basal angle and part of the original basal margin is incorporated with the masticatory margin, developing denticles. The original subapical tooth (purple dot in A) remains the subapical tooth (purple dot in B). The position of the fimbriate line on the inner surface of the mandible (purple outline in D and E) supports hypothesis 2.

Wilson 1987; Bolton 1994, 2003). However, this characterization is rather unfortunate from the perspective of broader insect morphology. Most insects with biting, 'orthopteroid' mouthparts have more-or-less triangular or wedge-shaped mandibles, such as cockroaches (e.g., Wipfler et al. 2016), beetles (e.g., Hörnschemeyer et al. 2013), or 'symphytan' Hymenoptera (Beutel and Vilhelmsen 2007). Characteristic for this mandibular type is a broad base which narrows laterally and medially to its pointed apex, often with additional subapical teeth. This is distinctly different from the condition observed in most ant species.

Ant mandibles have a narrow base, and it is only the mandibular blade that is broadened proximally and narrows distally into a pointed apex. It is apparent that the ant mandible has been generally conceived of as 'triangular' because the blade is the most

visible feature in light and scanning electron microscopy. However, the three sides of the 'triangle' in this class of ant mandible are not formed by the mandibular base, the gnathal edge, and the lateral margin as in other groups of insects with wedge-shaped mandibles, but rather by the basal margin (usually without teeth), the masticatory margin (usually with teeth), and the lateral/outer margin (Fig. 10B). As the inner surface of the mandibular blade in this mandible class is always at least somewhat concave due to the mandible torque and curvature (Keller 2011), we propose to consistently call it 'shovel-shaped' rather than 'triangular'. This better reflects the form, which is a broad, concave surface that is set on a narrower shaft. Shovels have previously been used, especially in the German literature, to describe this typical mandibular shape, giving this terminology some precedent (e.g., Escherich 1917, 'schaufelförmig',

p. 19). In the extant ant species that we examined for this study, the shovel shape is very clearly developed, although with a comparatively long and narrow blade in *Protanilla* (see also Richter et al. 2021). A very similar shape also occurs in a few other groups of Aculeata such as the megachilid bees (Gonzalez et al. 2019). However, given the distant relationship to these bees, we consider this to be the result of independent evolution. We suggest that the shovel shape is part of the groundplan of the poneroformicine ants (Chars. 94 and 97; Fig. 7), and possibly of the entire crown Formicidae. The situation in Leptanillomorpha remains ambiguous and will be discussed in more detail below.

The hypothesis that the shovel shape is an innovation of the crown Formicidae is based on the observation that this morphology is completely absent among known stem group ants (Boudinot et al. 2022c). Of the five stem ant subfamilies, two are strongly defined by their highly specialized mandibles. Those of the †Haidomyrmecinae are elongated and dorsoventrally oriented 'scimitars' (Barden et al. 2020, Perrichot et al. 2020), whereas those of the †Zigrasimeciinae are short, broad, almost completely edentate 'death spoons' that bear spine-like setae (Cao et al. 2020). In contrast, the mandibles of †Brownimeciinae are simplified, being falcate and with a single apical tooth (Grimaldi et al. 1997). The mandibles of †Armaniinae have also been described as falcate and bidentate (Dlussky 1999) or in some cases edentate (Dlussky et al. 2004). The mandibles of †*Gerontoformica* are similar in shape to those of most other species of †Sphecomyrminae, being narrow, falcate, and bidentate (Fig. 10A; see, e.g., Wilson 1967a, b, Grimaldi et al. 1997, Barden and Grimaldi 2014, Boudinot et al. 2022b). Additionally, the more distantly related †*Camelomecia*-group has exceptional, *Tatuidris*-like mandibles (Barden and Grimaldi 2016; Boudinot et al. 2020, 2022c), which appear to have derived from a unique but as yet understudied set of modifications. The question which of these diverse mandibular shapes most closely approximates the groundplan of the total clade Formicidae is not easy to answer. The highly specialized condition in †Haidomyrmecinae can be ruled out with reasonable certainty and probably also the twisted spoon-shaped mandibles of †Zigrasimeciinae. Although our taxon sampling is too limited to provide a definitive answer to this question, there are good arguments that a falcate and relatively short mandible, likely with an apical and a subapical tooth, represents a plesiomorphic condition retained from the last common ancestor of Formicoidea and Apoidea, as already hypothesized by Wilson et al. (1967a, b), Dlussky and Fedoseeva (1988), and Bolton (2003).

As in the total clade Formicidae, mandibular shapes are also diverse across the entire Aculeata. However, the falcate shape with an apical and a preapical tooth occurs in all subgroups of the stinging wasps. Mandibles are often wedge-shaped shaped and tooth number is variable in Chrysidoidea (e.g., Boudinot et al. 2022c), but the falcate, bidentate to many-dentate shape is also found, e.g., in Bethylidae (Alencar and Azevedo 2013, Lanes et al. 2020). Although a mandible with a broad base and simple triangular to rectangular shape occurs in many genera of Vespidae (e.g., *Parischnogaster* in our sample, Polistinae: Silveira and Santos 2011, *Vespula*: Duncan 1939), the falcate bidentate form is found in the subfamily Masarinae (Zimmermann et al. 2021). Falcate mandibles with or without a subapical tooth also occur in pompiloid subfamilies such as Thynnidae (*Methocha* from our sample), Tiphiidae, and Mutillidae. In some cases, additional teeth are present proximad the subapical one and limited broadening of the blade also occurs (Osten 1982, 1988). Among Apoidea, falcate bidentate mandibles are also typical for many taxa of Ampulicidae (*Ampulex* in our sample), Sphecidae

(*Sceliphron* in our sample), and Crabronidae (Bohart and Menke 1976), and also for some bees, especially in Andrenidae (Michener and Fraser 1978). This prevalence across all clades makes it plausible that this shape is a retained plesiomorphy in †*Gerontoformica* and related stem group ants. This implies that all other mandibular shapes occurring in the total clade Formicidae must be derived from this groundplan condition. Although surprisingly little biomechanical work has been done on the shovel-shaped crown ant mandible, one obvious idea for its advantage over other types, such as the generally more falcate stem ant mandibles, may be that it is a very useful tool for digging in the soil or also in other materials. This could have allowed crown ants to inhabit the soil layers and build elaborate nests more effectively. This may have been a significant advantage when forest ecosystems collapsed at the K/Pg boundary (Vajda and Bercovici 2014). In the following, we discuss how mandibular shapes may have changed in the early evolution of ants, finally bringing forth a largely conserved shovel shape in Poneroformicines.

How Did the Shovel Shape of Extant Ants Evolve from the Falcate Condition?

Hypotheses and Comparisons The three main prerequisites for the formation of a shovel-shaped mandible are that: 1) the masticatory margin (i.e., the tooth-bearing part of the gnathal edge) is elongated, 2) more teeth are developed proximad the apical incisors, and 3) the mandibular blade is broadened basally. Important and clear positional markers are the apical tooth, the subapical tooth, and the basal angle, i.e., the angle between the masticatory and basal margin in a shovel-shaped mandible. Based on this premise, we propose two alternative hypotheses of transformation (Fig. 10A–C).

In the first scenario (1), the margin between the apical and subapical teeth—the original masticatory margin of †*Gerontoformica*—was elongated and additional teeth emerged between the ancestral two (Fig. 10B). If the elongation occurs in a single plane parallel to the longitudinal axis of the head, this automatically leads to the basal broadening of the blade and the orthogonal orientation of the basal margin. This implies that the basal angle of the shovel-shaped mandible is homologous to the subapical tooth of the falcate mandible, that the subapical tooth of crown ants is a newly acquired structure, and that the masticatory and basal margins retain their identity and merely change in length and orientation.

Alternatively (2), the original basal margin may have been extended at a defined site along its midlength, forming the basal angle, which is where the mandibular base widens medially. Consequently, the area of the basal margin distad this point was incorporated into the masticatory margin and developed teeth, whereas the proximal part remained edentate and assumed its orthogonal position (Fig. 10C). In this scenario, the subapical tooth of the falcate mandible is homologous to the subapical tooth of the shovel-shaped mandible, and the basal angle corresponds to a point on the basal margin that is not strictly defined in the falcate mandible. This hypothesis implies that the terms 'masticatory' and 'basal margin' are purely functional and do not always indicate homologous structures or regions in different species.

These hypotheses are not necessarily mutually exclusive. It cannot be excluded that broadening of the mandibular blade was achieved by alternative mechanisms in different taxa. Some mandibular varieties occurring within Formicidae could be explained, for example, by development of denticles between the apical and subapical teeth, as observed in *Cheliomyrmex* (Gotwald and Kupiec 1975). However, one distinct landmark supports the second hypo-thesis for the formation of the shovel-shaped mandible: the 'fimbriate line'.
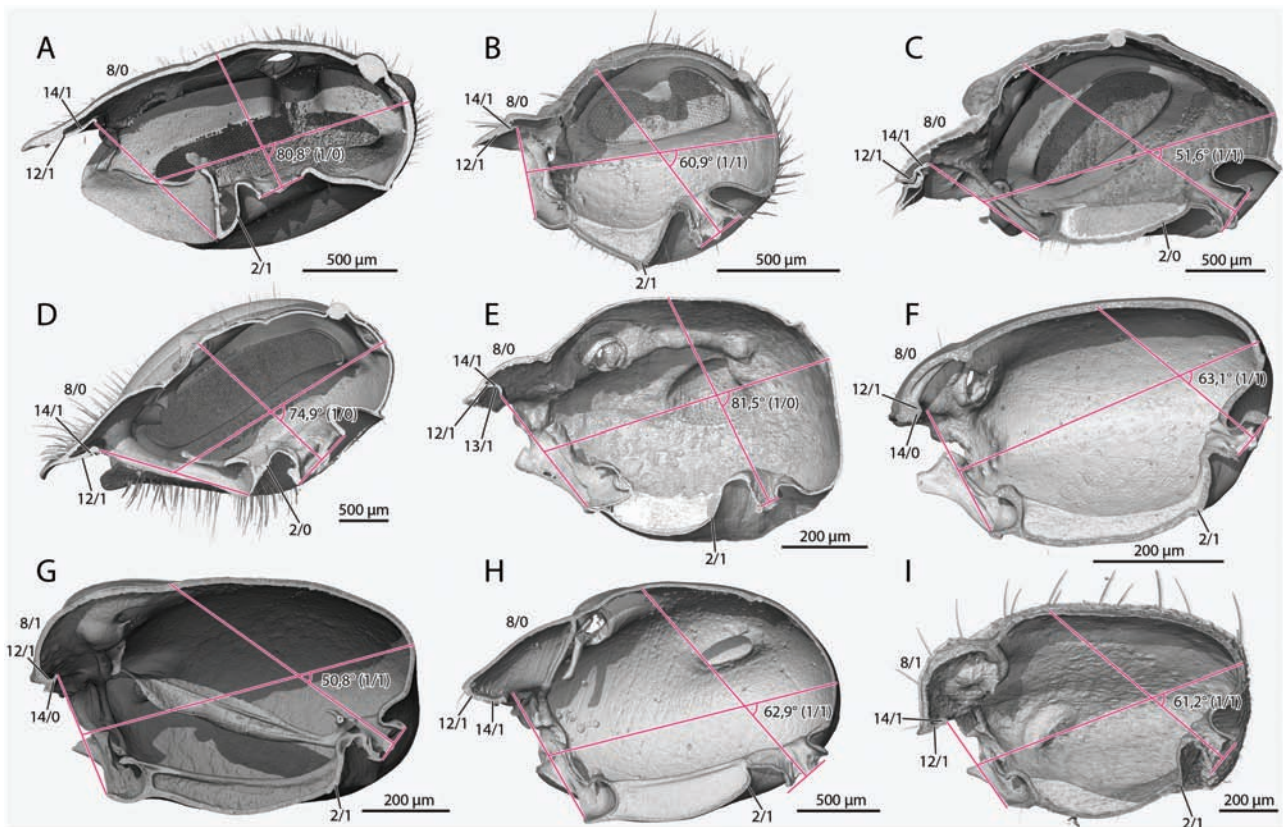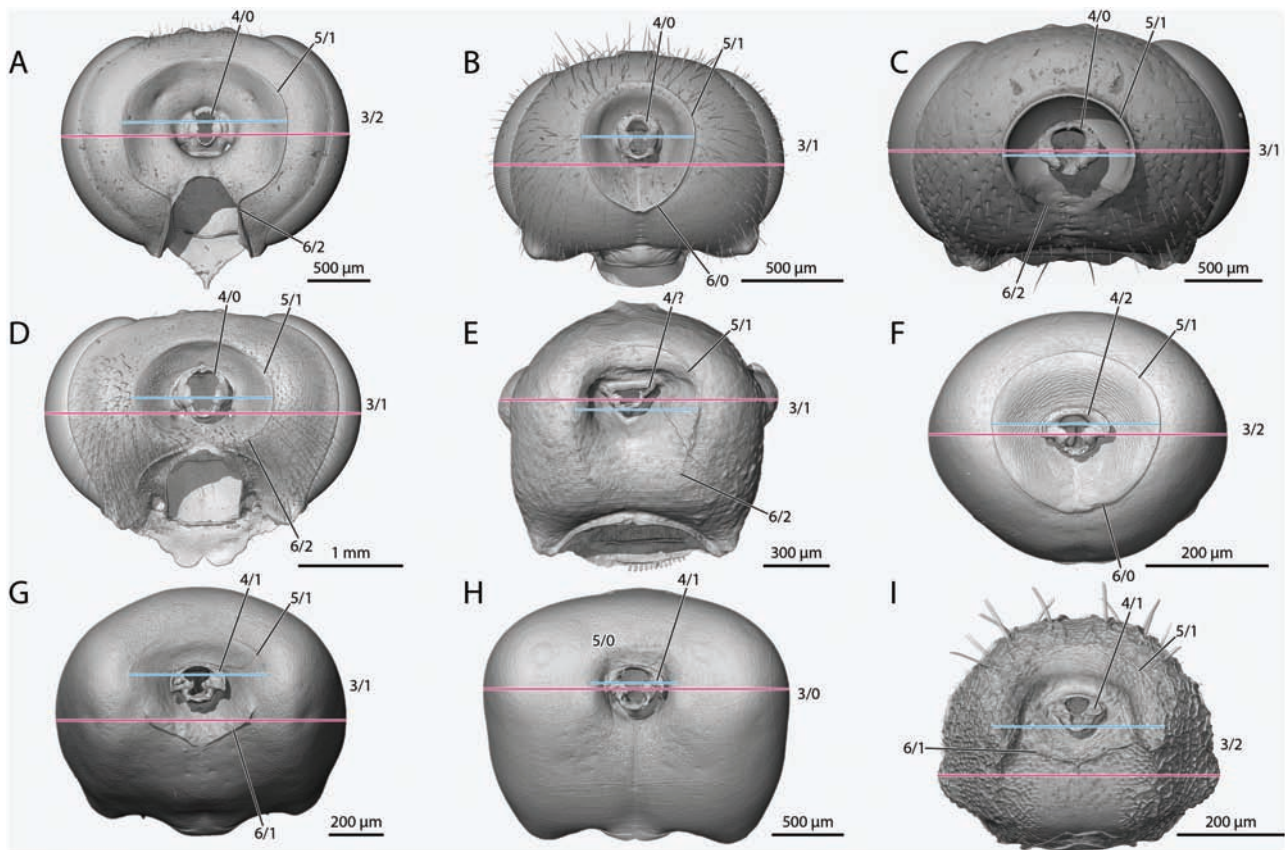
Char. 1, 2, 8, 12–14. 3D reconstruction of the head capsule in sagittal view, **A:** *Parischnogaster* sp., **B:** *Methocha* sp., **C:** *Ampulex* sp., **D:** *Sceliphron caementarium*, **E:** †*Gerontoformica gracilis*, **F:** *Protanilla lini*, **G:** *Brachyponera luteipes*, **H:** *Formica rufa*, **I:** *Wasmannia affinis*. **Char. 1:** 'head orientation angle', (**0**): above 70°, (**1**): below 70°. **Char. 2:** Subforaminal groove, (**0**): absent, (**1**): present. **Char. 8:** Orientation of the distal clypeus, (**0**): horizontal, (**1**): transverse. **Char. 12:** Clypeal inflection, (**0**): absent, (**1**): present. **Char. 13:** Clypeal inflection curvature, (**0**): straight, (**1**): concave. **Char. 14:** Clypeal inflection length, (**0**): long, (**1**): very short/reduced. General note for all character figures: If a character state is not labeled in some species, it is always the opposite of the one labeled in the others.

The fimbriate line is a groove with a series of hairs that extends along the medial ('masticatory') margin on the inner side of the mandible in crown Formicidae (Fig. 10E). In contrast, it runs along the 'basal margin' in †*Gerontoformica* (Fig. 10D), *Ampulex* (Char. 102C), and *Methocha* (Char. 102B). The line ends on or slightly proximad the subapical tooth in these genera and some bee species, whereas it almost reaches the tip of the apical tooth in *Sceliphron* (Char. 102D) and various bees (Michener and Fraser 1978). Only a very short line of setae is present on the inner side of the subapical tooth in *Parischnogaster* (Char. 102A). In all crown ants of our sample, this line of hairs subtends the masticatory margin proximad the subapical tooth (Char. 102F–I). Assuming that the fimbriate line roughly retains its relative position on the mandible, it appears likely that the line is indeed a part of the original basal margin which forms most of the crown formicid masticatory edge (scenario 2).

Even though the shovel-shaped mandible is also present in *Protanilla* of Leptanillinae (Richter et al. 2021), it is questionable whether this condition belongs to the groundplan of Leptanillomorpha, the sistergroup of the poneroformicine ants. In this clade, the enigmatic *Martialis heureka* Rabeling and Verhaagh, 2018 has a very elongate falcate mandible with one large subapical tooth and several small denticles both proximad and distad of it (Brandão et al. 2010). *Opamyrma hungvuong* Yamane, Bui and Eguchi, 2008, has a narrow, falcate mandible with just one apical tooth with several denticles along the 'basal' margin (Yamada et al. 2020). Species of the genus *Leptanilla* appear somewhat intermediate between the falcate and the shovel forms, possibly with irregular denticles inserted between the apical and subapical teeth

(Keller 2011). As the inner side of the mandible is not documented for any of these genera, their mandibular shapes are difficult to interpret. Considering the subordinate position of *Protanilla* in Leptanillomorpha, it is conceivable that the distinctly elongated shovel-shaped mandible found in this genus and other members of Anomalomyrmini/*Protanilla sensu lato* (e.g., Borowiec et al. 2011, Griebenow 2021) has evolved independently.

Mandibular Development The evolutionary transformations of the mandible could likely be better traced with an approach including developmental biology. By disentangling developmental processes shaping the mandibles of ant species, we may learn how these programs changed throughout evolution. Boudinot et al. (2021) presented several hypotheses on mandibular formation. This includes the developmental specification of the apical point, proximodistal elongation of the mandible, its torsion and curvature, the formation of the 'tooth line' (gnathal edge on the medial side, usually separated into masticatory and basal margin), the determination of the basal angle, the lateromedial expansion of the blade, and the formation of teeth at certain areas of the gnathal edge. We add here that there may be different ways in which the mandible is expanded, based on how different regions and margins are specified. This also means that teeth or denticles can be inserted in different regions. There are some hints in ant mandible morphology that there is actually a difference between individually specified 'teeth' or 'incisors' and 'denticles' that may better be described as serration of the gnathal edge specified by an iterative, space-dependent program (e.g., between

Char. 3–6. 3D reconstruction of the head capsule in view onto the occipital foramen, **A**: *Parischnogaster* sp., **B**: *Methocha* sp., **C**: *Ampulex* sp., **D**: *Sceliphron caementarium*, **E**: †*Gerontoformica gracilis*, **F**: *Protanilla lini*, **G**: *Brachyponera luteipes*, **H**: *Formica rufa*, **I**: *Wasmannia affinis*. **Char. 3**: Relative occipital region width, (**0**): < 30%, (**1**): < 30% < 50%, (**2**) > 50%. **Char. 4**: Upper postoccipital arch relative to lower, (**0**): same size, (**1**): larger, (**2**): much larger. **Char. 5**: Occipital carina, (**0**): absent, (**1**): present. **Char. 6**: Occipital carina extent, (**0**): complete circle, (**1**): separated into super- and subforaminal arches, (**2**): open.

the apical and subapical tooth or between apical tooth and basal angle). For example, we interpret as support of this idea the regular interchanging development of larger teeth and smaller denticles on the mandibles of *Brachyponera*, *Formica*, and many Dolichoderinae (e.g., Shattuck 1992) or the small intercalary denticles observed in some amblyoponines (Yoshimura and Fisher 2012).

Experimental manipulation of mandibular development, such as creating a falcate condition instead of a shovel-shaped mandible, may reveal how the points, margins, and zones of the mandible are morphogenetically defined, and thus prone to evolutionary transformations. As falcate mandibles similar to those of stem ant females such as †*Gerontoformica* do occur in males of some living ant species such as *Prionopelta* (Yoshimura and Fisher 2012), comparison of male and female development may be a promising step in this direction. Unfortunately, the investigation of the development of the insect mandible is still in its infancy. There are currently only few studies that specifically deal with this topic, most of them focused on beetles (Gotoh et al. 2011, 2014, 2017; Angelini et al. 2012; Coulcher et al. 2013; Okada et al. 2019) or termites (Sugime et al. 2019).

Several of the available studies on mandible patterning were focused on the formation of enlarged mandibles in male beetles. Dependent on nutrition, they are regulated by juvenile hormone (JH) expression at specific points in their development (Gotoh et al. 2011), but also more specifically by insulin-like growth factors (Okada et al. 2019) and depending on sex by interaction of *doublesex* with JH (Gotoh et al. 2014). In termite soldiers, expression of *dachshund*, regulated by several other factors, is responsible for elongation of

the medial part of the mandible (Sugime et al. 2019). An influence of *dachshund* on mandibular elongation was also observed in male stag beetles, where it additionally influenced the development of the serration of the blade, whereas larger teeth were regulated by other factors (*al* and *hth*) (Gotoh et al. 2017). It is possible, therefore, that the putative incisors and denticles could be regulated by different networks.

The expression patterns observed by Coulcher (2013) in *Tribolium castaneum* (Herbst, 1797) beetles suggest that the mandibular mola and the incisor develop from only one endite (in contrast to the two different endites that form the maxillary galea and lacinia). A mola does not occur in ants and was also not reported in any other hymenopteran groups with the exception of Xyelidae and a few other sawflies (Beutel and Vilhelmsen 2007). Similar studies on expression patterns in the early developing hymenopteran mandible could help clarify what happened to this part of the mandible during evolution and if it was exapted for a different function in the ant mandible, for example, if it could represent the part of the gnathal edge that is subtended by the fimbriate line. Similar synergistic effects of paleoentomology and evo devo research have, for example, been achieved in the elucidation of segmentation and limb identity patterns in the evolution of Arthropoda (Chipman and Edgecombe 2019), highlighting the value of considering paleontological findings in an evo devo framework (and vice versa).

Changes in the Mandibular Musculature

Not only the mandible but also its muscles have a distinct range of variation in total clade Formicidae. Gronenberg et al. (1997)
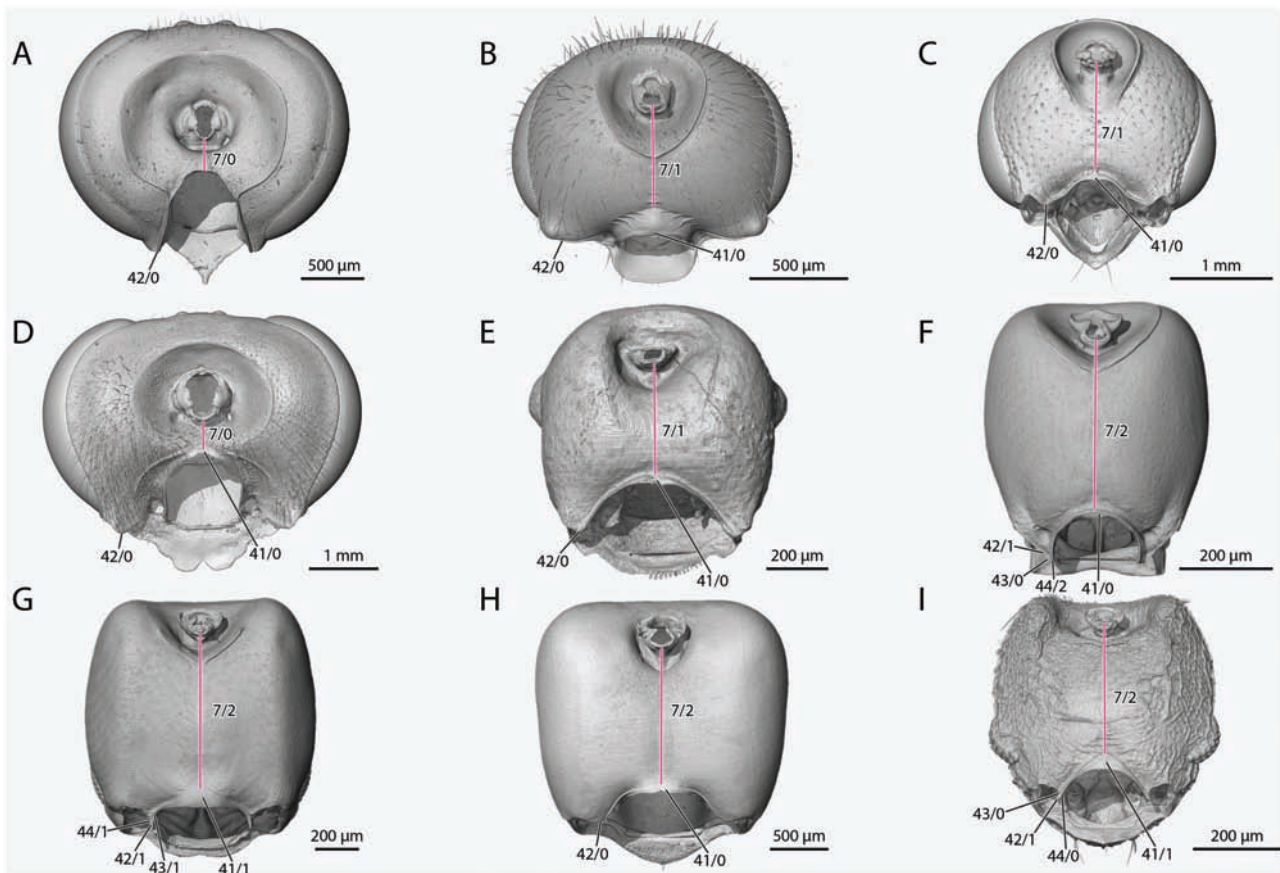
Char. 7, 41–44. 3D reconstruction of the head capsule in ventral view, **A:** *Parischnogaster* sp., **B:** *Methocha* sp., **C:** *Ampulex* sp., **D:** *Sceliphron caementarium*, **E:** †*Gerontoformica gracilis,* **F:** *Protanilla lini*, **G:** *Brachyponera luteipes*, **H:** *Formica rufa*, **I:** *Wasmannia affinis*. **Char. 7:** Length of the postgenal bridge relative to head length, (**0**): < 20%, (**1**): < 20% x < 50%, (**2**) > 50%. **Char. 41:** Medial portion of outer hypostomal carina, (**0**): not expanded, (**1**): expanded. **Char. 42:** Hypostomal teeth, (**0**): absent, (**1**): present. **Char. 43:** Hypostomal teeth orientation relative to outer hypostomal carina, (**0**): parallel, (**1**): angled. **Char. 44:** Hypostomal teeth shape, (**0**): thin, short, (**1**): thin, elongated, (**2**): broadly triangular.

recognized three different attachment types: 1) fibers with long sarcomeres attached to the apodeme via thin cuticular fibers, 2) fibers with long sarcomeres directly attached to the apodeme, and 3) directly attached fibers with short sarcomeres. Short fibers enable fast mandible closure, whereas long sarcomeres are suitable for slow but powerful closure. In modern ants, these fiber types occur in different proportions corresponding with the lifestyle. In other groups of Hymenoptera, only one fiber type was identified so far, with sarcomeres similar to the long variety of ants (Gronenberg et al. 1997). We confirm that only directly attached fibers occur in our outgroup taxa, although our µ-CT scan data were not of sufficient resolution to measure sarcomere lengths.

We also found only directly attached fibers in †*Gerontoformica*, indicating that the plesiomorphic condition of the adductor was maintained, which conforms with the plesiomorphic mandibular shape. Even scans with the highest resolution did not reveal the sarcomere length of all fibers, but we were able to measure some of the longer sarcomeres occurring in their mandibular adductor. We found that they are about 3.6 µm long on average, a value between the ranges of 'long' and 'short' sarcomeres reported by Gronenberg et al. (1997) for modern ants, although closer to the average 'short' length. Additionally, parts of some fibers had much longer sarcomeres of about 7 µm, and in some other regions no sarcomeres were visible at all (Fig. 2D). Two central bundles of fibers showed no visible sarcomeres along the complete fiber length. As these bundles

correspond in position with fibers with short sarcomeres in living ants (Gronenberg et al. 1997; Richter et al. 2020, 2021), we assume that the sarcomeres here are too short to be visualized with our maximum resolution. A similar effect was observed in µ-CT scans of *Protanilla lini* (Richter et al. 2021). This tentatively suggests that two of three different fiber types of living ant species were already present in †*Gerontoformica*.

It has to be noted that the mandibular muscles of our fossil were deformed and not perfectly preserved. This likely explains the heterogeneous appearance of some of the 'long' sarcomere fibers but may potentially also create the impression that different fiber types are present. Henwood (1992a) observed significant shrinkage of muscle fiber size in fossilized insect flight muscles from Dominican amber. Therefore, we cannot exclude shrinkage that may have affected the sarcomere length in our case. Nevertheless, two conclusions appear justified based on our data. The absence of fibers that attach via fibrillae is a plesiomorphy retained by †*Gerontoformica*, whereas a certain level of sarcomere length differentiation is an apomorphic condition compared to aculeatan outgroup taxa. Based on the measured short sarcomere length it appears likely that the mandibular flexor of †*Gerontoformica* was mainly suitable for fast closure, which would have been advantageous for prey capture, suggesting that these Cretaceous ants may have been effective predators.

The lack of fibers attached by filaments may also play a role here. The initially hypothesized advantage of the filaments was an
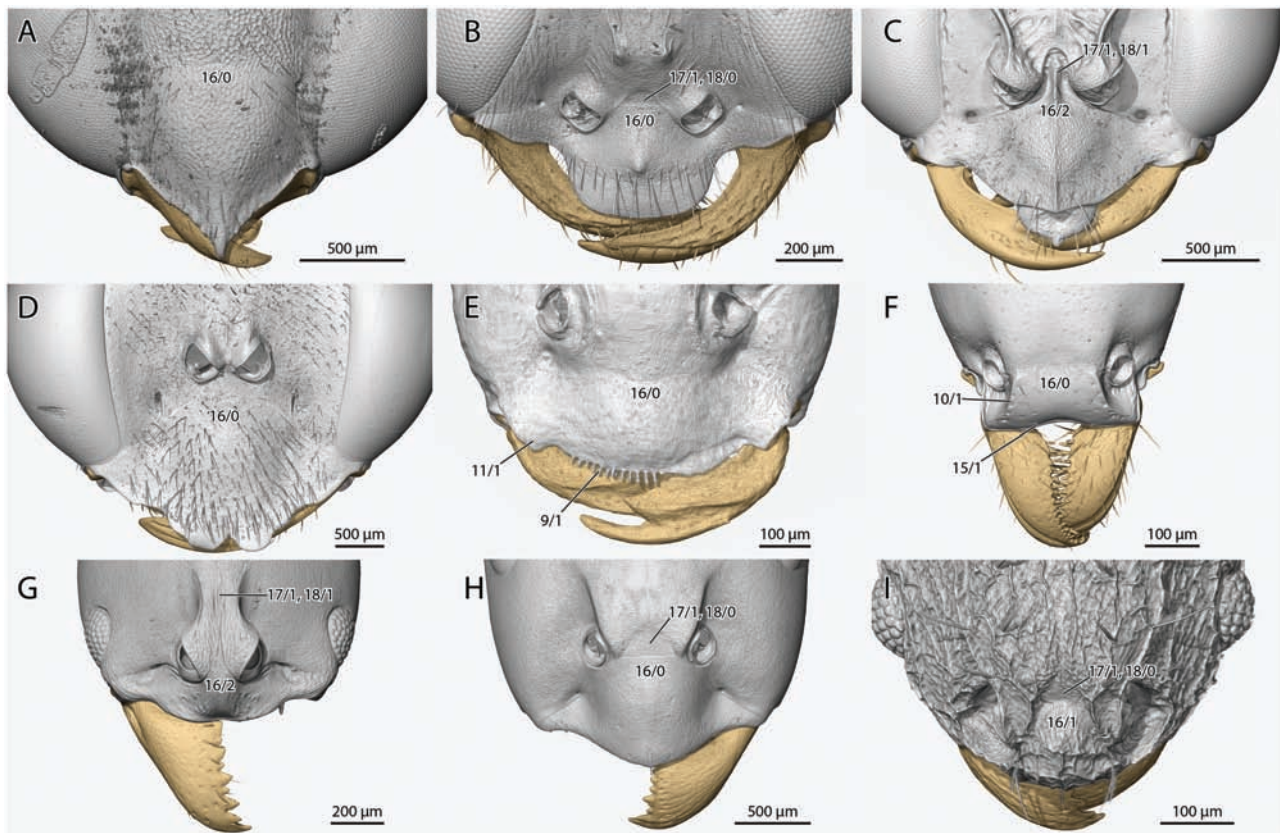
Char. 9–11, 15–18. 3D reconstruction of the clypeus in dorsal view, **A:** *Parischnogaster* sp., **B:** *Methocha* sp., **C:** *Ampulex* sp., **D:** *Sceliphron caementarium*, **E:** †*Gerontoformica gracilis,* **F:** *Protanilla lini*, **G:** *Brachyponera luteipes*, **H:** *Formica rufa*, **I:** *Wasmannia affinis*. **Char. 9:** Clypeal chaetae, (**0**): absent, (**1**): present. **Char. 10:** Medial portion of clypeus raised at right angle, (**0**): absent, (**1**): present. **Char. 11:** Anterolateral clypeal process, (**0**): absent, (**1**): present. **Char. 15:** Anterior clypeal margin concave, (**0**): absent, (**1**): present. **Char. 16:** Posterior clypeal margin shape, (**0**): straight, (**1**): curved, (**2**): pointed. **Char. 17:** 'Frontal triangle', (**0**): absent, (**1**): present. **Char. 18:** 'Frontal triangle' shape, (**0**): distinct triangle, (**1**): indistinct ovoid.

optimal usage of space in the head, increasing the number of fibers inserting on the apodeme (Gronenberg et al. 1997, Paul et al. 1999). However, Püffel et al. (2021) more recently argued that this could be also achieved by enlarging the main apodeme and adding additional main branches of it, rather than thin fibrillae. Considering the large apodeme branches of †*Gerontoformica gracilis*, this is likely the solution realized in this species. It is conceivable that fibers attached via fibrillae are advantageous energetically compared to an enlargement of the tendon, which requires space and considerable amounts of cuticular material. Presumably, this could thus be another step on the way to 'inexpensive' hence more expendable workers, which is a key to ant success hypothesized by Peeters and Ito (2015). Alternatively, Püffel et al. (2021) also list consequences of how filament-attachment can alter how muscle contraction translates to apodeme motion. Filament-attached fibers are shorter and thus slower. As a consequence, their absence in †*Gerontoformica gracilis* also supports the idea of rapidly closing mandibles and the idea that it is a functional optimization for this species' needs.

Specimens of other stem group ants with a well-preserved 0md1 muscle could be very informative in the context of highly divergent mandibular shapes in †Haidomyrmecinae (Barden et al. 2020) and †Zigrasimeciinae (Cao et al. 2020). Living specialized genera like *Odontomachus* (Gronenberg et al. 1997) and *Strumigenys* (Booher et al. 2021) are characterized by mandibular muscle fiber composition and arrangement that is specialized for certain types of mandibular movement. It is thus conceivable that these unusual stem group ants also possessed specialized arrangements of different fiber types. An analysis of their mandibular muscle fibers may allow us to infer how their mandibles were used and thus get closer to understanding their lifestyle. Our results show that such analyses may indeed be possible if the right fossils are found, allowing for the pursuit of a new avenue to study the potential lifestyle of 100-million-year-old species.

Conclusions

We present the first detailed and nearly complete 3D-reconstruction of cephalic structures of a Cretaceous insect. The preservation in the head of our specimen of †*Gerontoformica gracilis* is higher than in most or all previously described fossils with internal soft tissue preservation. Our study highlights the potential of investigating amber fossils using high resolution μ-CT. We were able to reconstruct and analyze histological details such as different brain regions, individual gland cells, the digestive tract, and most of the cephalic muscles down to the level of individual sarcomeres. In a comparison of our fossil to living ants and several wasp outgroup taxa, this allowed us to define more than 80 characters that have never been used in phylogenetic reconstructions of ants before. Although our taxon sampling was too limited for an exhaustive analysis of character evolution, parsimony-based character mapping on current molecular trees still recovered a high number of character transitions, especially for the total and crown clades of
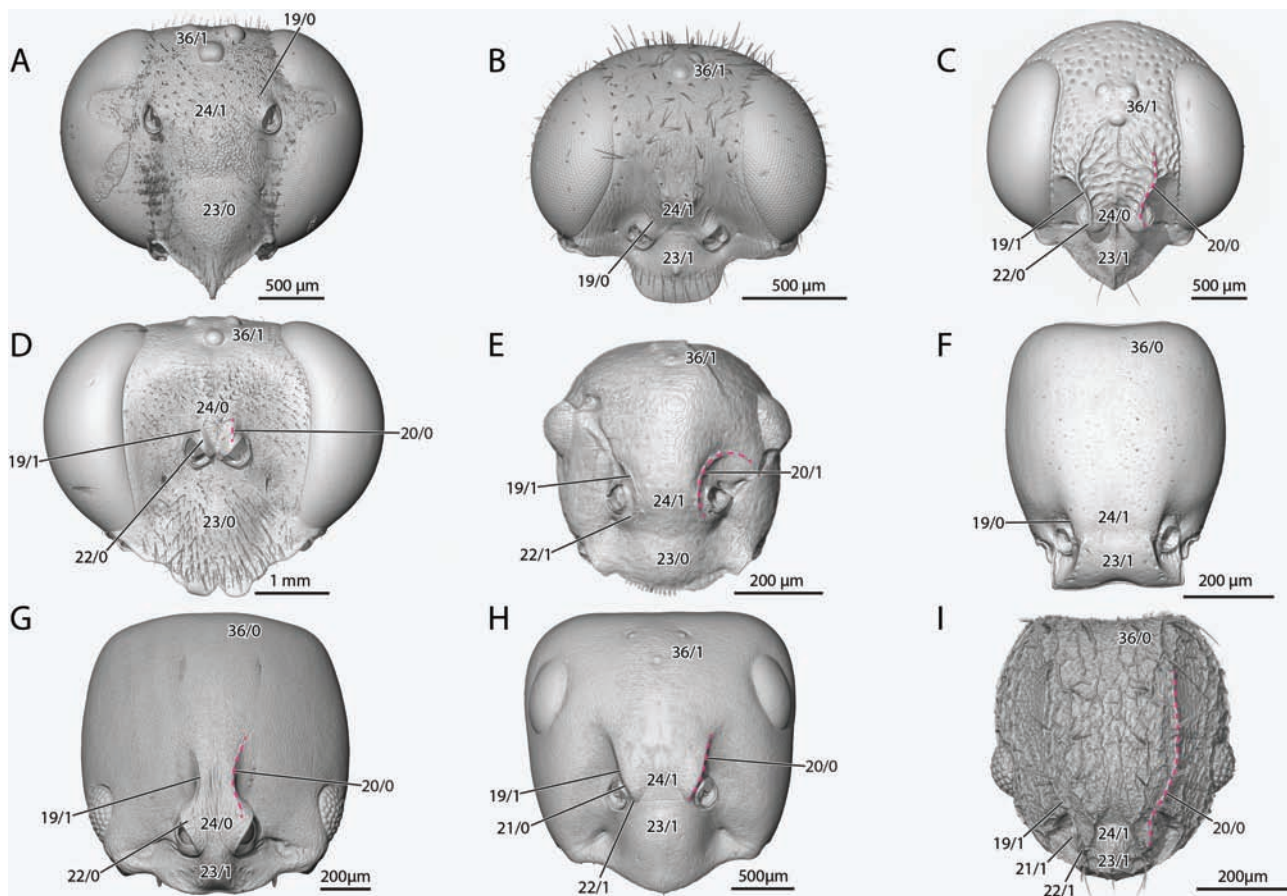
Char. 19–24, 36. 3D reconstruction of the head capsule in dorsal view, **A**: *Parischnogaster* sp., **B**: *Methocha* sp., **C**: *Ampulex* sp., **D**: *Sceliphron caementarium*, **E**: †*Gerontoformica gracilis*, **F**: *Protanilla lini*, **G**: *Brachyponera luteipes*, **H**: *Formica rufa*, **I**: *Wasmannia affinis*. **Char. 19**: Frontal carina/ protuberance, (**0**): absent, (**1**): present (marked with magenta dotted line). **Char. 20**: Frontal carina shape, (**0**): longitudinally oriented, (**1**): half circle. **Char. 21**: Frontal lobe, (**0**): absent, (**1**): present. **Char. 22**: Frontal carina anterior terminus, (**0**): on torulus, (**1**): medial to torulus. **Char. 23**: Posterior clypeal margin, (**0**): not reaching between toruli, (**1**): reaching between toruli. **Char. 24**: Distance between toruli, (**0**): less than one torulus diameter, (**1**): more than one torulus diameter. **Char. 36**: Ocelli, (**0**): absent, (**1**): present.

the Formicidae. From these results we hypothesize scenarios for the early evolution of ants.

Among the newly defined characters, we recovered a basally curved pedicel, presence of the pharyngeal gland, shortened dorsal tentorial arms, and a transverse line of setae on the labrum as synapomorphies of the total clade Formicidae. Potential apomorphies of crown Formicidae are two characters of the rarely studied hypostoma, the specific shape of the mandibular atala, the 'shovel shape' of the mandible, muscle fibers attached via filaments to the mandibular adductor, and the separation of the longitudinal epipharyngeal muscle into two distinctive pairs. We discuss the evolution of these and several other characters and what their implications may have been for the lifestyle of stem group ants. Well-developed paraglossae, transverse ridges in the buccal tube, and the specific morphology of the mandibles and their adductor muscles indicate that these ants may have been efficient predators. We furthermore discuss different hypotheses how falcate mandibles of †*Gerontoformica* and related stem group ants may have transformed into the shovel shape that is typical for many crown Formicidae. This shovel shape may have been one of the key features allowing the survival of crown ants after the collapse of the forest system at the K/Pg boundary, enabling them to dig elaborate underground nests more effectively.

Supplementary Data

Supplementary data are available at *Insect Systematics and Diversity* online.

Character List

Characters that were used in phylogenetic analysis for the first time in this study are marked with *. In some cases, similar character statements can be found in the literature, although the exact definition differs from the one here employed; these features are marked with ~.

Variability categories:

1. Variability little known: Variation detected but only investigated in few species, so overall variability and phylogenetic informative value uncertain.
2. Variability incompletely explored. Variation occurs beyond what is coded here for the investigated taxa but is difficult to define as discrete characters/ states. More detailed evaluation involving additional taxa may reveal more information. This is also true for shape characters that might benefit from different types of analyses if more taxa are considered.
3. Variability known but not sampled. Variation is known from the literature beyond what is documented and coded here, but
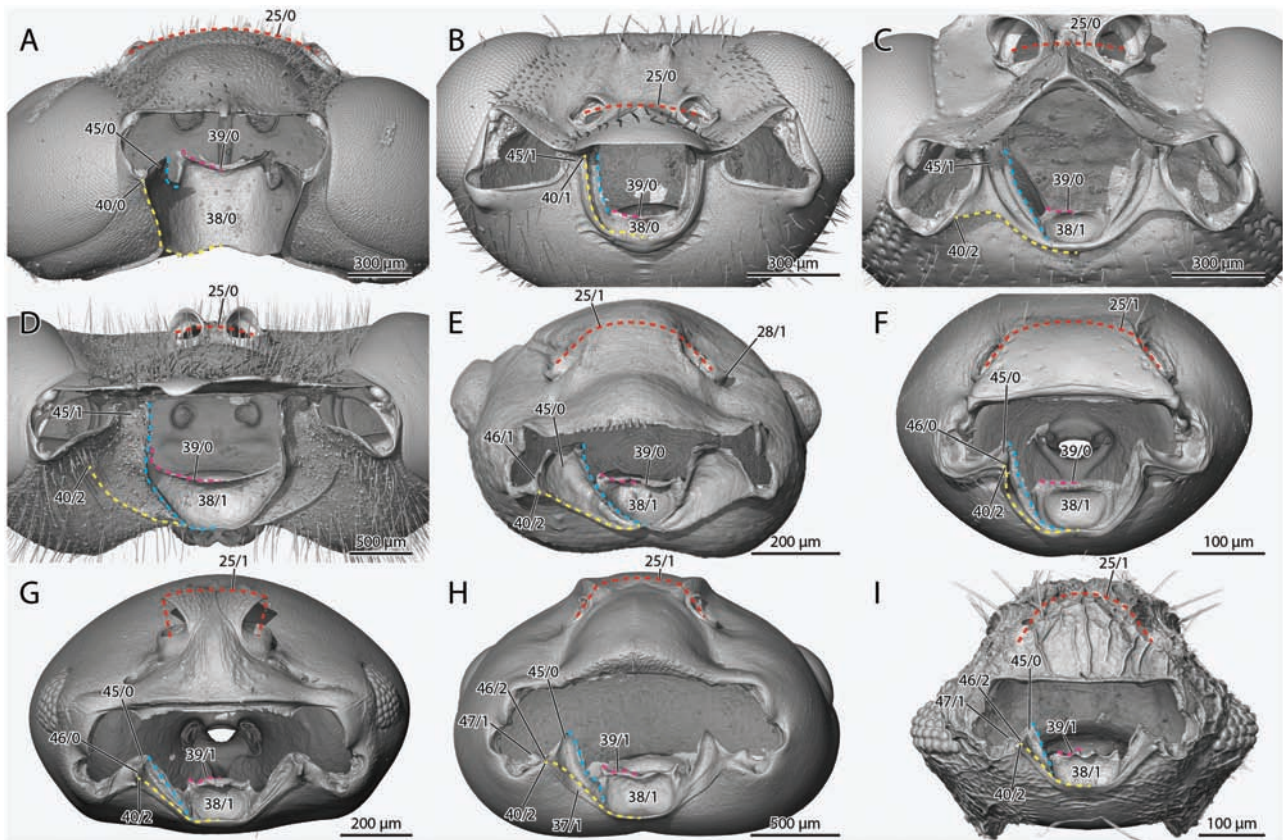
Char. 25, 28, 37–40, 45–47. 3D reconstruction of the head capsule in oral view, **A:** *Parischnogaster* sp., **B:** *Methocha* sp., **C:** *Ampulex* sp., **D:** *Sceliphron caementarium*, **E:** †*Gerontoformica gracilis*, **F:** *Protanilla lini*, **G:** *Brachyponera luteipes*, **H:** *Formica rufa*, **I:** *Wasmannia affinis*. **Char. 25:** Frontal region between toruli (marked by red dotted line), (**0**): flat, (**1**): bulging. **Char. 28:** Lateral torular arch, (**0**): as high or lower as medial arch, (**1**): higher than medial arch. **Char. 37:** Lateral outer hypostomal carina shape (marked by yellow dotted line), (**0**): straight, (**1**): twisted inward 90°. **Char. 38:** Hypostomal groove, (**0**): undivided, (**1**): divided by inner hypostomal carina (marked by cyan dotted line). **Char. 39:** Oral hypostomal carina shape, marked by magenta dotted line (**0**): straight or evenly curved, (**1**): sinuous/ shouldered. **Char. 40:** Lateral termination outer hypostomal carina, (**0**): at pleurostomal fossa, (**1**): at hypostomal triangular process apex, (**2**): between hypostomal triangular process and pleurostomal fossa. **Char. 45:** Hypostomal triangular process fusion to clypeus, (**0**): absent, (**1**): present. **Char. 46:** Alignment of hypostomal corner with hypostomal triangular process, (**0**): aligned, (**1**): shifted medially with connecting margin straight to convex, (**2**): shifted medially with connecting margin concave. **Char. 47:** Hypostomal knob medial to the pleurostomal fossa, (**0**): absent, (**1**): present.

this variation not presently covered due to our limited taxon sampling.

4. Variability known and sampled. Variation known, coded here and also previously used in phylogenetic analyses (but worded differently here in some cases).

Head capsule

1.~ Head orientation. Head orientation or relative mouth orientation, as defined by the angle between the normal vector of the "occipital plane" (the plane of the occipital foramen) and a longitudinal line drawn through the head that is itself defined by two points, one of the oral foramen and one which is the most distant from the oral point; (1) the oral point is the center point of a line between the inner margin of the clypeal inflection and the distalmost point of the hypostoma, and (2) the distant point is the point of the head capsule cuticle that is furthest away from the first point: This angle more than 70° (**0**), or less than 70° (**1**).

Given the complicated nature of hymenopteran head orientation, we attempted to measure an angle in the head that would give an impression of "anatomical head orientation", expressing how much the anatomy of the head itself would tend towards

prognathism (or an orthognathous orientation). We defined this angle as the following: On render images of sagittal sections through the head we drew a line from the oral margin of the clypeal inflection to the distalmost point of the hypostomal carina. From the middle point of this line, we drew a line to the posterior margin of the head in a way as to maximize the length of this line. Second, we drew a line through the occipital foramen, connecting the distalmost dorsal and ventral points of the postocciput. In †*Gerontoformica*, the dorsal margin of the postocciput is truncated, so we instead drew the shortest possible line from this point to the ventral arch of the postocciput. Finally, we set an orthogonal line through the midpoint of this occipital plane and measured the angle between this orthogonal line and the longitudinal headline generated previously using the measurement tool. We discretized the resulting angles into two character states, but alternatively, this variable could be treated as a continuous character, evaluating the exact angles. The measured angle is most likely correlated with other characters defined here. Traditionally, the orientation of the head is coded so as to distinguish between the "prognathous" condition on one hand and "hypognathous" or "orthognathous" condition on the other. Note, however, that both latter terms occur as synonyms in the Hymenoptera literature but are otherwise clearly distinguished (see, e.g., Beutel et al. 2014). This traditional coding
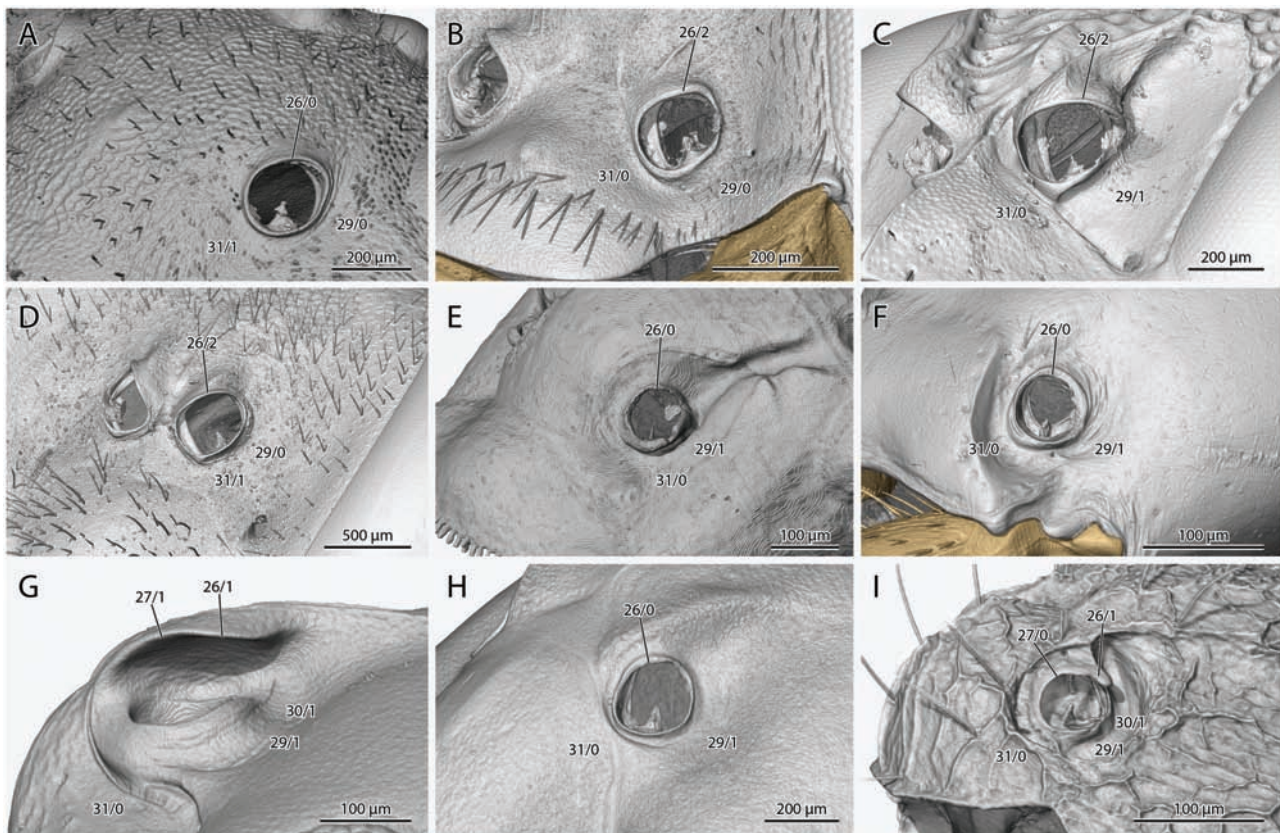
Char. 26, 27, 29–31. 3D reconstruction of the torulus in oblique dorsal frontolateral view with the exception of G which is laterally oriented to better illustrate the structures, **A**: *Parischnogaster* sp., **B**: *Methocha* sp., **C**: *Ampulex* sp., **D**: *Sceliphron caementarium*, **E**: †*Gerontoformica gracilis*, **F**: *Protanilla lini*, **G**: *Brachyponera luteipes*, **H**: *Formica rufa*, **I**: *Wasmannia affinis*. **Char. 26**: Medial torular arch, (**0**): not expanded, (**1**): expanded as posterolaterally oriented lobe, (**2**): expanded anteriorly directed lobe. **Char. 27**: Posterolaterally directed torular lobe, (**0**): continuous with lateral arch, (**1**): disassociated from lateral arch. **Char. 29**: Shape of area posterolaterad the torulus (**0**): flat, (**1**): at least slightly concave. **Char. 30**: Peritorular groove, (**0**): absent, (**1**): present. **Char. 31**: Position of toruli relative to epistomal sulcus (**0**): directly at, (**1**): at least somewhat separated.

is generally based on the orientation of the longitudinal axis of the head relative to the longitudinal axis of the remaining body (although see Ward and Brady 2003 for a coding closer to the one suggested here). However, the traditional coding clearly oversimplifies the phenomenon of the orientation of the head within Hymenoptera (see discussion).

Hymenoptera were very likely orthognathous in their groundplan (Beutel and Vilhelmsen 2007), and a prognathous condition has obviously evolved several times independently. These independent origins were achieved by complex and varying character transformations, which suggests that coding individual structural features linked with the cephalic orientation will be more informative than a summary statement "prognathism". A more complete understanding of the phenomenon will require increased taxon sampling and more-detailed structural investigations. This will likely be facilitated by 3D geometric morphometrics analyses. In the present list, we have provisionally included this "cephalic angle" character as an approximation of hypognathous and prognathous conditions to give a general overview of changes in the cephalic orientation, including the orientation of the occipital foramen. The other character clearly affecting the head orientation (and thus also the calculated angle) is the length of the postgenal bridge (Char. 7), but other features related to the shape of the occipital and postoccipital regions (Char. 3–6) may also play a role, and also further modifications in these areas as well as the oral foramen area (not coded here).

In our taxon sampling, only *Parischnogaster*, *Sceliphron* and †*Gerontoformica* had a high angle indicating a more orthognathous orientation, with the caveats of flexibility and in the case of †*Gerontoformica* the incomplete preservation of the postocciput. That all other taxa have a clearly lower angle indicating prognathism signifies the several independent modifications of cephalic orientation within Aculeata. Category 4 (as "prognathism", e.g. Baroni Urbani et al. 1992: char. 1, Prentice 1998, Beutel and Vilhelmsen 2007: char. 2, Keller 2011: char. 1, Barden and Grimaldi 2016: char. 1, Boudinot et al. 2022c: char. 11).

2.* Subforaminal groove presence. Shape of region of postgenal bridge directly below postocciput: without impression, thus almost on same level as remaining postgenal bridge (**0**), impressed, thus with strong bend or angle in sagittal view, forming distinct subforaminal groove (**1**).

If present, the subforaminal groove is integrated into the overall concavity of the occipital region. The angle and groove were observed to be present in all studied ant species including †*Gerontoformica*, at least to some degree (the groove is less distinct in *Formica*). Among outgroups, the groove is also very distinct in *Methocha*. The postgenal bridge of *Parischnogaster* is very short and sharply curved, thus we have coded the groove as present. In contrast, the postgenal bridge of *Ampulex* and *Sceliphron* is only very slightly convex, thus the subforaminal groove is absent. Category 2.

3.~ Relative occiput size. Diameter of occipital concavity relative to width of posterior half of head capsule (as seen from posterior
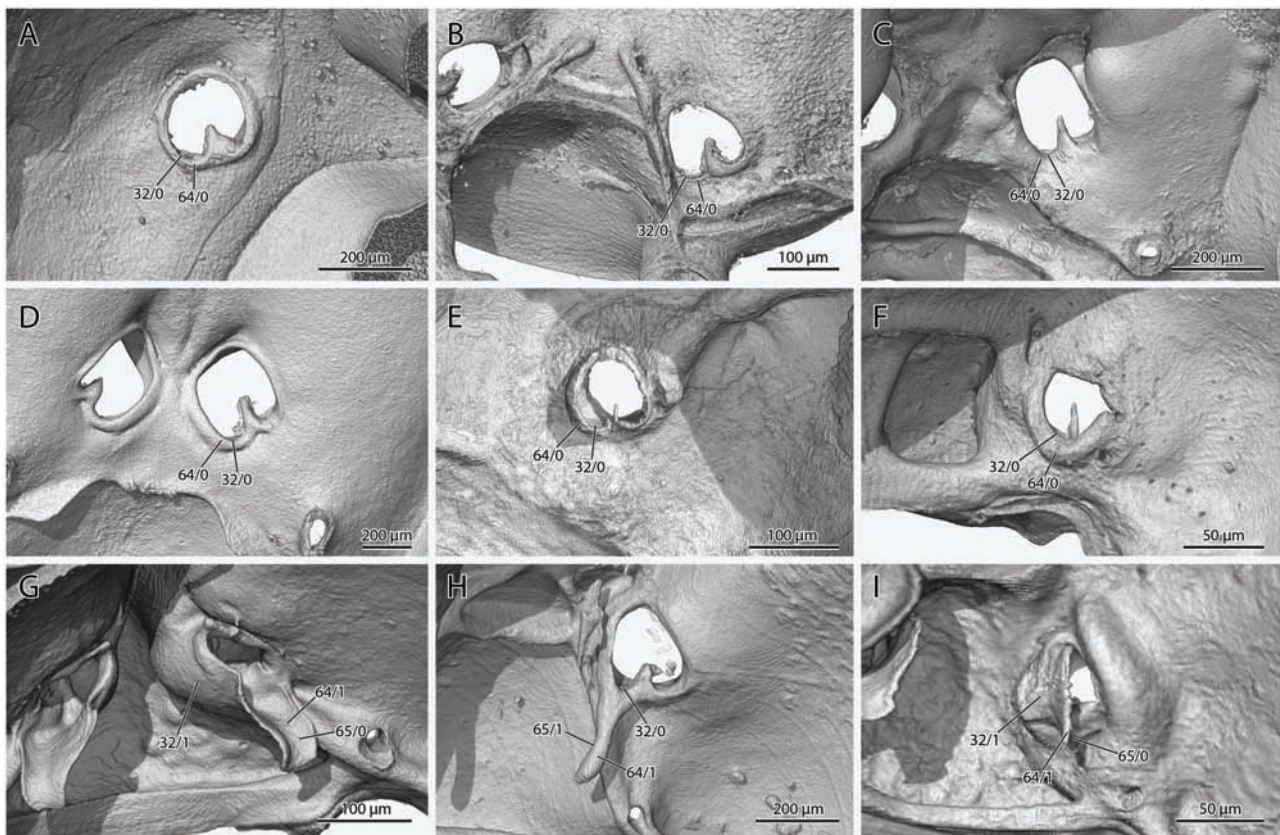
Char. 32, 64, 65. 3D reconstruction of the antennal foramen and torulus in internal view, **A**: *Parischnogaster* sp., **B**: *Methocha* sp., **C**: *Ampulex* sp., **D**: *Sceliphron caementarium*, **E**: †*Gerontoformica gracilis,* **F**: *Protanilla lini*, **G**: *Brachyponera luteipes*, **H**: *Formica rufa*, **I**: *Wasmannia affinis*. **Char. 32**: Antennal acetabulum, (**0**): flat, (**1**): bulbous cavity. **Char. 64**: Torular apodeme, (**0**): absent, (**1**): present. **Char. 65**: Torular apodeme shape, (**0**): flat sheet, (**1**): cylindrical rod.

view, with the occipital foramen in viewing plane): less than 30% (**0**), or between 30 and 50% (**1**), or more than 50%, thus "hypertrophied" (**2**).

State 1 of this character applies to most taxa considered here, but there are two exceptions. *Formica rufa* displays only a small concavity surrounding the postocciput, whereas the occipital region comprises a large proportion of the head capsule in *Protanilla lini* (hypertrophied). The categories chosen here are arbitrarily discretized, but they can also be evaluated as a continuous character. Boudinot et al. 2022c coded a "hypertrophied" occipital region as characteristic of *Opamyrma* (Leptanillinae), with an occipital region that covers the whole head width. Category 2.

4.* Postocciput shape. Size of dorsal/ posterior postoccipital arch relative to ventral/ anterior arch: of similar size (**0**), or distinctly larger (**1**), or dorsal arch massively widened and elongated (**2**).

The postocciput is divided into dorsal and ventral arches by a pair of condyles at midheight (these being the "postoccipital condyles"). The dorsal and ventral arches of the postocciput are of similar lateromedial width in the sampled outgroup taxa, giving the externally visible foramen a roughly circular to oval shape. In the ants, however, the dorsal arch is distinctly enlarged and widened relative to the ventral arch, giving the foramen a roughly triangular or mushroom-shaped appearance. In *Protanilla lini*, the dorsal arch is exceptionally large, and in addition to its increased width, it is much longer and more massive than the ventral one, possibly correlated with the pronounced forward orientation of the head (Richter et al. 2021); this feature also affects the "head orientation angle" discussed above. The postocciput in the investigated species of *Parischnogaster* is greatly reduced and not collar-like as in the

other taxa included. The reduced condition of *Parischnogaster* is also observed in previously investigated vespid species (e.g., Duncan 1939), but not in most other groups of Aculeata (Zimmermann and Vilhelmsen 2016), suggesting that this condition is possibly an apomorphy of the Vespidae. Zimmermann and Vilhelmsen (2016) describe distinctly extended dorsolateral corners of the occipital foramen for several non-aculeate apocritans, but based on their images we interpret this as a different character than the one described here as it does not relate to an expansion of the postoccipital collar. Category 1.

5. Occipital carina: absent (**0**), or present (**1**).

Among our sample of taxa, the carina is absent only in *Formica*. Presence of the carina is variable across Formicidae (Boudinot et al. 2022c) and often relevant on lower taxonomic levels within the family (e.g., in Myrmeciinae, Hasegawa and Crozier 2006). Occipital carina presence is also variable among Aculeata (missing, e.g., in *Sapyga*, Zimmermann and Vilhelmsen 2016) and the Hymenoptera more broadly. Vilhelmsen (2011) did not interpret the carina as a part of the groundplan but did note its presence in several symphytan lineages and general occurrence in Apocrita. Category 4 (e.g. Vilhelmsen 2011: char. 20, Zimmermann and Vilhelmsen 2016: char. 32, Boudinot et al. 2022c: char. 21).

6. ~(Reductive.) Occipital carina. Extent and completeness: completely encircling occipital concavity (**0**), or separated into superforaminal arch and subforaminal carina (**1**), or reaching onto postgenal bridge but not connecting as a complete circle and lacking subforaminal carina (**2**).

Among the taxa here sampled, the carina reaches onto the postgenal bridge without completely closing as a circle in
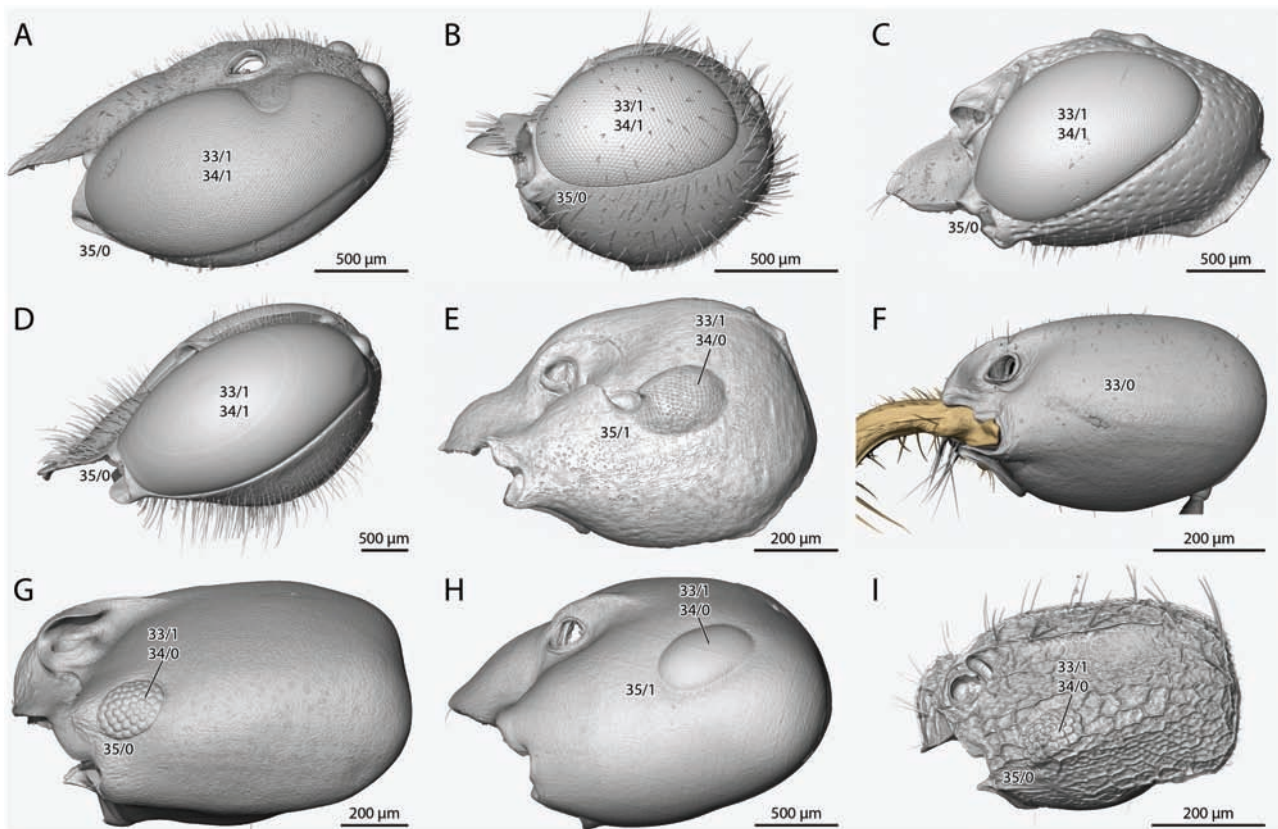
Char. 33–35. 3D reconstruction of the head capsule in lateral view, **A:** *Parischnogaster* sp., **B:** *Methocha* sp., **C:** *Ampulex* sp., **D:** *Sceliphron caementarium,* **E:** †*Gerontoformica gracilis,* **F:** *Protanilla lini,* **G:** *Brachyponera luteipes,* **H:** *Formica rufa,* **I:** *Wasmannia affinis.* **Char. 33:** Compound eyes, (**0**): absent, (**1**): present. **Char. 34:** Compound eye size, (**0**): covering less than half head width, (**1**): covering at least half head width. **Char. 35:** Compound eye position, (**0**): anterior half of head, (**1**): posterior half of head.

†*Gerontoformica*, *Ampulex*, *Sceliphron*, and *Parischnogaster*. Note that the terminal points of the carina on the ventral/ posterior surface of the head capsule depends on the combination of (1) degree of postgenal bridge elongation, (2) variation in the shape of the carina, and (3) relative size of the occipital region. For example, the hypostomal bridges of *Parischnogaster* and *Sceliphron* are similar in length, but the occiput is larger in the former and the carina contacts the hypostomal carina (also due to the deeply concave hypostomal region), while the occiput is smaller in the latter and the carina peters out before the hypostoma. Completely enclosed occipital regions are known in various crown ants, such as *Martialis*, *Thaumatomyrmex*, some *Aphaenogaster*, and some *Apterostigma*, among others, and is also confirmed here for *Protanilla* (Richter et al. 2021) and the outgroup genus *Methocha*. A ridge-like structure completely enclosing the occipital concavity is also present in *Brachyponera* and *Wasmannia*, although in a different way to the previously mentioned taxa. Specifically, the primary carina is obliterated before reaching the postgenal bridge but a secondary carina is present at the margin of the subforaminal groove. The condition (**1**) in these genera is conceivably a variation of the completely encircling character state. However, as the polarity and the sequence of transformations are currently unclear, it is treated as a separate state of an unordered character. Dependent on presence in Char. 5. Category 3. (Similar characters in Vilhelmsen 2011, char. 21, Zimmermann and Vilhelmsen 2016, char. 33, Boudinot et al. 2022c, char. 22)

7.~ Postgenal bridge. Length of bridge relative to length of head capsule (measured as ratio between length from hypostomal sulcus to lower margin of occipital foramen and head length): less than 20% (**0**), or 20–50% (**1**), or more than 50% (**2**).

The states defined here are arbitrarily discretized but can be treated alternatively as a continuous character. As noted above, this character affects the angle used to define prognathism (Char. 1), but because the angle of the head depends on different factors, it is not strictly correlated with the postgenal bridge length. In species with a wide angle, for instance, the postgenal bridge can be relatively long (as in †*Gerontoformica*, 42 % versus the 12% of *Parischnogaster*, both with a comparable angle around 80°). A strongly elongated postgenal bridge (leading to a ratio of more than 50%) is characteristic of crown ants, especially so for *Protanilla* and *Brachyponera* (both 64%). †*Gerontoformica*, *Ampulex*, and *Methocha* show a moderately elongated bridge (around 40%), while the bridges of *Parischnogaster* and *Sceliphron* are very short (12 %). Category 2. (Similar characters in Vilhelmsen 2011, char. 14, Sharkey et al. 2012, char. 12, Boudinot et al. 2022c, char. 10)

8.* Clypeus. Orientation: clypeus evenly sloping in lateral view, continuing curvature of frontal (facial) region (**0**), or clypeus strongly curved, approximately vertically oriented orally, forming distinct angle with frontal surface (**1**).

This condition is arguably correlated with the relative position of the antennal sockets, as the approximately vertical condition occurs in taxa with toruli located close to the anterior cephalic margin (see also character 4 of Keller 2011). However, the clypeus appears gently sloping in *Protanilla* (Richter et al 2021), even though the antennal sockets are very close to the anterior edge of the head. This suggests that that the clypeal slope and the position of the antennal sockets
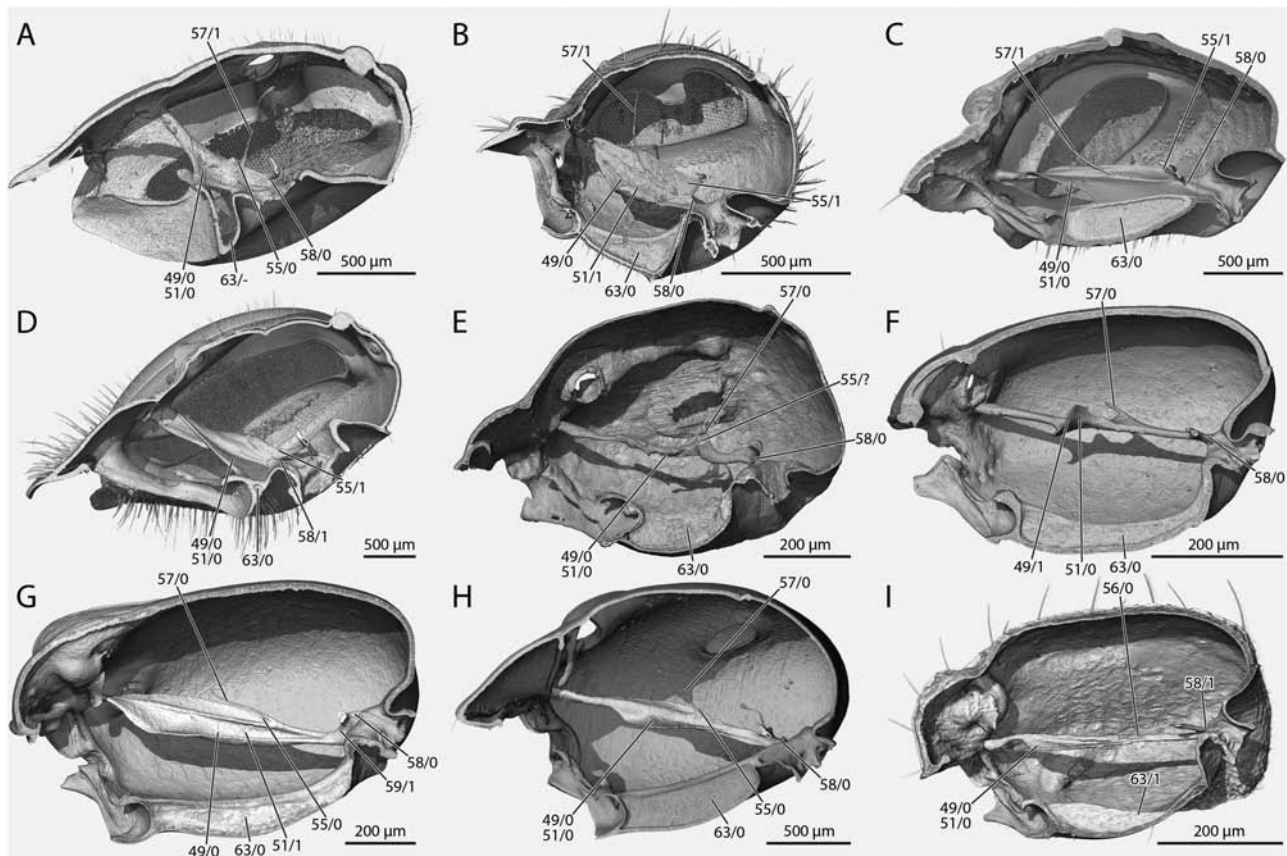
Char. 49, 51, 55–59, 63. 3D reconstruction of the tentorium in sagittal view, **A:** *Parischnogaster* sp., **B:** *Methocha* sp., **C:** *Ampulex* sp., **D:** *Sceliphron caementarium*, **E:** †*Gerontoformica gracilis,* **F:** *Protanilla lini,* **G:** *Brachyponera luteipes,* **H:** *Formica rufa,* **I:** *Wasmannia affinis.* **Char. 49:** Medial tentorial lamella orientation to anterior arm, (**0**): parallel, (**1**): twisted, perpendicular. **Char. 51:** Medial tentorial lamella shape, (**0**): flat, (**1**): deeply concave. **Char. 55:** Extent of lateral tentorial lamella, (**0**): up to dorsal tentorial arm, (**1**): up to tentorial bridge. **Char. 56:** Dorsal tentorial arm, (**0**): absent, (**1**): present. **Char. 57:** Dorsal tentorial arm length, (**0**): less than 1/3. of anterior arm, (**1**): more than 1/3 of anterior arm. **Char. 58:** Posterior tentorial arm length, (**0**): not reduced, distinct arm, (**1**): reduced, no distinct arm. **Char. 59:** Anterior arm bent ventrad posteriorly, (**0**): absent, (**1**): present. **Char. 63:** Postgenal ridge, (**0**): reaching postocciput, (**1**): not reaching postocciput.

may not be strictly correlated. Among sampled taxa, the vertical orientation occurs only in *Brachyponera* and *Wasmannia*, suggesting that this is a derived condition within Formicidae. In *Methocha* and *Ampulex*, the clypeus curves slightly upward relative to the frontal curvature. This is coded as (0) here. Category 2.

9. Chaetae ("traction setae") on anterior clypeal margin: absent (**0**), or present (**1**).

Presence of a row of distinctly thickened setae, or chaetae, on the anterior margin of the clypeus is characteristic for †*Gerontoformica* (e.g., Barden and Grimaldi 2014), certain other stem group ants such as †Zigrasimeciinae (e.g., Perrichot 2014; Cao et al. 2020), and some extant taxa such as Amblyoponinae (e.g., Yoshimura and Fisher 2012; Ward and Fisher 2016). Specific differences in the configuration of these chaetae may also turn out as phylogenetically informative for a broader sampling of taxa (see, e.g., Boudinot et al. 2022c, Keller 2011 Char. 2). Such setae were not observed in any of the other taxa considered here. Category 3. (Barden and Grimaldi 2016: char. 3, Boudinot et al. 2022c: char. 97)

10. Clypeus shape. Median clypeal portion distinctly raised with approximately right-angled lateral and posterior margins (**0**), or clypeus not raised or if raised without right-angled margins (**1**).

A shelf-like medial clypeal portion occurs in *Protanilla* in our taxon sampling, but a similar shape of the anterior clypeus was also found in the leptanilline *Opamyrma* (Yamada et al. 2020), indicating that this condition might be secondarily lost in *Leptanilla*. It does

not occur outside of Leptanillinae in this exact configuration (see also, e.g., Baroni Urbani et al. 1992; Boudinot 2015). Category 2. (Baroni Urbani et al. 1992: char. 5, Boudinot et al. 2022c: char. 83)

11. Lateral clypeal lobes. Anterolateral portions of clypeus extended as roughly triangular lobate process: absent (**0**), or present (**1**).

This condition is unique to †*Gerontoformica* in our taxon sampling, but similar processes also occur in other stem ants. Category 4. (Boudinot et al. 2022c: char. 90)

12. Anterior inflection of clypeus: absent (**0**), or present (**1**).

In all groups of Hymenoptera, the true distal (oral) margin of the clypeus is inflected and thus lies below the remaining clypeal region and points backwards (/dorsad) instead of forwards (/ventrad) (Beutel and Vilhelmsen 2007). Consequently, the apparent "distal margin" of the clypeus is in fact the clypeal inflection point (here usually termed "anterior margin of clypeus"). This character is phylogenetically uninformative within Hymenoptera but coded here as it is linked with the following two characters. Category 4. (e.g. Beutel and Vilhelmsen 2007: char. 10, Vilhelmsen 2011: char. 11)

13.* (Reductive.) Shape of inflected clypeal surface in sagittal section: straight or convex (**0**), or concave (**1**).

Based on our 3D-reconstruction, the inflected (posteriorly directed) clypeal surface is distinctly concave in †*Gerontoformica*. It is straight in all other evaluated taxa except for *Ampulex*, where a strongly convex bulge is present distally with a proximal shallow
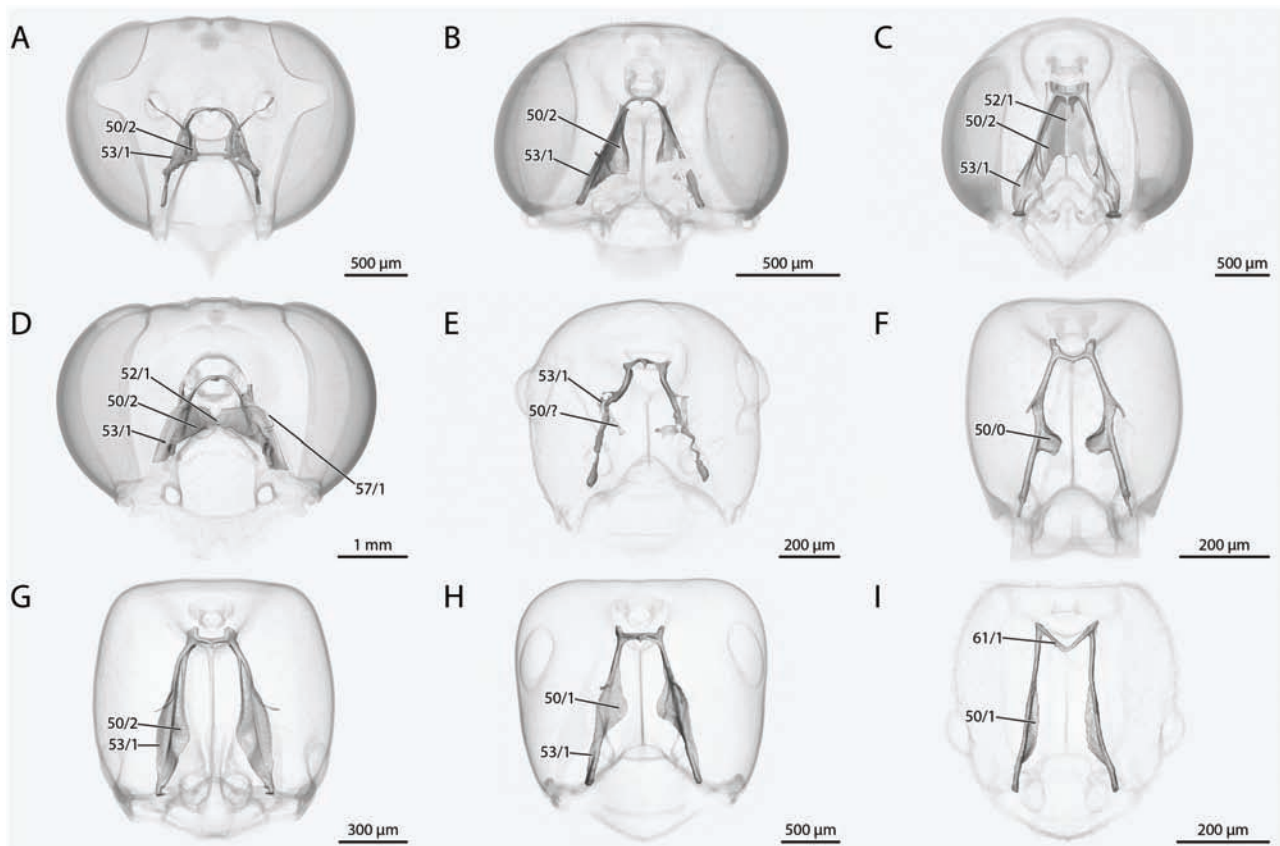
Char. 50, 52, 53, 61. 3D reconstruction of the tentorium in dorsal/ facial view, **A:** *Parischnogaster* sp., **B:** *Methocha* sp., **C:** *Ampulex* sp., **D:** *Sceliphron caementarium,* **E:** †*Gerontoformica gracilis,* **F:** *Protanilla lini,* **G:** *Brachyponera luteipes,* **H:** *Formica rufa,* **I:** *Wasmannia affinis.* **Char. 50:** Medial tentorial lamella size, (**0**): short lobe, (**1**): mid-sized lobe, (**2**): spanning most of anterior arm. **Char. 52:** Secondary tentorial bridge, (**0**): absent, (**1**): present. **Char. 53:** Lateral tentorial lamella, (**0**): absent, (**1**): present. **Char. 61:** Anteroposterior tentorial bridge shape, (**0**): straight or curved, (**1**): V-shaped.

concavity connected to the highly modified labrum. Detailed investigation of other stem group ants should be conducted, as the condition observed in †*Gerontoformica* might be an artefact. Dependent on presence in Char. 12. Category 1.

14.* (Reductive.) Length of clypeal inflection along midline: very short, almost completely reduced (**0**), or long and distinct (**1**).

The clypeal inflection has never been investigated in detail before, and the range of its variability is largely unknown. An almost completely reduced inflection was observed in *Protanilla lini* and *Brachyponera luteipes*, although that of *Wasmannia affinis* is also comparatively short. The clypeal inflection is especially long in all outgroup taxa, although it varies distinctly in shape and extension. Scoring the shape and length of the inflection are a first approximation to a phylogenetic assessment of this characteristic hymenopteran feature. Dependent on presence in Char. 12. Category 1.

15.* Clypeus form. Laterodistal corners of clypeus produced anteriorly, resulting in flat median concavity: absent (**0**), or present (**1**).

The presence was only observed in *Protanilla* so far (Richter et al. 2021) and is variable within the genus and the closely related genus *Anomalomyrma* (see all images under *Protanilla* and *Anomalomyrma* on antweb.org) in the level of depression of the median concavity. The produced laterodistal clypeal corners end with the distal clypeal knobs, which are part of the modified mandibular articulation. The lateral inflected clypeal surfaces are broad and cover the mandibular bases in frontal view, while the inflected surface is short medially (see Char. 17).

16. Clypeus shape. Curvature of posteromedian margin of clypeus: straight (**0**), or curved (**1**), or pointed (**2**).

The range of variation is arguably linked with Character 24, as the pointed condition occurs mainly in taxa with a very thin and strip-like clypeus, where the antennae are closely approximated medially. However, the clypeus is not thin and strip like in *Ampulex*, which shares the closely approximated antennae, and it still has a pointed margin pointing between the approximated antennal sockets. Therefore, the character is retained as independent until more taxa are coded for this feature. Category 3. (partly treated in Keller 2011: char. 5)

17. "Frontal triangle". Supraclypeal area close to epistomal sulcus distinctly visible as groove or with different surface sculpture: absent (**0**), or present (**1**).

The supraclypeal area or "frontal triangle" is an enigmatic structure. When it is developed, it often has an extremely distinct cuticular structure. Sometimes its area is internally very clearly delimited by ridges, as in *Formica* and *Methocha*, although the area is interestingly not very distinct externally in the latter taxon. Such clear borders or margins are absent in all other species investigated and only cuticular structure and more or less indistinct sulci delimit it externally (as in *Ampulex*, *Brachyponera* and *Wasmannia*). A differentiated supraclypeal area is missing completely in *Parischnogaster*, *Sceliphron*, and *Protanilla*. When present, its position between the antennal sockets and clypeus suggests a certain degree of correlation with the specific condition of these surrounding structures. A clear influence on the shape of the area can be attributed to the distance
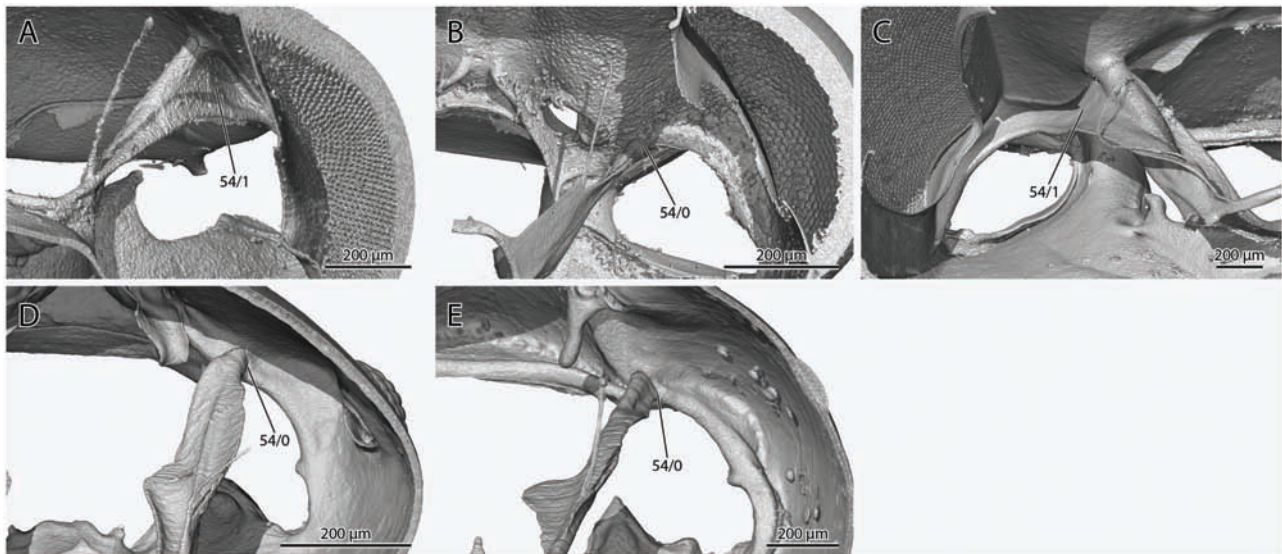
Char. 54. 3D reconstruction of the tentorium in inner posterior view, **A**: *Parischnogaster* sp., **B**: *Ampulex* sp., **C**: *Sceliphron caementarium*, **D**: *Brachyponera luteipes*, **E**: *Formica rufa*. Note that *Methocha*, †*G. gracilis*, *Protanilla*, and *Wasmannia* are not illustrated for convenienve as their states are sufficiently illustrated by the selected taxa. **Char. 54**: Lateral tentorial lamella fused to head capsule, forming buttress, (**0**): absent, (**1**): present.

between the toruli. The function of this distinctive cuticular area is completely unknown. In *Formica*, our sampled taxon where this feature is most distinct, it lies directly above the antennal ampulla. However, the ampulla is also present in a similar position in species without differentiated supraclypeal area, thus a direct functional association is questionable. Functional and phylogenetic aspects of this structural specialization deserve further attention in the future. Category 2. (partly treated in Keller 2011: char. 5)

18. (Reductive.) Shape of supraclypeal area: distinct and triangular (**0**), or indistinct, elongate and ovoid (**1**).

It is difficult to define the posterior extent of the clypeus and the anterior margin of the supraclypeal area in some species, such as *Brachyponera luteipes*. As the clypeus is highly compressed in *B. luteipes*, the epistomal ridges of both sides run longitudinally along the head capsule until they meet posteriorly. Internally, a part of this area forms the area of origin of the clypeobuccal muscles and can thus be tentatively identified as clypeal. However, the posterior part of this area, which is enclosed by ridges, contains the antennal ampulla, and a skeletal differentiation between these regions is lacking (Richter et al. 2020). This can be interpreted in different ways: the antennal ampulla has possibly "invaded" the clypeal area from elsewhere along the face. Alternatively, the "supraclypeal area" could be fused to the clypeus, or a differentiated supraclypeal area is simply missing. We suggest that the region adjacent to the antennal ampulla is the supraclypeal area in *Brachyponera* and we code its shape accordingly. This is supported by the state observed in *Ampulex*, where the clypeus is more clearly separated from the elongated oval supraclypeal area posterior to it, which is also the location of the antennal ampulla. In contrast, in *Sceliphron* (lacking a differentiated supraclypeal area), the antennal ampulla is located distinctly behind/above the toruli. Future investigations may reveal alternative interpretations. See also the interpretation of Keller (2011), Character 5, for this feature. Dependent on presence in Char. 17. Category 2.

19. Paired frontal carinae or longitudinal protuberances: absent (**0**), or present (**1**).

If present, these structural differentiations are paired longitudinal carinae or protuberances of the frontal area, extending posteriorly from the area of the antennal sockets to the frontal or even vertexal region. In some cases, they appear as weakly margined or unmargined protuberances, rather than as defined longitudinal carinae. Among our sampled taxa, the "protuberance" condition was observed in *Sceliphron* (very small, indistinct), but arguably also in *Formica*. Their function is not entirely clarified; they could deflect or reduce strain exerted by the mandibular adductor muscles; when well developed, they can also physically restrict antennal movements medially, thus preventing overextension and breakage of the proximal articulations of these appendages (Boudinot et al. 2022c). The carinae are coded as absent only in *Parischnogaster*, *Methocha*, and *Protanilla*. *Methocha* does have a pair of short protuberances on the face, but these are far posterad the toruli. Frontal carinae occur variably across the Aculeata (Boudinot et al. 2022c). Categories 2, 4. (Boudinot et al. 2022c: Char. 116)

20. (Reductive.) Orientation of frontal carinae: more-or-less longitudinally oriented along head capsule (**0**), or strongly curved and surrounding antennal socket as semicircle (**1**).

The semicircular shape of the frontal carinae is a specific condition found in †*Gerontoformica*. Shape differences of the frontal carina may yield additional characters in future investigations with a broader sample. Dependent on presence in Char. 19. Category 4. (Boudinot et al. 2022c: char. 120)

21. (Reductive.) Expansion of frontal carinae as "frontal lobes": absent (**0**), or present (**1**).

Frontal lobes are lateral lobe-like expansions of the frontal carinae at the level of the antennal sockets, which they often cover. The term "frontal lobes" has been also applied to other structures. The usage was disambiguated by Keller (2011), who distinguished the frontal lobes of the frontal carinae (Keller: Char. 16) from the medial lobes of the toruli (Keller: Char. 8) and from the posttorular flange (Keller: char. 14). The variation of the torular apparatus is complicated by the frontal carinae, which display multiple possible configurations, including distinct trends towards fusion of several possible involved structures. True "frontal lobes" are only present in *Wasmannia* among our sampled taxa. The complicated character complex deserves more attention in the future. Dependent on presence in Char. 19. Categories 2, 4. (Keller 2011: char. 16, Boudinot et al. 2022c: char. 123)

22.~ (Reductive.) Anterior termination point of frontal carinae: on top of antennal torulus (**0**), or mediad the antennal torulus (**1**).
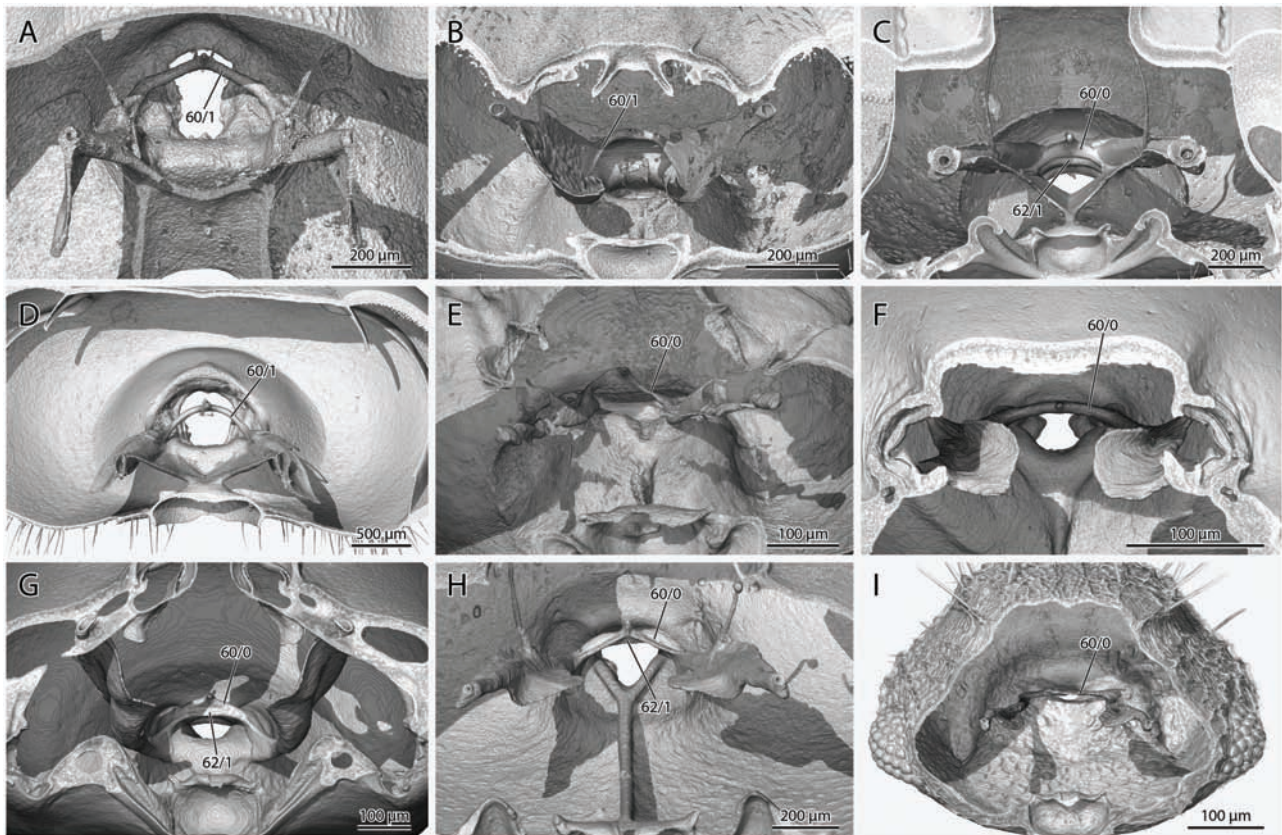
Char. 60, 62. 3D reconstruction of the tentorium in oral view, **A:** *Parischnogaster* sp., **B:** *Methocha* sp., **C:** *Ampulex* sp., **D:** *Sceliphron caementarium*, **E:** †*Gerontoformica gracilis*, **F:** *Protanilla lini*, **G:** *Brachyponera luteipes*, **H:** *Formica rufa*, **I:** *Wasmannia affinis*. **Char. 60:** Tentorial bridge height, (**0**): not raised more than two anterior arm diameters, (**1**): raised by more than two anterior arm diameters. **Char. 62:** Tentorial bridge ventral carina, (**0**): absent, (**1**): present.

The frontal carinae terminate on top of the toruli in *Ampulex* and *Brachyponera*, both of which have distinctly developed torular lobes of different shape (see Char. 26); the small humps corresponding to the carinae in *Sceliphron* also terminate on the medial torular arch. With the exception of *Brachyponera*, the carinae run mediad the toruli in all sampled total clade Formicidae including †*Gerontoformica*, which distinguishes the frontal carinae of ants from those of other aculeates, indicating either an independent origin of the structure or one or more lateromedial shifts of their anterior termination points. Dependent on presence in Char. 19. Category 4. (Similarly used by Boudinot et al. 2022c: char. 117)

23. Torulus position. Position of the toruli relative to clypeus: clypeus not reaching antennal sockets (**0**), or clypeus reaching or projecting between antennal sockets (**1**).

The position of the antennal sockets on the head varies considerably across our investigated taxa and Aculeata more generally. One consequence of this variation is that in many species, the torulus is very closely approximated to the anterior head margin which can lead to the phenomenon that its position is further anterior than the posterior margin of the clypeus, in some cases even pinching part of the lateral clypeus. The antennal sockets reach at least the clypeus in all investigated taxa with the exception of *Parischnogaster*, *Sceliphron*, and †*Gerontoformica*. Category 4. (discussed in Prentice 1998, Keller 2011: char. 5, similar in Brothers 1975: char. 5, used in Sharkey et al: char. 5, Boudinot et al. 2022c: 139)

24. Torulus position. Lateromedial distance between antennal sockets: one or less than one torulus diameter (**0**), or more than one torulus diameter (**1**).

State (**0**) describes the very closely set antennal toruli occurring in *Brachyponera*, *Sceliphron*, and *Ampulex*. The condition is characteristic for most Ponerini ants (Keller 2011) but also occurs in other groups of Formicidae and Aculeata (Boudinot et al. 2022c). All other sampled taxa have the toruli separated by more than one torulus diameter. Category 3, 4. (discussed in Prentice 1998, Keller 2011: char. 5, Boudinot et al. 2022c: char. 141).

25.∼ Frontal bulge. Frontal region between the antennal toruli: flat to weakly convex, at most slightly raised (**0**), or distinctly raised as frontal bulge (**1**).

We evaluated this condition in oral view. If one draws a line connecting the upper margin of the torular acetabula, the frontal region is either roughly parallel to this line (**0**) or raises clearly above it (**1**). The "flat" or non-bulging state occurs in all outgroup taxa we included, whereas the raised state occurs in all sampled members of total clade Formicidae including †*Gerontoformica*. While there is clearly variation in the degree of bulging, this is difficult to quantify so we chose to retain this simplified character statement. The bulging frontal region of the ants results in a torulus that appears to be more laterally directed rather than dorsally (or anteriorly if hypognathous). Keller (2011) described the orientation of the antennal socket apparatus as dorsal (char. 13) relative to the frontal plane, while Boudinot et al. (2022c) interpret the torulus of ants as laterally directed relative to the dorsal (anterior) direction of other Aculeata. Our definition of torular orientation based on the frontal bulge between them is an attempt to reconcile these observations. Category 2, 4. (different definition in Boudinot et al. 2022c: char. 142).
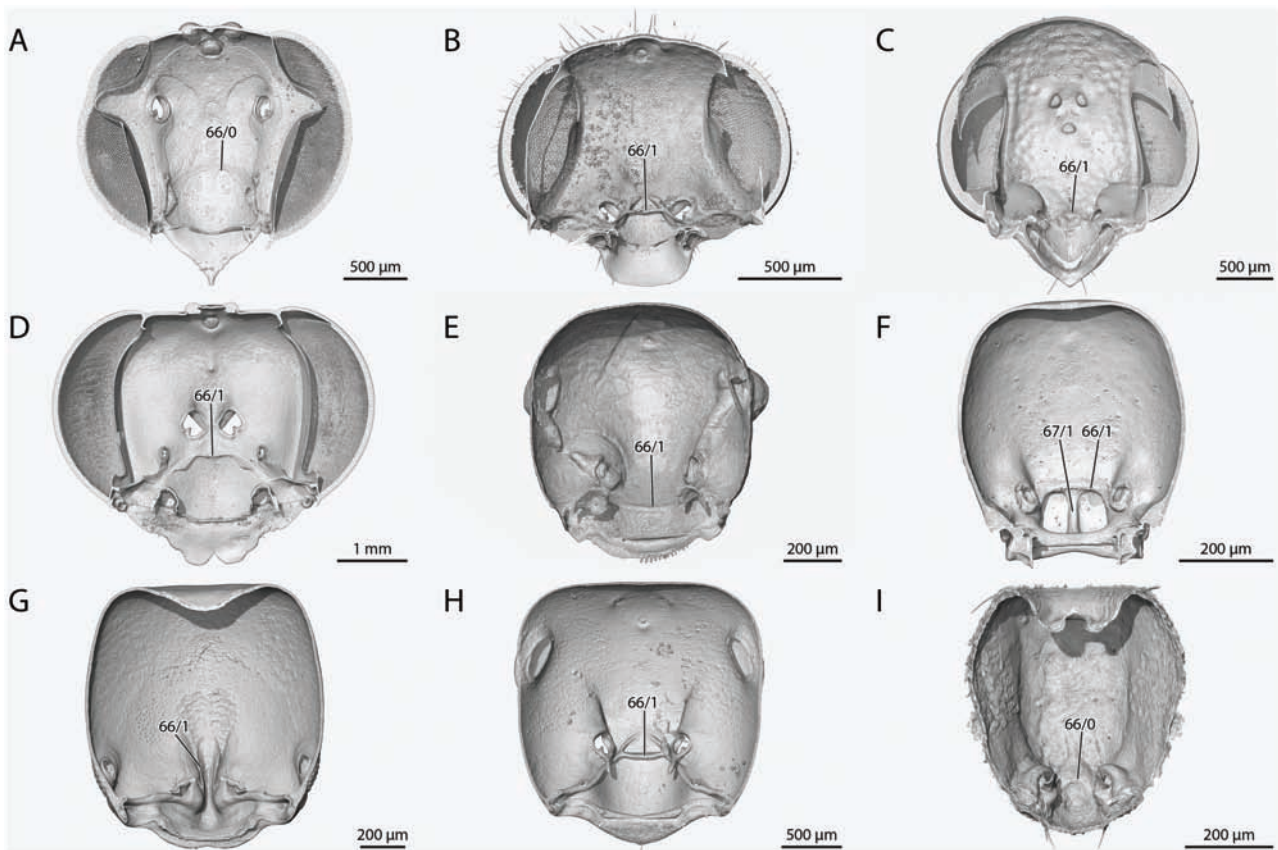
Char. 66, 67. 3D reconstruction of the head capsule cut open in ventral view, **A:** *Parischnogaster* sp., **B:** *Methocha* sp., **C:** *Ampulex* sp., **D:** *Sceliphron caementarium*, **E:** †*Gerontoformica gracilis*, **F:** *Protanilla lini*, **G:** *Brachyponera luteipes*, **H:** *Formica rufa*, **I:** *Wasmannia affinis*. **Char. 66:** Frontoclypeal/ epistomal strengthening ridge, (**0**): absent, (**1**): present. **Char. 67:** Longitudinal clypeal ridge, (**0**): absent, (**1**): present.

26.⁓ Expansion of median torular arch: no expansion (**0**), or expanded, forming posterolaterally expanded lobe (**1**), or expanded as anteriorly directed hood (**2**).

The antennal torulus of ants is extremely variable. It was analyzed in detail for the first time by Keller (2011), who distinguished different, partly interdependent characters. In addition to our coding scheme, further characters and states may be added with a broader taxon sampling. Note that states related to the presence of a posttorular flange (Keller 2011) are not included here, as they do not occur in the limited taxon sampling investigated in the present study. An important observation of Keller (2011) was that the medial and lateral arch of the torulus can vary more-or-less independently from each other, with the medial arch forming variously developed lobe-like expansions. Importantly, this "torular arch" or lobe is not to be confused with the "frontal lobe" which represents an expansion of the frontal carina (Char. 21), although the two different lobes may be fused to differing degrees in some taxa (A. Richter, unpubl. data of *Acromyrmex aspersus*). In our taxon sampling, unexpanded medial arches occur in *Parischnogaster*, †*Gerontoformica, Protanilla*, and *Formica*, while *Wasmannia* and *Brachyponera* show a posterolaterally expanded torular lobe, but see the note for the next character. The median torular arch of both apoid wasps included here is enlarged into a distinct, anteriorly directed hood, which is much larger in *Ampulex*. As a very small hood is also recognizable in *Methocha*, it is also coded as (**2**). Category 2, 4. (Brothers 1975: char. 6, Keller 2011: char. 8)

27.⁓ (Reductive.) Shape of median torular lobe when posterolaterally expanded: medium-sized and continuous with lateral arch (**0**), or large, disassociated from lateral arch (**1**).

Within Formicidae, lobe-like expansions of the median torular arch come in many shapes and can fuse with various other parts of the head cuticle (Keller 2011). Among our sampled taxa, a "normal" or "medium-sized" lobe occurs in *Wasmannia*. The lobe of *Brachyponera*, however, is comparatively large and disassociated from the lateral arch, forming a covered groove that surrounds the bulbus and bulbus neck of the scapus. Keller (2011) distinguished additional states such as a hypertrophied, even larger lobe (char. 8) and fusion of the torular lobe with the posttorular flange, but as these states do not occur among our sampled taxa, they were not defined here. Categories 2, 4. Dependent on state (1) in Char. 26. (Keller 2011: char. 8)

28.⁓ Shape of lateral torular arch: forming a simple rim (**0**), or expanded and barrel-shaped (**1**).

The distinction between these two states is somewhat arbitrary as height of the lateral arch is variable, as is the one of the medial one (see lobe characters above) and the height of the arches is at least partially linked. We tentatively coded the state of †*Gerontoformica* as expanded (**1**) here, as it is the only species where the lateral arch is at least slightly higher than the medial one. The character was previously applied to ponerine ants with a disassociated median arch (Keller, 2011, char. 9) but is treated more widely here to capture the expansion of the lateral arch in †*Gerontoformica*. Categories 2, 3. (Keller 2011: char. 9)
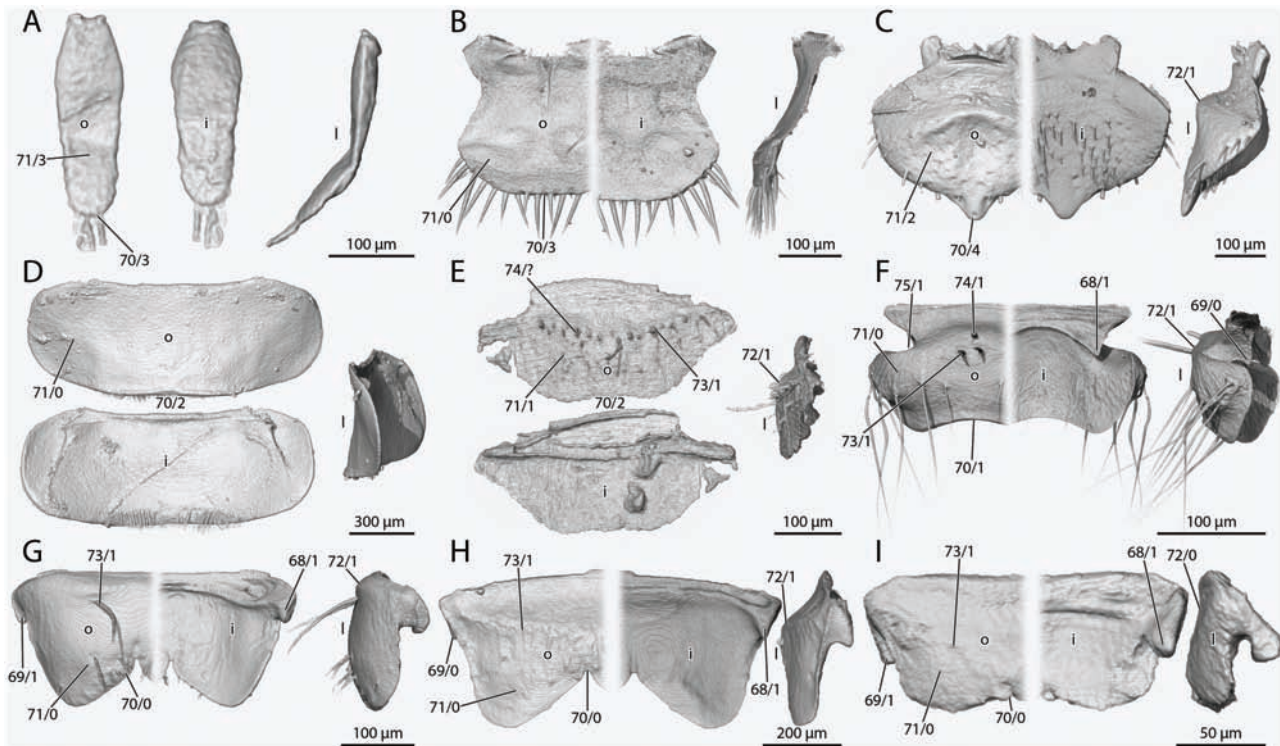
Char. 68–75. 3D reconstruction of the labrum in outer (o), inner (i), and lateral (l) view, **A:** *Parischnogaster* sp., **B:** *Methocha* sp., **C:** *Ampulex* sp., **D:** *Sceliphron caementarium*, **E:** †*Gerontoformica gracilis*, **F:** *Protanilla lini*, **G:** *Brachyponera luteipes*, **H:** *Formica rufa*, **I:** *Wasmannia affinis*. **Char. 68:** Proximolateral labral processes, (**0**): absent, (**1**): present. **Char. 69:** Proximolateral labral process orientation, (**0**): directed inward, (**1**): with a slight oblique lateral orientation. **Char. 70:** Distal labral margin shape, (**0**): emarginate, bi-lobed, (**1**): broadly concave, (**2**): straight/ slightly convex, (**3**): strongly convex, (**4**): convex with triangular distal point. **Char. 71:** Labrum shape, (**0**): rectangular, (**1**): trapezoidal, (**2**): broadly oval, (**3**): narrow, strip-like. **Char. 72:** Outer labral surface proximal, transverse elevation, (**0**): absent, (**1**): present. **Char. 73:** Transverse line of setae proximally on outer labral surface, (**0**): absent, (**1**): present. **Char. 74:** Labral chaetae, (**0**): absent, (**1**): present. **Char. 75:** Deep lateral grooves of labrum, (**0**): absent, (**1**): present.

29.* Shape of area bordering antennal toruli laterally: flat (**0**), or at least slightly concave (**1**).

The area immediately lateral to the torulus is almost always concave in Formicidae, even though the depth and extent of the concavity vary strongly. The area around the toruli is completely flat or slightly convex in the outgroup taxa except for *Ampulex*, which is also coded as concave (**1**). Category 2.

30.* (Additive.) Peritorular groove. Distinct groove posterior to antennal torulus: absent (**0**), or present (**1**).

The region surrounding the torulus varies considerably. It can be completely level with the surrounding cuticle but also form a deep "peritorular groove" that almost completely encloses the torulus. A deep peritorular groove is likely correlated with other features of the torular region, such as the position of the antennal foramina. The groove usually has distinctive, often smooth cuticular structure relative to the remaining head capsule. The presumably derived condition (**1**) is scored for *Wasmannia* and *Brachyponera*. Dependent on concavity (**1**) in Char. 29. Category 2.

31. Position of toruli relative to epistomal sulcus: toruli situated directly at or indenting the epistomal sulcus (**0**), or distinctly separated from epistomal sulcus (**1**).

The location of the torulus relative to the epistomal sulcus is highly variable across Aculeata. State (**1**) is found in *Parischnogaster* and *Sceliphron*. Prentice (1998) suggested toruli very close to the epistomal sulcus as the ancestral condition for Apoidea. This is arguably also the case for total clade Formicidae. The exact position of the toruli in relation to the epistomal sulcus and also the lateral, anterior, and posterior cephalic margins may yield more

phylogenetically informative characters when more taxa are investigated (see, e.g., Bolton 2003, Boudinot et al. 2022c). The present coding corresponds to Keller (2011) Char. 6. Categories 2, 4. (Prentice 1998, Keller 2011: char. 6, Boudinot et al. 2022c: char. 140)

32.~ Shape of torular acetabulum; flat and dish-like (**0**), or hemispherical, forming bulbous cavity (**1**).

Among the sampled taxa, the flat, dish-like condition is present in *Formica*, *Protanilla*, †*Gerontoformica* and all investigated outgroup taxa. This is usually associated with a rather simple external torulus, while the bulbous extension of the acetabulum of *Wasmannia* and *Brachyponera* corresponds with a lobate condition. The acetabulum of *Protanilla* is at least slightly enlarged relative to the other taxa with state 0. This suggests that finer differentiation is possibly useful with the addition of further taxa. Keller (2011) also recognized a "spherical" state (Keller's char. 10). However, the main criterion for this state was the depth of the antennal bulbus insertion into the torulus. The coding suggested here is restricted to the internally visible part of the acetabulum, which forms an internal bulbous chamber or not, at least in the taxa examined. As a consequence of the expansion of the acetabulum, the antennal foramen is directed posteriorly relative to the external torulus and is also laterally compressed, which results in an oval shape. Category 3. (Keller 2011, char. 10)

33. Compound eyes: absent in at least some females (**0**), or always present (**1**).

The compound eyes are treated as absent here if they are consistently absent in any caste or sex of a species. In a more
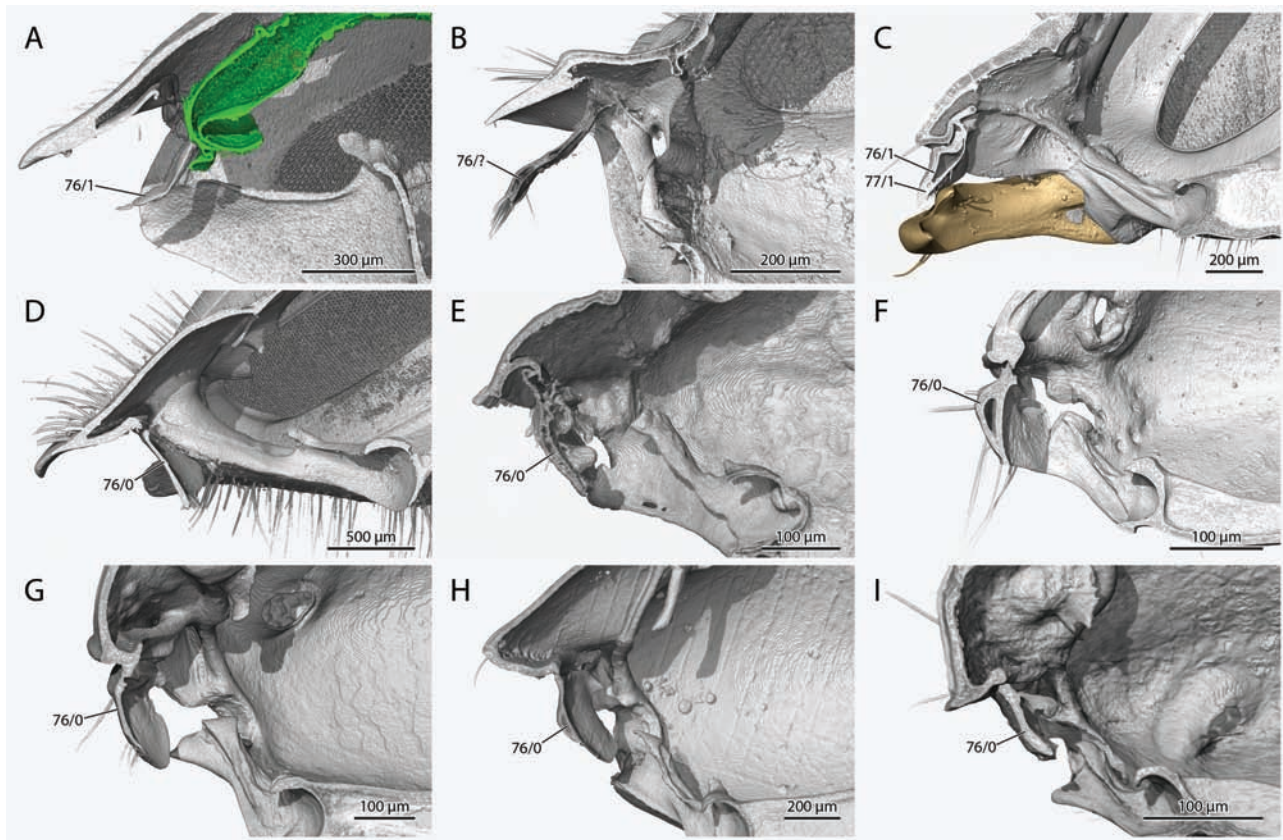
Char. 76, 77. 3D reconstruction of the labral attachment in sagittal view, **A:** *Parischnogaster* sp., **B:** *Methocha* sp., **C:** *Ampulex* sp., **D:** *Sceliphron caementarium*, **E:** †*Gerontoformica gracilis*, **F:** *Protanilla lini*, **G:** *Brachyponera luteipes*, **H:** *Formica rufa*, **I:** *Wasmannia affinis*. **Char. 76:** Orientation of the labrum in the retracted position relative to the clypeus, (**0**): perpendicular, (**1**): parallel. **Char. 77:** Position of the labrum relative to the mandibles, (**0**): below mandibles, (**1**): above mandibles.

complete analysis this should be separated into several characters for the different castes/ sexes that might have the eyes reduced. The compound eyes are reduced to various degrees or completely absent across total clade Formicidae, especially among workers, usually in association with a hypogaeic lifestyle (e.g., Wong and Guénard 2017). Among our taxon sampling, this occurs in the hypogaeic *Protanilla* and complete loss of worker eyes may be synapomorphic for the Leptanillomorpha (Boudinot et al. 2022c). The apparently rampant homoplasy of the character cannot be resolved *a priori* using external morphology alone. Category 4. (e.g. Baroni Urbani et al. 1992: char. 6, Boudinot et al. 2022c, char. 37)

34. (Reductive.) Size of compound eyes, as quantified by the maximum eye diameter relative to the length of the head, in at least some females: less than ½ of head length (**0**), or more than ½ of head length (**1**).

Compound eye size is generally reduced in females of total clade Formicidae. All of our sampled species have eyes that span less than half of their head length, while it is much larger in all considered outgroups. The relative size is known to be of alpha taxonomic value, and varies widely within total clade Formicidae and across Aculeata with some ecological relationships (e.g., Sosiak and Barden 2021, Jelley and Barden 2021). Dependent presence in Char. 33. Category 4. (Boudinot et al. 2022c: char. 36)

35. (Reductive.) Position of compound eye: anterior half of head capsule (**0**), or posterior half of head capsule (**1**).

The position of the lateral eyes is highly variable across total clade Formicidae, and coding as discrete character states can be problematic. One specific condition not coded here due to present taxon sampling is "eye very close to the anterior head margin, not separated from the clypeus by a distinct malar space" (see, e.g., Boudinot et al. 2022c: Char. 30). Among our sampled taxa, *Formica* and †*Gerontoformica* have the eye situated in the posterior head half and *Wasmannia* and *Brachyponera* in the anterior half. The outgroup taxa were coded as having the eyes on the anterior half of the head as the anterior ocular margin is at least very close to the anterior cephalic margin in all of them, although the eyes are very large and almost completely cover the lateral side of the head. Dependent on state (**1**) of Char. 33. Category 4. (Boudinot et al. 2022c: char. 38)

36. Ocelli: absent in at least some females (**0**), or present (**1**).

As with the compound eyes, presence of ocelli can vary strongly among different castes or sexes of one species. Absence is scored here if they are reduced completely in any sex or caste. An example of intraspecific variation are soldiers, e.g., in the genus *Carebara*, which retain one or two ocelli in comparison to complete absence in minor workers (Azorsa and Fisher 2018). Ocelli are absent in workers of *Protanilla*, *Brachyponera*, and *Wasmannia* in our taxon sampling. Overall, the presence or absence is variable in the worker caste of total clade Formicidae, with some degree of stability at the subfamily level (e.g., present in many Formicinae). Category 4. (e.g., Brothers 1975: char. 10, Keller 2011: char. 48, Boudinot et al. 2022: char. 41)

37.* Shape of lateral portion of hypostomal carina: straight (**0**), or flattened twisted inwards by about 90° (**1**).

Among the investigated taxa, this distinct twist was only observed in *Formica rufa*, but a similar condition is apparently present
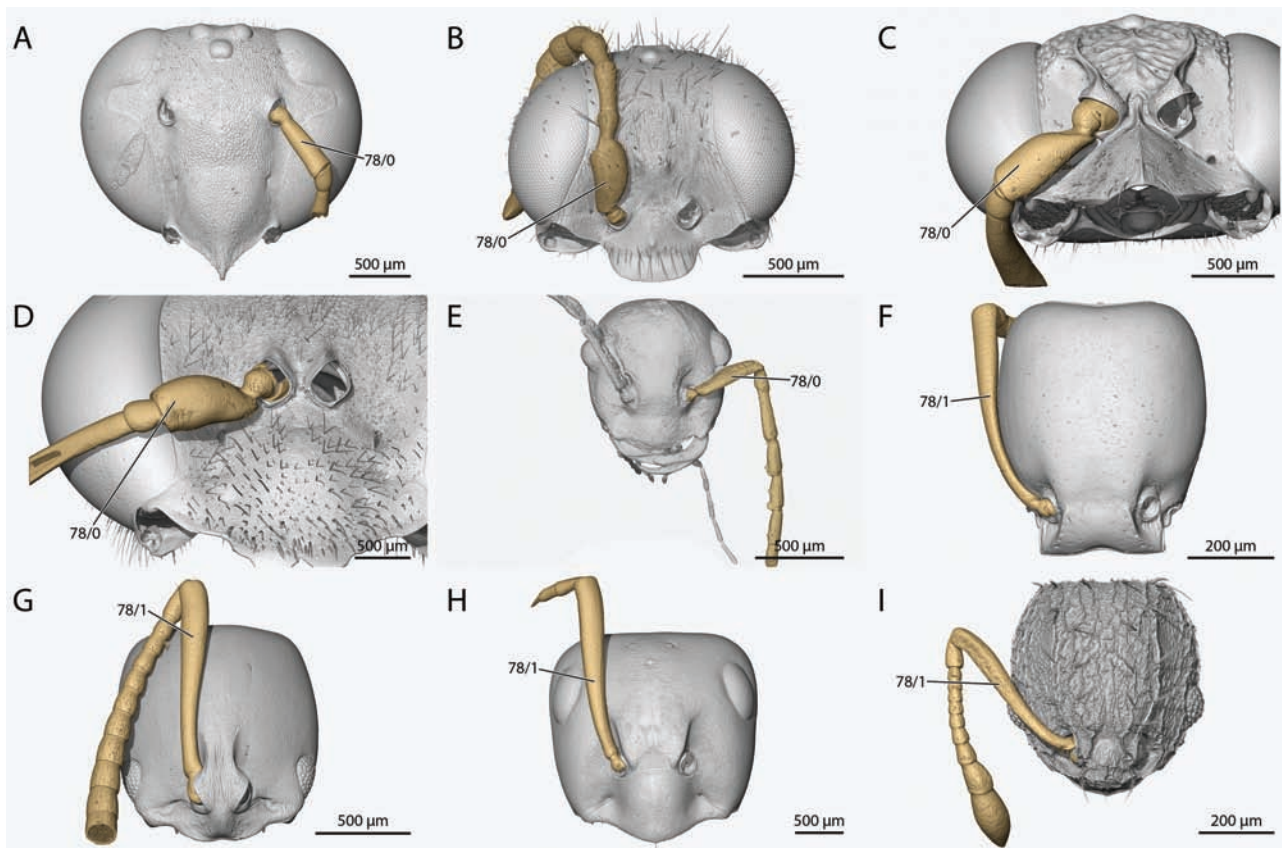
Char. 78. 3D reconstruction of the antenna in dorsal view, **A**: *Parischnogaster* sp., **B**: *Methocha* sp., **C**: *Ampulex* sp., **D**: *Sceliphron caementarium*, **E**: †*Gerontoformica gracilis,* **F**: *Protanilla lini*, **G**: *Brachyponera luteipes*, **H**: *Formica rufa*, **I**: *Wasmannia affinis*. **Char. 78**: Scapus length relative to flagellum, (**0**): less than half (**1**): at least half as long.

across many groups of Formicidae (see mouthpart images of Keller 2011 image atlas). Therefore, its phylogenetic significance deserves further scrutiny. Among the outgroups, only *Parischnogaster* shows a slight degree of twisting, less than the 90° observed in members of Formicidae. Category 1.

38.* Hypostomal groove: undivided (**0**), or divided in unpaired median and paired lateral portions by inner hypostomal carina (**1**)

The hypostomal groove is the area that is delimited by the points of the hypostomal processes laterally, the ventral (/ posterior) margin of the oral foramen dorsally (/anteriorly) and by the outer hypostomal carina ventrally (posteriorly). This groove is undivided in *Parischnogaster* and *Methocha* but divided to some extend by the inner hypostomal carina in the apoid and formicid taxa investigated here. In *Parischnogaster* and *Methocha*, this carina terminates medially at the hypostomal notch, thus not reaching into and dividing the hypostomal groove. In all other taxa, the carina extends into the groove instead, thus dividing it, but only in *Sceliphron* and †*Gerontoformica* it forms a completely continuous rim. The pattern observed here suggests state (**1**) as a potential synapomorphy of Formicoidea and Apoidea. Category 1.

39.* Oral margin of the hypostoma between the cardinal condyles: linear or continuous in curvature (**0**), or "shouldered", sinuous (**1**).

The oral margin of the hypostoma is linear or continuous in curvature in all taxa except for *Brachyponera*, *Formica* and *Wasmannia* in which it is shouldered, less so in *Formica* than the other two, but still distinct. While very little information is currently available on the hypostomal character system, the observed pattern

suggests state (**1**) as a potential autapomorphy of Formicidae excl. Leptanillomorpha. Category 1.

40.* Lateral termination of the outer hypostomal carina: laterally at mandibular articulation (**0**), or at the hypostomal process apex (**1**), or between mandibular articulation and hypostomal process (**2**).

The inner hypostomal carina varies in its lateral termination point. It terminates laterally at the mandibular articulation in *Parischnogaster*, at the hypostomal process apex in *Methocha* and between the mandibular articulation and the hypostomal process in all other investigated taxa. Category 1.

41.* Expansion of medial portion of hypostomal carina: medial portion about as wide as rest of carina (**0**), or medial portion expanded (**1**).

This character is highly variable across total clade Formicidae and informative at least at the generic level (Shattuck 1992; Keller 2011, ventral head images in image atlas). Among the species considered here, an expanded carina occurs in *Wasmannia affinis* and *Brachyponera luteipes*. Among our outgroups, the hypostomal carina is generally very wide in *Methocha*, but the medial portion is not specifically expanded, so this taxon was coded as (**0**). The width of the carina may turn out as functionally relevant in the context of improved mechanical protection of the maxillolabial complex base, together with the depth of the hypostomal cavity. Category 1.

42.* Lateral points of outer hypostomal carina extended into hypostomal teeth: absent or only forming corners, not teeth (**0**), or forming more or less sharp teeth (**1**).
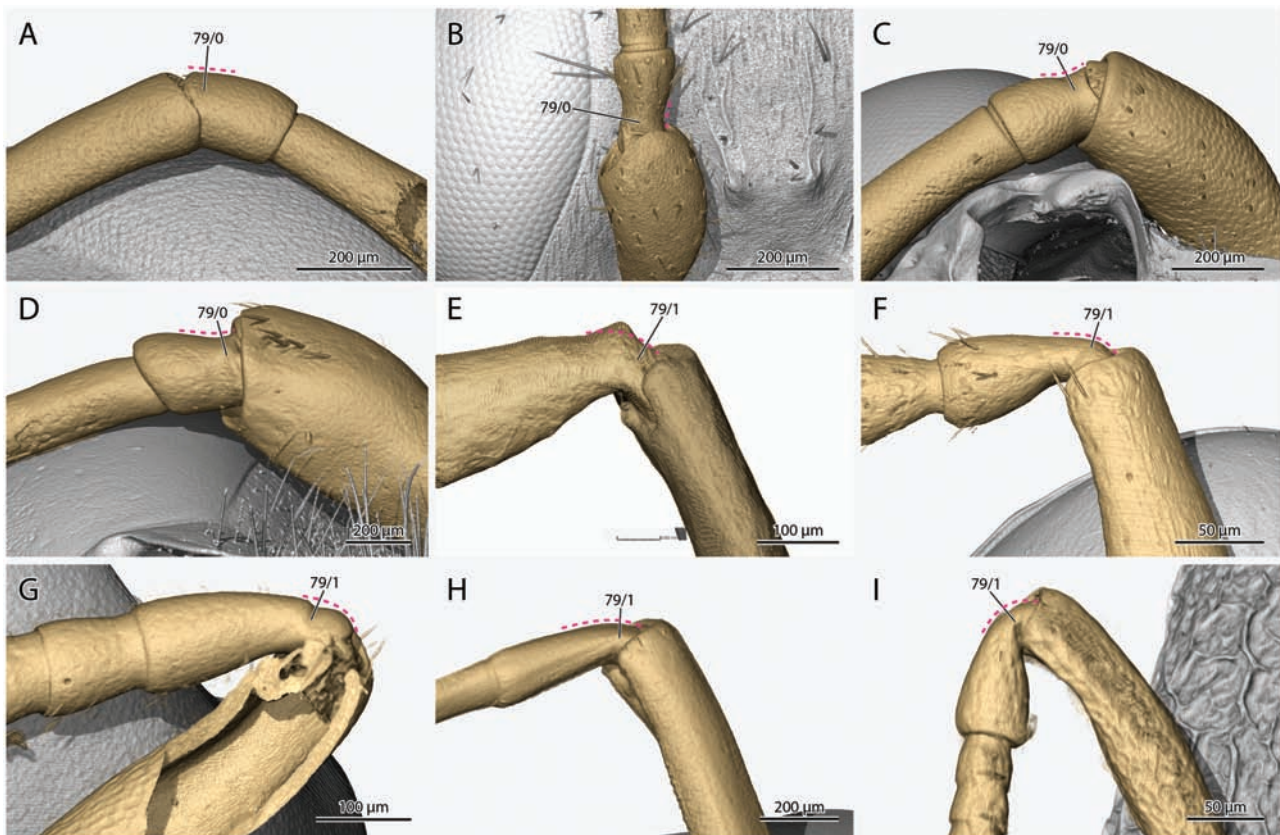
Char. 79. 3D reconstruction of the scapopedicellar articulation in lateral view, **A:** *Parischnogaster* sp., **B:** *Methocha* sp., **C:** *Ampulex* sp., **D:** *Sceliphron caementarium*, **E:** †*Gerontoformica gracilis*, **F:** *Protanilla lini*, **G:** *Brachyponera luteipes*, **H:** *Formica rufa*, **I:** *Wasmannia affinis*. **Char. 79:** Base of the pedicel, orientation marked by dotted magenta line, (**0**): cylindrical and straight, (**1**): pinched and curved.

Distinct hypostomal teeth are absent in the studied outgroup taxa and also in *Formica* and †*Gerontoformica*. They are often used in taxonomic work across Formicidae and other groups of Apocrita (e.g., Shattuck 1992, Wilson 2003, Miko et al. 2007), and might be phylogenetically informative on a lower level. Even if a distinct tooth is missing, at least a hypostomal corner can usually be observed at the junction of hypostoma and pleurostoma. Category 1.

43.* (Reductive.) Hypostomal teeth orientation relative to remainder of hypostomal carina: teeth forming continuation of remaining carina or at most gently curved (**0**), or teeth forming distinct angle with remaining carina (**1**).

The teeth are usually directly continuous with the carina. However, they form a distinct angle with the rest of the carina in some taxa such as *Brachyponera* (and some other ponerines such as species of *Diacamma*, see images in Keller 2011). Dependent on state (**1**) of Character 42. Category 1.

44.* (Reductive.) Shape of hypostomal teeth: thin and short (**0**), or thin and elongated (**1**), or broadly triangular (**2**).

These teeth are highly variable in shape (see images in Keller 2011). Among the sampled taxa, thin and short teeth occur in *Wasmannia affinis*, thin and long ones in *Brachyponera luteipes* and broadly triangular ones in *Protanilla lini*. Dependent on state (**1**) of Character 42. Categories 2, 4.

45. Triangular hypostomal process (paramandibular process) fusion with clypeus: not fused (**0**), or fused (**1**).

The hypostomal processes are triangular hypostomal projections (also termed paramandibular processes) directed towards the clypeus, which partially or completely separate the oral foramen from the mandibular foramen. The separation is complete when the process reaches the clypeus and fuses with it. Otherwise, a gap of varying distance remains between the hypostoma and clypeus. Fusion has not been observed in any species of total clade Formicidae so far. In our investigated outgroups it occurs in *Parischnogaster*, *Ampulex* and *Methocha*. This condition has certainly evolved several times independently and different instances of fusion might vary in structural details. Previously characterized by, e.g., Bohart and Menke (1976). Category 3. (e.g. Prentice 1998, Ohl and Spahn 2010)

46.* (Reductive) Alignment of the triangular (unfused) hypostomal (paramandibular) processes with the hypostomal corner: aligned (**0**), or shifted medially with a straight to convex connection (**1**), or shifted medially with a concave connection (**2**).

This character was never evaluated comparatively by myrmecologists before, thus the coding suggested here is a first approximation. The paramandibular process is perfectly aligned with the hypostomal corner in *Brachyponera luteipes* and *Protanilla lini*. In †*Gerontoformica* and *Parischnogaster* the paramandibular process is shifted mediad to the corner but has a straight or concave connection to it (between the tip of both). In *Formica* and *Wasmannia* the process is also distinctly shifted mediad, but the connection is clearly concave. This modification of the oral foramen is a possible synapomorphy of the clade containing Formicinae and Myrmicinae or even a more inclusive formicomorph clade. Dependent on unfused condition in Char. 45. Category 1.

47.* Development of knob shaped process between pleurostomal fossa and paramandibular process: absent (**0**), or present (**1**).

This knob was observed in *Formica* and *Wasmannia*. The current pattern suggests that this knob is generally present in Formicinae and Myrmicinae, whereas it is absent in all other sampled taxa. A
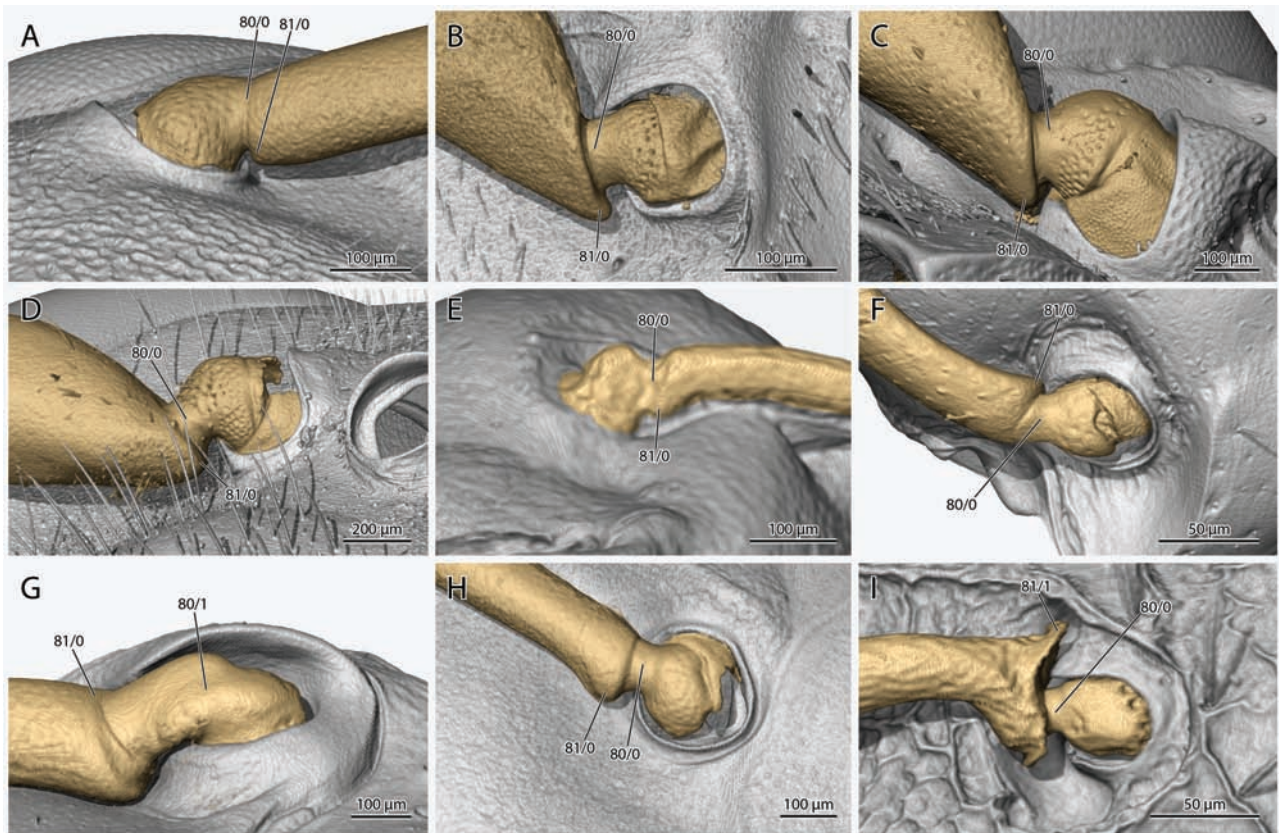
Char. 80, 81. 3D reconstruction of the scapus base in anterior view, **A**: *Parischnogaster* sp., **B**: *Methocha* sp., **C**: *Ampulex* sp., **D**: *Sceliphron caementarium*, **E**: †*Gerontoformica gracilis*, **F**: *Protanilla lini*, **G**: *Brachyponera luteipes*, **H**: *Formica rufa*, **I**: *Wasmannia affinis*. **Char. 80**: Bulbus neck orientation, (**0**): straight, (**1**): angled. **Char. 81**: Scapus base distad the bulbus neck, (**0**): not extended as flange, (**1**): extended as flange.

very slight elevation is also present in *Ampulex*, but we interpret this as a non-homologous differentiation. Category 1.

Endoskeleton:

48.* Medial tentorial lamella: absent (**0**), or present (**1**).

Generally present in ants and other apocritan groups. We were able to confirm the presence of this lamella for †*Gerontoformica*, although the preservation was insufficient for a precise reconstruction of its shape. Consequently, the following characters based on the medial lamella are coded as unknown for the fossil. The presence or absence is possibly not informative for Aculeata (Zimmermann and Vilhelmsen 2016) but is retained here as several following characters depend on its presence. Category 3. (discussed in Zimmermann and Vilhelmsen 2016)

49.* (Reductive.) Orientation of medial tentorial lamella relative to anterior tentorial arm: lamella and arm parallel (**0**), or lamella twisted and almost perpendicular to anterior arm (**1**).

The medial lamella is not twisted in the investigated apoid wasps and most ants. Its free margin runs roughly parallel to the anterior tentorial arm, although it can be slightly curved or sinuous. The lamella is strongly twisted in *Protanilla lini*, with its free margin roughly perpendicular to the anterior arm and its upper/ anterior surface facing the antennal socket in the anterior cephalic region. Dependent on presence in Char. 48. Categories 1, 2.

50.* (Reductive.) Length of medial tentorial lamella relative to anterior tentorial arm: lamella forming short lobe, ≤ 1/3 as long as anterior arm (**0**), or lamella forming elongated lobe ≥ 1/3 as long as

anterior arm but less than 3/4 (**1**), or lamella extending along most or entire length of anterior arm (**2**).

The length and shape of the medial lamella are highly variable. It forms a rather short lobe in *Protanilla*, a longer lobe of varying width in *Formica* (wide), *Wasmannia* (narrow) and *Opamyrma* (narrow, Yamada et al. 2020). In *Brachyponera* and the outgroup taxa it extends along almost the entire anterior arm, ending shortly anterad the tentorial bridge; it reaches all the way to the posterior head capsule close to the posterior tentorial pits in the sampled apoids, where it is extended as secondary tentorial bridge (see character 52). Dependent on presence in 48. Categories 1, 2

51.* (Reductive.) Shape of surface of medial tentorial lamella: mostly flat (**0**), or deeply concave (**1**).

The surface of the lamella is more-or-less flat in most examined species, including the apoid outgroups. By contrast, it is deeply concave in *Brachyponera* and *Methocha*. Dependent on presence in 48. Category 1.

52.~ (Reductive.) Anterior tentorial arms ventrally connected to head capsule by flat extensions forming secondary tentorial bridge: absent (**0**), or present (**1**).

The anterior tentorial arms are connected by flat extensions with the postgenal ridge and the head capsule posteriorly in *Ampulex* and *Sceliphron*, and to the hypostoma and the head capsule posteriorly in *Parischnogaster*, which lacks a postgenal ridge. A similar condition was described for several other aculeates and non-aculeatan apocritans (Zimmermann and Vilhelmsen 2016). In the species studied by us, the secondary bridge is continuous with the medial lamellae and could thus also be conceived as an expansion
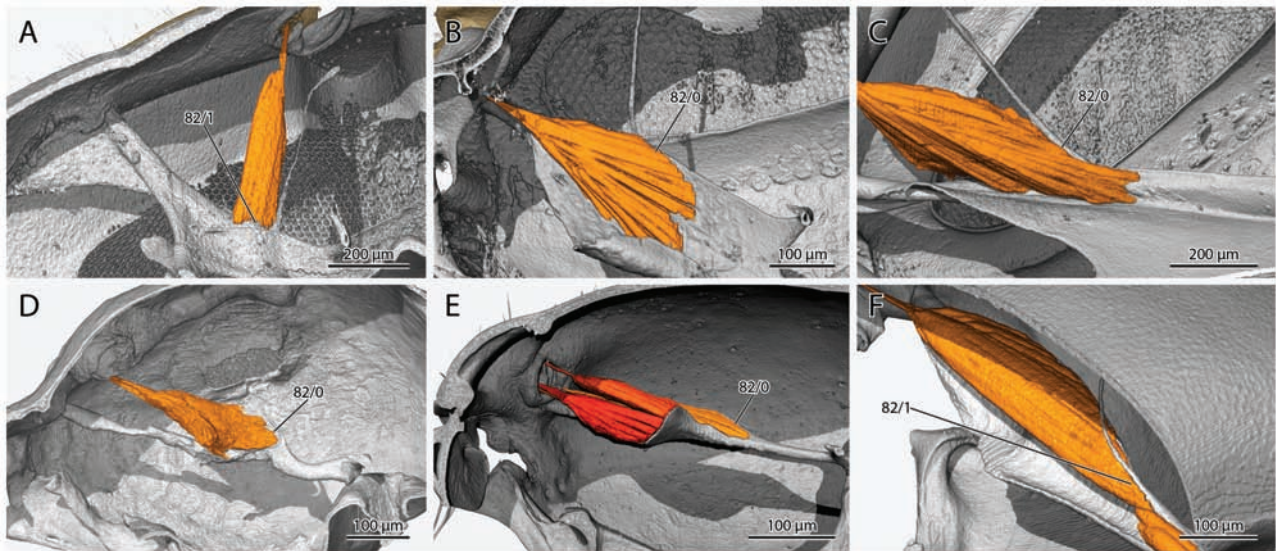
Char. 82. 3D reconstruction of *M. scapopedicellaris lateralis* (0an3), **A**: *Parischnogaster* sp., **B**: *Methocha* sp., **C**: *Ampulex* sp., **D**: †*Gerontoformica gracilis,* **E**: *Protanilla lini,* **F**: *Brachyponera luteipes.* **Char. 82**: Origin of 0an3, (**0**): extending onto dorsal tentorial arm, (**1**): not extending onto dorsal tentorial arm.

of these structures, but Zimmermann and Vilhelmsen (2016) documented species in which both a medial lamella and a secondary bridge are present without connection. The secondary bridge is absent in all studied species of total clade Formicidae, although a structure possibly corresponding to or analogous to it can be seen in the myrmicine *Melissotarsus* (Khalife et al. 2018). Dependent on presence in 48. Categories 1, 4. (Prentice 1998, Zimmermann and Vilhelmsen 2016: char. 9)

53.* Lateral tentorial lamella: absent (**0**), or present (**1**).

The lateral lamella is narrower than the medial lamella in all species studied here and those evaluated by Zimmermann and Vilhelmsen (2016); usually it extends over a longer distance on the anterior arm. The preservation of †*Gerontoformica* is not sufficient for a reliable assessment except that a lateral lamella is present. In the fossil, the lamella appears to be very broad. However, the recognizable antennal musculature and reconstructed cuticular fragments suggest that it is short. In all other taxa in which it is present, the lamella is at least slightly twisted along its length, oriented dorsad at its posterior end and turning laterad or ventrad close to the anterior tentorial pit. Category 1, 3. (discussed in Zimmermann and Vilhelmsen 2016)

54. (Reductive.) Lateral tentorial lamella fused with head capsule, forming broad buttressing ridge: absent (0), or present (1).

This condition is present in *Parischnogaster* and *Sceliphron* among the studied taxa. The buttressing ridge occurs widely in different groups of Apoidea (Paroculoclypeal brace of Prentice 1998) and Vespidae (Duncan 1939, fig. 10), but has not been observed in any ant species. Dependent on presence in Char. 53. Category 1, 4. (Prentice 1998)

55.* (Reductive) Posterior extent of lateral lamella: reaching dorsal tentorial arm (**0**), or reaching tentorial bridge (**1**).

The lateral lamella of the tentorium reaches up to the dorsal arm in the studied species of total clade Formicidae, when the arm is present, and in *Parischnogaster*. It reaches all the way to the tentorial bridge in *Ampulex, Sceliphron,* and *Methocha.* Dependent on presence in Char. 53. Category 1.

56. Dorsal tentorial arms: absent (**0**), or present (**1**).

The arms are generally quite reduced in ants and Aculeata more generally but are completely absent only in *Wasmannia* among taxa

currently sampled. The dorsal arms of Aculeata consist of a tubular evagination of the anterior arm which is connected to a thread-like cuticular extension (Prentice 1998, Zimmermann and Vilhelmsen 2016). The arms show some variation in length and shape; for example, they are strongly curved in *Sceliphron* and curved in a different way in *Methocha*, terminate in a bulbous expansion in *Formica* and *Parischnogaster*, and almost reach the frontal area of the head capsule in *Ampulex*. Category 3. (Similar in Zimmermann and Vilhelmsen 2016: char. 1)

57.* (Reductive.) Length of dorsal tentorial arms relative to length of anterior arms: at most 1/3. (**0**), or longer than 1/3. (**1**).

The dorsal tentorial arm is generally reduced in Aculeata compared to other Hymenoptera (Zimmermann and Vilhelmsen 2016), but it is especially short in the studied ant species (all scored as state 0), indicating further reduction. In all investigated non-ant aculeates, the dorsal arm reaches roughly 2/3 of the length of the anterior arm. Zimmermann and Vilhelmsen (2016) also consider fusion of the dorsal tentorial arm with the head capsule (their character 1), but this was so far never described for any Aculeata. Category 1.

58.* Posterior tentorial arm length: distinguishable as distinct arm (**0**), or very short, basically not distinguished as individual arm (**1**).

In many hymenopteran taxa (Zimmermann and Vilhelmsen 2016), the posterior arms are very reduced to the point of not being recognizable as individual structures anymore. In this case the tentorial bridge originated right below/ in front of the postoccipital collar. Alternatively, this can be formulated as fusion of the posterior arm with the head capsule. When the arms are distinct, they are known to vary in length (e.g., long arms in *Leptanilla*, Lopez et al. 1994). Among the taxa investigated here, the posterior arms are reduced to the degree of near absence in *Wasmannia, Brachyponera,* and *Sceliphron.* Category 1, 3.

59.* Posterior ends of anterior tentorial arms bent ventrad and fused to the head capsule below the occipital foramen: absent (**0**), or present (**1**).

This is a specific state observed in *Brachyponera*, in contrast to the straight anterior arm in all other known species (see also Zimmermann and Vilhelmsen 2016); it is currently unknown if it is unique to this genus or occurs in other taxa. Category 1.
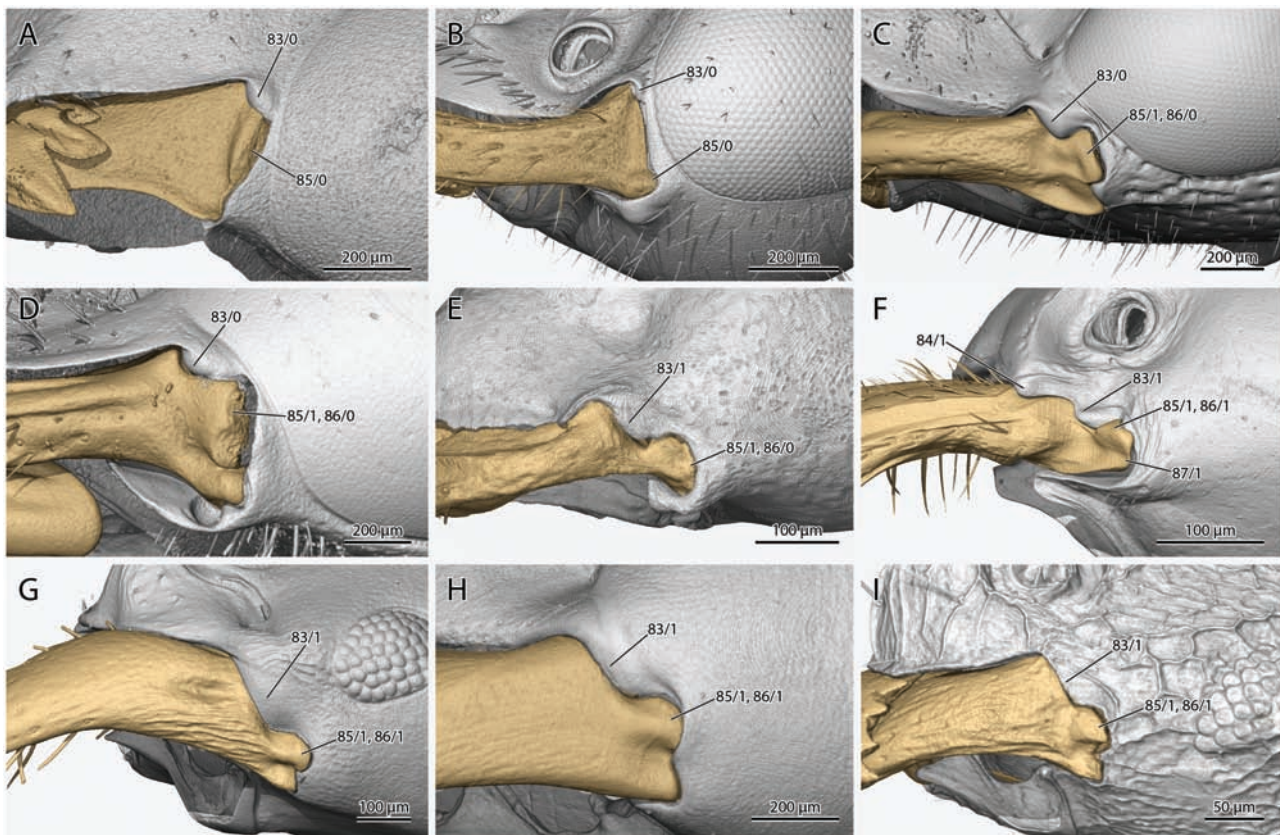
Char. 83–87. 3D reconstruction of the mandibular base in lateral view, **A:** *Parischnogaster* sp., **B:** *Methocha* sp., **C:** *Ampulex* sp., **D:** *Sceliphron caementarium*, **E:** †*Gerontoformica gracilis*, **F:** *Protanilla lini*, **G:** *Brachyponera luteipes*, **H:** *Formica rufa*, **I:** *Wasmannia affinis*. **Char. 83:** Elongation of secondary mandibular articulation, (**0**): up to moderately elongated, (**1**): elongated, at least reaching mandible mid-height. **Char. 84:** Distal clypeal knob, (**0**): absent, (**1**): present. **Char. 85:** Atala shape, (**0**): very small, (**1**): large. **Char. 86:** Large atala developed as distinct, long process, (**0**): absent (broad bulge), (**1**): present. **Char. 87:** Mandibular condyle, (**0**): not reduced, (**1**): reduced, fused with atala.

60.~ Tentorial bridge, dorsoventral curvature above anterior arms in oral view: straight or low arched, not raised more than two times anterior arm diameter (**0**), or bridge high, raised by more than two times anterior arm diameter (**1**).

The curvature of the tentorial bridge is highly variable; our characterization is only a very rough attempt at capturing this information. As seen in oral view, the tentorial bridge is raised as a high arch above the anterior arms in *Parischnogaster*, *Methocha*, and *Sceliphron*. In *Ampulex* and all species of total clade Formicidae, including †*Gerontoformica*, the bridge is either a straight rod between the anterior arms or only lowly arched above them, not raised by more than about two times the diameter of the anterior arms. Category 3. (Ronquist et al. 2012: char. 20)

61.* Tentorial bridge shape. Angle of bridge relative to anterior arms, as observed in dorsal view: more-or-less perpendicular, forming a straight rod (**0**), or acutely angled anterad, V-shaped (**1**).

The anteroposteriorly oriented V-shape was found in *Wasmannia* among our sampled taxa. It is currently entirely unknown if this is a unique feature of the species or genus or occurs in other taxa as well. Category 1.

62.* Ventral carina on tentorial bridge: absent (**0**), or present (**1**).

A flat carina is present on the (fronto-)ventral side of the tentorial bridge in *Formica*, *Brachyponera*, and *Ampulex*. Because presence of this feature is clearly highly variable, it likely has little phylogenetic value. Category 1.

63.* Postgenal ridge length. Extent of ridge relative to postgenal bridge: extending across entire postgenal bridge to the postocciput (**0**), or ending before reaching the postocciput (**1**).

The postgenal ridge usually extends across the length of the postgenal bridge, thus reaching the postocciput posteriorly. The only exception among our sampled species is *Wasmannia* where the ridge becomes obliterated at about the mid-length of the bridge; preliminary renders suggest that this is also the condition in *Leptanilla* (A. Richter, unpubl. data). *Sceliphron* is somewhat ambiguous to code as both the ridge and the external surface of the bridge are very short. The actual postgenal ridge in this apoid genus does not reach the postocciput, but rather is fused to the secondary tentorial bridge; it is the secondary bridge that reaches the postocciput. Although this is an unusual condition, due to the continuity of the ridge and secondary bridge, we decided to apply state (**0**) for *Sceliphron*. The ridge is completely absent in *Parischnogaster*, so this character was coded as inapplicable. Category 2.

64.* Torular apodeme: absent (**0**), or present (**1**).

The torular apodeme is a distinct internal process on the anteromedial side of the torular sclerite. It is present in the poneroformicine clade (*Brachyponera*, *Wasmannia*, *Formica*), but does not occur in *Protanilla*, †*Gerontoformica*, or any of the sampled outgroup taxa. We have also observed the apodeme in the male of *Dorylus* (Boudinot et al. 2021). Category 1.

65.* (Reductive.) Shape of torular apodeme: flat, broad plate (**0**), or cylindrical rod (**1**).
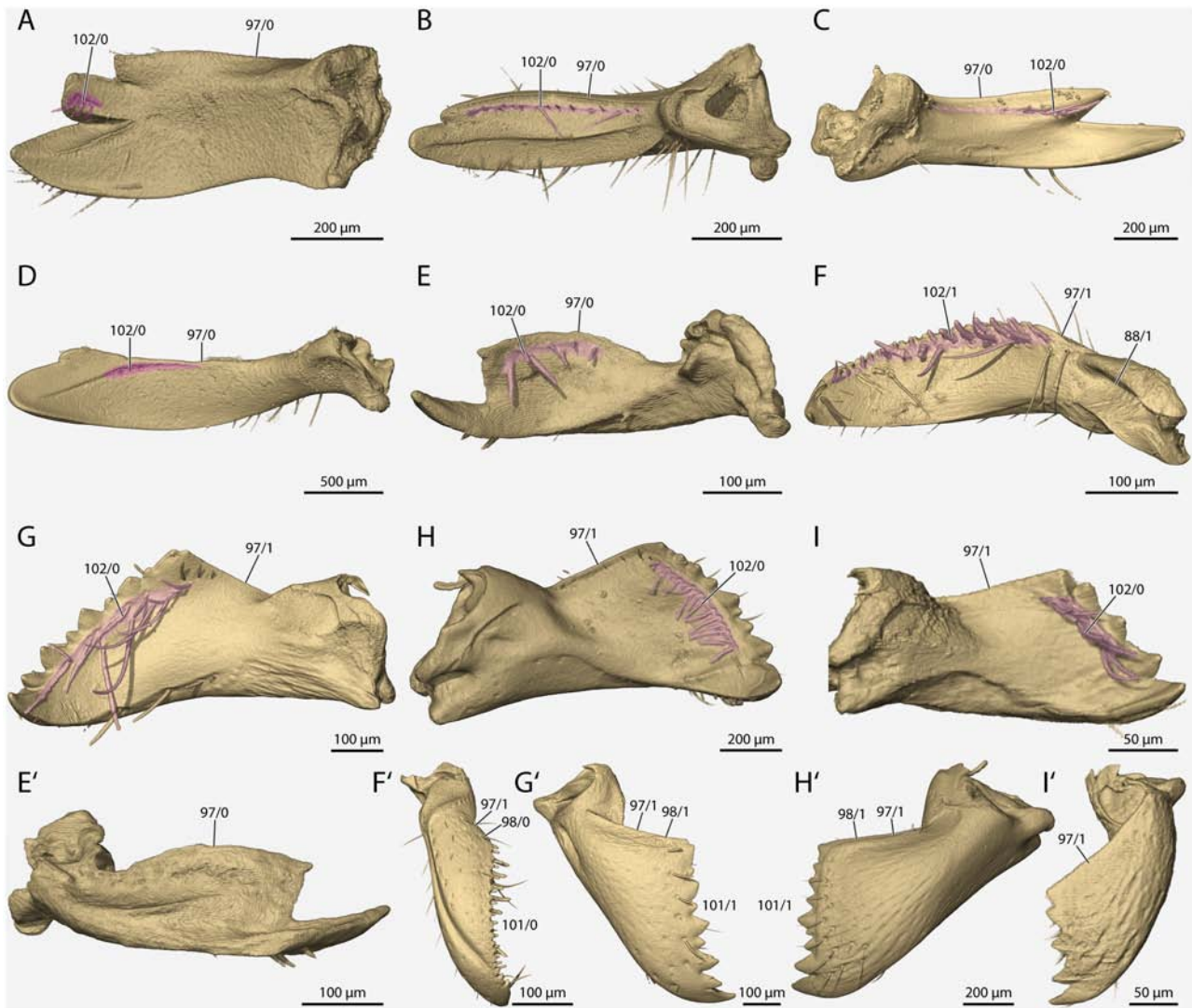
Char. 88, 97, 98, 101, 102. 3D reconstruction of the inner **(A–I)** or outer **(J–N)** surface of the mandible, **A:** *Parischnogaster* sp., **B:** *Methoca* sp., **C:** *Ampulex* sp., **D:** *Sceliphron caementarium*, **E, E':** †*Gerontoformica gracilis*, **F, F':** *Protanilla lini*, **G, G':** *Brachyponera luteipes*, **H, H':** *Formica rufa*, **I, I':** *Wasmannia affinis*. **Char. 88**: Ventral mandibular groove, (**0**): absent, (**1**): present. **Char. 97**: mandibular blade broadened basally, (**0**): absent, (**1**): present. **Char. 98**: Basal margin length relative to mandibular base, (**0**): less than 0.5x, (**1**): more than 0.5x. **Char. 101**: Mandibular denticle size relative to mandible size, (**0**): minute, fine serration, (**1**): variable size, distinctly larger. **Char. 102**: Setae on fimbriate line developed as stout chaetae, (**0**): absent, (**1**): present.

As the torular apodeme was only recently rediscovered and described (Richter et al. 2019, 2020, 2021, Boudinot et al. 2021) after it was first mentioned by Lubbock (1877), very limited information on its distribution and variation is presently available. The apodeme is developed as a flat plate-like structure in *Brachyponera* and *Wasmannia*; this plate is straight in the latter but concave and bent downwards in the former. The downcurved condition was also observed in *Dorylus* (Boudinot et al. 2021). In *Formica*, the apodeme forms a straight cylindrical rod, a shape that was also described by Lubbock (1877) for a *Lasius* species. Further investigation may reveal more detailed differences in shape. Dependent on presence in Char. 64. Category 1.

66.* Frontoclypeal strengthening ridge: absent (**0**), or present (**1**).

The frontoclypeal strengthening ridge, corresponding to the externally visible epistomal sulcus, is present in most taxa investigated here. However, it is completely reduced in *Wasmannia* and *Parischnogaster*. It is also distinctly reduced in *Ampulex* but is still recognizable, thus coded as present. Category 1.

67.* Longitudinal clypeal ridge: absent (**0**), or present (**1**).

The presence of a broad longitudinal internal ridge on the clypeus is detectable externally as a darkened strip. The ridge likely a unique feature of *Protanilla*; its development should also be evaluated in *Anomalomyrma*. The function of the ridge is presently unknown. Category 1.

Labrum:

68.⌣ Proximolateral labral processes: absent (**0**), or present (**1**).

Proximolateral labral processes (labral arms) are a highly characteristic feature of the labrum of ants. Their evolutionary origin is currently unknown (see, e.g., Richter et al. 2020). In our specimen of †*Gerontoformica*, the processes were not visible, but they have been observed in scans of other specimens of the genus (V. Perrichot, unpubl. data), thus the state was coded as unknown for the fossil treated here. The processes interact in some way with the labrum in all species of Formicidae (Keller 2011); the kind of
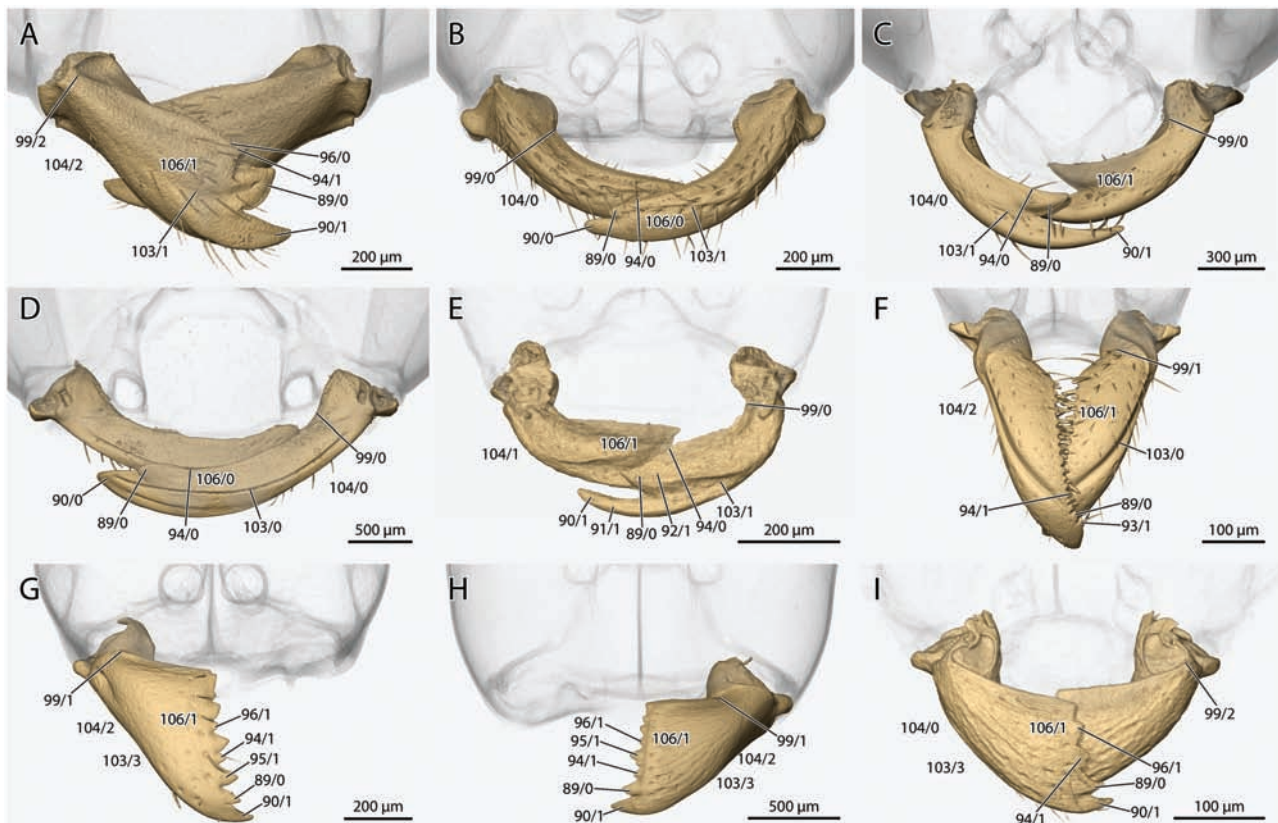
Char. 89–96, 99, 103, 104, 106. 3D reconstruction of the mandibles in dorsal view, **A:** *Parischnogaster* sp., **B:** *Methocha* sp., **C:** *Ampulex* sp., **D:** *Sceliphron caementarium*, **E:** †*Gerontoformica gracilis*, **F:** *Protanilla lini*, **G:** *Brachyponera luteipes*, **H:** *Formica rufa*, **I:** *Wasmannia affinis*. **Char. 89**: Subapical incisor, (**0**): present, (**1**): absent. **Char. 90**: Shape of the apical incisor tip, (**0**): rounded, (**1**): sharply pointed. **Char. 91**: Apical incisor shape, (**0**): broad, not elongated, (**1**): thin, elongated. **Char. 92**: Subapical incisor shape, (**0**): at most as broad as apical incisor, (**1**): distinctly broader. **Char. 93**: Denticles between apical and subapical incisor, (**0**): absent, (**1**): present. **Char. 94**: Denticles on gnathal margin proximad of subapical tooth, (**0**): absent, (**1**): present. **Char. 95**: Teeth on gnathal margin proximad of subapical tooth, (**0**): absent, (**1**): present. **Char. 96**: Number of teeth or denticles on gnathal margin proximad of subapical tooth, (**0**): one, (**1**): more than one. **Char. 99**: Termination point of basal margin on mandibular stem, (**0**): medial, (**1**): central, (**2**): lateral. **Char. 103**: Acetabular groove, (**0**): extending from mandibular acetabulum to subapical tooth, (**1**): only distal part developed, (**2**): only basal part developed, (**3**): no groove observable. **Char. 104**: Lateromedial curvature of mandibular base relative to entire mandible, (**0**): same curve, (**1**): stronger curve, (**2**): straight/ less curved. **Char. 106**: Medial torsion of mandibular blade, (**0**): not torqued, (**1**): torqued.

interaction is dependent on both the shape and position of the labral processes as well as the shape of the distal maxilla. In the following characters, we code the shape differences of the labral arms and the maxilla that are involved in the interaction individually for each structure. However, we also note that these are not strictly independent characters due to their close functional integration. Thus, for strict topology searches—rather than character mapping as performed here—it may be preferable to code these structures based on their functional interactions as was done by Keller (2011, chars. 32 + 33). Our aim in splitting the labral and maxillary shape characters is to get a better view of the evolutionary patterns of shape differences leading to the different kinds of interactions. A focused study on maxillary-labral interaction is both needed and forthcoming. Categories 2, 4. (discussed in Keller 2011: char. 32)

69.~ (Reductive.) Labral process orientation: perpendicular to labrum, thus directed orally at full labral closure (**0**), or oblique and laterally directed, such that at least part of process is visible in external view of the labrum (**1**).

The general shape of the labral processes is hook-like. When the processes are perpendicular to the labrum, they are usually short and triangular, and interact with the basal maxillary palpomere, which is the case in *Protanilla* and *Formica*. When they are directed at least slightly laterally, they are usually larger, and with broad, blunt tips, as observed in *Brachyponera* and *Wasmannia*. Labral arms of this shape interact with the stipes, although the specific interaction can vary considerably depending on distal stipes and labral arm shape. Dependent on state 1 for Char. 68. Category 4. (discussed in Keller 2011: char. 32)

70.* Shape of distal labral margin: emarginate, thus bi-lobed (**0**), or broadly concave (**1**), or straight to slightly convex (**2**), or markedly convex (**3**), or convex with a triangular distal point (**4**).

The distal labral margin is bilobed with a median emargination or concavity in many, if not most ants (*Brachyponera*, *Wasmannia* and *Formica* in our sample). However, numerous exceptions occur (see, e.g., Gotwald 1969), and a bilobed labrum is also found in other groups of Aculeata (e.g., *Pison spinulae*, see Cowley 1959). The distal edge is straight without any emargination in †*Gerontoformica* and *Sceliphron*, and broadly concave in *Protanilla lini*. The labrum of *Methocha* is broadly convex and its distal margin is set with thick, spine-like setae. A convex margin also occurs in *Ampulex*, which is further differentiated by presence of a triangular, unpaired projection distally; this is treated as an independent character state here (state **4**). The labrum of *Parischnogaster* is reduced to a thin
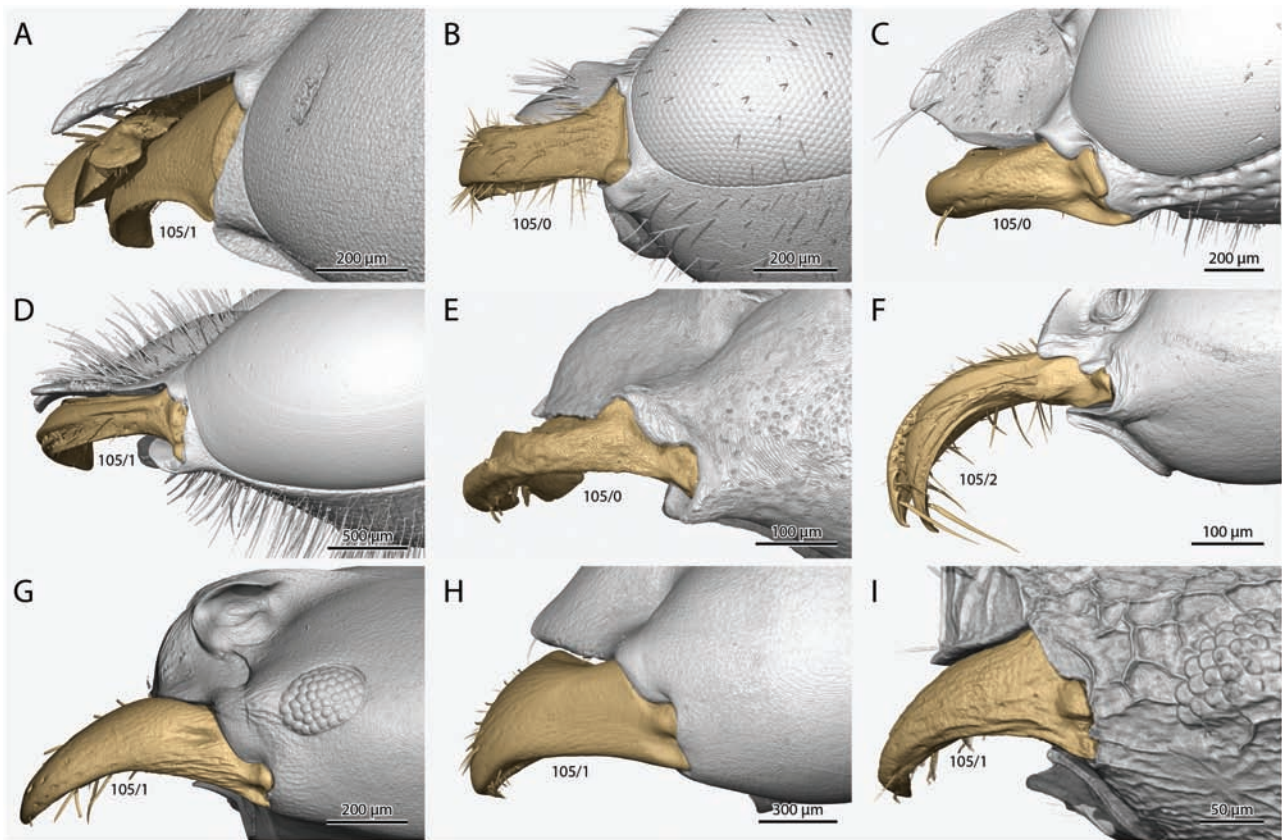
Char. 105. 3D reconstruction of the mandible in lateral view, **A:** *Parischnogaster* sp., **B:** *Methocha* sp., **C:** *Ampulex* sp., **D:** *Sceliphron caementarium,* **E:** †*Gerontoformica gracilis,* **F:** *Protanilla lini*, **G:** *Brachyponera luteipes*, **H:** *Formica rufa*, **I:** *Wasmannia affinis*. **Char. 105**: Dorsoventral curve of mandible, (**0**): straight to slightly curved, (**1**): gently curved throughout, (**2**): strong downward curve.

strip, similar to what was previously described for other members of Vespidae (Duncan 1939); this condition has been recognized as a potential autapomorphy of the family (Carpenter 1982). As the distal margin of this strip-like labrum is convex, it was coded as (**3**) here. Category 3.

71.⁓ Shape of labrum: rectangular (**0**), or trapezoidal, tapering towards proximolateral edges (**1**), or rounded and broadly oval, (**2**), or narrow and strip-like (**3**).

The labrum of all presently sampled crown Formicidae is roughly rectangular. A trapezoidal, very broad labrum is present in †*Gerontoformica*. The labrum of *Protanilla* is interpreted as rectangular here, and more specific features are treated in other character statements. A rounded-ovoid shape of the labrum is a characteristic of *Ampulex*. As mentioned above (Char. 70), *Parischnogaster* shows the typical strip-like vespid labrum. As exemplified by this and the previous character, labral shape is highly variable within Aculeata and requires investigation with a much larger taxon sampling to reveal more phylogenetically informative features. Indeed, several highly specialized shapes have been observed among crown ants, such as in Basicerotina (e.g., Longino, 2013 Longino and Boudinot 2013, Probst et al. 2019). Category 3. (previously used, e.g., Sharkey et al 2012: char. 24)

72.* Elevation of proximal transverse line of aboral labral surface: absent, surface completely flat (**0**), present, at least as slightly elevated transverse "hump" (**1**).

State (**1**) of this character is a preliminary characterization of the transverse labral elevation which was most characteristically observed in †*Gerontoformica* and *Formica*. The presumably derived

condition is also present in *Ampulex* and *Protanilla*, even though it is unclear whether the elevation is homologous to the one observed in the previously mentioned taxa, considering the highly derived shape of the labrum in both genera. On the labrum of *Brachyponera* a hump is present, but not as centrally on its surface, instead directly at its very proximal margin. We also code the hump as present in this taxon, but homology is not entirely clear at this point. The labrum of *Sceliphron* and *Parischnogaster* and also *Wasmannia* is very flat. While the proximal surface is slightly convex in *Methocha*, the labrum is overall concave and we do not presently consider the distal convexity as representing a hump as scored for the other taxa, so *Methocha* is scored as (**0**). Category 1, 2.

73.* Setae on proximal transverse line of external shield (aboral surface) of labrum: transverse line not marked by setae (**0**), or line marked by row or at least pair of setae (**1**).

We anticipate that the setation along the proximal transverse line can be coded in more detail with an expanded taxon sample. When the transverse line on the proximal oral surface is not well defined, either elevated (Char. 72) or marked by a row of setae, its identity is difficult to verify. This suggests that the developmental specification may be lost and that the setae have lost their individuated spatial identities. At least two setae in the region we interpret as the transverse line of the labrum are present in all investigated taxa of total clade Formicidae while no setae are present in a transverse line in any of our outgroup taxa. Interestingly, in the apoid wasps *Ampulex* and *Sceliphron* numerous short setae can be found on the inner side of the labrum, which is glabrous in all other investigated taxa. This is potentially an apomorphic
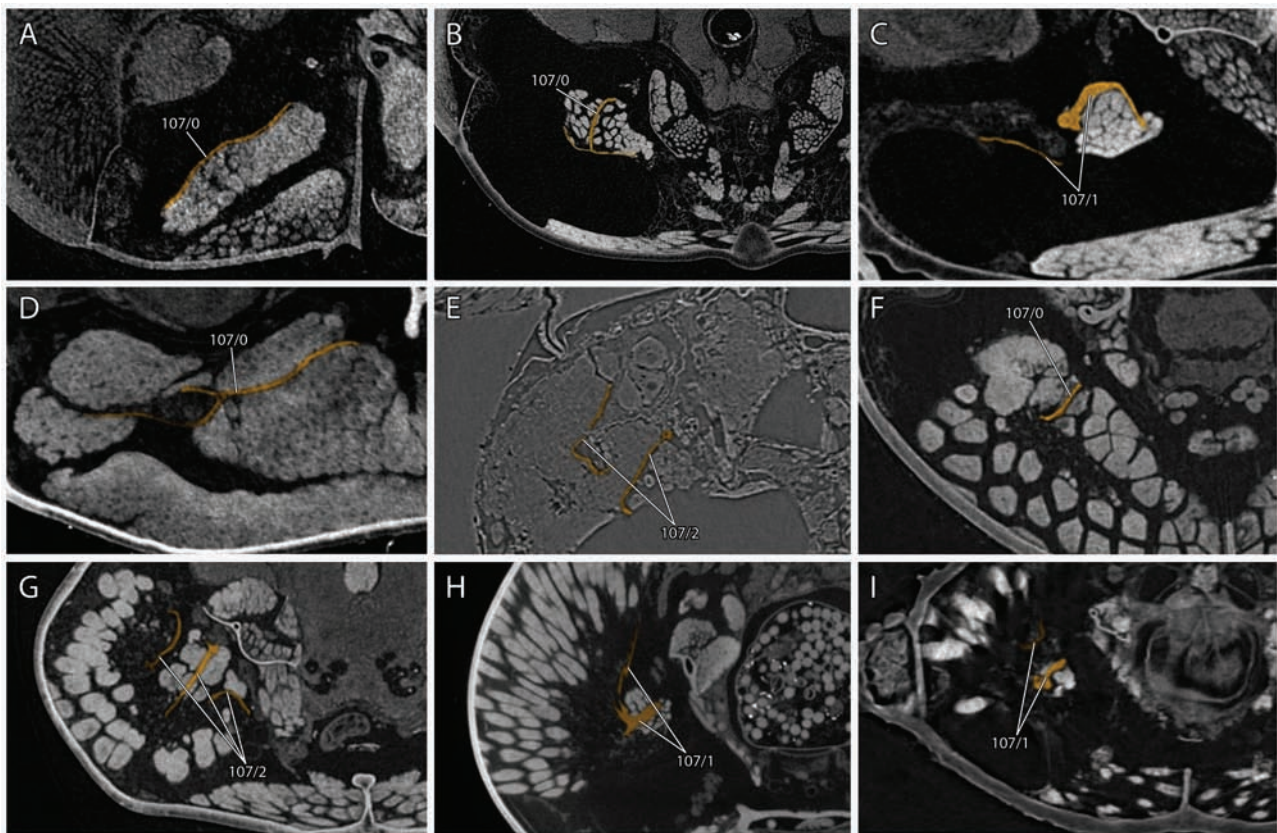
Char. 107. Tomographic transverse section through the *M. craniomandibularis internus* (0md1), apodeme marked in dark yellow, **A:** *Parischnogaster* sp., **B:** *Methocha* sp., **C:** *Ampulex* sp., **D:** *Sceliphron caementarium*, **E:** †*Gerontoformica gracilis*, **F:** *Protanilla lini*, **G:** *Brachyponera luteipes*, **H:** *Formica rufa*, **I:** *Wasmannia affinis*. **Char. 107:** 0md1 apodeme subdivisions, (**0**): one branch, (**1**): two branches, (**2**): three branches. Note: see also next figure.

feature of Apoidea and may be relevant for the function of the labrum. Category 1.

74. Labrum with at least one thick "chaeta" with riffled surface structure: absent (**0**), or present (**1**).

This character occurs in *Protanilla* in our taxon sampling, but also in *Apomyrma* and other representatives of Amblyoponinae (e.g., Keller 2011), in *Opamyrma* (Yamada et al. 2020), and in several stem group ants but not †*Gerontoformica* according to (Boudinot et al. 2022c). The setae reconstructed on the labrum of our †*Gerontoformica* fossil appear to have the short, "chaeta" shape, but may be truncated due to preservation, so it was coded as (**?**) here. Category 4. (e.g. Keller 2011: char. 28, Boudinot et al. 2022c: char. 76)

75.* Labrum with deep lateral grooves interacting with medial mandibular margin: absent (**0**), or present (**1**).

Deep lateral labral grooves were not observed or reported in any genus except *Protanilla*. Category 1.

76.* Labrum direction at closure: directed downward (perpendicular to the clypeus) (**0**), or directed anterad (parallel to the clypeus) (**1**).

The labrum is nearly vertically oriented in most aculeate species we investigated but faces forward in *Ampulex*, *Parischnogaster*, and *Methocha*. The *Methocha* specimen we scanned has a clearly extended maxillolabial complex, indicating that its labrum may also be in the "open" condition, thus we conservatively coded the condition as (**?**). Interestingly, muscle 0lb2 is missing in *Methocha* and *Ampulex*, possibly correlated with this modified orientation. A connection between presence/ absence of this muscle and labral position at rest is also suggested by the very small condition of

0lb2 in *Parischnogaster*, which has a strip-like and reduced labrum. Category 1, 3.

77.~ Position of labrum relative to mandibles: below mandibles (mostly hidden below closed mandibles) (**0**), or located above mandibles (exposed) (**1**).

The labrum is highly modified in the investigated *Ampulex* species, placed above the mandibles at rest. This feature has not been used in phylogenetic reconstruction involving the family before (Prentice 1998, Ohl and Spahn 2010). While it is currently unknown if this unusual feature is generally present in Ampulicidae or only some species, preliminary data on *Dolichurus* (A. Richter, unpubl. data) indicate it as a autapomorphy of the family. The labrum is generally concealed by the mandibles in Aculeata but above them in some non-aculeate Hymenoptera (Vilhelmsen 1996). Category 1, 3. (similar in Vilhelmsen 1996: char. 1)

Antenna

Note: Variation in the relative length and shape of antennomeres is certainly informative at lower taxonomic levels and can be coded when more taxa are considered, but no important variation was obvious among the presently investigated taxa.

78. Scapus length relative to funiculus (pedicel plus flagellum): less than half as long (**0**), or more than half as long (**1**).

Adopted from Boudinot (2020) Char. 156. Elongation of the scapus relative to the remaining antenna is an apomorphy of crown group ants. Other measures of scape length relative to the head can be employed (e.g., Borysenko 2017, Boudinot et al. 2022c) but are likely not very informative on the level investigated here. Category 4.
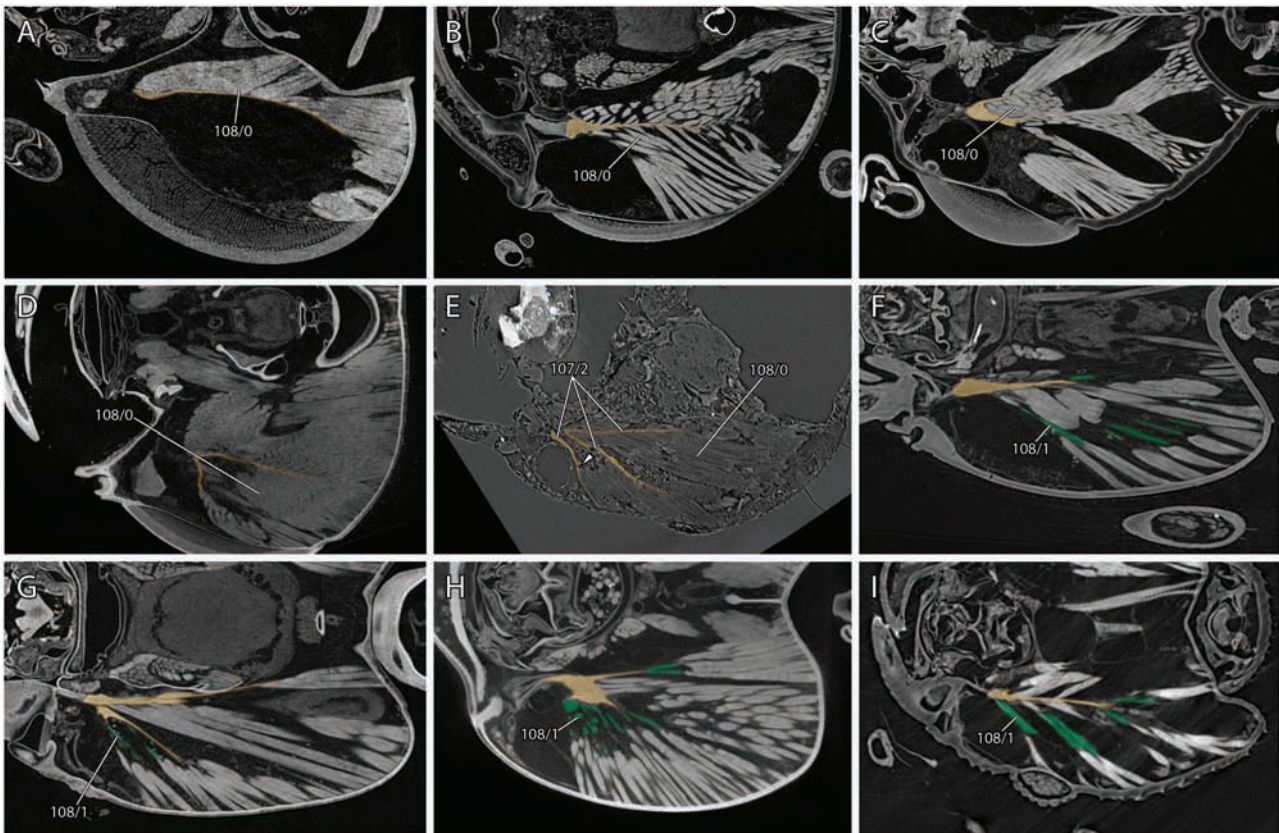
Char. 107, 108. Tomograph in frontal plane through the *M. craniomandibularis internus* (0md1), apodeme marked in light brown, cuticular fibrillae marked in green, **A:** *Parischnogaster* sp., **B:** *Methocha* sp., **C:** *Ampulex* sp., **D:** *Sceliphron caementarium,* **E:** †*Gerontoformica gracilis,* **F:** *Protanilla lini,* **G:** *Brachyponera luteipes,* **H:** *Formica rufa,* **I:** *Wasmannia affinis.* **Char. 107:** 0md1 apodeme subdivisions, (**0**): one branch, (**1**): two branches, (**2**): three branches. **Char. 108:** 0md1 with some fibers attached to thin cuticular fibrillae, (**0**): absent, (**1**): present.

(e.g., Baroni Urbani et al. 1992: char. 9, Barden and Grimaldi 2016: char. 12, Boudinot et al. 2022c: char. 156)

79.~ Base of pedicel: straight (**0**), or "pinched" and curved (**1**).

The pedicel in the outgroup taxa is a simple cylindrical sclerite ring throughout its whole length. The pedicel of the investigated ants, however, is anteroposteriorly pinched at its base and with a slight anterad curve at the location of this constriction. We interpret this anatomical detail as the defining feature of the typical geniculate antenna of crown clade Formicidae, together with the relatively elongated scape coded above. Likely, this also correlates with a deep notch on the anterior side of the scapus tip flanked by expanded flanges, as it was observed in all representatives of total clade Formicidae including †*Gerontoformica* here. This condition has gone almost unnoticed previously and was not mentioned in summaries of ant synapomorphies (e.g., Bolton 2003, Boudinot 2015). It was first described by Dlussky and Fedoseeva (1988) for stem ants and by Borysenko (2017) for all total clade Formicidae, but never used in a formal analysis. Category 1. ("geniculate antenna" used by, e.g., Keller 2011: char. 21)

80.~ Bulbus neck shape: straight (**0**), or distinctly curved (**1**).

The bulbus neck is the short segment of the scapus connecting the bulbus (radicle) with the main scapus shaft. The bulbus neck is distinctly curved in *Brachyponera,* likely in relation to the presence of a large torular lobe which enforces this bulbus neck shape to fit into the tight space available. All other investigated species have a straight bulbus neck. Shape differences of the bulbus were previously coded by Keller (2011) (Characters 18, 19), Category 3. (discussed in Keller 2011: char. 19)

81.~ Base of main scapus shaft: simple, not extended as a flange (**0**), or extended as a distinct flange encircling the scapus and overhanging the radicle (**1**).

The main shaft of the scapus is separated from the radicle (bulbus neck) by a groove. The base of the main scapus shaft distad of this groove is produced into a broad flange in *Wasmannia* and many other species of the subfamily Myrmicinae (e.g., Keller 2011). Such flanges can also occur in other groups of Aculeata and are, for example, a diagnostic feature of Mutillidae (Brothers 1975). Category 3. (Brothers 1975: char. 14)

82.* Extent of the origin area of *M. tentorioscapalis lateralis* 0an3: extending onto the dorsal tentorial arm (**0**), or not extending onto the dorsal tentorial arm (**1**).

Prentice (1998) assumed that no antennal muscles originate on the dorsal tentorial arm in Apoidea. However, one muscle, *M. tentorioscapalis lateralis* 0an3, frequently does originate on this part of the tentorium, at least partially, according to our observations. At least a few fibers need to be observed clearly originating on the arm to be coded as state (**0**), which is the case in the outgroup taxa with the exception of *Parischnogaster.* For total clade Formicidae, this was the case in *Protanilla* and †*Gerontoformica.* State 1 is coded for the remaining crown ant species and was also applied when the dorsal tentorial arm is missing (*Wasmannia*). Category 1.

Mandible:

83. Elongation of secondary (dorsal) mandibular articulation: small to moderately elongated, never contacting mandible midheight
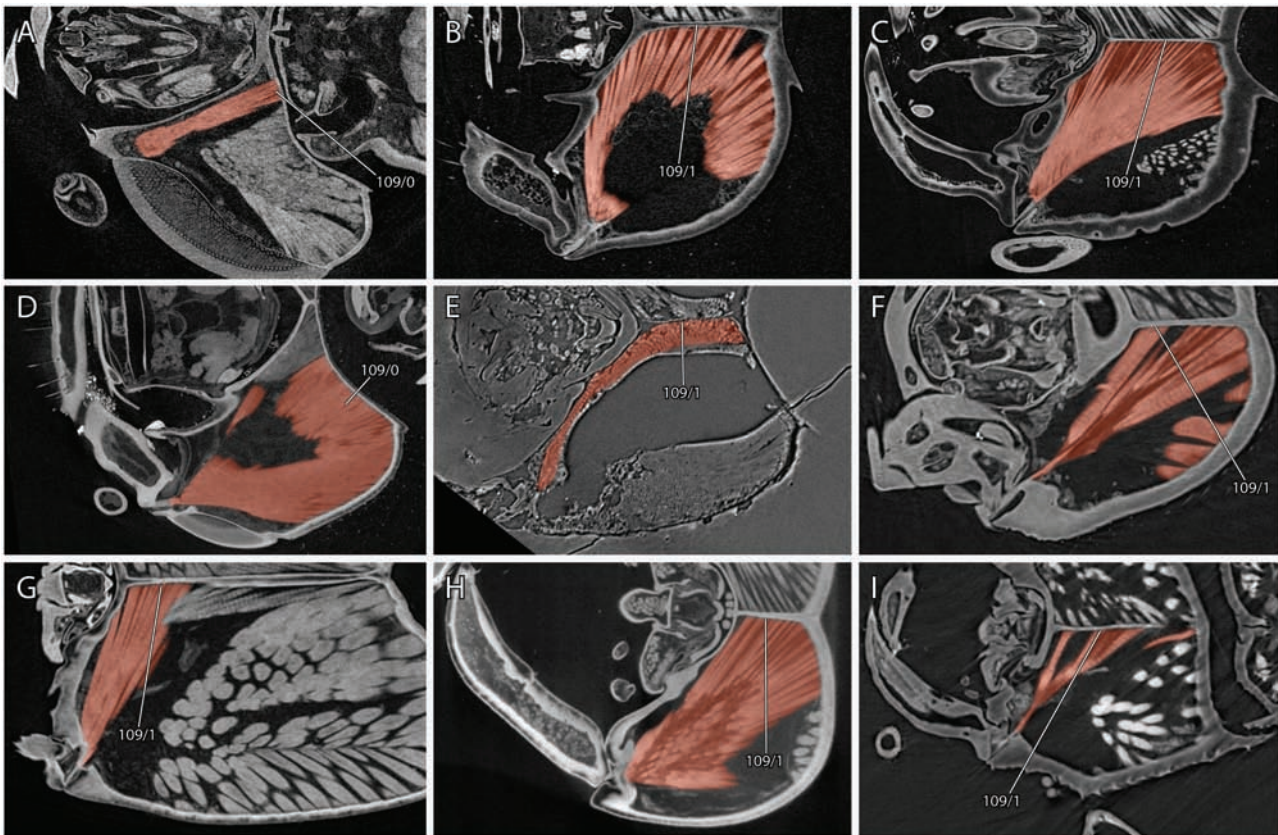
Char. 109. Tomographic oblique frontal section through the *M. craniomandibularis externus* (0md3), muscle marked in red, **A:** *Parischnogaster* sp., **B:** *Methocha* sp., **C:** *Ampulex* sp., **D:** *Sceliphron caementarium*, **E:** †*Gerontoformica gracilis,* **F:** *Protanilla lini*, **G:** *Brachyponera luteipes*, **H:** *Formica rufa*, **I:** *Wasmannia affinis*. **Char. 109**: 0md3 origin area, (**0**): exclusively on head capsule, (**1**): at least partly on postgenal ridge.

(**0**), or very elongated, at least contacting or surpassing mandible midheight (**1**).

The enlarged secondary mandibular articulation is a characteristic and most certainly autapomorphic feature of total clade Formicidae (see Boudinot et al. 2022c). We appreciate here for the first time the very variable sizes of the condyle occurring across Aculeata. The condyle is especially tiny in *Methocha*, small in *Parischnogaster* and distinctly elongated in *Ampulex*. However, only within total clade Formicidae the articulation is consistently enlarged to cover at least the midheight of the mandible. There exists variation of this structure beyond this character statement, for example the distinct redesign in *Protanilla* (Richter et al, 2021) (see following character), and the consistent large and shield-like state of Dolichoderinae and Aneuretinae (B. Boudinot, unpubl. data). Category 1, 4. (Boudinot et al. 2022c: char. 44)

84.* Development of distal clypeal knob articulating with a groove on the dorsal mandibular base: absent (**0**), or present (**1**).

As mentioned above, the dorsal mandibular articulation is modified in *Protanilla lini*. In this species, the laterodistal corners of the clypeus are elongated and expanded into small distal clypeal knobs. The knobs articulate with a flat groove of the dorsal mandibular base. This feature was only observed in *Protanilla* but can be assumed to be present in *Anomalomyrma* (Borowiec et al. 2011) based on images; it is likely autapomorphic for Anomalomyrmini. Category 1.

85.* Size of the lateral mandibular base: no atala or only a very small atala (abductor swelling) visible (**0**), or distinct atala (abductor swelling) associated with abductor muscle apodeme developed (**1**).

The lateral mandibular base is the site of insertion of the tendon of *M. craniomandibularis internus* 0md3, i.e., the mandibular abductor (opener). It is highly variable in shape and size across the studied taxa. The distinct swelling that is often present in this region was previously termed abductor swelling (Michener and Fraser 1978) and more recently, the term atala was introduced for this process (Richter et al. 2020). We observe a very small swelling in *Parischnogaster* and *Methocha* (**0**) and a larger one of variable shape in all other taxa (**1**). At this point, according to the definition of Richter et al. (2020), we call all these swellings/ processes "atala", but a more thorough study of the variation may make it possible and desirable to separate between a more undefined "abductor swelling" and the "atala" as a distinct process as it occurs in Formicidae. This and the following characters are only a first attempt to understand this variation. Category 2.

86.* (Reductive.) Large atala (abductor swelling) developed as distinct, rounded process: absent (**0**), or present (**1**).

The atala as a rounded process of the lateral mandibular base is usually at least as large or larger than the mandibular condyle, as can be observed on the mandibles of most crown Formicidae, although variation in size occurs within the group (Khalife et al. 2018, Richter et al, 2021). The swelling is much broader and more angular in *Ampulex* and *Sceliphron* and has a somewhat intermediate condition in †*Gerontoformica* where it is not well defined, broad and rounded (coded as [**0**] here). Dependent on state (**1**) in Char. 85. Category 1.

87.* Reduction of mandibular condyle and fusion with atala (abductor swelling): condyle and atala not fused (**0**), or fused (**1**).
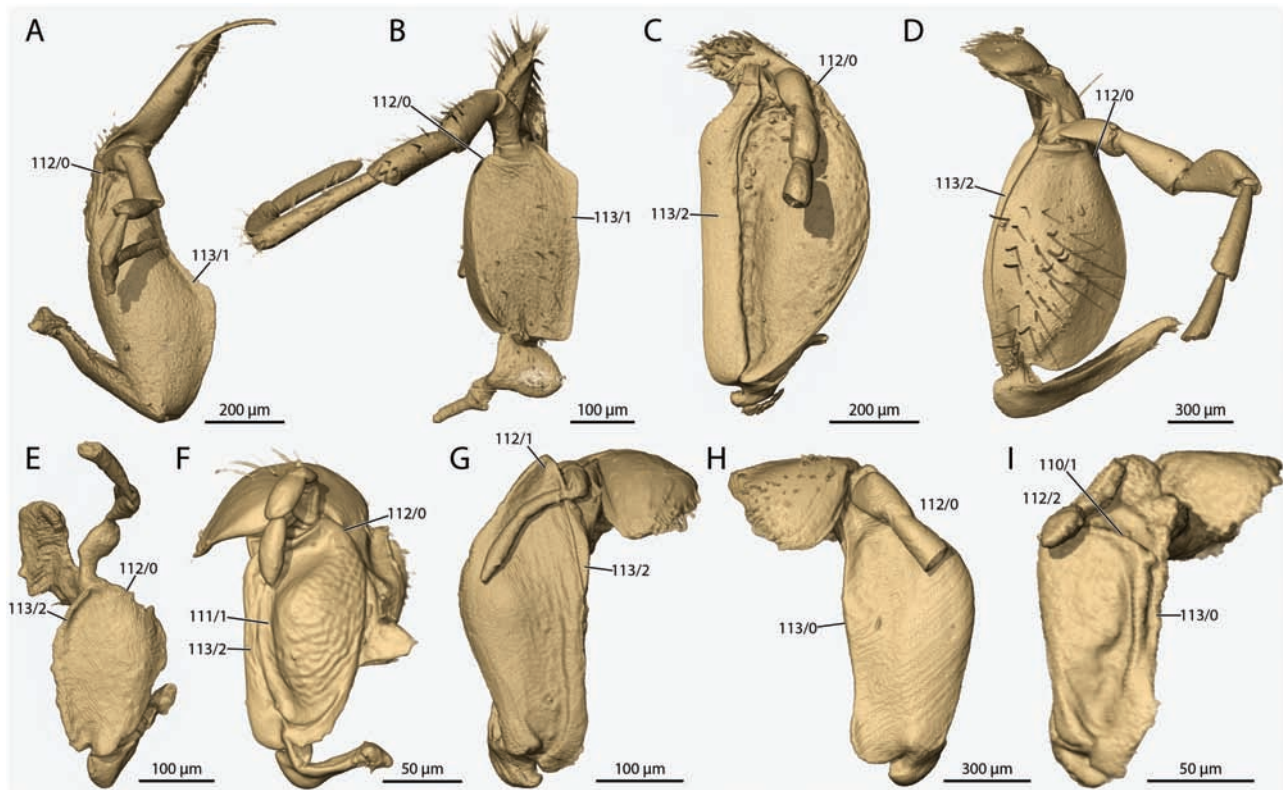
Char. 110–113. 3D reconstructions of the maxilla in external view onto the stipital sclerite, **A:** *Parischnogaster* sp., **B:** *Methocha* sp., **C:** *Ampulex* sp., **D:** *Sceliphron caementarium*, **E:** †*Gerontoformica gracilis*, **F:** *Protanilla lini*, **G:** *Brachyponera luteipes*, **H:** *Formica rufa*, **I:** *Wasmannia affinis*. **Char. 110**: transverse stipital groove, (**0**): absent, (**1**): present. **Char. 111**: longitudinal stipital groove, (**0**): absent, (**1**): present. **Char. 112**: Shape of distal stipital margin laterad palpus, (**0**): flat, (**1**): acute process, (**2**): laterally extended shoulder. **Char. 113**: Medial stipital flange, relative to stipital surface, (**0**): not raised, (**1**): raised in gentle curve, (**2**): raised in distinct step.

The mandibular condyle is reduced or fused with the atala in *Protanilla*. As a single ventrolateral articulatory process also occurs in *Harpegnathos* (e.g., Zhang et al. 2020), it is plausible that similar conditions might have evolved independently. As it is conceivable that such a fusion also occurs with a very small abductor swelling, it is not treated as reductive character dependent on atala presence here. However, this may be refined as more is learned about the lateral mandibular base. Categories 1, 2.

88.* Development of a ventral mandibular groove that interacts with the hypostomal (paramandibular) process: absent (**0**), or present (**1**).

This groove and its interaction with the hypostomal process have only been observed in *Protanilla* thus far. They are part of the complex restructuring of the mandibular base in this genus (Richter et al. 2021). Categories 1, 2.

89.~ Subapical ("pollex") incisor: developed (**0**), or not developed (**1**).

See the discussion for an explanation of the tooth-bearing margin of the mandible and our interpretation of mandibular patterning. When the subapical tooth is not developed, as is the case for example in some Scoliidae (Osten 1982) or various male ants with modified mandibles (see, e.g., Boudinot et al. 2021), the only mandibular tooth is the apical incisor, which is situated at the distal tip of the mandible and is always developed. The subapical incisor is present in all species investigated by us, although it is very flat and rounded in *Sceliphron*. Category 4. (Boudinot et al. 2022c: char. 63).

90.* Shape of apical incisor tip: rounded (**0**), or sharply pointed (**1**).

The tip of the apical incisor is rounded and blunt in *Sceliphron*, *Methocha* (and many other wasp taxa, e.g., Bohart and Menke 1976), but sharp and pointed in all studied ants, and also in *Ampulex*, and *Parischnogaster*. The shape of the apical tooth is mirrored in the subapical tooth in all species investigated here, indicating that they are closely coupled. Variation of the incisor form is likely at least partly correlated with nesting behavior and diet. Scoliids (Osten 1982), *Methocha*, and *Sceliphron* excavate from or dig into the soil and have rounded teeth, while species with predatory habits likely need a sharp point. Category 3.

91.* Shape of apical incisor: broad, not elongated, triangular (**0**), or thin, elongated, and curved (**1**).

This character statement specifically captures the shape of the apical tooth in †*Gerontoformica* (**1**), which is thin, elongated, and clearly different from that of other sampled taxa in shape. However, this is only a very rough first attempt to capture shape variation of a structure that is known to vary considerably across crown clade Formicidae (e.g., Shattuck 1992, Bolton 1994) and other groups of Aculeata (e.g., Bohart and Menke 1976). Categories 3, 4.

92.* Shape of the subapical incisor: at most as broad as the apical incisor (**0**), or distinctly broader (**1**).

As with the previous character, this statement is aimed at capturing the unique shape in †*Gerontoformica* specifically. The expansion of the tooth creates a broad, flat flange on the medial margin of the mandible. This flange, which carries the fimbriate line ventrally, is potentially used in the context of pressing prey against the stout clypeal chaetae. While it cannot be completely ruled out that the extreme flattening of the tooth observed by us is a fossilization artefact,
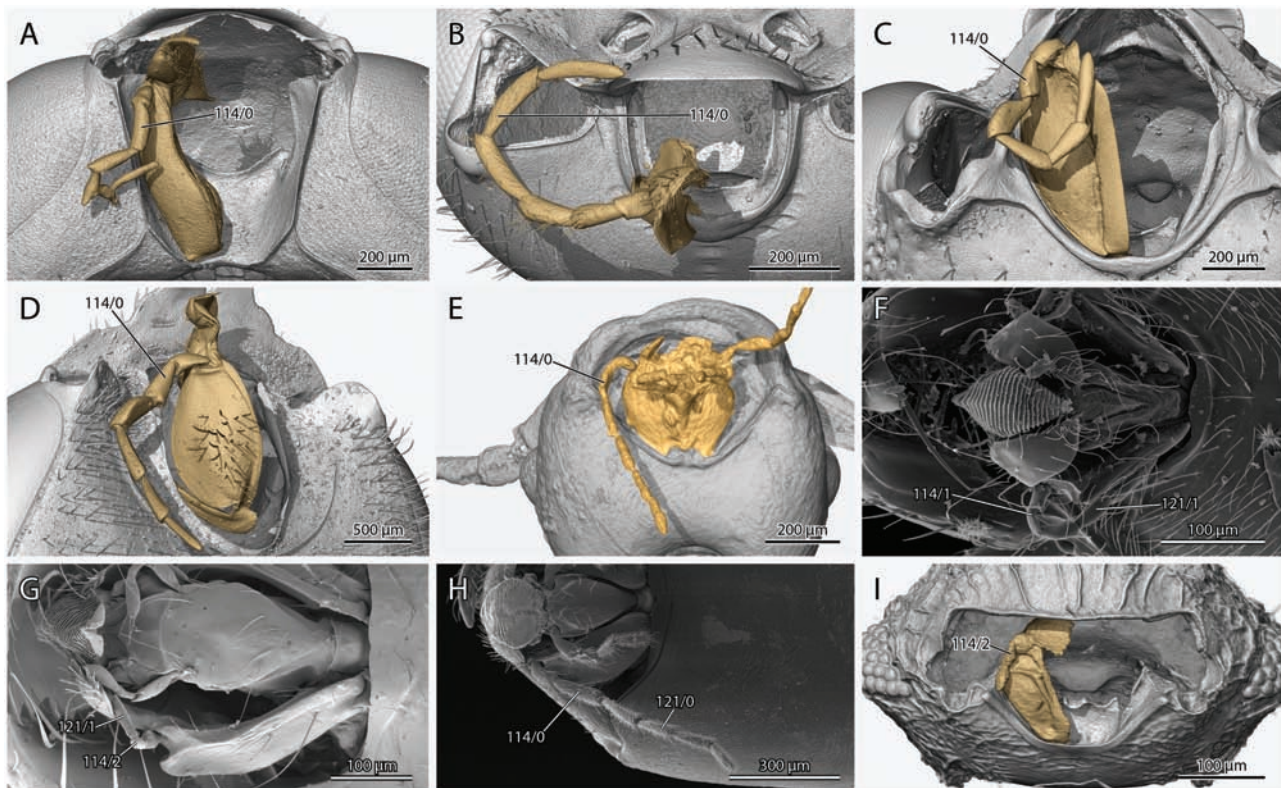
Char. 114, 121. 3D reconstructions and SEM images of the maxilla *in situ* in oral view (**A–D, I**) or the maxillolabial complex in ventral view (**E–H**), **A:** *Parischnogaster* sp., **B:** *Methocha* sp., **C:** *Ampulex* sp., **D:** *Sceliphron caementarium*, **E:** †*Gerontoformica gracilis,* **F:** *Protanilla lini*, **G:** *Brachyponera luteipes*, **H:** *Formica rufa*, **I:** *Wasmannia affinis*. **Char. 114**: Maxillary palpomere count, (**0**): 6, (**1**): 4, (**2**): 3. **Char. 121**: Sensilla density on maxillary palp, (**0**): dense, (**1**): sparse.

the general shape can be found in other species of †*Gerontoformica* as well (Barden and Grimaldi 2014). Category 3.

93.— Development of intercalary denticle(s) between apical and subapical incisors: absent (**0**), or present (**1**).

As we have outlined in the discussion, we distinguish between "denticles" developed between the apical and subapical incisors on the one hand and "denticles" developed on the gnathal margin proximad of the incisors on the other. In our sampled taxa, we observe denticles between the incisors only in *Protanilla*. According to our interpretational scheme, they also occur in other ant taxa such as *Leptanilla* (Keller 2011 images) and are common and of taxonomic importance in trap-jaw ants and genera such as *Strumigenys* (e.g., Booher and Hoenle, 2021). Additional teeth in this specific region are common in different apoid taxa (e.g., Bohart and Menke 1976, Michener and Fraser 1978). Category 3. (Boudinot et al. 2022c: chars. 64–67)

94.— Development of denticles on gnathal margin proximad subapical incisor: absent (**0**), or present (**1**).

In all aculeate outgroups considered here, as well as in †*Gerontoformica*, the gnathal margin proximad the subapical incisor is developed as a smooth carina without any additional teeth or denticles. In the species of Formicidae, various distributions of denticles are developed on this margin. Teeth and serrations of vastly different sizes, shapes and distributions occur in most ants and also many non-ant aculeatan groups (Gotwald 1969, Bohart and Menke 1976, Michener and Fraser 1978, Prentice 1998). Category 3. (Boudinot et al. 2022c: chars. 64–67)

95.— Development of teeth on gnathal margin proximad the subapical incisor: absent (**0**), or present (**1**).

As described in the previous character statement, teeth and denticles can variably be developed proximad the subapical incisor. As we distinguish between the two types of triangular tooth-line processes here, we code them as independent character statements. The validity of this approach to understand tooth-line evolution at a deeper level will ultimately have to be evaluated with developmental analyses. Based on size, species, of the ant genera *Wasmannia* and *Protanilla* do not show "teeth" in this region according to our strict definition, as all processes of their respective mandibles are distinctly smaller than apical and subapical incisors. Category 4. (Boudinot et al. 2022c: chars. 64–67)

96.— (Reductive) Number of teeth or denticles developed on the gnathal margin proximad the subapical incisor: only 1 (**0**), or more than one (**1**).

We distinguish here only the case if one additional denticle (or tooth) is developed (as in *Parischnogaster*) and if several additional teeth or denticles are present (as in *Brachyponera*, *Formica*, in both of which teeth alternate with denticles), but ultimately, different numbers of teeth (and denticles) could be analyzed in detail. A problem with the character definition in *Parischnogaster* is the absence of the markers described in the discussion to define apical and subapical incisor relative to additional teeth/ dentition. The fimbriate line is an indistinct groove on the inner side of the subapical tooth. If we retain our interpretation that the distal end of this line marks the subapical tooth, this means we need to interpret the additional denticle as occurring proximad the subapical tooth, thus arriving at the coding scheme proposed here. Interestingly, a similarly placed and sized denticle compared to *Parischnogaster* also occurs in other vespids such as polistines, in case of this subfamily with an additional distal incisor, so this denticle is termed tooth
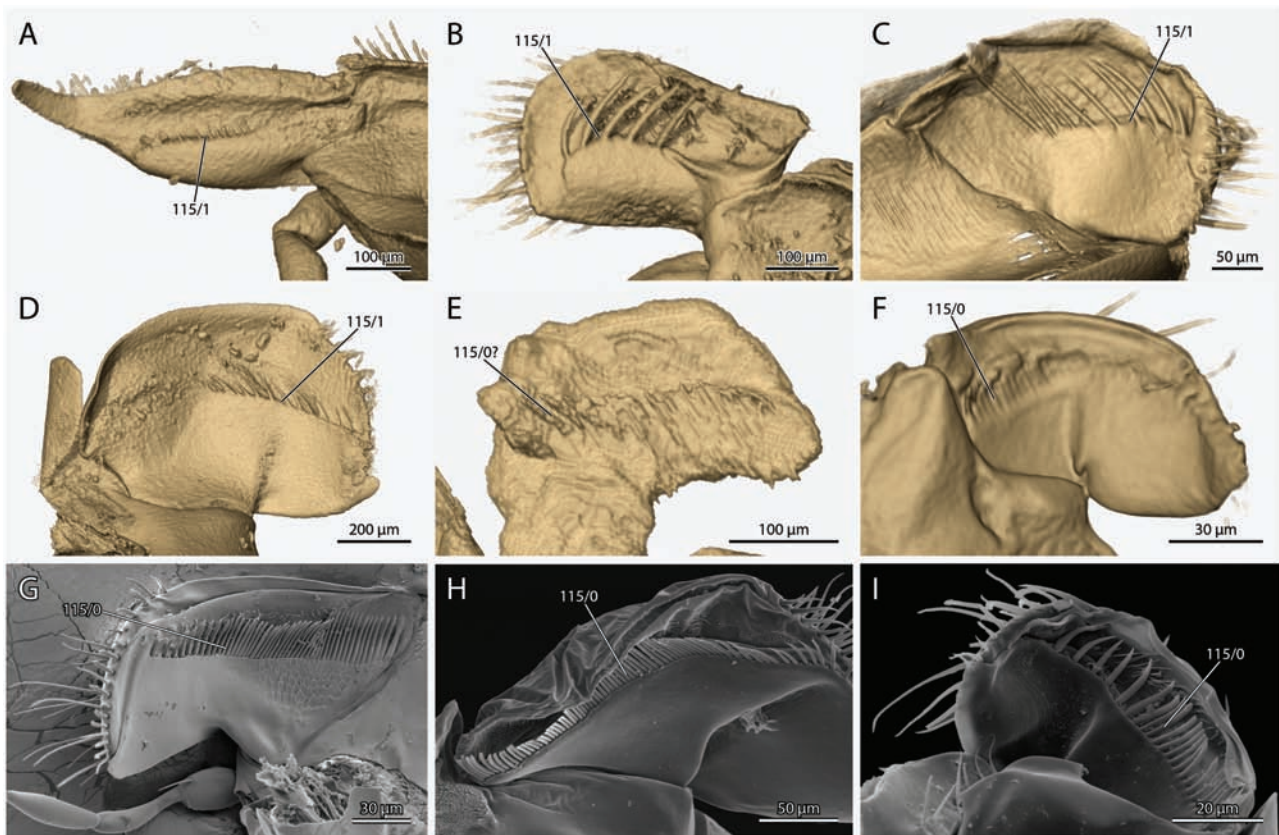
Char. 115. 3D reconstructions and SEM images of the inner surface of the galea, showing the maxillary comb, **A**: *Parischnogaster* sp., **B**: *Methocha* sp., **C**: *Ampulex* sp., **D**: *Sceliphron caementarium*, **E**: †*Gerontoformica gracilis*, **F**: *Protanilla lini*, **G**: *Brachyponera luteipes*, **H**: *Formica rufa*, **I**: *Wasmannia affinis*. **Char. 115**: Maxillary comb seta density, (**0**): most setae set closer than 1 seta base diameter, (**1**): most setae set apart farther than 1 seta base diameter.

4 by Silveira and Santos (2011). Dependent on presence of teeth and denticles (Char. 94, 95). Category 3, 4. (Boudinot et al. 2022c: chars. 64–67)

97.* A true "basal margin" developed, i.e., gnathal margin of mandible is lateromedially expanded distad to "basal angle": absent (**0**), or present (**1**).

The lateromedial expansion of the mandible distad to a defined point on the gnathal margin, which is traditionally called the "basal angle" results in the incorporation of the distal portion of the gnathal margin (which is subtended by the fimbriate line) with the apical incisor zone. This results in the formation of an elongated "masticatory margin" with the "basal margin" at an angle to it, or in other words the "triangular mandible" as traditionally described for the ants (Gotwald 1969), which is termed shovel shaped mandible here. This feature is present in all crown Formicidae considered in this study. The expansion resulting in the shovel shaped mandible shape can be modified and reduced within Formicidae in many different ways (e.g., trap-jaw ants: Gronenberg 1995, Gronenberg 1996, dorylines: Boudinot et al. 2021, *Cataglyphis bombycina*: Molet et al. 2014, Myrmeciinae: Ogata and Taylor 1991), but the initial expansion is very likely an autapomorphy of the crown group, possibly excluding Leptanillomorpha. Notably, while a shovel shaped mandible as defined here does occur in *Protanilla*, the expansion of the mandibular blade is minimal and the gnathal margin is not partly incorporated with the incisors in *Martialis* (Rabeling et al. 2008), *Leptanilla* (image atlas of Keller 2011) and *Opamyrma* (Yamada et al. 2020), at least according to our interpretation. The mandible of *Leptanilla* needs closer reexamination to test this assumption. The

multitude of variations of mandibular shape related to this condition can likely be coded in detail, but the task of discretizing them into well-defined variables will be challenging. Validation from the perspective of the developmental character concept will be crucial. Category 2.

98.* (Reductive.) Length (expansion) of basal margin relative to mandibular base: less than 0.5x (**0**), or more than 0.5x (**1**).

This character was defined to distinguish between the very small basal margin of *Protanilla* and the well-developed one of the other crown ant taxa. Comparisons with *Leptanilla* and *Opamyrma* (Yamada et al. 2020) indicate that the basal margin of *Protanilla* might be the result of a parallel development to the crown ants. A finer grained taxon sampling across the Formicidae will be necessary to elucidate the evolution of this feature. Dependent on presence in Char. 97. Category 1.

99.* Location of proximal terminus of the gnathal/ basal margin on the mandibular base: close to medial margin (**0**), or centrally/ dorsally (**1**), or completely crossing it (**2**).

In most aculeate species the proximal terminus of the gnathal margin is on the medial base of the mandible, right above the insertion point of the 0md1 adductor apodeme (see, e.g., Bohart and Menke 1976, Michener and Fraser 1978). Among our taxon sampling this occurs in *Methocha*, *Sceliphron*, *Ampulex* and †*Gerontoformica*. In many taxa however, especially in those with a true "basal margin", the terminus of this edge is shifted. In *Formica* and *Protanilla*, it is centrally on the mandibular base and in *Parischnogaster*, *Brachyponera*, and *Wasmannia* it is located laterally on the mandibular base, completely crossing it. This pattern
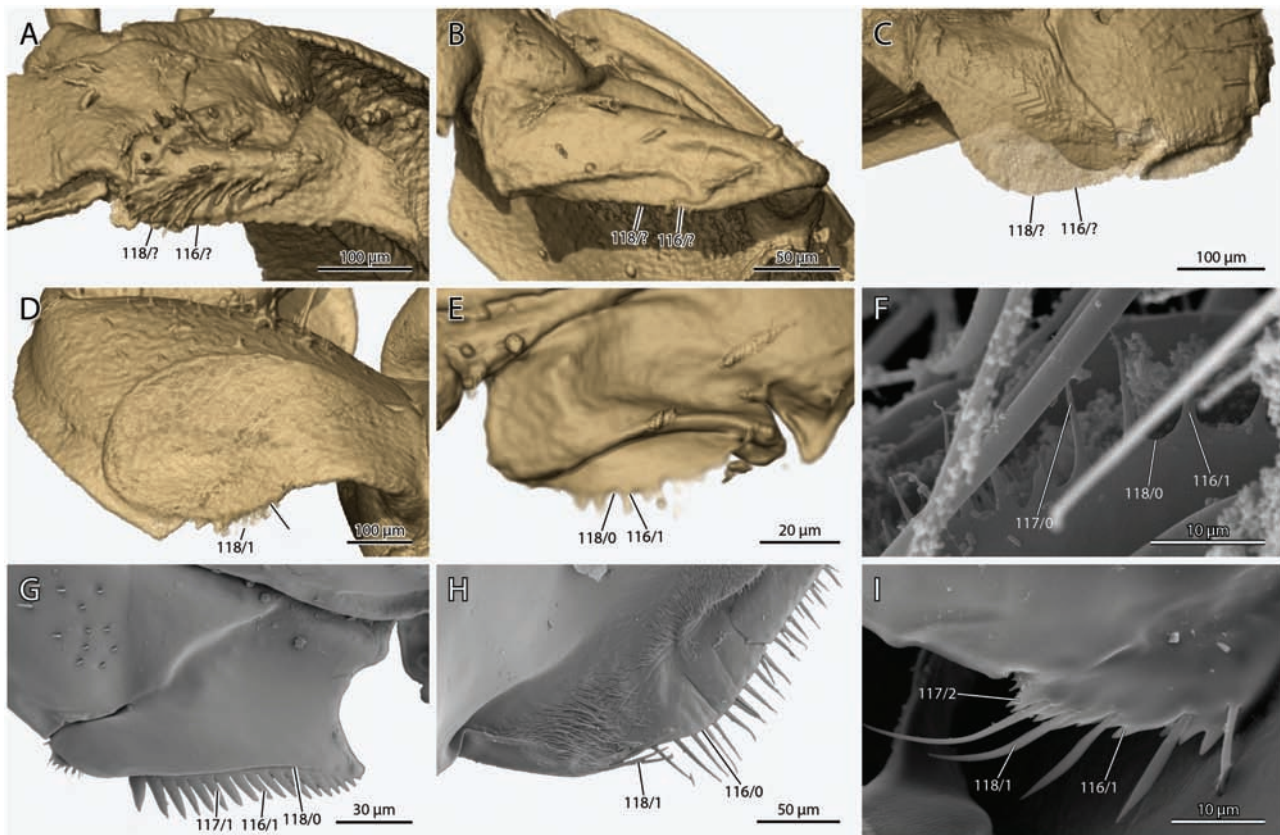
Char. 116–118. 3D reconstructions and SEM images of the lacinial margin, **A:** *Parischnogaster* sp., **B:** *Methocha* sp., **C:** *Ampulex* sp., **D:** *Sceliphron caementarium*, **E:** †*Gerontoformica gracilis*, **F:** *Protanilla lini*, **G:** *Brachyponera luteipes*, **H:** *Formica rufa*, **I:** *Wasmannia affinis*. **Char. 116**: Lacinial margin shape, (**0**): flat, unarmed, (**1**): with unarticulated spines/ denticles. **Char. 117**: Unarticulated spine shape, (**0**): sparse thin hair-like spines, (**1**): dense thick spines (**2**): sparse, short irregular denticles. **Char. 118**: Articulated setae on lacinial margin, (**0**): absent, (**1**): present.

indicates that this feature is highly variable; it will be interesting to investigate the potential mechanical consequences of such a shift. Category 1.

100. (Reductive.) Development of serration on basal margin (if present): lacking (**0**), or present (**1**).

As the mandible is extraordinarily diverse across ants and related taxa and the distinction between basal and masticatory margin is not always straightforward, these character states will not always be easy to assign. This condition does not occur among the taxa sampled in this study but is an important feature of the gnathal margin in many ants, for instance of Amblyoponinae (Yoshimura and Fisher 2012). This is a focal point of this study thus we code it here to stress this variability of the basal margin. Dependent on presence in Char. 94 and 97. Category 4. (Boudinot et al. 2022c: char. 61)

101.* (Reductive.) Size of denticles (serration) on masticatory margin relative to mandible size: minute, serration extremely fine (**0**), or denticles of variable size but distinctly larger (**1**).

The serration is extremely fine in *Protanilla*, but also in species of other ant taxa such as *Tatuidris* (Brown and Kempf 1967) and †*Zigrasimecia* (Cao et al. 2020). Serration or denticle size is highly variable, and this can be reinforced by having different sizes on the mandible of one species, in which case there might be a pattern of alternating incisors and denticles. In the species mentioned above, all teeth (including the apical incisors and all denticles) are very small. It is thus not clear if this distinctly tiny serration is a completely

different program or is just one extreme state in the continuous size variation of mandibular dentition. Dependent on presence in Char. 94. Category 1.

102. Development of specialized, stout chaetae on fimbriate line: absent (**0**), or present (**1**).

Specialized chaetae are present along the inner mandibular hair line of *Protanilla lini* and similar dense brushes of long and thick, pointed setae are also present in †*Zigrasimecia* (Cao et al. 2020) and *Tatuidris* (Brown and Kempf 1967). It is likely that a similar condition has evolved several times convergently or in parallel. The hairline is generally present in ants and Aculeata and thus "available" for variation such as this one. Category 4. (Boudinot et al. 2022c: char. 68)

103.* Degree of development of acetabular groove: well-developed, connecting acetabulum and subapical tooth (**0**), or base reduced, only distal part present (**1**), or distal part reduced, only base is present (**2**), or no groove is observable (**3**).

Among the sampled taxa, only *Sceliphron* and *Protanilla* show a well-developed acetabular groove (**0**). In *Methocha*, *Ampulex*, and *Gerontoformica*, only a distal portion of the groove is more or less clearly developed. In all other species no trace of the groove could be observed, but a basal portion is present variably across Formicidae, especially Formicinae and Dolichoderinae (B. Boudinot, unpubl. data). Even if no groove is visible, some taxa still show a line of hairs (e.g., *Opamyrma*, Yamada et al. 2020), that might mark its location. The groove was used as an
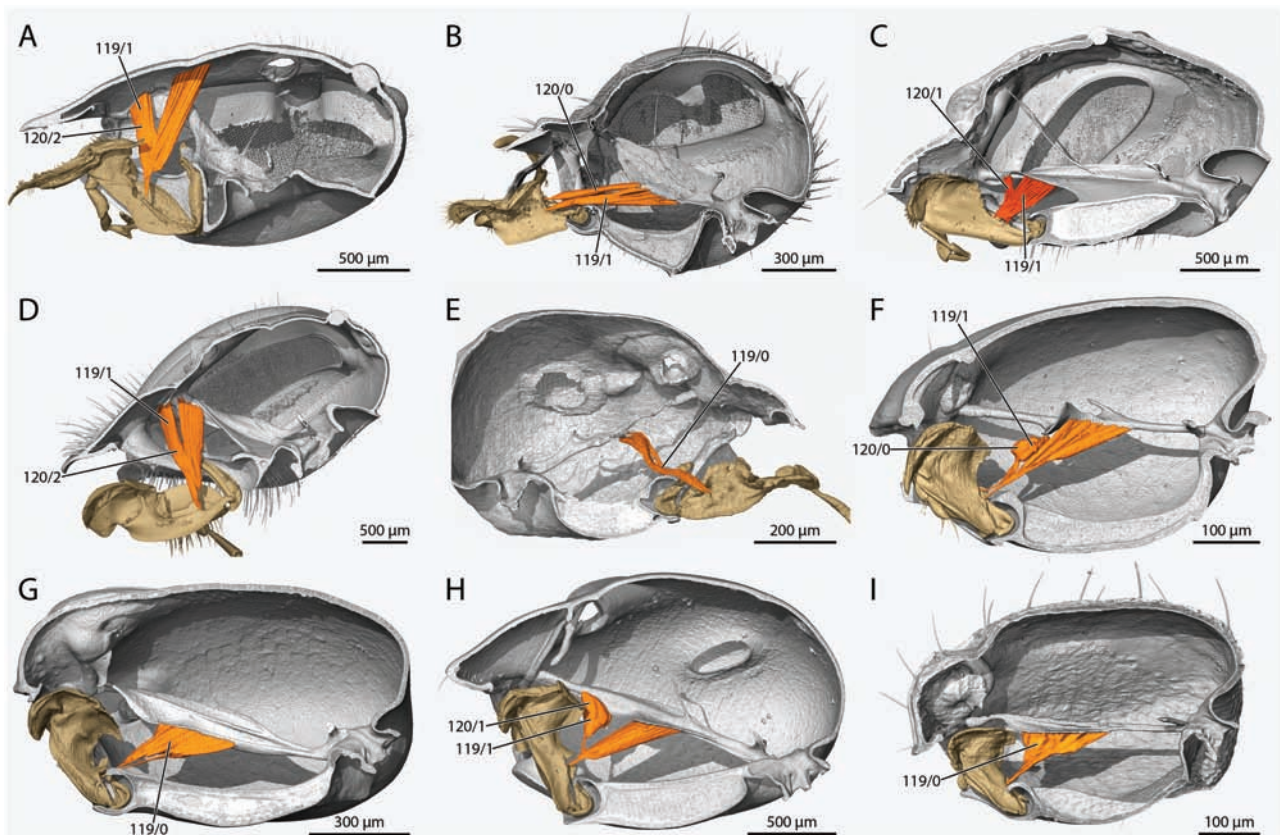
Char. 119, 120. 3D reconstructions of the maxilla and *M. tentoriostipitalis* (0mx4) in sagittal view, **A:** *Parischnogaster* sp., **B:** *Methocha* sp., **C:** *Ampulex* sp., **D:** *Sceliphron caementarium*, **E:** †*Gerontoformica gracilis*, **F:** *Protanilla lini*, **G:** *Brachyponera luteipes*, **H:** *Formica rufa*, **I:** *Wasmannia affinis*. **Char. 119:** 0mx4 bundle count, (**0**): 1, (**1**): 2. **Char. 120:** Origin of anterior bundle of 0mx4, (**0**): on medial tentorial lamella, (**1**): on anterior tentorial arm anterad lamella, (**2**): on head capsule at or close to epistomal ridge.

important marker on the mandibles of bees by Michener and Fraser (1978), and it is clear that a very similar concavity occurs widely across Aculeata. However, the relevance and homology of the groove across Aculeata has yet to be shown conclusively (see also Hermann et al. 1971). Category 1.

104.* Lateromedial curvature of mandibular base relative to entire mandible: same curve (**0**), stronger curve (**1**), or straight (**2**).

A gentle medial curve is common in all mandibles we compared. While in most outgroup species and *Wasmannia*, the curve is even throughout the appendage, the mandibles of †*Gerontoformica* are characterized by a much sharper curve in their proximal third, and those of *Parischnogaster*, *Protanilla*, *Brachyponera* and *Formica* are almost entirely straight in their proximal region and only bent medially in their distal part. As a marker for this character, we took the curve of the outer mandibular margin in dorsal (/frontal) view. This is clearly only a small aspect of mandibular shape variation and likely has little explanatory power on its own. However, the present characterization represents a first approximation of some of the shape variation observed in mandibles across Aculeata and especially crown clade Formicidae (Gotwald 1969). This applies to the next two characters as well. A three-dimensional shape analysis of mandibles will likely yield insights in this context and is forthcoming. Category 1, 2.

105.* Curvature of mandible in dorsoventral plane: straight to almost straight (**0**), or at most gently curved throughout (**1**), or mandible with a strong downward curve (**2**).

We assessed the dorsoventral curvature of the mandibles in lateral view with the lateral margin of the clypeus in a horizontal orientation. The curvature of the ventral mandibular margin and the (downward) displacement of the apical incisor tip relative to the mandibular condyle were used as criterion. The mandibles in *Methocha*, *Ampulex*, and †*Gerontoformica*, are almost entirely straight, while those of most extant ant species (of *Wasmannia*, *Brachyponera*, *Formica*), and species of *Parischnogaster* and *Sceliphron* are at least slightly curved downward in lateral view. The mandible of *Protanilla* is instead very strongly curved downward. Dorsoventral mandibular curvature also strongly influences the angle of the masticatory margin relative to the longitudinal axis of the head, together with other aspects such as torsion of the mandible around its proximodistal axis (Character 106). The orientation of the masticatory margin likely has important functional implications. Interestingly, it approaches a parallel orientation in presumed predators such as *Brachyponera* (also *Protanilla* but with a strong downward curve distally) and is almost entirely parallel in †*Gerontoformica*. In more "generalist" ants such as species of *Wasmannia* and *Formica*, the masticatory margin is at a distinct 45° angle relative to the longitudinal angle of the head, this being caused by the slight downward curve of the apical tooth relative to the remaining blade. The mandible of these ants is more "shovel"-shaped instead of "scissor"-shaped. As the angle can currently not be disentangled from other qualities such as the downward curve and overall torsion of the mandible (see Char. 106), we will not code it individually, although it might be
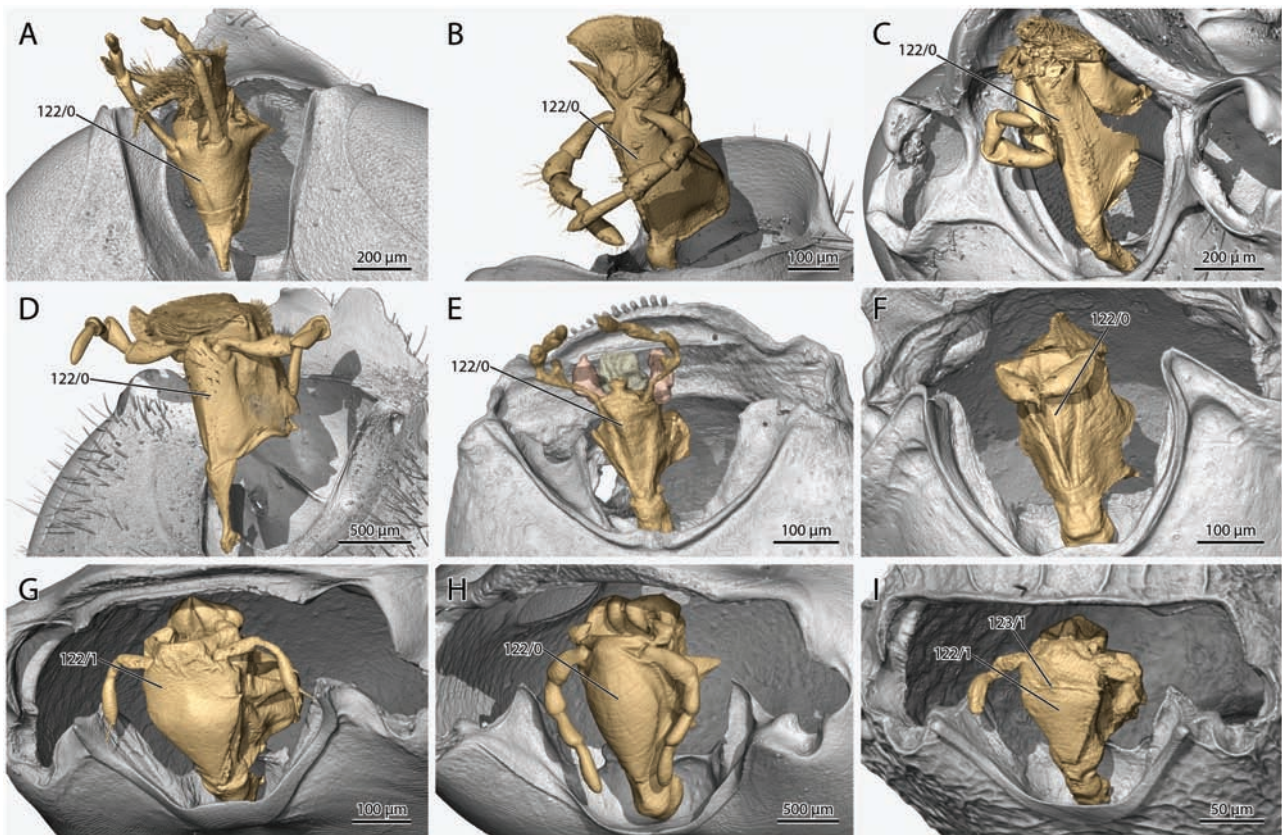
Char. 122, 123. 3D reconstructions of the labium *in situ* in ventrolateral view, **A:** *Parischnogaster* sp., **B:** *Methocha* sp., **C:** *Ampulex* sp., **D:** *Sceliphron caementarium*, **E:** †*Gerontoformica gracilis*, **F:** *Protanilla lini*, **G:** *Brachyponera luteipes*, **H:** *Formica rufa*, **I:** *Wasmannia affinis*. **Char. 122:** Curvature of ventral premental face, (**0**): convex, (**1**): flat. **Char. 123:** Transverse premental groove, (**0**): absent, (**1**): present.

interesting to analyze it biomechanically in the future. Category 1, 2.

106.~ Medial torsion of the mandibular blade; mandible not torqued (**0**), or torqued (**1**).

In a mandible with medial torsion of the blade, its external surface is visible in dorsal (frontal) view and the edge of the gnathal margin in frontal/ caudal (dorsal/ ventral) view. In a mandible without torsion, the external surface is visible in frontal (ventral) view and the edge of the gnathal margin in dorsal (frontal) view. The effect of the torsion is modified by the curvature of the mandible (see characters above) and is not always complete at 90°, but mandibles with any visible degree of torsion were coded as (**1**) here. Among the sampled taxa, only *Sceliphron* and *Methocha* do not have a torqued mandible. This character corresponds to Keller (2011: char. 29) and Rasnitsyn and Quicke (2002: char. 104) and is interpreted by the latter as a autapomorphy of Aculeata excl. Chrysidoidea. Category 2. (e.g. Keller 2011: char. 29).

107.* *M. craniomandibularis internus* 0md1 apodeme subdivisions: one branch (**0**), or two branches (**1**), or three branches (**2**).

One branch occurs in *Parischnogaster*, *Methocha*, *Sceliphron*, and *Protanilla*, two in *Ampulex*, *Formica*, and *Wasmannia*, and three in †*Gerontoformica* and *Brachyponera*. *Methocha* and *Sceliphron* are coded as having one branch, but the structure is "anchor shaped", giving it a tripartite appearance. The apodeme shape is complicated in †*Gerontoformica* with a broad sheet that is cone shaped distally and extends into three main branches. Due to the limited preservation, it cannot be excluded that the apodeme

is more accurately described as two branches with a complicated shape resulting in the three part appearance. The second branch in *Formica*, *Wasmannia* and to a certain degree also *Ampulex* is much thinner and shorter than the main branch. In all species, an accessory branch occurs that branches from the main branch to a muscle bundle originating around the occipital foramen, this was not considered in the number of branches for this character. Category 1, 2.

108.* *M. craniomandibularis internus* 0md1, fibrillar fibers: absent (**0**), or present (**1**).

In most crown ants, at least a part of the fibers of 0md1 are attached to the apodeme through thin cuticular fibrillae (Gronenberg et al. 1997). In †*Gerontoformica* and all sampled outgroups, such fibers are absent, although we cannot completely exclude that a few very short cuticular fibrillae may be present in the extinct ant genus. The pattern observed in the taxa under investigation here indicates that this condition might be an apomorphy of the crown ants. However, fiber composition is without a doubt extremely variable within this clade (Gronenberg et al. 1997). Consequently, our interpretation is a working hypothesis. Category 3.

109.* Location of origin of *M. craniomandibularis externus* 0md3: exclusively on lateral or ventral head capsule (**0**), or with a significant portion on postgenal ridge (**1**).

The origin of a sizeable portion of 0md3 on the postgenal ridge is one of the main features of total clade Formicidae, potentially allowing for more delicate control of the mandibles. A prerequisite of this condition is the elongation of the postgenal ridge. Potentially,
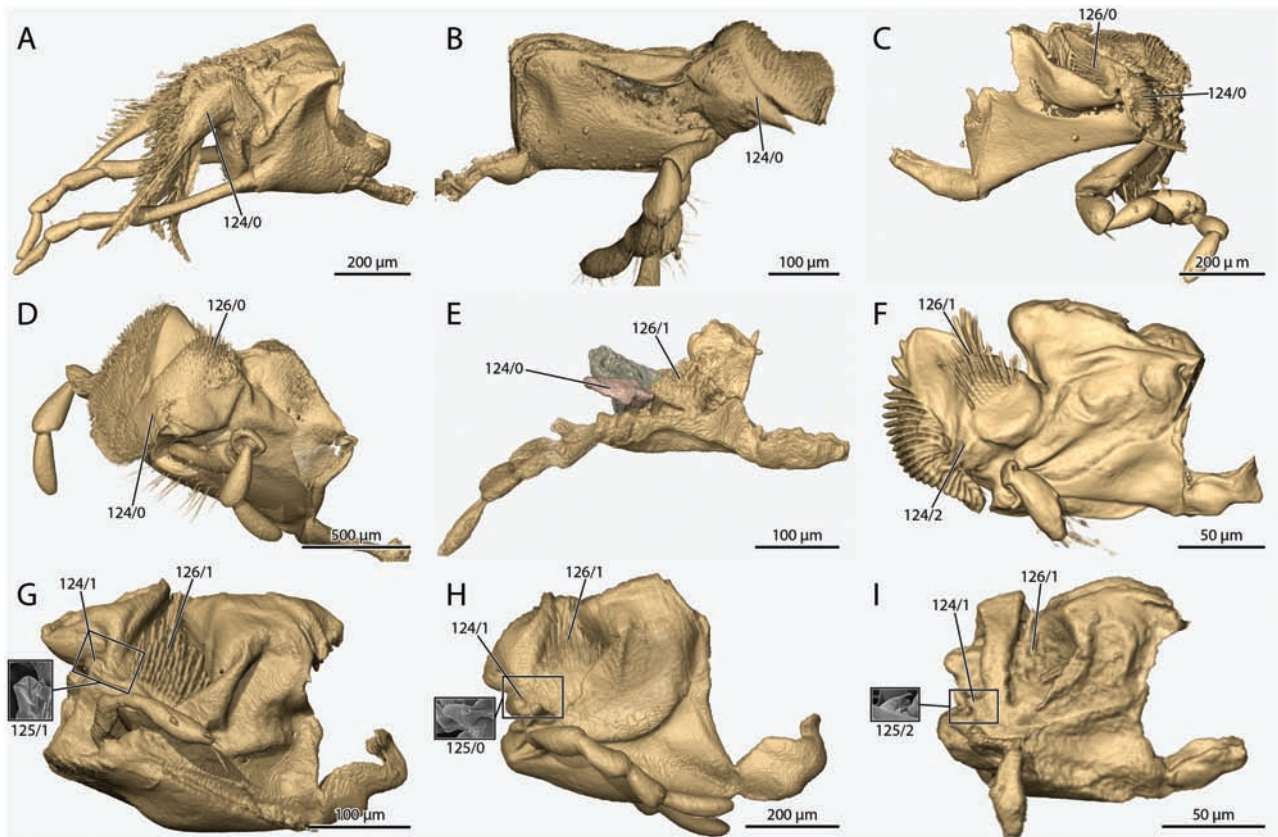
Char. 124–126. 3D reconstructions of the labium in lateral view, **A:** *Parischnogaster* sp., **B:** *Methocha* sp., **C:** *Ampulex* sp., **D:** *Sceliphron caementarium*, **E:** †*Gerontoformica gracilis*, **F:** *Protanilla lini*, **G:** *Brachyponera luteipes*, **H:** *Formica rufa*, **I:** *Wasmannia affinis*. **Char. 124**: Paraglossa size, (**0**): as long as glossa, (**1**): much shorter than glossa, (**2**): very reduced, no lobe visible. **Char. 125**: Shape of small paraglossae, (**0**): lobe covered in microtrichia-denticles, (**1**): lobe with apical conical sensilla, (**2**): lobe with long, flat apical microtrichia. **Char. 126**: Position of basiparaglossal brush relative to glossa, (**0**): level to, (**1**): proximal to.
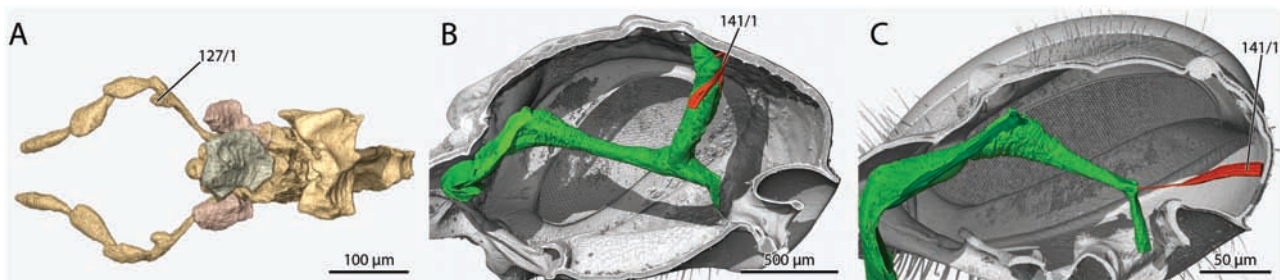
Char. 127, 141. 3D reconstructions of the labium of, **A:** †*Gerontoformica gracilis* in dorsal view and the pharynx with *M. verticopharyngalis* (0phy1) in **B:** *Ampulex* sp., **C:** *Sceliphron caementarium*. **Char. 127**: Medial process of first labial palpomere, (**0**): absent, (**1**): present, (**2**): very reduced, no lobe visible. **Char. 141**: 0ph1, (**0**): absent, (**1**): present.

an elongated postgenal bridge is always associated with this shift of muscle origin, considering this also occurs in *Ampulex* and *Methocha* and is only absent (**0**) in *Parischnogaster* and *Sceliphron*. Category 1.

Maxilla:

110. Development of transverse groove close to distal margin of external surface of stipital sclerite, curving into longitudinal groove at medial margin: absent (**0**), or present (**1**).

In different species of Formicidae, a variety of different grooves occurs on the external surface of the stipes (see, e.g., Keller 2011 char. 35). The specific type of groove described here was observed in *Wasmannia*,

which is the only representative in our sample with this condition. When adding additional taxa with a stipital groove in phylogenetic analyses, their precise anatomy and precision should be considered to account for independent origins of this feature as much as possible. A transverse stipital groove is, as far as presently known, always associated with a tight closure of the oral foramen, as it interacts with the distal labral margin. Categories 1, 4. (Keller 2011: char. 35)

111.* Development of longitudinal stipital groove: absent (**0**), or present (**1**).

A longitudinal groove along the medial region of the stipes partly receives the maxillary and/or labial palpus in *Protanilla* when the maxillolabial complex is retracted (Richter et al. 2021). As this
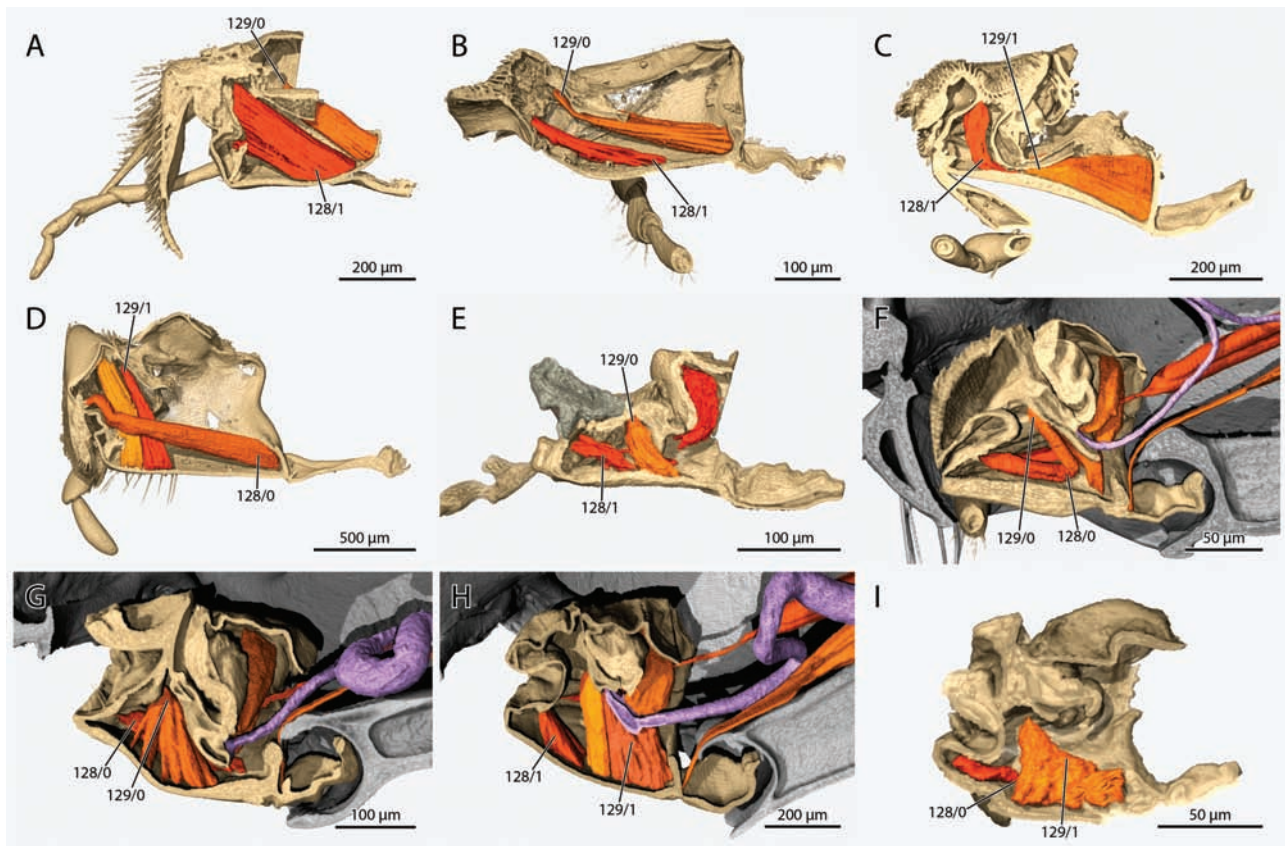
Char. 128, 129. 3D reconstructions of the labium and its inner muscles in sagittal view, **A:** *Parischnogaster* sp., **B:** *Methocha* sp., **C:** *Ampulex* sp., **D:** *Sceliphron caementarium*, **E:** †*Gerontoformica gracilis*, **F:** *Protanilla lini*, **G:** *Brachyponera luteipes*, **H:** *Formica rufa*, **I:** *Wasmannia affinis*. **Char. 128:** Origin area of *M. praementoparaglossalis* (0la11) relative to origin of M. *praementoglossalis* (0la12), (**0**): at level of or proximad, (**1**): distad. **Char. 129:** *M. praementosalivarialis* (0hy7), (**0**): absent, (**1**): present.

character was not coded in previous analyses of ant morphology (Keller 2011), it might be unique to the species or a small group (e.g., Anomalomyrmini) including it. Category 1.

112.~ Shape of distal stipital margin directly laterad palpus insertion: flat, not produced (**0**) or produced into acute process (**1**), or produced into flat, laterally expanded shoulder (**2**).

The shape of the distal stipital portion is closely associated with the maxillolabral interaction type (see Char. 66). A short acute process as in state (**1**) occurs in *Brachyponera luteipes* and an acute process of various dimensions occurs in most other species of Poneria ("poneroids"), but also some other Formicidae (Keller 2011). A laterally expanded but mostly flat shoulder (**2**) occurs in *Wasmannia* and other species of Myrmicinae as well as in Ectatomminae and some Dorylinae (Keller 2011). This feature was treated by Keller (2011: char. 33), but reanalysis with 3D-information of an expanded taxon sampling will be highly beneficial to understand the evolution of this functionally significant character. Category 2, 4. (discussed in Keller 2011: char. 33)

113.* Principal carina of stipes (medial stipital flange) relative to external stipital surface: not raised (**0**), or only slightly raised in gently curve (**1**), or raised in distinct step (**2**).

The external stipital sclerite is medially produced into a flange that is termed as principal carina of the stipes in Apocrita (e.g., Duncan 1939, Popovici et al. 2014; Prentice 1998: stipital carina). The carina is present to some degree in all investigated species. In *Ampulex*, *Sceliphron*, †*Gerontoformica*, *Protanilla*, and *Brachyponera* the flange is at least partly raised in a distinct step from the remaining

external stipital surface. It is only slightly raised in a gentle curve instead of an angle in *Methocha* and *Parischnogaster* and is not distinctly raised in *Formica* and *Wasmannia*. The observed pattern indicates that this is a highly variable character state. It is included here to stress the variability of the stipital flange and to inspire more detailed observation to better understand its functional significance and evolutionary trajectories. Category 1.

114. Maxillary palpomere count: 6 (**0**), or 4 (**1**), or 3 (**2**).

Palpomere count is a highly variable feature within crown clade Formicidae (*e.g.*, Bolton 1994, 2003, Keller 2011) and across Apocrita more generally (e.g., Boudinot 2020). The groundplan number of Formicoidea and Aculeata is most certainly six palpomeres (Bolton 2003), which occurs in all of our outgroups as well as in †*Gerontoformica* and *Formica*. *Protanilla* has four, and *Brachyponera* and *Wasmannia* have three maxillary palpomeres. Category 4. (e.g., Keller 2011: char 36)

115.* Maxillary comb, density of setae: set closer than one seta diameter (**0**), or set at least one seta base diameter apart (**1**).

The maxillary comb is a straight line of thick setae set on the inner side of the galea. In all species of crown Formicidae, a majority of the setae are set very close to each other with less than one seta diameter space between them. Only in the very distal part of the comb does the distance between setae increase beyond this level. In the observed outgroups however, all setae in the comb are set distinctly further apart, i.e., by at least one seta base diameter. As the number of setae generally seems to be higher in ants, seta count may be an alternative way of capturing this
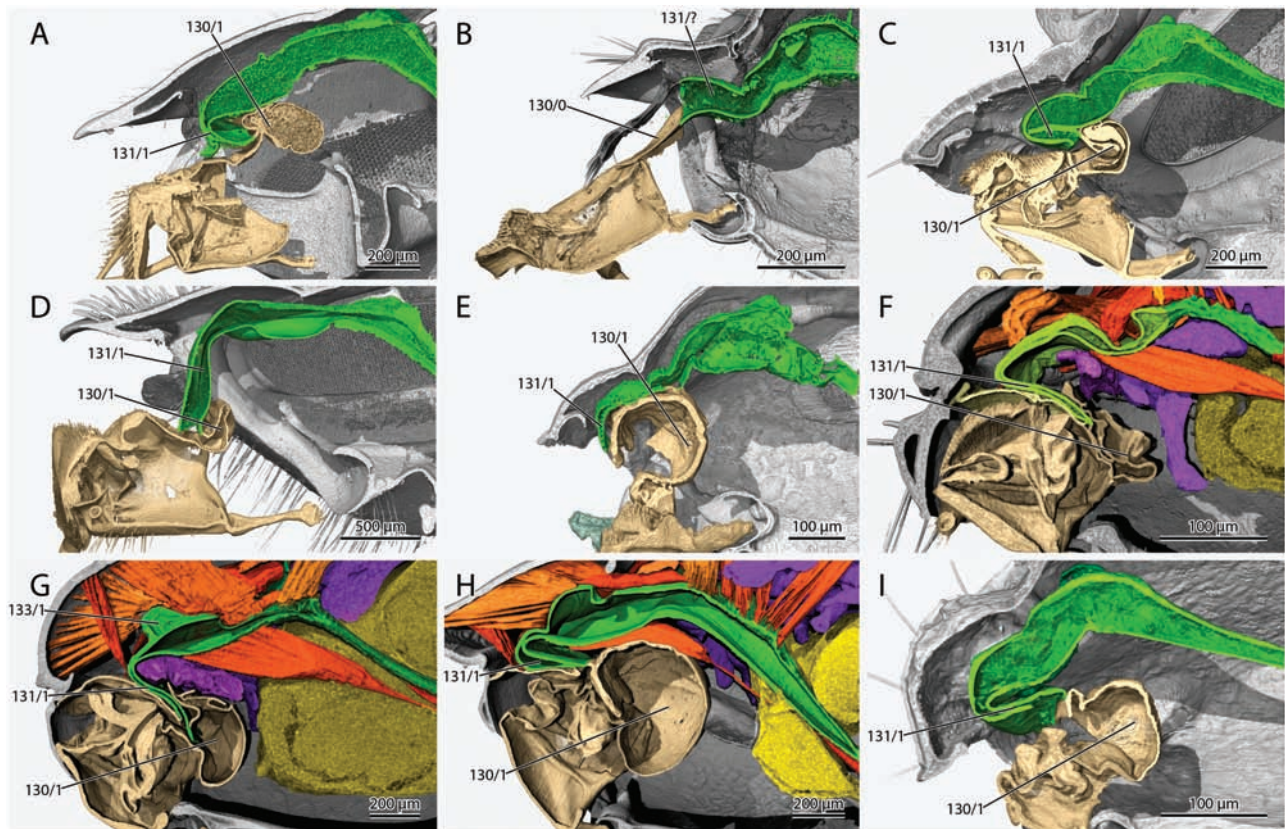
Char. 130, 131, 133. 3D reconstructions of the distal cephalic digestive tract in sagittal view, **A:** *Parischnogaster* sp., **B:** *Methocha* sp., **C:** *Ampulex* sp., **D:** *Sceliphron caementarium*, **E:** †*Gerontoformica gracilis*, **F:** *Protanilla lini*, **G:** *Brachyponera luteipes*, **H:** *Formica rufa*, **I:** *Wasmannia affinis*. **Char. 130:** Infrabuccal pouch, (**0**): absent, (**1**): present. **Char. 131:** Buccal tube orientation, (**0**): straight, (**1**): distinctly curved downward. **Char. 133:** Sclerotized keel on epipharyngeal wall of prepharynx, (**0**): absent, (**1**): present.

variation. Although the presence of the brush can be confirmed for †*Gerontoformica*, the quality of the reconstruction is not sufficient to assess the character state. The close position appears more likely based on the µ-CT data, but we conservatively code †*Gerontoformica* as (**?**). Category 1.

116.* Shape of lacinial margin: flat and unarmed (**0**), or with unarticulated spines or denticles (**1**).

The armament of the lacinial margin is highly variable, with either unarticulated spines of differing shape, or articulated setae, or combinations of the two. Previous evaluations of the lacinial margin did not differentiate between articulated setae and unarticulated processes (Gotwald 1969). This and the following two characters are intended to represent an initial survey of the different occurring configurations, but more detailed investigations will be necessary to understand the significance of this feature and to code it more precisely in character statements. As these characters and states represent fine details, µ-CT scanning data can only confidently resolve them if the resolution of the data is very high. This limits their application based on the available data. We were able to confirm the presence of spines or denticles (**1**) for *Protanilla* and *Brachyponera* based on both µ-CT scanning data and SEM images, and for *Wasmannia* only based on SEM images. SEM images confirmed the absence in *Formica*. Spines or denticles were not observed in any other taxa, but as only µ-CT scanning data were available for these, we conservatively coded them as (**?**). For †*Gerontoformica*, neither this nor the following to characters could be applied, as the lacinia is not sufficiently preserved. Category 1.

117.* (Reductive.) Shape of comb of unarticulated spines on lacinia: sparse row of thin spines ending in hair-like extensions (**0**), or dense row of short, thick, pointed spines (**1**), or sparse row of short, irregular denticles (**2**).

In *Wasmannia*, irregular denticles (**2**) are interspersed with longer setae, while in *Brachyponera* (**1**) and *Protanilla* (**0**) only spines of variable shape are present, and setae are lacking. Dependent on state (**1**) in Char. 116. Category 1.

118.* Articulated setae on lacinial margin: absent (**0**), or present (**1**).

Articulated setae could be confirmed on the lacinial margin of *Formica* and *Wasmannia* based on SEM images (not visible in µ-CT data). They are also tentatively coded as present (**1**) here in *Sceliphron* and *Ampulex*, but low scan resolution makes it challenging to differentiate between setae with articulations and spines without it. In *Methocha* and *Parischnogaster* several setae were confirmed based on µ-CT data on the external lacinial surface, but none very close to the lacinial margin. They were tentatively treated as absent (**0**) here. Category 2.

119.~ Development of *M. tentoriostipitalis* 0mx4: present as only one recognizable bundle (**0**), or as two clearly separated bundles (**1**).

In all species that were included here, two tendons which insert very close to each other on the stipes can be recognized. However, in some cases these tendons are associated with clearly separated muscle bundles while in other cases they are set so close to each other that only one bundle can be recognized. The variability of this feature could be associated with tentorial shape and potentially also general space available in the head. In †*Gerontoformica*,
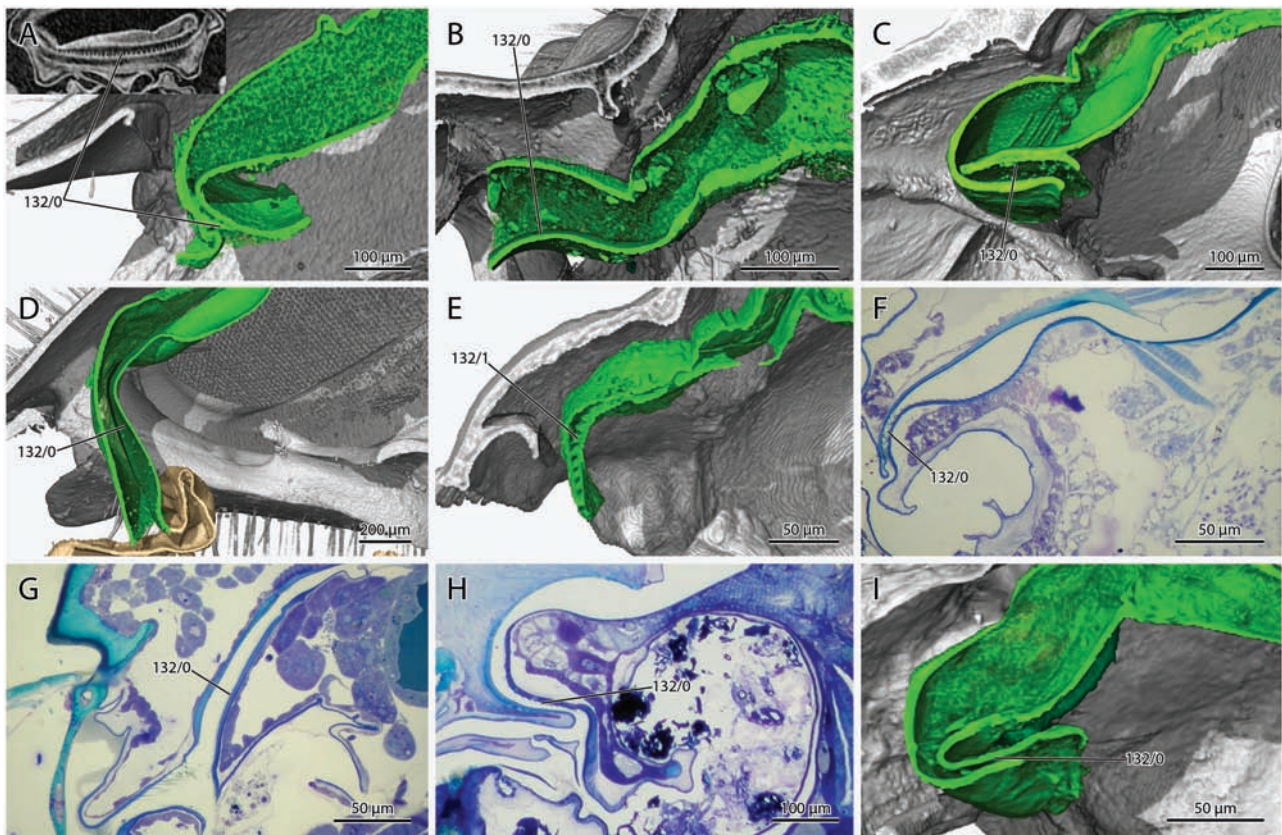
Char. 132. 3D reconstructions and histological sections of the distal prepharynx in sagittal view, **A:** *Parischnogaster* sp., **B:** *Methocha* sp., **C:** *Ampulex* sp., **D:** *Sceliphron caementarium,* **E:** †*Gerontoformica gracilis,* **F:** *Protanilla lini,* **G:** *Brachyponera luteipes,* **H:** *Formica rufa,* **I:** *Wasmannia affinis.* **Char. 132:** Transverse ridges within buccal tube, (**0**): fine or not visible, (**1**): coarse and massive.

only one bundle was observed, but it cannot be excluded that the second bundle is not preserved. One bundle is also present in *Brachyponera* and *Wasmannia,* while all other taxa have clearly separated muscles. In *Ampulex* and *Methocha,* the two bundles also have clearly separated points of insertion, but this condition was not observed in any of the investigated total clade Formicidae. This feature was previously coded by Zimmermann and Vilhelmsen (2016: char. 19) as the distinction of having two independent insertions on the stipes or just one. Category 3. (Zimmermann and Vilhelmsen 2016: char. 18)

120.* (Reductive.) Origin of anterior portion of 0mx4, if developed as two separate bundles: on medial tentorial lamella (**0**), or anterad lamella on anterior tentorial arm (**1**), or on head capsule close to or on the frontoclypeal strengthening ridge (**2**).

As discussed above, the condition of this muscle is likely at least partly dependent on tentorial shape. The anterior bundle originates on the medial tentorial lamella in *Methocha* and *Protanilla* (**0**) and on the anterior tentorial arm in *Ampulex* and *Formica* (**1**). In *Sceliphron* and *Parischnogaster,* both bundles of the muscle are shifted far anterad compared to other species, which is related to the more orthognathous head orientation and the anterior bundle (both bundles in *Parischnogaster*) originates on the head capsule rather than the tentorium (**2**). We note further that in *Parischnogaster* the anterior bundle originates on a lobe formed by the epistomal ridge. Dependent on presence of two bundles in Char. 116. Category 1.

121.~ Density of maxillary palp setation: dense, with more than 20 setae on each palpomere on average (**0**), or sparse, with less than 20 setae on each palpomere on average (**1**).

This is only a very rough categorization. The number of 20 setae is arbitrary, but among the investigated species, there is a very clear difference between the densely covered palpomeres of *Formica* and the less densely covered ones of all other taxa, although *Methocha* is very close to the threshold defined here. †*Gerontoformica* seems to have a sparse cover of setae on the palpus, but our photographs are of insufficient resolution to clarify this with certainty. As with some other characters, this feature would require SEM or similar high-resolution study of all involved taxa for fully satisfactory evaluation. All outgroup taxa had to be coded as (**?**) for this feature. The dense setation of the maxillary palp is individuated into adpressed shorter setae and longer, thicker, erect setae in *Formica.* This was not further considered as it is not applicable to any other taxon in the current sample but might be worth evaluating among other ants. Based on the images of Keller (2011) sparse or very sparse setation is widespread across Formicidae, but dense setation similar to *Formica* occurs also in other Formicinae, Dolichoderinae, Myrmeciinae, Pseudomyrmecinae and a few species across other subfamilies, such as in *Platythyrea* in Ponerinae. Denser setation, although less dense than in the previous examples, also occurs in *Discothyrea* (Proceratiinae), Paraponerinae and Myrmicinae. This suggests overall high variability across the subfamilies. Hashimoto (1991) used the density of labial palp sensilla for phylogenetic inference and based on our observations sensilla density is similar in maxillary and labial palp, so only maxillary palp setation is coded here as proxy for both palp pairs. Category 2.
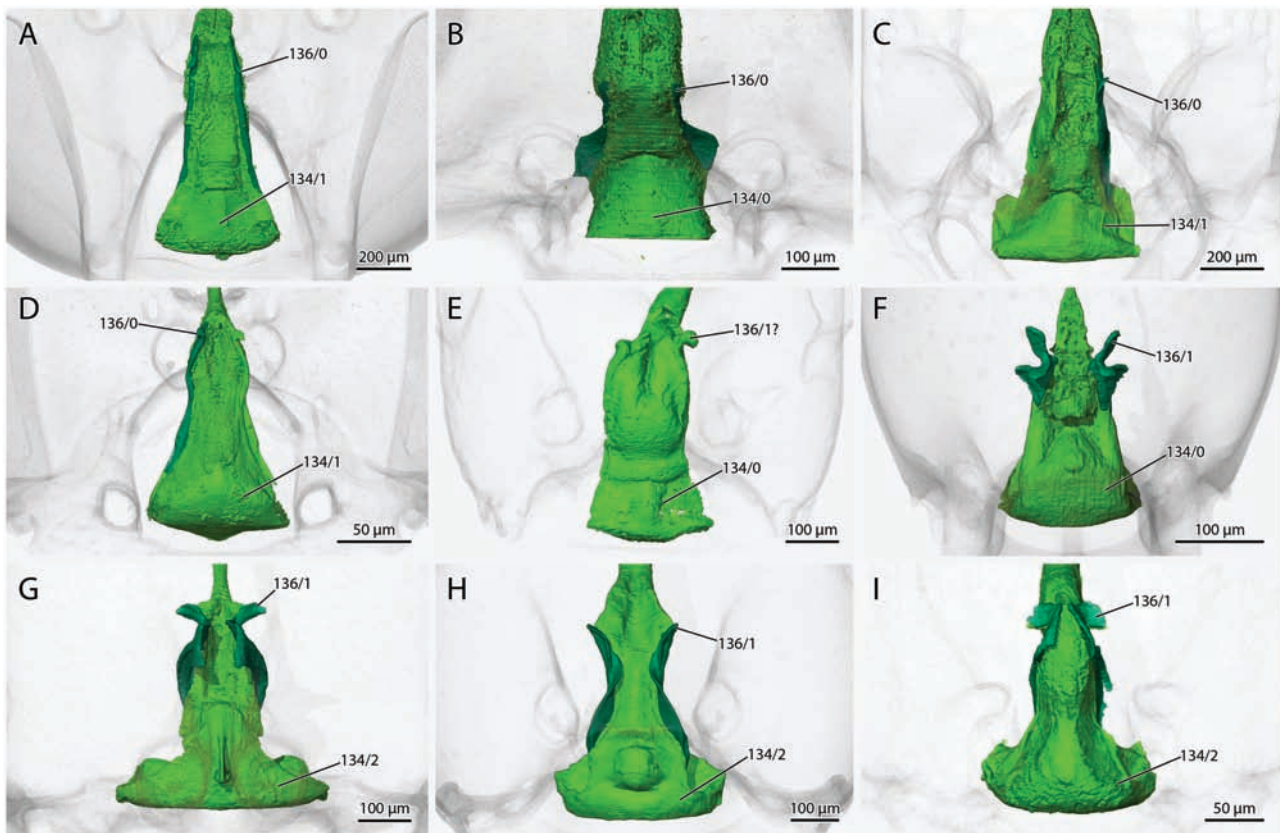
Char. 134, 136. 3D reconstructions of the prepharynx with oral arms in dorsal view, **A**: *Parischnogaster* sp., **B**: *Methocha* sp., **C**: *Ampulex* sp., **D**: *Sceliphron caementarium*, **E**: †*Gerontoformica gracilis*, **F**: *Protanilla lini*, **G**: *Brachyponera luteipes*, **H**: *Formica rufa*, **I**: *Wasmannia affinis*. **Char. 134**: Distal prepharynx/ buccal tube widening relative to proximal prepharynx at level of anatomical mouth, (**0**): not widened, (**1**): evenly widening throughout, (**2**): abruptly widened. **Char. 136**: Oral arm process length, (**0**): small, roughly as long was wide, (**1**): large, longer than wide.

Labium:

122.~ Curvature of ventral (aboral) surface of prementum: convex (**0**), or flat (**1**).

Keller (2011) combined this character with overall premental shape in his char 44. A convex premental surface is almost always associated with a roughly oval, oblong shape, whereas a flat surface correlates with a diamond-shaped outline. As the distinctly convex prementum of †*Gerontoformica* is rather triangular than oval, we include only the curvature in our definition of this character. Separate coding of the shape may turn out as useful when more species are investigated. Interestingly, the flat shape seems to be associated with taxa with a tighter closure of the oral foramen, which are species of *Brachyponera* and *Wasmannia* in our sampling (see Chars. related to maxillolabial-labral interaction, 68, 69, 110, 112, 123). All other taxa show the convex condition. Category 4. (Keller 2011: char. 44)

123. Transverse premental groove: absent (**0**), or present (**1**).

If present, the premental groove is part of the maxillolabial-labral locking mechanism of the oral foramen. In our taxon sampling it occurs only in *Wasmannia*, but it has certainly originated several times independently across Formicidae (Keller 2011). Category 4. (Keller 2011: char. 45)

124.* Paraglossae, size: large lobes, length similar to glossa (**0**), or small, reduced lobes (**1**), or completely reduced, no lobe visible (**2**).

We observed relatively large paraglossae for all outgroup taxa and in our †*Gerontoformica* fossil; all sampled crown Formicidae have smaller paraglossae. To the best of our knowledge, the form

of the paraglossae has not been reported from the ant fossil record. Available images of ant fossils in the literature or on AntWeb.org are insufficient due to resolution and/or viewing angle to confirm this feature in other stem group Formicidae. Likewise, none of the fossils immediately available to us have been preserved with their mouthparts extended outwards. It cannot be entirely excluded that the large lobes we observed in †*Gerontoformica* are an artefactual feature based, for example, on unnaturally inflated membranous paraglossae. However, as outgroup taxa such as *Sceliphron* and *Ampulex* also show paraglossae of relatively similar dimensions to those recovered for †*Gerontoformica*, we are inclined to trust our reconstruction. The paraglossae are thin and pointed in *Parischnogaster* and *Methocha*, and in the former elongated together with the rest of the maxillolabial complex. Among the extant ant species, small paraglossae are observable in *Brachyponera*, *Formica* and *Wasmannia*, while no paraglossae were found in *Protanilla lini*. The presence of small paraglossae of varying shape was previously reported to occur in Ponerinae, Amblyoponinae, Paraponerinae, some Formicinae, and Myrmicinae by Gotwald (1969), who did not find any paraglossae in Dorylinae, Myrmeciinae, Pseudomyrmecinae, Dolichoderinae, and most Formicinae. Due to the inconspicuous size of most ant paraglossae, reexaminations might reveal paraglossal presence in many species that were previously considered as lacking them. Category 3.

125.~ (Reductive.) Shape and vestiture of small/ reduced paraglossae: lobes covered in denticles (**0**), or smooth lobes
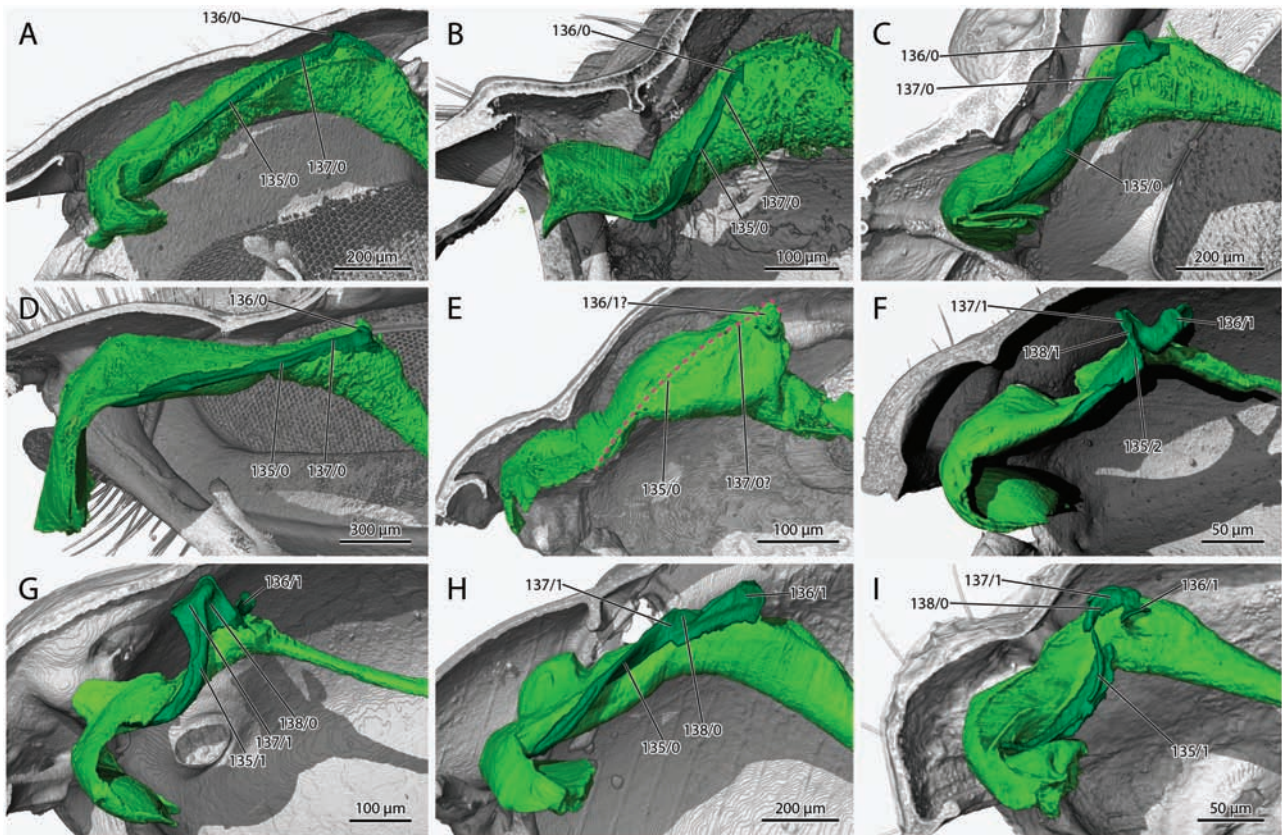
Char. 136–138. 3D reconstructions of the prepharynx with oral arms in lateral view, **A**: *Parischnogaster* sp., **B**: *Methocha* sp., **C**: *Ampulex* sp., **D**: *Sceliphron caementarium*, **E**: †*Gerontoformica gracilis*, **F**: *Protanilla lini*, **G**: *Brachyponera luteipes*, **H**: *Formica rufa*, **I**: *Wasmannia affinis*. **Char. 135**: Curve of the oral arms, (**0**): linear, gently curved, (**1**): strongly curved, almost sinuate, (**2**): angled. **Char. 136**: Oral arm process length, (**0**): small, roughly as long was wide, (**1**): large, longer than wide. **Char. 137**: Oral arm dorsal plate/ lamellae, (**0**): absent, (**1**): present. **Char. 138**: Oral arm dorsal plate/ lamellae, orientation relative to oral arm overall, (**0**): parallel, (**1**): perpendicular.
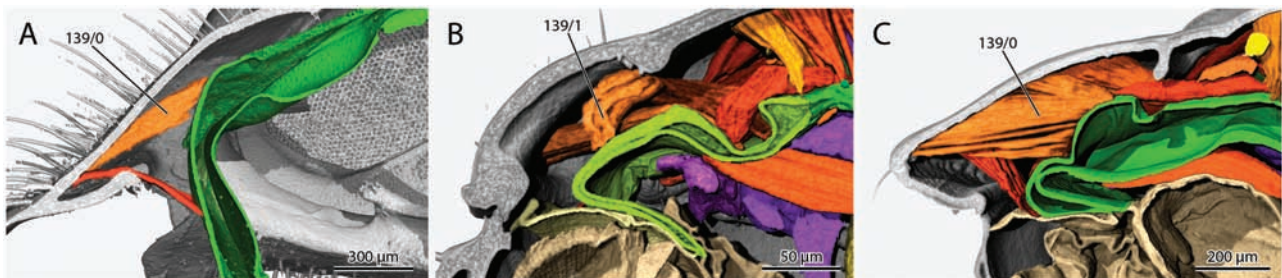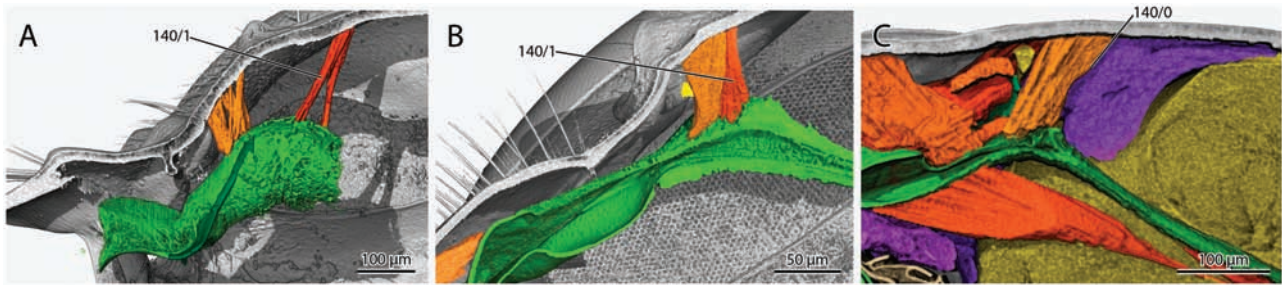

Char. 139. 3D reconstructions of the distal prepharynx in sagittal view, with *M. clypeopalatalis* (0ci1), **A**: *Parischnogaster* sp., **B**: *Methocha* sp., **C**: *Ampulex* sp., **D**: *Sceliphron caementarium*, **E**: †*Gerontoformica gracilis*, **F**: *Protanilla lini*, **G**: *Brachyponera luteipes*, **H**: *Formica rufa*, **I**: *Wasmannia affinis*. **Char. 139**: 0ci1a, (**0**): origin distally on clypeus and insertion on buccal tube (**1**): origin on epistomal sulcus and insertion proximad buccal tube.

with apical conical sensilla (**1**), or barrel-shaped with long apical microtrichia (**2**).

The small lobes we interpret as reduced paraglossae have highly variable shapes and vestitures in the three sampled species that were coded as (**1**) in Char. 121. A small lobe covered in denticles occurs in *Formica* (**0**). A smooth lobe with an apical conical sensilla was found in *Brachyponera* (**1**). The barrel-shape with "spines" (here interpreted as long microtrichia) assigned to *Wasmannia* (**2**) was also observed for other Myrmicinae by Keller (2011) and may be a characteristic of this subfamily. Dependent on state (**1**) in Char. 121. Category 3. (Keller 2011: char. 46)

126.* Position of basiparaglossal brush relative to glossa: on level (**0**), or proximad (**1**).

The basiparaglossal brush and the basiparaglossal plate/ sclerite, on which it inserts, are located at the level of the glossa and directed posteriorly (assuming prognathy and extended position of the labium) in *Ampulex* and *Sceliphron*. They are set distinctly proximad the glossa and face dorsad in all of the investigated total clade Formicidae including †*Gerontoformica*. In *Parischnogaster* and *Methocha* only very short setae are present at the base of the paraglossa, while a similar condition is also observed in *Vespula* (Baranek et al. 2018). As homology with the basiparaglossal brush

Char. 140. 3D reconstructions of the distal prepharynx in sagittal view, at level of anatomical mouth with frontobuccal muscles, **A:** *Methocha* sp., **B:** *Sceliphron caementarium*, **C:** *Brachyponera luteipes*. **Char. 140:** *M. frontobuccalis posterior* (0bu3), (**0**): absent (**1**): present.
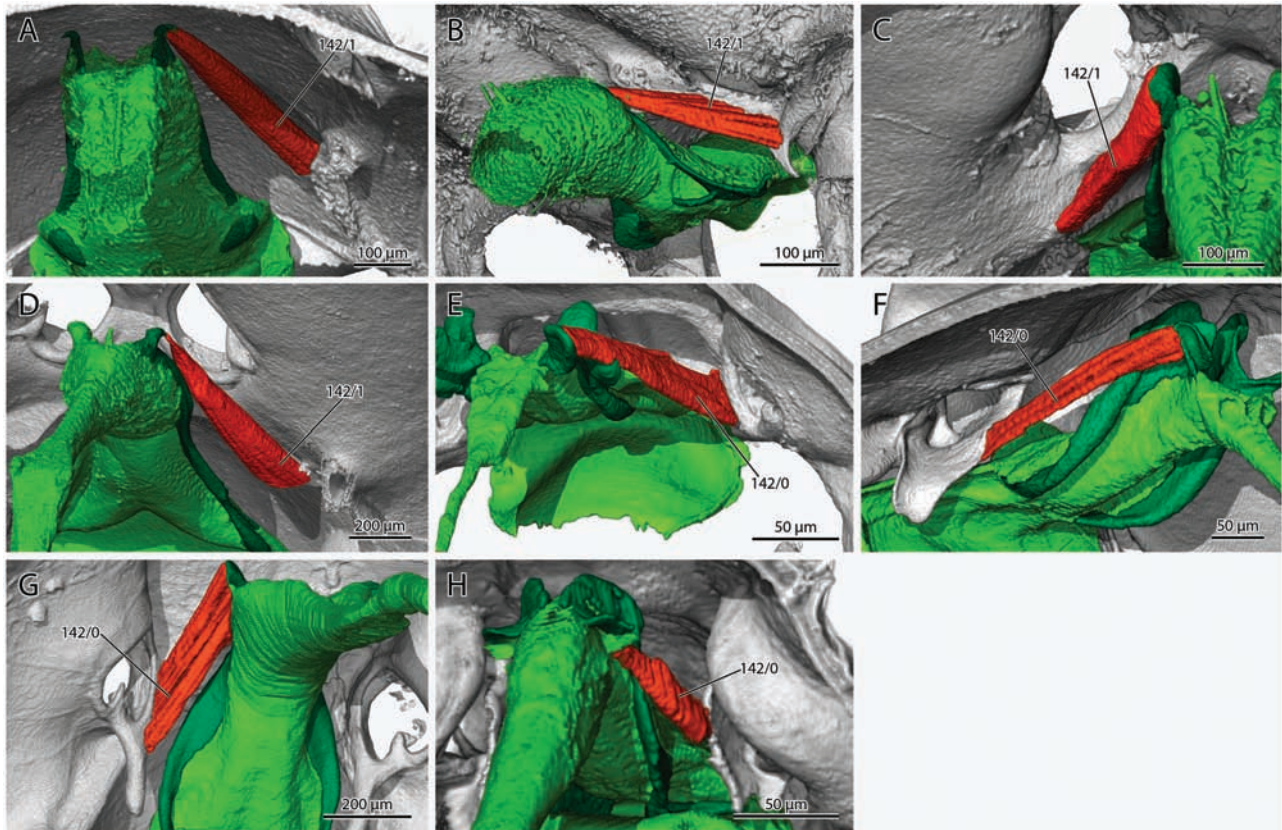
Char. 142. 3D reconstructions of the distal prepharynx in posterolateral view, with *M. tentriooralis* (0hy2), **A:** *Parischnogaster* sp., **B:** *Methocha* sp., **C:** *Ampulex* sp., **D:** *Sceliphron caementarium*, **E:** *Protanilla lini*, **F:** *Brachyponera luteipes*, **G:** *Formica rufa*, **H:** *Wasmannia affinis*. †*Gerontoformica gracilis* not included as 0hy2 could not be reconstructed. **Char. 142:** *M. tentriooralis* (0hy2) origin, (**0**): on antennal torulus/ torular apodeme, (**1**): epistomal ridge.

of Formicoidea and Apoidea is uncertain at this point, this character was conservatively coded as inapplicable. Category 3.

127.* Development of medial process distally on first labial palpomere: absent (**0**), or present (**1**).

A lobe-like process on the first labial palpomere was observed in our scanned specimen of †*Gerontoformica gracilis*. We recently observed that this process is absent in †*G. sternorhabda* (Boudinot et al. in press). Otherwise, no similar processes have been reported for another ant, extant or extinct, thus a broader survey is necessary. Category 1.

128.* Location of *M. praementoparaglossalis* 0la11 origin area on the prementum: at level of 0la 12 or proximad of it (**0**), or distinctly distad 0la12 (**1**).

The distal condition appears to be associated with the very large 0la12 in *Formica* which fills out most of the proximal labium internally. Interestingly this state is also observed in †*Gerontoformica* (with a much smaller 0la12). The muscle is also clearly distad of 0la12 in both vespoid outgroup taxa. In all other taxa the 0la11 origin is at the level of or proximad the origin of 0la12. Muscle arrangement within the labium is probably affected by premental and general labial shape but possibly also has functional implications. Category 1.

129. *M. praementosalivarialis* 0hy7: absent (**0**), or present (**1**).

This muscle was interpreted as absent in Aculeata by [Zimmermann and Vilhelmsen (2016)](#), but muscle fibers connecting the prementum and salivarium and/or the salivary duct have
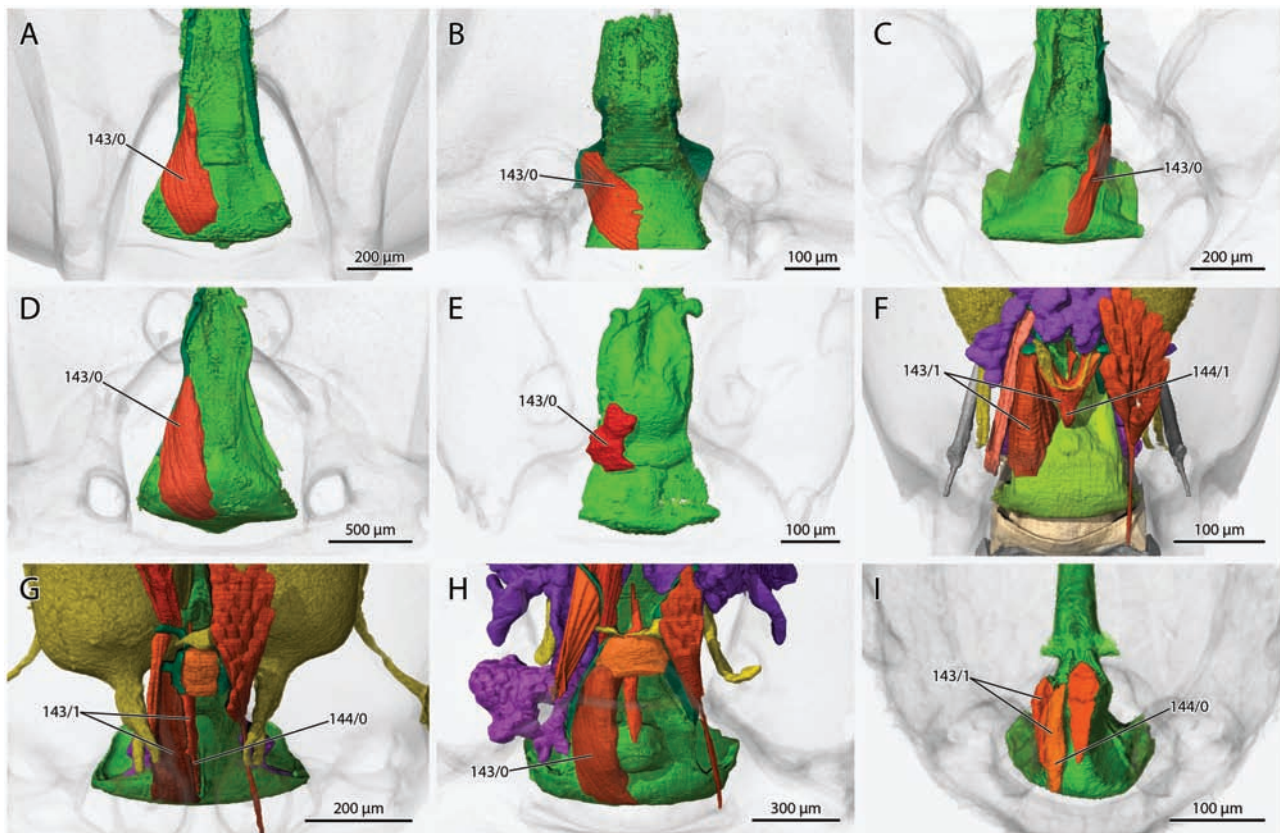
Char. 143, 144. 3D reconstructions of the distal prepharynx in dorsal view, with *M. pharyngoepipharyngalis* (0pe1), **A**: *Parischnogaster* sp., **B**: *Methocha* sp., **C**: *Ampulex* sp., **D**: *Sceliphron caementarium*, **E**: †*Gerontoformica gracilis*, **F**: *Protanilla lini*, **G**: *Brachyponera luteipes*, **H**: *Formica rufa*, **I**: *Wasmannia affinis*. **Char. 143**: *M. pharyngoepipharyngalis* (0pe1), number of bundles in the lateral portion, (**0**): 1, (**1**): 2. **Char. 144**: *M. pharyngoepipharyngalis* (0pe1), lateral 2 bundles, insertion of medial bundle, (**0**): directly by of lateral bundle, (**1**): centrally on prepharynx with bundles from both sides fusing.

been found in several ant species (*Protanilla lini*, *Formica rufa*, *Wasmannia affinis*). In this study, we also observed at least a few fibers connecting to the salivarium rather than the glossa in both *Sceliphron* and *Ampulex*, so we coded the muscle as present for both. We observed that this muscle is absent in *Parischnogaster* and *Methocha*. We did not find the muscle in †*Gerontoformica*, but it cannot be excluded that this is due to insufficient preservation. Presently, it is unclear whether the muscle was retained in the last common ancestor of Aculeata and (Formicoidea + Apoidea) and was preserved (or reappeared) in the latter clade. It is also possible that the observed muscle bundles are in fact an expansion of *M. praementoglossalis* 0la12 onto the salivarium. Category 1, 4. (Zimmermann and Vilhelmsen 2016: char. 14)

Digestive tract:

130. Infrabuccal pouch: absent (0), or present (1).

The infrabuccal pouch is present in the groundplan of Hymenoptera (Beutel and Vilhelmsen 2007) and was found in almost all taxa we compared here, but interestingly it is absent in *Methocha*. It is conceivable that it is stretched out because of the extended labiomaxillary complex of the investigated specimen, but in other investigated specimens with extended maxillolabial complex the pouch was still present (e.g., Richter et al. 2020, 2021), so this is in any case a unique state. We also observed clear variation in the size of the pouch, but this is difficult to evaluate, as the pouch size varies massively with different filling states (Wang et al. 2019). If this

problem can be addressed, pouch size might be an informative character, as it appears especially large in some total clade Formicidae such as †*Gerontoformica* and *Formica*. Category 2. (e.g., Beutel and Vilhelmsen 2007: char. 37)

131. Orientation of distal prepharynx (cibarium) with mouthparts in retracted position: mostly straight (0), or distinctly curved (1).

A strongly bent or curved prepharynx is a characteristic feature of Aculeata and at least some other Apocrita according to Zimmermann and Vilhelmsen (2016). In the ant literature, this bent part of the prepharynx is known as the "buccal tube", which can be somewhat separated from the following prepharynx by its armament of microtrichia (e.g., Forbes 1938), although the bent portion does not always strictly coincide with differences in the vestiture (Whelden 1957, Richter et al. 2021). The curved condition is generally present in the species sampled by us but is less pronounced in specimens with extended maxillolabial complex, which results in "straightening" of the prepharynx. This applies to *Sceliphron* and was previously reported for *Protanilla lini* (Richter et al. 2021). A special case was observed in *Methocha*, in which the prepharyngeal shape differs distinctly from that of the other taxa we examined; additionally, the lumen is rectangular rather than crescent-shaped and it is rather short and very wide. The prepharynx of *Methocha* is also not bent, although this may be due to the extended condition of its maxillolabial complex. However, it is striking that the anterior prepharynx appears actually bent upwards rather than downwards, indicating that even with the mouthparts in a retracted position, the
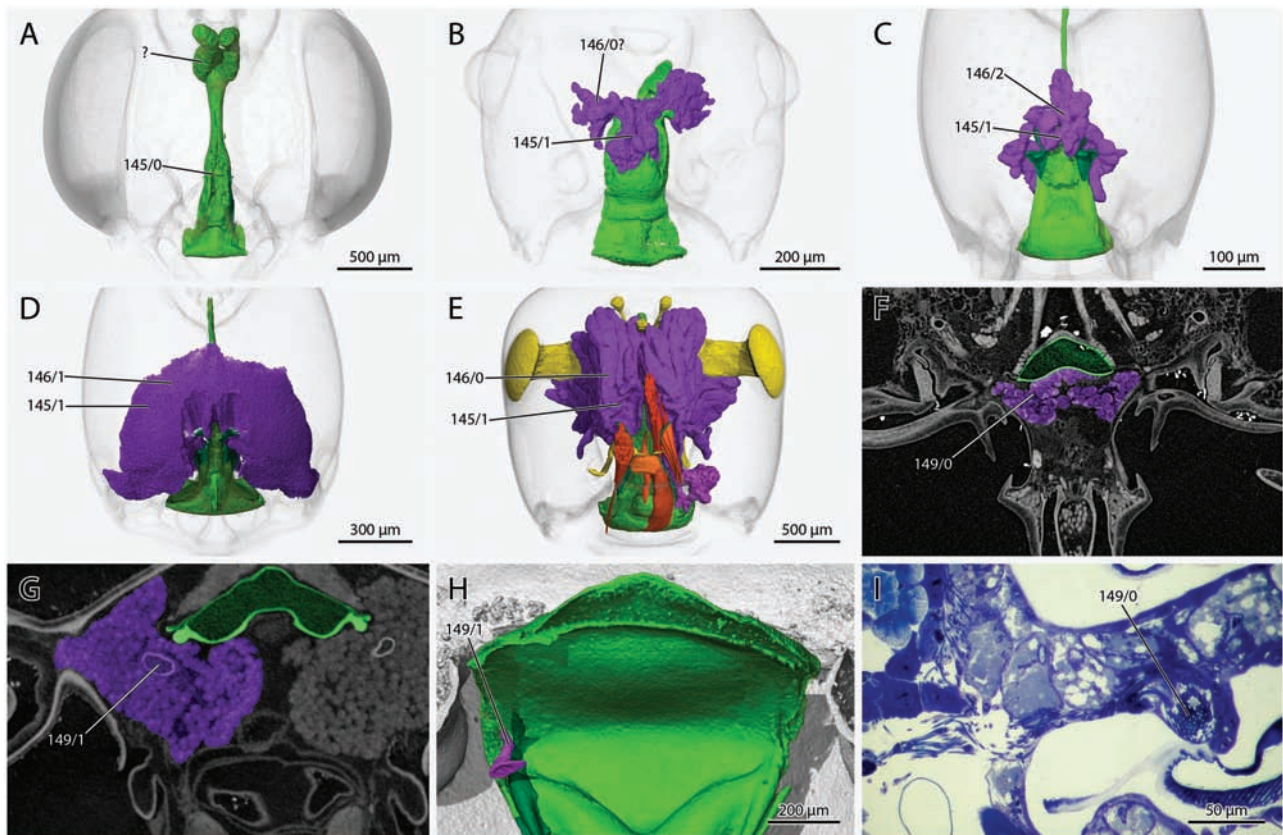
Char. 145, 146, 149. The prepharyngeal and pharyngeal glands, 3D reconstructions, µ-CT sections, and histological sections, **A:** *Ampulex* sp dorsal view of pharynx, **B:** †*Gerontoformica gracilis*, dorsal view of pharynx and pharyngeal gland, **C:** *Protanilla lini*, dorsal view of pharynx and pharyngeal gland, **D:** *Brachyponera luteipes*, dorsal view of pharynx and pharyngeal gland **E:** *Formica rufa*, dorsal view of pharynx and pharyngeal gland, **F:** *Methocha* sp. sagittal section of prepharyngeal gland, **G:** *Sceliphron caementarium*, sagittal section of prepharyngeal gland, **H:** *Sceliphron caementarium* 3D reconstruction of prepharyngeal gland opening in ventral view, **I:** *Formica rufa*, frontal histological section of prepharyngeal gland opening. **Char. 145**: Pharyngeal gland, (**0**): absent, (**1**): present. **Char. 146**: Pharyngeal gland shape, (**0**): several finger-like tubes, (**1**): one large, connected lobe, (**2**): irregularly shaped bulbous lobes. **Char. 149**: Opening of prepharyngeal gland, (**0**): many small ducts opening on sieve-like plate, (**1**): large duct opening at single orifice.

distinct curve observed in other aculeates might not be present. As we do not have a *Methocha* specimen with retracted mouthparts available to test this hypothesis, we code this species as (**?**) and encourage further anatomical investigation of the Thynnoidea. Category 2, 4. (Zimmermann and Vilhelmsen 2016: char. 11)

132.* Development of thick internal transverse ridges on distal prepharynx: absent (**0**), or present (**1**).

The distal prepharynx of all investigated species bears rows of microtrichia pointing in the direction of the functional mouth opening. Only †*Gerontoformica* shows massive transverse ridges in this region (**1**). While it cannot be ruled out completely that this is an artefact, this seems unlikely given the strength of these structural modifications. At the very least, if these ridges represent rows of microtrichia that are clumped together and appear large compared to the other investigated species. *Parischnogaster* has one very distinctly developed row of long, spine-like microtrichia arranged as a transverse comb in its buccal tube. It is possible that there is further meaningful variation of this character system, but evaluation of the internal prepharyngeal wall in sufficient detail requires considerable effort, including SEM and/ or histological investigation. Category 1, 2.

133.* Dorsal prepharyngeal wall close to buccal tube with longitudinal keel: absent (**0**), or present (**1**).

The dorsal prepharyngeal wall is at least slightly sclerotized or thickened in all species we investigated, although the degree and

extent of sclerotization/ thickening varies. As µ-CT scans are not an ideal method to assess sclerotization, this aspect will require application of other techniques to precisely assess. Strong sclerotization has been shown for some ant species such as *Brachyponera luteipes* with histological sections (Richter et al. 2020). This species additionally carries a fin-shaped dorsal longitudinal keel which serves as attachment area for part of *M. clypeopalatalis* 0ci1b and part of *M. pharyngoepipharyngalis*. In *Formica* this area is humped, and in *Parischnogaster* a small but conspicuous fold is visible at this location, but it is relatively flat in the other investigated species. Only the distinct keel of *Brachyponera* was coded here, as the state in *Formica* and *Parischnogaster* could represent temporary formations of the flexible prepharyngeal cuticle. Category 1, 2.

134.* Width of distal prepharynx/ buccal tube relative to prepharynx between buccal tube and frontal ganglion: not or at most slightly widened (**0**), or widening gradually throughout prepharynx (**1**), or buccal tube abruptly widened (**2**).

In most taxa investigated by us, the distal prepharynx, particularly the region of the buccal tube, is distinctly widened compared to the proximal prepharynx at the level of the anatomical mouth opening. In *Parischnogaster*, *Ampulex*, and *Sceliphron*, it widens gradually and evenly throughout its length (**1**). In †*Gerontoformica* and *Protanilla* the prepharynx does not widen distinctly in its distal region but is distinctly wider than the pharynx (which is the case in all species). In all Poneroformicia (*Brachyponera*, *Formica*, *Wasmannia*), the buccal

tube is distinctly and abruptly widened compared to the proximal prepharynx. These differences in prepharyngeal shape might be explained with diet preferences, but in the case of †*Gerontoformica* could also be the result of an artefact. Category 1.

135.* Shape of oral arms in lateral view: gently curved, almost linear (**0**), or strongly curved, almost sinuate (**1**), or angled, appearing kinked (**2**).

This and the following characters are an attempt to discretize the observed variation of the prepharyngeal oral arms. This sclerite is certainly very diverse across ants and deserves focused study in the future. In all outgroup taxa and *Formica*, the oral arms gently curve from the ventral side of the distal prepharynx to the dorsal side of the proximal prepharynx. We also tentatively assume this state for †*Gerontoformica*, but as the oral arms are not clearly visible in our dataset this interpretation is based on the folds we interpret to represent the oral arms. Conservatively, we coded this and the following characters as (**?**) for this taxon. Interestingly, the strongly curved (*Brachyponera* and *Wasmannia*) or angled states (*Protanilla*) only occur within different groups of crown ants. Category 1.

136.* Shape of posterior oral arm processes: as long as wide (**0**), or longer than wide (**1**).

In all investigated taxa the oral arms always have at least one distinct process close to their aboral/proximal end which receives the insertions of *M. frontooralis* (0hy1) and *M. tentoriooralis* (0hy2). Boudinot et al. (2021) labeled this the "posterior process of the oral arm" to differentiate it from the ant-specific "anterior process of the oral arm". The length and position of the posterior process was used as a phylogenetic character for bees and termed "apodeme of frontal muscle on pharyngeal rod" by Porto and Almeida (2021). We generally found a significant degree of difference of the oral arms ("pharyngeal rods") and their processes within total clade Formicidae and relative to the outgroup taxa. The arms appear "simple" in the outgroups and "complex", with more different shapes and sizes of the different parts of the rods in ants. The processes receiving the oral muscles are longer than wide (**1**) in all ant species investigated by us. They range in size from large (*Protanilla*, *Brachyponera*) to relatively small (*Formica*, *Brachyponera*), and may be parallel to the prepharynx (*Formica*), or directed laterad (*Brachyponera*, *Wasmannia*) or dorsolaterad (*Protanilla*). In the investigated outgroups, they are relatively shorter (**0**) and are knob-like (*Sceliphron*), hook-like (*Parischnogaster*), flat and lobate (*Ampulex*), or not produced from the alimentary canal at all (*Methocha*). The processes are not preserved well enough in †*Gerontoformica* to confidently evaluate (coded as**?**). Category 1, 2.

137.* Second pair of oral arm processes orad/distad the posterior processes: absent (**0**), or present, developed as dorsal plates ("oral arm lamellae") (**1**).

In all extant ant species that we have examined, the oral arms have an additional pair of processes which occur orad/distad the primary processes (see Char. 136). Because of their position, we have labeled them as the "anterior processes of the oral arms" (Boudinot et al. 2021). The anterior processes are produced into dorsal plates (oral arm lamellae) of varying size and shape. In *Protanilla* and *Brachyponera*, the plates are large, while in *Formica* and *Wasmannia* they are only slightly produced from the remaining oral arms. *M. oralis transversalis* (0hy9) and the lateral portions of *M. pharyngoepipharyngalis* (0pe1) both originate, at least in part, on these processes. The anterior processes were not found in any of the outgroups and the mentioned muscles simply originate on the unmodified arms. The oral arms of *Methocha* are expanded, but the expansion is of the distal region of the arms, directed laterad the prepharynx and serving as anterior insertion

site of the lateral portion of *M. pharyngoepipharyngalis* (0pe1). Category 1.

138.* (Reductive) Orientation of primary axis of anterior oral arm processes: mostly parallel to prepharynx (**0**), or mostly transverse to prepharynx (**1**).

The dorsal plates are parallel to the prepharynx in *Brachyponera*, *Formica*, and *Wasmannia*, but are twisted into a transverse orientation in *Protanilla*. Dependent on presence in Char. 136. Category 1.

139.* *M. clypeopalatalis* 0ci1a: originating distally or centrally on clypeus and inserting on buccal tube (**0**), or originating on frontoclypeal ridge and inserting on prepharynx proximad the buccal tube (**1**).

Condition (**1**) is only known in *Protanilla* and is probably due to the presence of the mid-clypeal ridge which occupies the usual origin area of this muscle and shifts it posteriorly. Interestingly, its insertion area is also shifted away from the buccal tube and thus the functional mouth opening, suggesting that it does not perform the role this muscle usually does. Category 1.

140.* *M. frontobuccalis posterior* 0bu3: absent (**0**), or present (**1**).

This muscle is absent or at least highly reduced in *Brachyponera* and *Wasmannia*. Its loss has probably repeatedly occurred across the total clade Formicidae, possibly related to diet preference. The muscle was not recognizable in †*Gerontoformica*, possibly due to poor preservation (coded as**?**). Category 1.

141.* *M. verticopharyngalis* 0ph1: absent (**0**), or present (**1**).

This muscle is absent in all previously investigated worker ants but present in the investigated outgroups as well as in one investigated male ant specimen (Boudinot et al. 2021). Its absence likely depends on available space in the posterior part of the head capsule. Category 3.

142.* *M. tentoriooralis* 0hy2 origin: on antennal torulus/ torular apodeme (**0**), or on clypeofrontal ridge (**1**).

The muscle originates on the inner torulus of the antennal insertion in all investigated ants, but on the frontoclypeal ridge in all outgroup terminals. Usually, the ridge forms an expanded lobe of varying shape and size as site of origin, but this is not the case in *Ampulex*. In *Methocha*, the lobe of the frontoclypeal ridge that the muscle originates on is located directly approximate the antennal socket but was still coded as (**1**). The original origin of this muscle on the tentorium (Wipfler et al. 2011) was not observed for any species in our sampling, but it was found in several species of Apocrita and also the aculeate *Sapyga* (Sapygidae) by Zimmermann and Vilhelmsen (2016). Category 1.

143.* *M. epipharyngopharyngalis* 0pe1, unilateral number of bundles of lateral portion: 1 (**0**), or 2 (**1**).

Only one unilateral bundle of *M. epipharyngopharyngalis* and a single dorsal bundle are present in most examined taxa. However, two clearly separated bundles were observed in *Protanilla*, *Brachyponera* and *Wasmannia*. Category 1.

144.* (Reductive.) *M. epipharyngopharyngalis* Mpe, lateral portion, insertion of the medial bundle: directly mesad of lateral bundle (**0**), or mesad on prepharynx, with the bundles of both sides merging medially (**1**).

If the lateral portion of *M. epipharyngopharyngalis* consists of two bundles, the lateral bundle always originated on the dorsal plates of the oral arms and inserts laterally on the prepharynx close to the buccal tube. The medial portion however inserts directly mesad of the lateral bundle on the lateral prepharynx in *Wasmannia* (**0**) and medially on the center of the prepharynx in *Protanilla*, with the bundles from both sides merging (**1**). Dependent on state (**1**) in Char. 143. Category 1.

Glands:

Note: It is probable that more gland characters can be scored with a wider taxon sampling.

145.* Pharyngeal gland: absent (**0**), or present (**1**).

This gland with its typical shape and opening location close to the anatomical mouth opening has only been observed and documented in Formicidae (e.g., Peregrine 1973, Schoeters and Billen 1996) and Philanthinae (Apoidea, e.g., Strohm et al 2007, Weiss et al. 2015). It may be present in Scoliidae and other groups of Aculeata, but reliable data are missing. The gland was not found in *Sceliphron* and *Ampulex*. In *Ampulex*, Herzner et al. (2011) observed two tube-shaped pharyngeal expansions posterad the brain. However, in contrast to the interpretation of these authors, we consider the homology of these diverticula and the pharyngeal gland as uncertain. As the shape, position and structure of the former are very different from any pharyngeal gland described within ants, at least two of three of Remane's homology criteria are not fulfilled. It appears more likely that the pharyngeal diverticula evolved independently, and their function is unknown at present. The convergent evolution interpretation is also supported by the fact that *M. verticopharyngalis* (0ph1), which always inserts on the postcerebral pharynx if present, attaches on these diverticula in the *Ampulex* specimen investigated by us. It is conceivable that an underlying developmental program facilitates the expansion and differentiation of parts of the cephalic pharynx into glandular diverticula such as the postpharyngeal gland or these special extensions of the fore gut in *Ampulex*. Weiss et al. (2015) hypothesize that "simple" diverticula of the pharynx evolved first within Apoidea, and then complex pharyngeal glands only evolved within Philanthinae. More research will be necessary to clarify the genetic background and evolutionary history of these structures associated with the cephalic digestive tract. Category 1.

146.* (Reductive.) Shape of pharyngeal gland: several finger-like tubes (**0**), or one large, connected lobe (**1**), or irregularly shaped bulbous lobes (**2**).

The finger-like tube shape was coded for *Formica* and *Wasmannia*, a large, connected lobe is confirmed for *Brachyponera* and several other ponerines (Gama and Cruz Landim 1982, Schoeters and Billen 1996), and the irregular lobes characterize the gland of *Protanilla*. The gland is not sufficiently preserved in †*Gerontoformica* for a reliable assessment, but the reconstruction indicates at least several lobes or possibly finger-like tubes. Dependent on presence in Char. 145. Category 1, 3.

147.* Cardo base gland: absent (**0**), or present (**1**).

Only present in *Formica* and *Wasmannia* in our taxon sampling, but also present in other species of Formicinae and Myrmicinae (Boonen and Billen 2016). Previously known as maxillary gland, but improved terminology introduced by Xu et al. (2020). Category 1, 3.

148.* Galeolacinial gland: absent (**0**), or present (**1**).

This gland was found in *Protanilla* thus far and was also confirmed for this genus by Billen (2013). Category 1.

149.* Duct of the prepharyngeal gland: many small ducts opening on sieve-like plate (0), or one large duct opening at single orifice (1).

A single large duct was only observed in *Sceliphron* in our sampling, but it also occurs in other groups of Aculeata (see, e.g., Porto and Almeida 2021). Sieve plates are the common opening type in Formicidae (Boonen and Billen 2016). The shape and size of the gland itself is also highly variable. Category 2, 3.

Authors' Contributions

AR: conceptualization, processing μCT-scan data, parsimony analysis, image plates, writing manuscript, review/editing manuscript. BEB: conceptualization, Bayesian analysis, review/editing manuscript. SY: providing fossil, photographs, review/editing manuscript. JK: μCT-scanning, review/editing manuscript. RGB: conceptualization, review/editing manuscript.

References Cited

Alekseev, V. I., J. Mitchell, R. C. McKellar, M. Barbi, H. C. E. Larsson, and A. Bukejs. 2021. The first described turtle beetles from Eocene Baltic amber, with notes on fossil Chelonariidae (Coleoptera: Byrrhoidea). Foss. Rec. 24: 19–32.

Alencar, I. D., and C. O. Azevedo. 2013. Reclassification of Epyrini (Hymenoptera: Bethylidae): a tribal approach with commentary on their genera. Syst. Ent. 38: 45–80.

Anderson, K. E., J. A. Russell, C. S. Moreau, S. Kautz, K. E. Sullam, Y. Hu, U. Basinger, B. M. Mott, N. Buck, and D. E. Wheeler. 2012. Highly similar microbial communities are shared among related and trophically similar ant species. Molec. Ecol. 21: 2282–2296.

Angelini, D. R., F. W. Smith, A. C. Aspiras, M. Kikuchi, and E. L. Jockusch. 2012. Patterning of the adult mandibulate mouthparts in the red flour beetle, *Tribolium castaneum*. Genetics 190: 639–654.

Azorsa, F., and B. Fisher. 2018. Taxonomy of the ant genus *Carebara* Westwood (Formicidae, Myrmicinae) in the Malagasy Region. ZooKeys 767: 1–149.

Balashov, I. 2021. The first records of mollusks from mid-Cretaceous Hkamti amber (Myanmar), with the description of a land snail, *Euthema myanmarica* n. sp. (Caenogastropoda, Cyclophoroidea, Diplommatinidae). J. Paleontol. 95: 9941–1003.

Baranek, B., K. Kuba, J. Bauder, and H. Krenn. 2018. Mouthpart dimorphism in male and female wasps of *Vespula vulgaris* and *Vespula germanica* (Vespidae, Hymenoptera). Dtsch. Entomol. Z. 65: 61–74.

Barba-Montoya, J., M. Dos Reis, H. Schneider, P. C. Donoghue, and Z. Yang. 2018. Constraining uncertainty in the timescale of angiosperm evolution and the veracity of a Cretaceous Terrestrial Revolution. New Phytol. 218: 819–834.

Barden, P. 2017. Fossil ants (Hymenoptera: Formicidae): ancient diversity and the rise of modern lineages. Myrmecol. News 24: 1–30.

Barden, P., and D. Grimaldi. 2012. Rediscovery of the bizarre Cretaceous ant *Haidomyrmex* Dlussky (Hymenoptera: Formicidae), with two new species. Am. Mus. Novit. 2012: 1–16.

Barden, P., and D. Grimaldi. 2013. A new genus of highly specialized ants in Cretaceous Burmese amber (Hymenoptera: Formicidae). Zootaxa 3681: 405–412.

Barden, P., and D. Grimaldi. 2014. A diverse ant fauna from the Mid-Cretaceous of Myanmar (Hymenoptera: Formicidae). PLoS One 9: e93627.

Barden, P., and D. Grimaldi. 2016. Adaptive radiation in socially advanced stem-group ants from the Cretaceous. Curr. Biol. 26: 1–7.

Barden, P., H. W. Herhold, and D. A. Grimaldi. 2017. A new genus of hell ants from the Cretaceous (Hymenoptera: Formicidae: Haidomyrmecini) with a novel head structure. Syst. Entomol. 42: 837–846.

Barden, P., V. Perrichot, and B. Wang. 2020. Specialized predation drives aberrant morphological integration and diversity in the earliest ants. Curr. Biol. 30: 3818–3824.e4.

Belokobylskij, S. A., D. A. Dubovikoff, A. R. Manukyan, and D. M. Zharkov. 2021. Braconid parasitoids of ants (Hymenoptera, Braconidae, Euphorinae, Neoneurini) from Baltic amber with a discussion of records of fossil larvae parasitizing ant workers. J. Hym. Res. 84: 29–43.

Benton, M. J., P. Wilf, and H. Sauquet. 2021. The angiosperm terrestrial revolution and the origins of modern biodiversity. New Phytol. 233: 2017–2035.

Beutel, R. G., and F. Haas. 2000. Phylogenetic relationships of the suborders of Coleoptera (Insecta). Cladistics 16: 103–141.

Beutel, R. G., and L. Vilhelmsen. 2007. Head anatomy of Xyelidae (Hexapoda: Hymenoptera) and phylogenetic implications. Org. Div. Evol. 7: 207–230.

Beutel, R. G., F. Friedrich, T. Hörnschemeyer, H. Pohl, F. Hünefeld, F. Beckmann, R. Meier, B. Misof, M. F. Whiting, and L. Vilhelmsen. 2011. Morphological and molecular evidence converge upon a robust phylogeny of the megadiverse Holometabola. Cladistics 27: 341–355.

Beutel, R. G., F. Friedrich, X.-K. Yang, and S.-Q. Ge. 2014. Insect morphology and phylogeny: a textbook for students of entomology. Walter de Gruyter, Berlin, 532pp.

Billen, J., E. Bauweleers, R. Hashim, and F. Ito. 2013. Survey of the exocrine system in *Protanilla wallacei* (Hymenoptera, Formicidae). Arthropod Struct. Devel. 42: 173–183.

Blüthgen, N., and H. Feldhaar. 2010. Food and shelter: how resources influence ant ecology, Pp 115–136. in L. Lach, C. Parr, and K. Abbott, editors. Ant ecology. Oxford University Press, New York.

Bohart, R. M., and A. S. Menke. 1976. Sphecid wasps of the world: a generic revision. University of California Press, Berkeley.

Bolton, B. 1994. Identification guide to the ant genera of the world. Harvard University Press, Cambridge, MA, 222 pp.

Bolton, B. 2003. Synopsis and classification of Formicidae. Mem. Amer. Entomol Inst. 71: 1–370.

Booher, D. B., and P. O. Hoenle. 2021. A new species group of *Strumigenys* (Hymenoptera, Formicidae) from Ecuador, with a description of its mandible morphology. ZooKeys 1036: 1.

Booher, D. B., J. C. Gibson, C. Liu, J. T. Longino, B. L. Fisher, M. Janda, N. Narula, E. Toulkeridou, A. S. Mikheyev, and A. V. Suarez. 2021. Functional innovation promotes diversification of form in the evolution of an ultrafast trap-jaw mechanism in ants. PLoS Biol. 19: e3001031.

Boonen, S., and J. Billen. 2016. Functional morphology of the maxillary and propharyngeal glands of *Monomorium pharaonis* (L.). Arthropod Struct. Dev. 45: 325–332.

Borowiec, M. L., A. Schulz, G. D. Alpert, and P. Baňař. 2011. Discovery of the worker caste and descriptions of two new species of *Anomalomyrma* (Hymenoptera: Formicidae: Leptanillinae) with unique abdominal morphology. Zootaxa 2810: 1–14.

Borowiec, M. L., C. Rabeling, S. G. Brady, B. L. Fisher, T. R. Schultz, and P. S. Ward. 2019. Compositional heterogeneity and outgroup choice influence the internal phylogeny of the ants. Mol. Phylog. Evol. 134: 111–121.

Borysenko, L. H. 2017. Description of a new genus of primitive ants from Canadian amber, with the study of relationships between stem-and crown-group ants (Hymenoptera: Formicidae). Insecta Mundi 570: 1–57.

Boudinot, B. E. 2015. Contributions to the knowledge of Formicidae (Hymenoptera, Aculeata): a new diagnosis of the family, the first global male-based key to subfamilies, and a treatment of early branching lineages. Euro. J.Taxon 120: 1–62.

Boudinot, B. E., V. Perrichot, and J. C. M. Chaul. 2020. †*Camelosphecia* gen. nov., lost ant-wasp intermediates from the mid-Cretaceous (Hymenoptera, Formicoidea). ZooKeys 1005: 21–55.

Boudinot, B. E., O. T. D. Moosdorf, R. G. Beutel, and A. Richter. 2021. Anatomy and evolution of the head of *Dorylus helvolus* (Formicidae: Dorylinae): Patterns of sex-and caste-limited traits in the sausagefly and the driver ant. J. Morph. 282: 1616–1658.

Boudinot, B. E., M. L. Borowiec, and M. M. Prebus. 2022a. Phylogeny, evolution, and classification of the ant genus *Lasius*, the tribe Lasiini, and the subfamily Formicinae (Hymenoptera: Formicidae). Syst. Entomol. 47: 113–151.

Boudinot, B. E., A. Richter, J. Katzke, J. C. M. Chaul, R. A. Keller, E. P. Economo, R. G. Beutel, and S. Yamamoto. 2022b. Evidence for the evolution of eusociality in stem ants and a systematic revision of †*Gerontoformica* (Hymenoptera, Formicidae). Zool. J. Linn. Soc. zlab097.

Boudinot, B. E., Z. Khouri, A. Richter, Z. H. Griebenow, T. van de Kamp, V. Perrichot, and P. Barden. 2022c. Evolution and systematics of the Aculeata and kin (Hymenoptera), with emphasis on the ants (Formicoidea: †@@@ idae fam. nov., Formicidae). bioRxiv: 2022.2002.2020.480183.

Brady, S. G., T. R. Schultz, B. L. Fisher, and P. S. Ward. 2006. Evaluating alternative hypotheses for the early evolution and diversification of ants. Proc. Natl. Acad. Sci. U.S.A. 103: 18172–18177.

Brandão, C., J. Diniz, and E. Tomotake. 1991. *Thaumatomyrmex* strips millipedes for prey: a novel predatory behaviour in ants, and the first case of sympatry in the genus (Hymenoptera: Formicidae). Insectes Soc. 38: 335–344.

Brandão, C. R. F., J. L. M. Diniz, and R. M. Feitosa. 2010. The venom apparatus and other morphological characters of the ant *Martialis heureka* (Hymenoptera, Formicidae, Martialinae). Pap. Avulsos Zool. (São Paulo) 50: 413–423.

Branstetter, M. G., J. T. Longino, P. S. Ward, and B. C. Faircloth. 2017. Enriching the ant tree of life: enhanced UCE bait set for genome-scale phylogenetics of ants and other Hymenoptera. Method. Ecol. Evol. 8: 768–776.

Brothers, D. 1975. Phylogeny and classification of the aculeate Hymenoptera, with special reference to Mutillidae. Univ. Kans. Sci. Bull. 50: 483–648.

Brown, W. L., and W. W. Kempf. 1967. *Tatuidris*, a remarkable new genus of Formicidae (Hymenoptera). Psyche 74: 183–190.

Brunke, A. J., D. Żyła, S. Yamamoto, and A. Solodovnikov. 2019. Baltic amber Staphylinini (Coleoptera: Staphylinidae: Staphylininae): a rove beetle fauna on the eve of our modern climate. Zool. J. Linn. Soc. 187: 166–197.

Bukejs, A., and A. A. Legalov. 2020. The first record of Brentidae (Coleoptera) in Eocene Rovno amber with description of a new fossil species of *Toxorhynchus* Scudder, 1893. Foss. Rec. 23: 169–177.

Bukejs, A., J. Bezděk, V. I. Alekseev, K. Kairišs, and R. C. McKellar. 2020a. Description of the male of fossil *Calomicrus eocenicus* Bukejs et Bezděk (Coleoptera: Chrysomelidae: Galerucerinae) from Eocene Baltic amber using x-ray microtomography. Foss. Rec. 23: 105–115.

Bukejs, A., C. A. M. Reid, and M. Biondi. 2020b. *Groehnaltica batophiloides*, a new genus and species of flea-beetles (Coleoptera: Chrysomelidae) from Baltic amber, described using x-ray microtomography. Zootaxa 4859: 397–409.

Brazeau, M. D. 2011. Problematic character coding methods in morphology and their effects. Biol. J. Linn. Soc. 104: 489–498.

Brothers, D. J., and A. S. Lelej. 2017. Phylogeny and higher classification of Mutillidae (Hymenoptera) based on morphological reanalyses. J. Hymenopt. Res. 60: 1–97.

Cao, H., B. E. Boudinot, Z. Wang, X. Miao, C. Shih, D. Ren, and T. Gao. 2020. Two new iron maiden ants from Burmese amber (Hymenoptera: Formicidae: †Zigrasimeciini). Myrmecol. News 30: 161–173.

Carpenter, J. M. 1982. The phylogenetic relationships and natural classification of the Vespoidea (Hymenoptera). Syst. Ent. 7: 11–38.

Carpenter, J. M., and C. K. Starr. 2000. A new genus of hover wasps from Southeast Asia (Hymenoptera: Vespidae; Stenogastrinae). Am. Mus. Nov. 2000: 1–12.

Chipman, A. D., and G. D. Edgecombe. 2019. Developing an integrated understanding of the evolution of arthropod segmentation using fossils and evo-devo. Proc. Royal Soc. B 286: 20191881.

Coiro, M., J. A. Doyle, and J. Hilton. 2019. How deep is the conflict between molecular and fossil evidence on the age of angiosperms? New Phytol. 223: 83–99.

Coulcher, J. F., and M. J. Telford. 2013. Comparative gene expression supports the origin of the incisor and molar process from a single endite in the mandible of the red flour beetle *Tribolium castaneum*. EvoDevo 4: 1–12.

Cowley, D. R. 1959. Studies on the biology and anatomy of *Pison spinolae* Shuckard (Hymenoptera, Sphecidae). M.Sc. Thesis, Auckland University, New Zealand.

Davidson, D. W., A. Kopchinskiy, K. A. Salim, M. Grujic, L. Lim, C. C. Mei, T. H. Jones, D. Casamatta, L. Atanasova, and I. S. Druzhinina. 2016. Nutrition of Borneo's 'exploding' ants (Hymenoptera: Formicidae: *Colobopsis*): a preliminary assessment. Biotropica 48: 518–527.

Duplais, C., V. Sarou-Kanian, D. Massiot, A. Hassan, B. Perrone, Y. Estevez, J. T. Wertz, E. Martineau, J. Farjon, and P. Giraudeau. et al. 2021. Gut bacteria are essential for normal cuticle development in herbivorous turtle ants. Nat. Comm. 12: 676.

Dlussky, G. 1996. Ants (Hymenoptera: Formicidae) from Burmese amber. Paleontol. J. 30: 449–454.

Dlussky, G. 1999. The first find of the Formicoidea (Hymenoptera) in the Lower Cretaceous of the Northern Hemisphere. Paleont. J. 33: 274–277.

Dlussky, G., E. Fedoseeva. 1988. Origin and early stages of evolution in ants. Cretaceous biocenotic crisis and insect evolution. Nauka, Moskva, pp. 77–144.

Dlussky, G. M., D. Brothers, and A. P. Rasnitsyn. 2004. The first Late Cretaceous ants (Hymenoptera: Formicidae) from southern Africa, with comments on the origin of the Myrmicinae. Insect Syst. Evol. 35: 1–13.

Duncan, C. D. 1939. Contribution to the biology of North American vespine wasps. Ann. Entomol. Soc. Am. 8: 1–272.

Dunlop, J. A., D. Penney, N. Dalüge, P. Jäger, A. McNeil, R. S. Bradley, P. J. Withers, and R. F. Preziosi. 2011. Computed tomography recovers data from historical amber: an example from huntsman spiders. Sci. Nat. 98: 519–527.

Edgecombe, G. D., S. Richter, and G. D. Wilson. 2003. The mandibular gnathal edges: homologous structures throughout Mandibulata?. Afr. Invertebr. 44: 115–135.

Engel, M. S., and D. A. Grimaldi. 2005. Primitive new ants in cretaceous amber from Myanmar, New Jersey, and Canada (Hymenoptera: Formicidae). Am. Mus. Novit. 2005: 1–24.

Engelkes, K., F. Friedrich, J. U. Hammel, and A. Haas. 2018. A simple setup for episcopic microtomy and a digital image processing workflow to acquire high-quality volume data and 3D surface models of small vertebrates. Zoomorphol. 137: 213–228.

Escherich, K. 1917. Die Ameise: Schilderung ihrer Lebensweise. Vierweg and Sohn, Braunschweig.

Farish, D. 1972. The evolutionary implications of qualitative variation in the grooming behaviour of the Hymenoptera (Insecta). Anim. Behav. 20: 662–676.

Fedoseeva, E. B. 2001. [Morphofunctional aspects of the head capsule topography in Aculeata (Hymenoptera)]. Zh. Obshch. Biol. 62: 157–170 (in Russian).

Forbes, J. 1938. Anatomy and histology of the worker of *Camponotus herculeanus pennsylvanicus* De Geer (Formicidae, Hymenoptera). Ann. Entomol. Soc. Am. 31: 181–195.

Gama, V., and C. da Cruz Landim. 1982. Estudo comparativo das glândulas do sistema salivar das formigas (Hymenoptera, Formicidae). Naturalia (São José do Rio Preto) 7: 145–165.

Gibson, G. A. 1986. Evidence for monophyly and relationships of Chalcidoidea, Mymaridae, and Mymarommatidae (Hymenoptera: Terebrantes). Can. Entomol. 118: 205–240.

Glancey, B. M., R. Vander Meer, A. Glover, C. Lofgren, and S. Vinson. 1981. Filtration of microparticles from liquids ingested by the red imported fire ant *Solenopsis invicta* Buren. Insectes Soc. 28: 395–401.

Gonzalez, V. H., G. T. Gustafson, and M. S. Engel. 2019. Morphological phylogeny of Megachilini and the evolution of leaf-cutter behavior in bees (Hymenoptera: Megachilidae): evolution of leaf-cutter behavior in bees. J. Melittology. 85: 1–123.

Gotoh, H., R. Cornette, S. Koshikawa, Y. Okada, L. C. Lavine, D. J. Emlen, and T. Miura. 2011. Juvenile hormone regulates extreme mandible growth in male stag beetles. PLoS One 6: e21139.

Gotoh, H., H. Miyakawa, A. Ishikawa, Y. Ishikawa, Y. Sugime, D. J. Emlen, L. C. Lavine, and T. Miura. 2014. Developmental link between sex and nutrition; doublesex regulates sex-specific mandible growth via juvenile hormone signaling in stag beetles. PLoS Genet. 10: e1004098.

Gotoh, H., R. A. Zinna, Y. Ishikawa, H. Miyakawa, A. Ishikawa, Y. Sugime, D. J. Emlen, L. C. Lavine, and T. Miura. 2017. The function of appendage patterning genes in mandible development of the sexually dimorphic stag beetle. Dev. Biol. 422: 24–32.

Gotwald, W. H. 1969. Comparative morphological studies of the ants: with particular reference to the mouthparts (Hymenoptera: Formicidae). Memoirs of the Cornell University Agricultural Experiment Station No. 408: 1–150.

Gotwald, W. H.Jr, and B. M. Kupiec. 1975. Taxonomic implications of doryline worker ant morphology: *Cheliomyrmex morosus* (Hymenoptera: Formicidae). Ann. Entomol. Soc. Am. 68: 961–971.

Gotwald, W., and R. Schaefer. 1982. Taxonomic implications of doryline worker ant morphology: *Dorylus* subgenus Anomma (Hymenoptera: Formicidae). Sociobiology 7: 187–204.

Griebenow, Z. H. 2021. Synonymization of the male-based ant genus *Phaulomyrma* (Hymenoptera: Formicidae) with *Leptanilla* based upon Bayesian total-evidence phylogenetic inference. Invertebr. Syst. 35: 603–636.

Grimaldi, D., and D. Agosti. 2000. A formicine in New Jersey Cretaceous amber (Hymenoptera: Formicidae) and early evolution of the ants. Proc. Natl. Acad. Sci. U.S.A. 97: 13678–13683. doi:10.1073/pnas.240452097.

Grimaldi, D., and M. S. Engel. 2005. Evolution of the insects. Cambridge University Press, Cambridge, UK.

Grimaldi, D., E. Bonwich, M. Delannoy, and S. Doberstein. 1994. Electron microscopic studies of mummified tissues in amber fossils. Am. Mus. Nov. 3097: 1–31.

Grimaldi, D., D. Agosti, and J. M. Carpenter. 1997. New and rediscovered primitive ants (Hymenoptera: Formicidae) in Cretaceous amber from New Jersey, and their phylogenetic relationships. Am. Mus. Nov. 3208: 1–43.

Grimaldi, D. A., E. Peñalver, E. Barrón, H. W. Herhold, and M. S. Engel. 2019. Direct evidence for eudicot pollen-feeding in a Cretaceous stinging wasp (Angiospermae; Hymenoptera, Aculeata) preserved in Burmese amber. Commun. Biol. 2: 408.

Gronenberg, W. 1995. The fast mandible strike in the trap-jaw ant *Odontomachus*. I. Temporal properties and morphological characteristics. J. Comp. Physiol. A. 176: 391–398. doi:10.1007/bf00219064.

Gronenberg, W. 1996. The trap-jaw mechanism in the dacetine ants *Daceton armigerum* and *Strumigenys* sp. J. Exper. Biol. 199: 2021–2033.

Gronenberg, W., J. Paul, S. Just, and B. Hölldobler. 1997. Mandible muscle fibers in ants: fast or powerful? Cell Tiss. Res. 289: 347–361.

Gronenberg, W., C. R. F. Brandão, B. H. Dietz, and S. Just. 1998. Trap-jaws revisited: the mandible mechanism of the ant *Acanthognathus*. Physiol. Entomol. 23: 227–240.

Guo, X., P. A. Selden, and D. Ren. 2021. Maternal care in mid-Cretaceous lagonomegopid spiders. Proc. R. Soc. B. 288: 20211279.

Hasegawa, E., and R. H. Crozier. 2006. Phylogenetic relationships among species groups of the ant genus *Myrmecia*. Mol. Phylogenet. Evol. 38: 575–582.

Hashimoto, Y. 1991. Phylogenetic study of the family Formicidae based on the sensillum structures on the antennae and labial palpi (Hymenoptera, Aculeata). Jap. J. Entomol. 59: 125–140.

Heethoff, M., L. Helfen, and R. A. Norton. 2009. Description of *Neoliodes dominicus* n. sp. (Acari, Oribatida) from Dominican amber, aided by synchrotron x-ray microtomography. J. Palaeontol. 83: 153–159.

Henwood, A. 1992a. Soft-part preservation of beetles in Tertiary amber from the Dominican Republic. Palaeontol. 35: 901–912.

Henwood, A. 1992b. Exceptional preservation of dipteran flight muscle and the taphonomy of insects in amber. Palaios. 7: 203–212.

Hermann, H. R., A. N. Hunt, and W. F. Buren. 1971. Mandibular gland and mandibular groove in *Polistes annularis (L.) and Vespula maculata* (L.) (Hymenoptera: Vespidae). Int. J. Insect Morphol. Embryol. 1: 43–49.

Herzner, G., W. Goettler, J. Kroiss, A. Purea, A. G. Webb, P. M. Jakob, W. Rössler, and E. Strohm. 2007. Males of a solitary wasp possess a postpharyngeal gland. Arthropod Struct. Dev. 36: 123–133.

Herzner, G., J. Ruther, S. Goller, S. Schulz, W. Goettler, and E. Strohm. 2011. Structure, chemical composition and putative function of the postpharyngeal gland of the emerald cockroach wasp, *Ampulex compressa* (Hymenoptera, Ampulicidae). Zoology (Jena). 114: 36–45. doi:10.1016/j.zool.2010.10.002.

Hölldobler, B., and **E. O. Wilson**. 1990. The ants. Harvard University Press, Cambridge, MA.

Hopkins, M. J., and **K. St. John**. 2021. Incorporating hierarchical characters into phylogenetic analysis. Syst. Biol. 70: 1163–1180.

Hörnschemeyer, T., J. Bond, P. G. Young, and **A. Deans**. 2013. Analysis of the functional morphology of mouthparts of the beetle *Priacma serrata*, and a discussion of possible food sources. J. Insect Sci. 13: 1–14.

Ivens, A. B. F., A. Gadau, E. T. Kiers, and **D. J. C. Kronauer**. 2018. Can social partnerships influence the microbiome? Insights from ant famers and their trophobiont mutualists. Molec. Ecol. 27: 1898–1914.

Jacobs, H.-J. 2007. Grabwespen Deutschlands. Goecke & Evers, Keltern.

Jałoszyński, P., X. -Z. Luo, J. U. Hammel, S. Yamamoto, and **R. G. Beutel**. 2020. The mid-Cretaceous †*Lepiceratus* gen. nov. and the evolution of the relict beetle family Lepiceridae (Insecta: Coleoptera: Myxophaga). J. Syst. Palaeontol. 18: 1127–1140.

Janet, C. 1905. Anatomie de la tête du *Lasius niger*. Imprimerie-Librairie Ducourtieux et Gout, Limoges, Paris.

Jasso-Martínez, J. M., A. Donath, D. Schulten, A. Zaldívar-Riverón, and **M. Sann**. 2021. Midgut transcriptome assessment of the cockroach-hunting wasp *Ampulex compressa* (Apoidea: Ampulicidae). PLoS One 16: e0252221.

Jelley, C., and **P. Barden**. 2021. Vision-linked traits associated with antenna size and foraging ecology across ants. Insect Syst Diver. 5: 9.

van de Kamp, T., S. Rolo, and **T. Baumbach**. 2014. Scanning the past–synchrotron x-ray microtomography of fossil wasps in amber. Entomol. heute 26: 151–160.

Keller, R. A. 2011. A phylogenetic analysis of ant morphology (Hymenoptera: Formicidae) with special reference to the Poneromorph subfamilies. Bull. Amer. Mus. Nat. Hist. 355: 1–90.

Keller, R. A., C. Peeters, and **P. Beldade**. 2014. Evolution of thorax architecture in ant castes highlights trade-off between flight and ground behaviors. ELife 3: e01539.

Keyser, D., and **F. Friedrich**. 2017. An exceptionally well preserved new species of ostracod (Crustacea) with soft parts in Baltic amber. Hist. Biol. 29: 53–62.

Khalife, A., R. A. Keller, J. Billen, F. Hita Garcia, E. P. Economo, and **C. Peeters**. 2018. Skeletomuscular adaptations of head and legs of *Melissotarsus* ants for tunnelling through living wood. Front. Zool. 15: 30.

Khramov, A., A. Bashkuev, and **E. Lukashevich**. 2020. The fossil record of long-proboscid nectarivorous insects. Entomol. Rev. 100: 881–968.

Klunk, C. L., M. A. Argenta, A. Casadei-Ferreira, E. P. Economo, and **M. R. Pie**. 2021. Mandibular morphology, task specialization and bite mechanics in *Pheidole* ants (Hymenoptera: Formicidae). J. Roy. Soc. Interface 18: 20210318.

Kolibáč, J., V. I. Alekseev, K. Kairišs, and **A. Bukejs**. 2021. Systematic placement and new data on the checkered beetles *Aberrokorynetes* Winkler and *Visokorynetes* Winkler (Coleoptera: Cleridae) from Eocene Baltic amber obtained from x-ray tomography. Hist. Biol. 1–9.

Krenn, H. W., V. Mauss, and **J. Plant**. 2002. Evolution of the suctorial proboscis in pollen wasps (Masarinae, Vespidae). Arthropod Struct. Dev. 31: 103–120.

Krenn, H. W., J. D. Plant, and **N. U. Szucsich**. 2005. Mouthparts of flower-visiting insects. Arthropod Struct. Dev. 34: 1–40.

Kundrata, R., A. Bukejs, A. S. Prosvirov, and **J. Hoffmannova**. 2020. X-ray micro-computed tomography reveals a unique morphology in a new click-beetle (Coleoptera: Elateridae) from the Eocene Baltic amber. Sci. Rep. 10: 20158.

Labandeira, C. C., J. Kvaček, and **M. B. Mostovski**. 2007. Pollination drops, pollen, and insect pollination of Mesozoic gymnosperms. Taxon. 56: 663–695.

Lanes, G. O., R. Kawada, C. O. Azevedo, and **D. J. Brothers**. 2020. Revisited morphology applied for systematics of flat wasps (Hymenoptera, Bethylidae). Zootaxa. 4752: 1–127.

Larabee, F. J., W. Gronenberg, and **A. V. Suarez**. 2017. Performance, morphology and control of power-amplified mandibles in the trap-jaw ant *Myrmoteras* (Hymenoptera: Formicidae). J. Exp. Biol. 220: 3062–3071.

Larabee, F. J., A. A. Smith, and **A. V. Suarez**. 2018. Snap-jaw morphology is specialized for high-speed power amplification in the Dracula ant, *Mystrium camillae*. R. Soc. Open Sci. 5: 181447.

Lattke, J. E., and **G. A. R. Melo**. 2020. New haidomyrmecine ants (Hymenoptera: Formicidae) from mid-Cretaceous amber of northern Myanmar. Cretac. Res. 114: 104502.

Lattke, J., T. Delsinne, G. Alpert, and **R. Guerrero**. 2018. Ants of the genus *Protalaridris* (Hymenoptera: Formicidae), more than just deadly mandibles. Europ. J. Entomol. 115: 268–295.

Lewis, P. O. 2001. A likelihood approach for estimating phylogeny from discrete morphological character data. Syst. Biol. 50: 913–925.

Li, Y.-D., S. Yamamoto, D. -Y. Huang, and **C.-Y. Cai**. 2021. New species of *Paraodontomma* from mid-Cretaceous Burmese amber with muscle tissue preservation (Coleoptera: Archostemata: Ommatidae). Pap. Avul. Zool. 61: e20216153.

Lin, X., C. C. Labandeira, C. Shih, C. L. Hotton, and **D. Ren**. 2019. Life habits and evolutionary biology of new two-winged long-proboscid scorpionflies from mid-Cretaceous Myanmar amber. Nat. Comm. 10: 1235.

Linnaeus, C. 1758. Systema naturae per regna tria naturae, secundum classes, ordines, genera, species, cum characteribus, differentiis, locis. Tomus I. Editio decima, reformata. L. Salvii, Holmiae [= Stockholm], 824 pp.

Liu, W., P. T. Rühr, and **T. Wesener**. 2017. A look with μ-CT technology into a treasure trove of fossils: the first two fossils of the millipede order Siphoniulida discovered in Cretaceous Burmese amber (Myriapoda, Diplopoda). Cretac. Res. 74: 100–108.

Longino, J. T. 2013. A revision of the ant genus *Octostruma* Forel 1912 (Hymenoptera, Formicidae). Zootaxa 3699: 1–61.

López, F., M. Martínez, and **J. Barandica**. 1994. Four new species of the genus *Leptanilla* (Hymenoptera: Formicidae) from Spain-relationships to other species and ecological issues. Sociobiology 24: 179–212.

Longino, J. T., and **B. E. Boudinot**. 2013. New species of Central American *Rhopalothrix* Mayr, 1870 (Hymenoptera, Formicidae). Zootaxa 3616: 301–324.

Lösel, P. D., T. van de Kamp, A. Jayme, A. Ershov, T. Faragó, O. Pichler, N. Tan Jerome, N. Aadepu, S. Bremer, S. A. Chilingaryan, et al. 2020. Introducing Biomedisa as an open-source online platform for biomedical image segmentation. Nat. Commun. 11: 1–14.

Lubbock, J. 1877. On some points in the anatomy of ants. J. Microsc. 18: 120–142.

Lucky, A., M. D. Trautwein, B. S. Guénard, M. D. Weiser, and **R. R. Dunn**. 2013. Tracing the rise of ants-out of the ground. PLoS One 8: e84012.

Luque, J., L. Xing, D. E. G. Briggs, E. G. Clark, A. Duque, J. Hui, H. Mai, and **R. C. McKellar**. 2021. Crab in amber reveals an early colonization of nonmarine environments during the Cretaceous. Sci. Adv. 7: eabj5689.

Maddison, W. P., and **D. R. Maddison**. 2021. Mesquite: A modular system for evolutionary analysis. Version 3.7 http://mesquiteproject.org. 2021.

Mao, Y., K. Liang, Y. Su, J. Li, X. Rao, H. Zhang, F. Xia, Y. Fu, C. Cai, and **D. Huang**. 2018. Various amberground marine animals on Burmese amber with discussions on its age. Palaeoentomology 1: 91–103. doi:10.11646/palaeoentomology.1.1.11.

Martínez-Delclòs, X., D. E. G. Briggs, and **E. Peñalver**. 2004. Taphonomy of insects in carbonates and amber. Palaeogeogr. Palaeoclimatol. Palaeoecol. 203: 19–64.

McCoy, V. E., C. Soriano, and **S. E. Gabbott**. 2016. A review of preservational variation of fossil inclusions in amber of different chemical groups. Earth Environ. Sci. Trans. R. Soc. Edinb. 107: 203–211.

McCoy, V. E., C. Soriano, M. Pegoraro, T. Luo, A. Boom, B. Foxman, and **S. E. Gabbott**. 2018. Unlocking preservation bias in the amber insect fossil record through experimental decay. PLoS One 13: e0195482.

McKenna, K. Z., G. P. Wagner, and **K. L. Cooper**. 2021. Chapter One—A developmental perspective of homology and evolutionary novelty, pp. 1–38. In: S. F. Gilbert (ed.), Current Topics in Developmental Biology, vol. 141. Academic Press, Cambridge, MA.

Meurville M.-P., L. A. C. 2021. Trophallaxis: the functions and evolution of social fluid exchange in ant colonies (Hymenoptera: Formicidae). Myrmecol. News 31: 1–30.

Michener, C. D., and **A. Fraser**. 1978. A comparative anatomical study of mandibular structure in bees (Hymenoptera: Apoidea). Univ. Kans. sci. bull. 51: 463–482.

Miko, I., L. Vilhelmsen, N. F. Johnson, L. Masner, and **Z. Penzes. 2007.** Skeletomusculature of Scelionidae (Hymenoptera: Platygastroidea): head and mesosoma. Zootaxa 1571: 1–78.

Molet, M., V. Maicher, and **C. Peeters. 2014.** Bigger helpers in the ant *Cataglyphis bombycina:* increased worker polymorphism or novel soldier caste? PLoS One 9: e84929.

Moreau, C. S., C. D. Bell, R. Vila, S. B. Archibald, and **N. E. Pierce. 2006.** Phylogeny of the ants: diversification in the age of the angiosperms. Science 312: 101–104.

Nabozhenko, M. V., K. Kairišs, and **A. Bukejs. 2020.** The oldest fossil darkling beetle of the genus *Neomida* Latreille, 1829 (Coleoptera: Tenebrionidae) from Eocene Baltic amber examined with X-ray microtomography. Zootaxa 4768: 435–442.

Nel, A., G. Perrault, and **D. Néraudeau. 2004.** The oldest ant in the lower Cretaceous amber of Charente-maritime (SW France) (Insecta: Hymenoptera: Formicidae). Geol. Acta. 2: 23–30.

Nelsen, M. P., R. H. Ree, and **C. S. Moreau. 2018.** Ant-plant interactions evolved through increasing interdependence. Proc. Natl. Acad. Sci. U.S.A. 115: 12253–12258.

Nguyen, V., B. Lilly, and **C. Castro. 2014.** The exoskeletal structure and tensile loading behavior of an ant neck joint. J. Biomech. 47: 497–504. doi:10.1016/j.jbiomech.2013.10.053.

Nixon, K. C. 1999–2002. WinClada ver. 1.0000 Published by the author, Ithaca, NY.

Ogata, K., and **R. Taylor. 1991.** Ants of the genus *Myrmecia* Fabricius: a preliminary review and key to the named species (Hymenoptera: Formicidae: Myrmeciinae). J. Nat. Hist. 25: 1623–1673.

Ohl, M., and **P. Spahn. 2010.** A cladistic analysis of the cockroach wasps based on morphological data (Hymenoptera: Ampulicidae). Cladistics 26: 49–61.

Okada, Y., M. Katsuki, N. Okamoto, H. Fujioka, and **K. Okada. 2019.** A specific type of insulin-like peptide regulates the conditional growth of a beetle weapon. PLoS Biol. 17: e3000541.

Osten, T. 1982. Vergleichend-funktionsmorphologische Untersuchungen der Kopfkapsel und der Mundwerkzeuge ausgewälter 'Scolioidea' (Hymenoptera, Aculeata): mit 2 Tabellen. Stuttg. Beitr. Naturk. A (Biol.) 354: 1–60.

Osten, T. 1988. Die Mundwerkzeuge von *Proscolia spectator* Day (Hymenoptera: Aculeata): ein Beitrag zur Phylogenie der 'Scolioidea'. Stuttg. Beitr. Naturk. A (Biol.) 411: 1–30.

Paul, J., and **W. Gronenberg. 1999.** Optimizing force and velocity: mandible muscle fibre attachments in ants. J. Exper. Biol. 202: 797–808.

Paul, J., F. Roces, and **B. Hölldobler. 2002.** How do ants stick out their tongues? J. Morphol. 254: 39–52. doi:10.1002/jmor.10011.

Peeters, C., and **F. Ito. 2015.** Wingless and dwarf workers underlie the ecological success of ants (Hymenoptera: Formicidae). Myrmecol. News 21: 117–130.

Peeters, C., R. A. Keller, A. Khalife, G. Fischer, J. Katzke, A. Blanke, and **E. P. Economo. 2020.** The loss of flight in ant workers enabled an evolutionary redesign of the thorax for ground labour. Front. Zool. 17: 1–13.

Penney, D., M. Dierick, V. Cnudde, B. Masschaele, J. Vlassenbroeck, L. van Hoorebeke, and **P. Jacobs. 2007.** First fossil Micropholcommatidae (Araneae), imaged in Eocene Paris amber using x-ray computed tomography. Zootaxa 1623: 47–53.

Penney, D., D. I. Green, A. McNeil, R. S. Bradley, Y. M. Marusik, P. J. Withers, and **R. F. Preziosi. 2012.** A new species of *Craspedisia* (Araneae: Theridiidae) in Miocene Dominican amber, imaged using x-ray computed tomography. Paleont. J. 46: 583–588.

Peregrine, D., A. Mudd, and **J. Cherrett. 1973.** Anatomy and preliminary chemical analysis of the post-pharyngeal glands of the leaf-cutting ant, *Acromyrmex octospinosus* (Reich.) (Hym., Formicidae). Insectes Soc. 20: 355–363.

Perreau, M., and **P. Tafforeau. 2011.** Virtual dissection using phase-contrast x-ray synchrotron microtomography: reducing the gap between fossils and extant species. Syst. Entomol. 36: 573–580.

Perrichot, V. 2014. A new species of the Cretaceous ant *Zigrasimecia* based on the worker caste reveals placement of the genus in Sphecomyrminae (Hymenoptera: Formicidae). Myrmecol. News 19: 165–169.

Perrichot, V., A. Nel, D. Néraudeau, S. Lacau, and **T. Guyot. 2008.** New fossil ants in French cretaceous amber (Hymenoptera: Formicidae). Naturwiss. 95: 91–97.

Perrichot, V., B. Wang, and **M. S. Engel. 2016.** Extreme morphogenesis and ecological specialization among Cretaceous basal ants. Curr. Biol. 26: 1468–1472.

Perrichot, V., B. Wang, and **P. Barden. 2020.** New remarkable hell ants (Formicidae: Haidomyrmecinae stat. nov.) from mid-Cretaceous amber of northern Myanmar. Cretac. Res. 109: 104381.

Peters, R. S., L. Krogmann, C. Mayer, A. Donath, S. Gunkel, K. Meusemann, A. Kozlov, L. Podsiadlowski, M. Petersen, and **R. Lanfear. et al. 2017.** Evolutionary History of the Hymenoptera. Curr. Biol. 27: 1013–1018.

Piekarski, P. K., J. M. Carpenter, A. R. Lemmon, E. M. Lemmon, and **B. J. Sharonowski. 2018.** Phylogenomic evidence overturns current conceptions of social evolution in wasps (Vespidae). Mol. Biol. Evol. 35: 2097–2109.

Pohl, H., B. Wipfler, D. Grimaldi, F. Beckmann, and **R. G. Beutel. 2010.** Reconstructing the anatomy of the 42 million-year-old fossil †*Mengea tertiaria* (Insecta, Strepsiptera). Naturwiss. 97: 855–859.

Poinar, G. O., and **R. Hess. 1982.** Ultrastructure of 40-million-year-old insect tissue. Science 215: 1241–1242.

Popovici, O., I. Miko, K. Seltmann, and **A. Deans. 2014.** The maxillo-labial complex of *Sparasion* (Hymenoptera, Platygastroidea). J. Hym. Res. 37: 77–111.

Porto, D. S., and **E. A. Almeida. 2019.** A comparative study of the pharyngeal plate of Apoidea (Hymenoptera: Aculeata), with implications for the understanding of phylogenetic relationships of bees. Arthropod Struct. Dev. 50: 64–77.

Porto, D. S., and **E. A. Almeida. 2021.** Corbiculate bees (Hymenoptera: Apidae): exploring the limits of morphological data to solve a hard phylogenetic problem. Insect Syst. Div. 5: 2.

Porto, D. S., L. Vilhelmsen, and **E. A. B. Almeida. 2016.** Comparative morphology of the mandibles and head structures of corbiculate bees (Hymenoptera: Apidae: Apini). Syst. Entomol. 41: 339–368.

Prentice, M. A. 1998. The comparative morphology and phylogeny of apoid wasps (Hymenoptera: Apoidea). PhD dissertation, University of California, Berkeley.

Probst, R. S., B. D. Wray, C. S. Moreau, and **C. R. Brandão. 2019.** A phylogenetic analysis of the dirt ants, *Basiceros* (Formicidae: Myrmicinae): inferring life histories through morphological convergence. Insect Syst. Div. 3: 1–12.

Püffel, F., A. Pouget, X. Liu, M. Zuber, T. van de Kamp, F. Roces, and **D. Labonte. 2021.** Morphological determinants of bite force capacity in insects: a biomechanical analysis of polymorphic leaf-cutter ants. J. R. Soc. Interface 18: 20210424.

Rabeling, C., J. M. Brown, and **M. Verhaagh. 2008.** Newly discovered sister lineage sheds light on early ant evolution. Proc. Natl. Acad. Sci. USA. 105: 14913–14917.

Rambaut, A., A. J. Drummond, D. Xie, G. Beale, and **M. A. Suchard. 2018.** Posterior summarization in Bayesian phylogenetics using Tracer 1.7. Syst. Biol. 67: 901–904.

Rasnitsyn, A. P., and **D. L. Quicke. 2002.** History of insects. Kluwer Academic Publishers, Dordrecht, Netherlands.

Richter, A., R. A. Keller, F. B. Rosumek, E. P. Economo, F. Hita Garcia, and **R. G. Beutel. 2019.** The cephalic anatomy of workers of the ant species *Wasmannia affinis* (Formicidae, Hymenoptera, Insecta) and its evolutionary implications. Arthropod Struct. Dev. 49: 26–49.

Richter, A., F. H. Garcia, R. A. Keller, J. Billen, E. P. Economo, and **R. G. Beutel. 2020.** Comparative analysis of worker head anatomy of *Formica* and *Brachyponera* (Hymenoptera: Formicidae). Arthropod Syst. Phylogeny 78: 133–170.

Richter, A., F. Hita Garcia, R. A. Keller, J. Billen, J. Katzke, B. E. Boudinot, E. P. Economo, and **R. G. Beutel. 2021.** The head anatomy of *Protanilla lini* (Hymenoptera: Formicidae: Leptanillinae), with a hypothesis of their mandibular movement. Myrmecol. News 31: 85–114.

Riquelme, F., M. Hernández-Patricio, A. Martínez-Dávalos, M. Rodríguez-Villafuerte, M. Montejo-Cruz, J. Alvarado-Ortega, J. L. Ruvalcaba-Sil, and **L. Zúñiga-Mijangos. 2014.** Two flat-backed polydesmidan millipedes from the Miocene Chiapas-amber Lagerstätte, Mexico. PLoS One 9: e105877.

Ronquist, F., and **J. P. Huelsenbeck**. **2003**. MrBayes 3: Bayesian phylogenetic inference under mixed models. Bioinfo. 19: 1572–1574.

Ronquist, F., **S. Klopfstein**, **L. Vilhelmsen**, **S. Schulmeister**, **D. L. Murray**, and **A. P. Rasnitsyn**. **2012**. A total-evidence approach to dating with fossils, applied to the early radiation of the Hymenoptera. Syst. Biol. 61: 973–999.

Sann, M., **O. Niehuis**, **R. S. Peters**, **C. Mayer**, **A. Kozlov**, **L. Podsiadlowski**, **S. Bank**, **K. Meusemann**, **B. Misof**, **C. Bleidorn. et al**. **2018**. Phylogenomic analysis of Apoidea sheds new light on the sister group of bees. BMC Evol. Biol. 18: 71.

Sann, M., **K. Meusemann**, **O. Niehuis**, **H. E. Escalona**, **M. Mokrousov**, **M. Ohl**, **T. Pauli**, and **C. Schmid-Egger**. **2021**. Reanalysis of the apoid wasp phylogeny with additional taxa and sequence data confirms the placement of Ammoplanidae as sister to bees. Syst. Entomol. 46: 558–569.

Schädel, M., **M. Hyžný**, and **J. T. Haug**. **2021**. Ontogenetic development captured in amber—the first record of aquatic representatives of Isopoda in Cretaceous amber from Myanmar. Naupl. 29: e2021003.

Schoeters, E., and **J. Billen**. **1996**. The post-pharyngeal gland in *Dinoponera* ants (Hymenoptera: Formicidae): unusual morphology and changes during the secretory process. Int. J. Insect Morphol. Embryol. 25: 443–447.

Schmidt, J., and **P. Michalik**. **2017**. The ground beetle genus *Bembidion* Latreille in Baltic amber: review of preserved specimens and first 3D construction of endophallic structures using x-ray microscopy (Coleoptera, Carabidae, Bembidiini). ZooKeys 662: 101–126.

Schmidt, J., **I. Belousov**, and **P. Michalik**. **2016**. X-ray microscopy reveals endophallic structures in a new species of the ground beetle genus *Trechus* Clairville, 1806 from Baltic amber (Coleoptera, Carabidae, Trechini). ZooKeys 614: 113–127.

Schmidt, J., **S. Scholz**, and **D. R. Maddison**. **2021**. *Balticeler kerneggeri* gen. nov., sp. nov., an enigmatic Baltic amber fossil of the ground beetle family Trechinae (Coleoptera, Carabidae). Dtsch. Entomol. Z. 68: 207–224.

Sereno, P. C. 2007. Logical basis for morphological characters in phylogenetics. Cladistics 23: 565–587.

Sharkey, M.J., **J. M. Carpenter**, **L. Vilhelmsen**, **J. Heraty**, **J. Liljeblad**, **A. P. G. Dowling**, **S. Schulmeister**, **D. Murray**, **A. R. Deans**, **F. Ronquist, et al**. **2012**. Phylogenetic relationships among superfamilies of Hymenoptera. Cladistics 28: 80–112.

Shattuck, S. O. 1992. Generic revision of the ant subfamily Dolichoderinae (Hymenoptera: Formicidae). Sociobiology 21: 1–181.

Shavrin, A. V., and **K. Kairišs**. **2021**. A new species of *Eusphalerum* Kraatz, 1857 from the Eocene Baltic amber (Coleoptera, Staphylinidae, Omaliinae). Zootaxa 4966: 469–475.

Shi, G. H., **D. A. Grimaldi**, **G. E. Harlow**, **J. Wang**, **J. Wang**, **M. C. Yang**, **W. Y. Lei**, **Q. L. Li**, and **X. H. Li**. **2012**. Age constraint on Burmese amber based on UePb dating of zircons. Cret. Res. 37: 155–163.

Silveira, O. T., and **J. N. A. Santos, Jr**. **2011**. Comparative morphology of the mandibles of female polistine social wasps (Hymenoptera, Vespidae, Polistinae). Rev. Bras. Entomol. 55: 479–500.

Sinotte, V. M., **J. Renelies-Hamilton**, **B. A. Taylor**, **K. M. Ellegaard**, **P. Sapountzis**, **M. Vasseur-Cognet**, and **M. Poulsen**. **2020**. Synergies between division of labor and gut microbiomes of social insects. Front. Ecol. Evol 7: 503.

Sosiak, C. E., and **P. Barden**. **2021**. Multidimensional trait morphology predicts ecology across ant lineages. Funct. Ecol. 35: 139–152.

Soriano, C., **M. Archer**, **D. Azar**, **P. Creaser**, **X. Delclòs**, **H. Godthelp**, **S. Hand**, **A. Jones**, **A. Nel**, and **D. Néroudaux. et al**. **2010**. Synchrotron X-ray imaging of inclusions in amber. Compt. Rend. Palevol. 9: 6361–7368.

Strohm, E., **G. Herzner**, and **W. Goettler**. **2007**. A 'social' gland in a solitary wasp? The postpharyngeal gland of female European beewolves (Hymenoptera, Crabronidae). Arthropod Struct. Dev. 36: 113–122.

Strohm, E., **M. Kaltenpoth**, and **G. Herzner**. **2010**. Is the postpharyngeal gland of a solitary digger wasp homologous to ants? Evidence from chemistry and physiology. Insectes Soc. 57: 285–291.

Sugime, Y., **K. Oguchi**, **H. Gotoh**, **Y. Hayashi**, **M. Matsunami**, **S. Shigenobu**, **S. Koshikawa**, and **T. Miura**. **2019**. Termite soldier mandibles are elongated by dachshund under hormonal and Hox gene controls. Development 146: dev171942.

Tafforeau, P., **R. Boistel**, **E. Boller**, **A. Bravin**, **M. Brunet**, **Y. Chaimanee**, **P. Cloetens**, **M. Feist**, **J. Hoszowska**, **J. J. Jaeger. et al**. **2006**. Applications of x-ray synchrotron microtomography for non-destructive 3D studies of paleontological specimens. Appl. Phys. A 83: 195–202.

Taniguchi, R., **H. Nishino**, **H. Watanabe**, **S. Yamamoto**, and **Y. Iba**. **2021**. Reconstructing the ecology of a Cretaceous cockroach: destructive and high-resolution imaging of its micro sensory organs. Sci. Nat. 108: 1–8.

Taylor, R. W. 1978. *Nothomyrmecia macrops*: a living-fossil ant rediscovered. Science 201: 979–985. doi:10.1126/science.201.4360.979.

Urbani, C. B., **B. Bolton**, and **P. S. Ward**. **1992**. The internal phylogeny of ants (Hymenoptera: Formicidae). Syst. Entomol. 17: 301–329.

Vajda, V., and **A. Bercovici**. **2014**. The global vegetation pattern across the Cretaceous–Paleogene mass extinction interval: a template for other extinction events. Glob. Planet. Change 122: 29–49.

Vilhelmsen, L. 1996. The preoral cavity of lower Hymenoptera (Insecta): comparative morphology and phylogenetic significance. Zool. Script. 25: 143–170.

Vilhelmsen, L. 2011. Head capsule characters in the Hymenoptera and their phylogenetic implications. Zookeys: 343-361.

Wagner, G. P. 2007. The developmental genetics of homology. Nat. Rev. Genet. 8: 473–479.

Wagner, G. P. 2014. Homology, genes, and evolutionary innovation. Princeton University Press, Princeton.

Wang, C., **J. Billen**, **C. Wei**, and **H. He**. **2019**. Morphology and ultrastructure of the infrabuccal pocket in *Camponotus japonicus* Mayr (Hymenoptera: Formicidae). Insect. Soc. 66: 637–646.

Ward, P. S., and **S. G. Brady**. **2003**. Phylogeny and biogeography of the ant subfamily Myrmeciinae (Hymenoptera: Formicidae). Invertebr. Syst. 17: 361–386.

Ward, P. S., and **B. L. Fisher**. **2016**. Tales of dracula ants: the evolutionary history of the ant subfamily Amblyoponinae (Hymenoptera: Formicidae). Syst. Ent. 41: 683–693.

Weiss, K., **E. Strohm**, **M. Kaltenpoth**, and **G. Herzner**. **2015**. Comparative morphology of the postpharyngeal gland in the Philanthinae (Hymenoptera, Crabronidae) and the evolution of an antimicrobial brood protection mechanism. BMC Evol. Biol. 15: 291.

Weiss, K., **G. Herzner**, and **E. Strohm**. **2017**. Sexual selection and the evolution of male pheromone glands in philanthine wasps (Hymenoptera, Crabronidae). BMC Evol. Biol. 17: 1–20.

Whelden, R. M. 1957. Notes on the anatomy of *Rhytidoponera convexa* Mayr ('*violacea*' Forel) (Hymenoptera, Formicidae). Ann. Entomol. Soc. Am. 50: 271–282.

Wilson, E. O. 1987. Causes of ecological success: the case of the ants. The Sixth Tansley Lecture. J. Anim. Ecol. 56: 1–9.

Wilson, E.O. 2003. *Pheidole* in the New World: a dominant, hyperdiverse ant genus. Harvard University Press, Cambridge, MA.

Wilson, E. O., **F. M. Carpenter**, and **W. L. Brown, Jr. 1967a**. The first Mesozoic ants, with the description of a new subfamily. Psyche (Cambridge) 74: 1–19.

Wilson, E. O., **F. M. Carpenter**, and **W. L. Brown, Jr. 1967b**. The first Mesozoic ants. Sci. (Washington, D. C.) 157: 1038–1040.

Wipfler, B., **R. Machida**, **B. Müller**, and **R. G. Beutel**. **2011**. On the head morphology of Grylloblattodea (Insecta) and the systematic position of the order, with a new nomenclature for the head muscles of Dicondylia. Syst. Entomol. 36: 241–266.

Wipfler, B., **K. Weissing**, **K. -D. Klass**, and **T. Weihmann**. **2016**. The cephalic morphology of the American cockroach *Periplaneta americana* (Blattodea). Arthropod Syst. Phylogeny 74: 267–297.

Wong, M., and **B. Guenard**. **2017**. Subterranean ants: summary and perspectives on field sampling methods, with notes on diversity and ecology (Hymenoptera: Formicidae). Myrmecol. News 25: 1–16.

Xie, W., **P. O. Lewis**, **Y. Fan**, **L. Kuo**, and **M. -H. Chen**. **2011**. Improving marginal likelihood estimation for Bayesian phylogenetic model selection. Syst. Biol. 60: 150–160.

Xing, L., and **L. Qiu**. **2020**. Zircon UPb age constraints on the mid-Cretaceous Hkamti amber biota in northern Myanmar. Palaeogeogr. Palaeoclimatol. Palaeoecol. 558: 109960.

Xu, W., **H. He**, and **J. Billen**. **2020**. Morphology of the exocrine glands associated with the maxillolabial complex in the ant *Camponotus japonicus* Mayr, 1866 (Hymenoptera: Formicidae). Insectes Soc. 68: 59–67.

Yamada, A., **D. D. Nguyen**, and **K. Eguchi**. **2020**. Unveiling the morphology of the Oriental rare monotypic ant genus *Opamyrma* Yamane, Bui, and

Eguchi, 2008 (Hymenoptera: Formicidae: Leptanillinae) and its evolutionary implications, with first descriptions of the male, larva, tentorium, and sting apparatus. Myrmecol. News 30: 27–52.

Yamamoto, S., A. V. Shavrin, and K. Kairišs. 2021. A second fossil species of the enigmatic rove beetle genus *Charhyphus* in Eocene Baltic amber, with implications on the morphology of the female genitalia (Coleoptera: Staphylinidae: Phloeocharinae). Earth Environ. Sci. Trans. R. Soc. Edinb. 113: 39–50.

Yoder, M. J., I. Mikó, K. C. Seltmann, M. A. Bertone, and A. R. Deans. 2010. A gross anatomy ontology for Hymenoptera. PLoS One 5: e15991.

Yoshimura, M., and B. L. Fisher. 2012. A revision of male ants of the Malagasy Amblyoponinae (Hymenoptera: Formicidae) with resurrections of the Genera *Stigmatomma* and *Xymmer*. PLoS One 7: e33325.

Yu, T., R. Kelly, L. Mu, A. Ross, J. Kennedy, P. Broly, F. Xia, H. Zhang, B. Wang, and D. Dilcher. 2019. An ammonite trapped in Burmese amber. Proc. Natl. Acad. Sci. 116: 11345–11350.

Zhang, W., Z. He, Y. Sun, J. Wu, and Z. Wu. 2020a. A mathematical modeling method elucidating the integrated gripping performance of ant mandibles and bio-inspired grippers. J. Bionic. Eng. 17: 732–746.

Zhang, W., M. Li, G. Zheng, Z. Guan, J. Wu, and Z. Wu. 2020b. Multifunctional mandibles of ants: variation in gripping behavior facilitated by specific microstructures and kinematics. J. Insect Physiol. 120: 103993.

Zhang, W., Z. Wu, Z. Wang, Z. Wang, C. Li, H. Rajabi, and J. Wu. 2021. Double-rowed teeth: design specialization of the *H. venator* ants for enhanced tribological stability. Bioinspir. Biomim. 16: 055003.

Zimmermann, D., and L. Vilhelmsen. 2016. The sister group of Aculeata (Hymenoptera)-evidence from internal head anatomy, with emphasis on the tentorium. Arthropod Syst. Phylogeny 74: 195–218.

Zimmermann, D., S. Randolf, and V. Mauss. 2021. Morphological adaptations to silk production by adult females in the pollen wasp genus *Quartinia* (Masarinae, Vespidae)—a keystone character for ground nesting in dry sand habitats. Arthropod Struct. Dev. 62: 101045.

Żyła, D., S. Yamamoto, K. Wolf-Schwenninger, and A. Solodovnikov. 2017. Cretaceous origin of the unique prey-capture apparatus in mega-diverse genus: stem lineage of Steninae rove beetles discovered in Burmese amber. Sci. Rep. 7: 45904.